This is to certify that the
dissertation entitled

PROPERTIES AND SEPARATIONS OF
PLANT-DERIVED CHEMICALS

presented by

DUNG THI VU

has been accepted towards fulfillment
of the requirements for the

Ph.D. degree in Chemical Engineering

Carl T. Lira
Major Professor's Signature

5/8/07
Date

DATE DUE	DATE DUE	DATE DUE

PROPERTIES AND SEPARATIONS OF PLANT-DERIVED CHEMICALS

By

Dung Thi Vu

A DISSERTATION

Submitted to
Michigan State University
in partial fulfillment of the requirements
for the degree of

DOCTOR OF PHILOSOPHY

Department of Chemical Engineering and Material Science

2007

ABSTRACT

PROPERTIES AND SEPARATIONS OF PLANT-DERIVED CHEMICALS

By

Dung Thi Vu

Biorenewable processing is highly dependent on the feasibility of separations. This work considers the development of fractionation principles and thermodynamic properties useful for process designs in two main areas: fractionation of lipids; and measurement/prediction of properties for upgrading of organic acids and their derivatives.

Ricinolein can be separated from the other triglycerides in castor oil by adsorbing it onto acidic adsorbents or by concentrating it in the effluent stream of fixed-beds using non-polar adsorbents. Solvents play an important role in adsorption. Replacing hexane with ethanol, the hydroxylated triglycerin, which is preferentially adsorbed by Florisil in hexane, will be released in the effluent. The adsorbent capacity of Florisil to the total oil also significantly changes from 17 wt. % in hexane to 6 wt. % in ethanol.

Extractions of plant lipids usually use solvent mixtures of chloroform-methanol. However, chloroform is very toxic and a possible carcinogen in humans. A proposed process developed in this work successfully extracts sulfoquinovosyl diacylglycerol (SQDG) from alfalfa and isolates it from other plant lipids using non-chlorinated solvents. Lipases are deactivated during extraction using isopropanol at 50-55 ^{o}C. Hexane-methanol mixtures are used in extraction and subsequent liquid-liquid partitioning to remove proteins and phospholipids. The yield of SQDG using the

proposed process is comparable to literature and the amount of solvent used is less than 30 vol. % of the value reported in literature.

For purposes of upgrading of lactic acid, a model is developed for the oligomer distribution in aqueous solutions. The model is extended to multicomponent VLE in mixtures involving lactic acid and ethyl lactate oligomers. A *P-x-y* apparatus is also developed to measure VLE and VLLE at temperatures between 25 °C and 80 °C and pressures down to 0.7 kPa. Data pass either the area or point-to-point thermodynamic consistency test.

Finally, the Step Potential Equilibria and Dynamics (SPEAD) molecular simulation method is adapted for predicting vapor pressures of oxygenated compounds. A method is developed for optimization of five and nine variable functions. From this study, parameters for the secondary –OH, cyclic -O-, and -COO- groups are made available for use in SPEAD. Vapor pressures of esters containing up to 30 carbons are predicted within 25 % of the experimental values using these parameters.

Dedicated to my Lord and God, Jesus and his Holy mother Mary, for giving me the inspiration and stamina to complete this dissertation.

ACKNOWLEDGMENTS

I would like to thank Dr. Carl T. Lira for his guidance and support as my advisor through my Ph.D. studies. I am especially grateful for his patience and the encouragement he gave me to finish my dissertation. I also wish to thank Dr. Dennis Miller, Dr. Christoph Benning, and Dr. Mark Worden for serving on my committee. Special thanks to Dr. Miller for his support and giving me a chance to work with his research group on reactive distillation projects, to Dr. Christoph Benning for collaboration on sulfolipid project, and to Dr. Richard Elliott at the University of Ohio at Akron for collaboration and support on Step Potential Equilibria and Dynamics molecular simulation.

I also would like to thank my family Vu (Vũ), extended family, Chuck T. Wynn (Huỳnh Thiện Hùng), and Vivian Gendron for their help, support and unconditional love.

I also want to extend my appreciation to Dr. R. Leep and T. Dietz in the Department of Crop and Soil Sciences for providing alfalfa; to Dr. Navin Asthana and Dr. Aspi Kolah from Dr. Miller's Reactive Distillation Group, and Dr. Wayne Riekhof from Dr. Benning's sulfolipid project for their support. Thanks also go to undergraduate students, Jesse Wright and Brett Burkhart for their assistance in phase equilibrium experiments and the administration of the MSU Chemical Engineering Department.

TABLE OF CONTENTS

LIST OF TABLES

LIST OF FIGURES

PART 1:

SEPARATIONS OF PLANT-DERIVED CHEMICALS

Chapter 1 – Background on Ricinolein and SQDG

1.1 – Introduction on Castor Oil Separation

Castor oil is obtainable from castor bean (*Ricinus Communis*), which is extensively cultivated in India, Brazil and China [1]. At present, castor oil is the only source of commercially hydroxylated fatty acid containing up to 90 wt.% of ricinoleic acid, (*12-hydroxy-9Z-octadecenoic acid*), which can be easily obtained by hydrolysis of the corresponding triglycerides [2].

Triglycerides in castor oil are mostly triricinolein and diricinolein, derived from esterification of fatty acids with glycerol. In a typical castor oil, the fatty acids' contents are 85-90 wt.% of ricinoleic, 3-5 wt.% of linolenic, 2-5 wt.% of oleic, 1-2 wt.% of stearic, 1-3 wt.% of palmitic acid, and refined vegetable oils generally have less than 2 wt.% of non-glyceride components [3, 4].

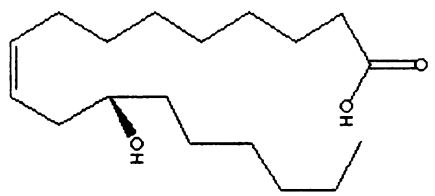

Figure 1.1 Structure of Ricinoleic Acid

Castor oil can be a renewable source of non-petroleum chemical feedstocks. In addition to its excellent emollient and lubricating properties, which have been utilized in wetting and dispersing dyes, pigments, and fillers in textiles and inks, castor oil also is an excellent plasticizer or a surfactant for a wide variety of natural and synthetic resins, waxes, polymers and elastomers due to its highly polar hydroxyl groups. Ricinoleic acid

is widely used in urethane-polymer, electronics, food, pharmaceutical, perfumes and cosmetic industries [1, 2, 5].

For specific applications, highly pure ricinoleic fatty acid content is desirable. Also, research is ongoing to genetically modify plants to selectively express functional lipids. However, purity is difficult to achieve. In general, distillation is impractical for separation of high molecular molecules such as triglycerides, due to their low vapor pressure. Emulsions and foam generation due to the presence of fatty acids in plant oils can also create difficulties in liquid-liquid extractions, and require large quantities of solvents for a complete separation. This would result in high capital, operating costs and difficulty in disposing or recovering large amount of organic solvents [6].

Solid-phase extraction can be an attractive alternative separation process for triglycerides. Chapter 2 in this dissertation will discuss the separation of triricinolein from non-hydroxylated glycerides in castor oil using adsorption. Basically, castor oil is blended with solvent then loaded into a column containing adsorbents, which have different affinity to hydroxylated and non-hydroxylated glycerides. The stronger affinity to one type of these glycerides allows adsorbents to preferentially bind non-covalently and retain the selected glyceride(s) in the column while the others flush through. Then, the adsorbed glyceride(s) are recovered from washing adsorbents with an appropriate solvent, and the adsorbents are regenerated for future use.

1.2 – Introduction on Plant Sulfolipids Separation

Glycerolipids, the major class of thylakoid membrane lipids, composed of glyceroglycolipids and glycerophospholipids, are derived from glycerol [7]. The most abundant glycerophospholipids, so-called phosphatides, in membranes are

phosphatidylglycerol (PG), *phosphatidylcholine* (PC), *phosphatidylethanolamine* (PE), and *phosphatidylinositol* (PI). The main glyceroglycolipids are *monogalactosyl-diacylglycerol* (MGDG), *digalactosyldiacylglycerol* (DGDG), and *sulfoquinovosyl-diacylglycerol* (SQDG) [8].

In this dissertation, the terms *glycolipids* and *phospholipids* are substituted for glycerolipids and glycerophospholipids, which have both C1 and C2 hydroxyl groups of the glycerol backbone esterified to the carboxyl groups of the two fatty acid chains. The C3 hydroxyl group of the glycerol is esterified to phosphoric moiety in phospholipids, and it attached to a sugar molecule in glycolipids. However, a glycolipid such as SQDG is called sulfolipid if its molecule contains a sulfur atom directly bonded to a carbon as $C–SO_3H$ [9, 10].

Figures 1.2 and 1.3 show the example structure of phospholipids and sulfolipids, phoshatidylcholine and SQDG, respectively. The acyl R_1 and R_2 groups in these molecules can be different in length and degree of saturation. For SQDG in particular, R_1COO- is often palmitic (C 16:0) and R_2COO- is linolenic (C18:3, $\Delta^{9,12,15}$) [11-14]. The IUPAC name of SQDG is 1,2-di-*O*-acyl-3-*O*-(6'-deoxy-6'-sulfo-α-D-glucopyranosyl)-*sn*-glycerol, and PC is 1,2-diacyl-*sn*-glycero-3-phosphorylcholine [15, 16].

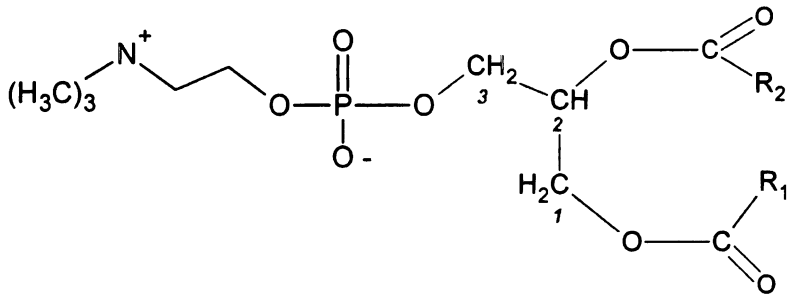

Figure 1.2 Structure of Phosphatidylchloline

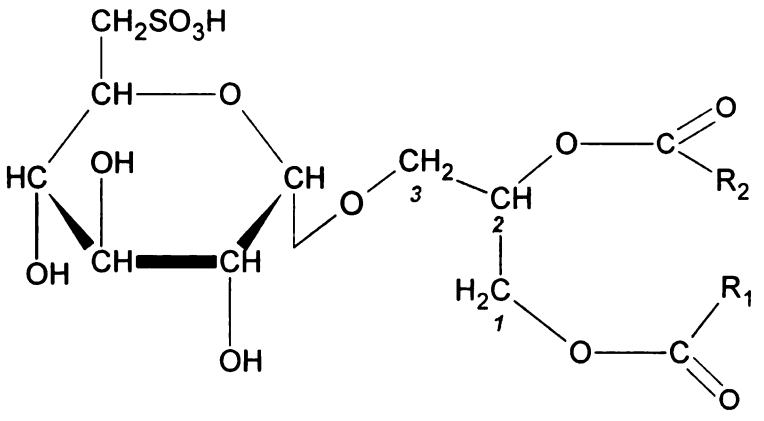

Figure 1.3 Structure of Sulfoquinovosyl Diacylglycerol [17]

Phospholipids have been known for more than 100 years, but the existence of MGDG and DGDG was unknown until 1956 [18], and SQDG was first recognized in 1959 by Benson [10]. Sulfolipids were late in being discovered, partly because of the lack of specific and sensitive reagents for detection of sulfate and sulfonate [19]. Since 1960, not only because of the demand for understanding their role in membrane structure and function, sulfolipids have also attracted considerable interest due to their excellent surfactant properties and more recently due to their activity against the AIDS virus [20].

As shown, phospholipids and sulfolipids are amphiphillic molecules, having a *hydrophobic* end (fatty acids) and a *hydrophilic* end (phosphoric acid or sugar). These molecules are associated and bound to proteins in plant membranes from their hydrophilic end. Thus, extractions of sulfolipids or phospholipids from plants require a dehydrating solvent such as methanol to rupture the lipid-protein linkages. However, the hydrophobic end does not allow it to be very soluble in this type of polar solvent. It is necessary to include a less polar solvent such as petroleum ether, chloroform, or diethyl ether. The most efficient solvents reported in literature for plant lipids extractions are

ethanol-diethyl ether (3:1 v/v) and methanol-chloroform (2:1 v/v), though they are toxic and chloroform in particular is a possible carcinogen in humans [11, 21].

Sulfolipids have been found in all green higher plants, algae, mosses, cyanobacteria, purple sulfur and non-sulfur bacteria [15, 22-26]. As mentioned, they are potentially an anti-AIDS virus, but a larger testing program including tests on humans with the AIDS virus cannot begin until sulfolipids can be obtained in much larger quantities [20]. Abundant sources of sulfolipids are necessary, but developments of new separation techniques using non-chlorinated solvents are also critical.

In this dissertation, a novel process to recover sulfolipids from plant extraction using non-chlorinated and less toxic solvents will be presented in chapter 3. The key source of interest is SQDG in alfalfa, planted on the Michigan State University campus. The yield of SQDG using the proposed process is comparable to literature and the amount of solvents used is less than 30 vol. % of the value reported in literature.

Chapter 2 – Selective Adsorption of Ricinolein Studies

2.1 – Overview

This chapter summarizes the adsorption studies to separate glycerides of ricinoleic acid from non-hydroxylated fatty acid esters in castor oil. Batch adsorptions are used to screen the adsorbent candidates, and the evaluation is based on the adsorption capacity of adsorbents to the total oil. Once the potential adsorbent is identified, its selectivity of hydroxylated triglycerides to the non-hydroxylated is further studied using fixed-bed adsorption.

Since all glycerides in soybean oil also are the glycerides in castor oil, soybean oil is blended with castor oil to vary the concentration of feed solutions in fixed bed adsorptions. This reduces errors in sample analyses, due to a very small portion of unsaturated fatty acid contents in castor oil, and provides fractionation studies over a wider range of compositions than possible in natural castor oil.

The effect of solvents and adsorption capacities of three different types of non-polar, acidic, and basic adsorbents are evaluated for hydroxylated and non-hydroxylated glycerides. As expected, ricinolein can be selectively adsorbed onto acidic adsorbents such as Florisil. In contrast, the non-hydroxylated glycerides are more selective to the non-polar adsorbents. The separations significantly improve when a less-polar solvent is used with Florisil, or a more polar solvent is used with a non-polar adsorbent.

2.2 – Adsorbent Selection

Fatty acids in soybean and castor oils can be categorized as non-hydroxylated (all acids except for ricinoleic acid) and hydroxylated acid (ricinoleic acid) as shown in Table

2-1. Separation using adsorption is expected to become attractive when the desired functional component is available in large concentration, with smaller amounts of other components. An objective in the design of adsorption columns is to adsorb the minor components. Because the ricinoleic acid content is high in castor oil, this study aims to adsorb non-hydroxylated triglycerides onto adsorbents and liberate the hydroxylated in the effluent in order to minimize the quantity of adsorbents. Thus, non-polar adsorbents which should have high affinity to the non-hydroxylated glycerides are more preferable candidates than the acidic or basic adsorbents. Economical adsorbents such as silica gels and activated carbon are first selected and the cost of regeneration is also considered.

Table 2-1 Triglyceride Contents in Soy-based and Castor Oils [2]

*Values in parenthesis are measured in this work.

Plant oil	Composition of Fatty Acids (wt.%)					
	non-hydroxylated					hydroxylated
	Palmitic	Stearic	Oleic	Linoleic	Linolenic	Ricinoleic
	C16:0	C18:0	C18:1	C18:2	C18:3	C18:1
Soybean	10.1	4.2	24.3	51.5	8.3	0.0
	(10.5)	*(4.3)*	*(25.1)*	*(53.5)*	*(6.6)*	(0.0)
Castor	1.0	1.0	3.0	4.2	0.3	89.5
	(1.2)	*(1.4)*	*(3.7)*	*(5.0)*	*(0.6)*	*(88.1)*

C16:0: *Hexadecanoic acid*
C18:0: *Octadecenoic acid*
C18:1: *9-Octadecanoic acid*
C18:2: *9,12-Octadecadienoic acid*
α-C18:3: *9,12,15-Octadecatrienoic acid*
Ricinoleic: 12-hydroxy-9Z-octadecenoic acid

2.3 – Batch Adsorption

Batch adsorptions of castor oil in ethanol solutions onto activated carbon, silica gels and a polymeric resin were performed. Castor oil [8001-79-4] was purchased from Sigma-Aldrich and the absolute ethanol of ACS/USP grade [64-17-5] from Pharmacia

was used as received. Silica gel [112926-00-8] of pore size 22 Å was from Supelco and 150 Å was from Analtech. Amberlite® XAD-2 nonionic polystyrene based resin of 90 Å [9060-05-3] was from Aldrich and activated carbon F-400 [7440-44-0] was from Calgon.

Activated carbon is a non-polar adsorbent, and silica gel is slightly acidic. They both have been applied to the clean up and purification of a wide range of synthetic and natural compounds. Amberlite® XAD-2 is also a non-polar adsorbent, commercially used to remove antibiotics, organic nitrogen, grease and various aromatic compounds from aqueous streams [27].

2.3.1 – Experimental Preparation and Analysis

Prior to use, adsorbents were washed using ethanol, and silica gels were pre-heated at 200 °C to eliminate the moisture. A predetermined quantity of adsorbent was added to an oil solution at room temperature. Equilibration was carried out overnight in a closed container to make sure that saturation of each batch was reached. Oil solution samples were filtered to remove any fine adsorbent particles before analyses were taken. Since the boiling point of castor oil is significantly higher than solvents, which were used to make the oil solutions, concentrations of total oil in samples were determined using the gravimetric method, after completely evaporating off solvents. Differences in the initial and final oil concentrations of the solutions were used to evaluate the adsorbent capacity.

2.3.2 – Results and Discussion

Results are summarized in Table 2-2. *Adsorption capacity* is defined as the maximum amount (gram) of castor oil that can be adsorbed onto one gram of the selected adsorbent. As shown, polymeric XAD-2 and silica gel at 22 Å had a low capacity to

castor oil in ethanol solvent. No adsorption seemed to occur with silica gel at 150 Å. The discrepancy in adsorption capacity of the two silica gels could be due to 1) the evaporation of ethanol in sample analyses using the gravimetric method, or 2) loss of solvent by evaporation during twelve-hour experiments or 3) the incomplete removal of moisture from silica gel. Assuming silica gel at 150 Å pore had the same adsorption capacity as the 22 Å pore type, it was verified that calculated concentrations of castor oil in batches 1-3 did not change after adsorption if only 3 % ethanol was evaporated. On the other hand, oil solutions using silica gel at 22 Å were more dilute, evaporating 10 % of ethanol only reduced half of the calculated adsorption capacity of this silica gel.

Table 2-2 Summary of Batch Adsorption Experiments in Ethanol

Adsorbent		Batch #	Load	Solvent	$q_{max,oil}$
Type	Source		g-adsorbent/ 1g-castor oil	g-ethanol/ 1g-castor oil	g-adsorbed oil/ 1g-adsorbent
Silica gel, pore ~150 Å	Analtech	1	1.2	1.4	0.000
		2	2.3	5.5	
		3	2.3	9.6	
		4	5.6	12.5	
Silica gel, pore ~ 22 Å	Supelco	5	14.5	5.5	0.013 ± 0.002
		6	9.9	12.5	
Amberlite XAD-2	Aldrich	7	6.3	11.2	0.013 ± 0.002
Activated Carbon	Calgon	8	3.3	8.9	0.06 ± 0.02
		9	7.3	8.3	
		10	11.0	14.4	
		11	12.8	17.2	

The evaporation of solvent could also be a reason causing the calculated capacity of XAD-2 in batch experiments lower than that obtained from fixed-bed adsorptions discussed below. It was observed that XAD-2 was significantly swollen, sticky, and difficult to remove from oil samples in batch adsorption.

Activated carbon has the largest adsorption capacity to castor oil among the selected adsorbents, but data are inconsistent. The inconsistency could be due to the defects sites on this adsorbent, caused by the presence of heteroatoms such as sulfur, chlorine, nitrogen, and metal oxides in the manufacturing process of carbon [28].

As discussed before, non-polar adsorbents were more favorable in this study. The acidic adsorbent, silica gel, showed the same capacity to castor oil as the non-polar polymeric XAD-2. But, packing and backwashing of silica gels at the experimental condition were difficult due to the fine texture. Therefore, silica gels were not included in fixed-bed adsorption studies.

2.4 – Fixed-bed Adsorption

In addition to the polymeric XAD-2 and activated carbon used in batch adsorptions, Florisil® [1343-88-0, 16-30 mesh, standard grade], and three different types of methylene-bridge divinylbenzene-styrene copolymer adsorbents were selected for fixed-bed adsorption studies: (Dowex® Optipore SD-2 [374558-57-3], Dowex® M-43 [195215-44-2], and Dowex® L-493 [211502-88-4]).

Florisil®, an acidic adsorbent, is a co-precipitate of silica and magnesia (MgO_3Si), extensively used in the chromatographic analysis of lipids and pesticides [29-31]. Dowex® Optipore SD-2, a non-polar adsorbent, containing the functional group of tertiary amine, has been used as an alternative to activated carbon, for decolorization, taste and odor removals in the processing of corn syrups and high fructose corn syrups. Dowex® M-43 is a weak-base exchange resin, used to remove mineral and organic acids such as acetic, formic, propionic, benzoic, halogen, sulfuric and phosphoric, from the air and solutions. Dowex® L-493 is a hydrophobic resin with non-catalytic activity,

considered a better option than carbon in removing natural organics from water. In general, polymeric materials have a low swell of ~ 5%, allowing for easy vessel design, can potentially be recovered for future use, and they do not require furnace regeneration. More details of the Dowex® adsorbents are available on the Dow Chemical web site [32].

2.4.1 – Fixed-bed Design

A fixed-bed was constructed using stainless steel of 3/8" OD x 6" length, shown in Figure 2.1. All feed tubes used in this design were 1/16" OD. Adsorbates in feed solution were fed to the fixed-bed using a micropump® (ELDEX, A-30-S model). Table 2-3 provides a summary of fixed-bed run conditions.

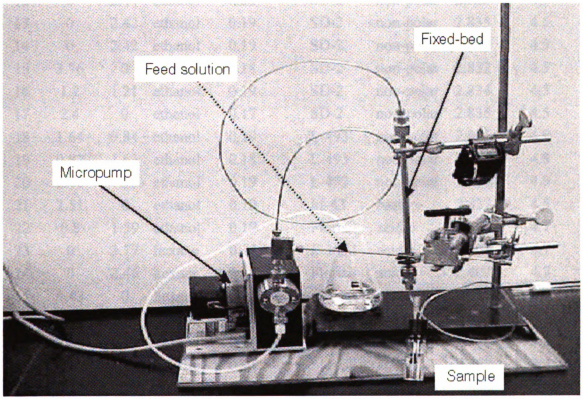

Figure 2.1 Fixed-Bed Design

Table 2-3 Summary of Fixed-bed Adsorption Experiments

	Feed Solution				Adsorbent			
Run #	Castor (wt.%)	Soy (wt.%)	Solvent	Flowrate (ml/min)	Name	Type	Amount (g)	Volume (ml)
1	1.05	0	ethanol	0.18	Carbon	non-polar	2.256	4.8
2	0.72	0	ethanol	0.30	Carbon	non-polar	2.256	4.8
3	0.68	0	ethanol	0.14	Carbon	non-polar	2.276	4.8
4	0.99	0	ethanol	0.18	Carbon	non-polar	2.276	4.8
5	1.01	0	ethanol	0.18	Carbon	non-polar	2.275	4.8
6	1	0	ethanol	0.16	XAD-2	non-polar	1.930	3.8
7	2.46	0	ethanol	0.16	XAD-2	non-polar	2.802	5.5
8	0	3.69	ethanol	0.18	SD-2	non-polar	2.833	5.0
9	0.8	1.6	ethanol	0.17	SD-2	non-polar	2.901	4.9
10	1.99	0.41	ethanol	0.19	SD-2	non-polar	2.836	4.8
11	0.38	1.99	ethanol	0.20	SD-2	non-polar	2.837	4.8
12	0	2.44	ethanol	0.20	SD-2	non-polar	2.826	4.5
13	0	2.42	ethanol	0.19	SD-2	non-polar	2.835	4.5
14	0	2.42	ethanol	0.19	SD-2	non-polar	2.832	4.5
15	3.76	0	ethanol	0.18	SD-2	non-polar	2.832	4.5
16	1.2	1.21	ethanol	0.19	SD-2	non-polar	2.834	4.5
17	2.4	0	ethanol	0.17	SD-2	non-polar	2.835	4.5
18	1.64	0.84	ethanol	0.19	L-493	non-polar	2.865	4.9
19	0.82	1.63	ethanol	0.18	L-493	non-polar	2.827	4.8
20	2.48	0	ethanol	0.19	L-493	non-polar	2.875	4.9
21	2.51	0	ethanol	0.19	M-43	basic	2.837	4.5
22	0.8	1.59	ethanol	0.19	Florisil	acidic	2.369	4.7
23	0	3.77	hexane	0.14	Florisil	acidic	2.408	4.7
24	0	2.46	hexane	0.14	Florisil	acidic	2.407	4.7
25	1.43	0	hexane	0.21	Florisil	acidic	2.427	4.7
26	1.29	1.3	hexane	0.18	Florisil	acidic	2.413	4.7
27	1.66	0.85	hexane	0.18	Florisil	acidic	2.468	4.8
28	0.8	1.68	hexane	0.17	Florisil	acidic	2.462	4.8
29	2.44	0	methanol	0.20	SD-2	non-polar	2.835	5.0
30	2.38	0	propanol	0.20	SD-2	non-polar	2.838	5.0
31	1.63	0.84	propanol	0.16	SD-2	non-polar	2.856	5.0
32	0.81	1.63	propanol	0.19	SD-2	non-polar	2.835	5.0

2.4.2 – Sample Analysis

Bed Volume – Before adsorbents were packed into the fixed-bed, the volume of wetted adsorbents (V_{ads}), the so-called one bed volume, was measured using either a buret or a graduated cylinder. The liquid flow was measured in bed volumes (*BedVol*) defined as $BedVol = F * T / V_{ads}$ where F is the actual flow rate (ml/min) of feed solution, T is time (minutes) at which the sample is collected.

Bed loading procedure – Debris was removed and adsorbents were washed using the elution solvent. Then, slurry of adsorbents was slowly poured into the column (up to 80 % of column's volume) and backwashing was performed to remove air bubbles.

Total oil concentration – Fractions containing about 2-3 g of the effluent from fixed-bed were collected over 15-20 minute periods. The gravimetric method was used to determine the total oil content in samples by evaporating solvent. For example, in run # 22, the initial oil concentration C_0 = 2.42 %, fraction 5 was collected between T = 65 min and T = 85 min; tared = 25.4993 g, weight of sample (solvent + oil + tared) = 28.6127 g. After evaporating off solvent, weight of sample (oil + tared) = 25.5696 g.

$$C = oil\ \% = \frac{(25.5696 - 25.4993)}{(28.6127 - 25.4993)} = 2.26\ \%, \text{ and } C/C_0 = \frac{2.26\ \%}{2.42\ \%} = 0.933$$

Glyceride concentrations and FAME method – After evaporating off the solvents to determine total oil concentration, samples of the effluents were converted to fatty acid methyl esters (FAME) to find out the contents of non-hydroxylated and hydroxylated triglycerides. A method was developed and verified to be compatible and more efficient than the standard esterification method (AOCS, Ce 2-66) [33]. The standard method requires the use of boron trifluoride (BF_3), which is extremely

flammable and decomposes on exposure to moisture. The alternative method, developed in this study, eliminated the use of nitrogen, glove box to store BF_3, and the heat to elevate the chemical reaction in converting triglycerides into fatty acids methyl esters.

A droplet of each sample was blended in about 1.5 ml of hexane. After dissolving in hexane, the sample was mixed with 0.5 ml of 2M KOH in methanol solution and shaken thoroughly for 30 seconds. Finally, 2 ml of aqueous saturated KCl was added to separate the methyl esters into the hexane phase.

The analyses of FAMEs were performed using gas chromatography. The chromatograph (GC) was a Perkin-Elmer model 8500 equipped with a FID detector and an Econo-Cap EC-WAX capillary column (15m x 0.53 mm ID x 1.2 μm). The column and standard triglycerides were purchased from Alltech Associate, Inc [34]. The GC used helium gas at 5ml/min and 5.0 psig. At t = 0 min, oven temperature (T_{oven}) = 65 °C; t = 4.5-12.5 min, T_{oven} = 200 °C, and t =15.8 – 21.8 min, T_{oven} = 250 °C.

Figure 2.2 is an example GC chromatogram of a castor-soybean oil mixture. Assuming the same response factor for all FAMEs, mass concentrations of the hydroxylated and non-hydroxylated glycerides in oil samples were determined from the corresponding GC peak areas. The calculated fatty acids contents in soy-based and castor oils from GC analyses using this assumption are in excellent agreement with literature, shown in Table 2-1. GC analyses were also done for castor-soy oil mixtures to compare with the calculated $C_{1,0}$ and $C_{2,0}$ using the weight method. Difference between the two methods was about 7 %, which is acceptable for GC analyses.

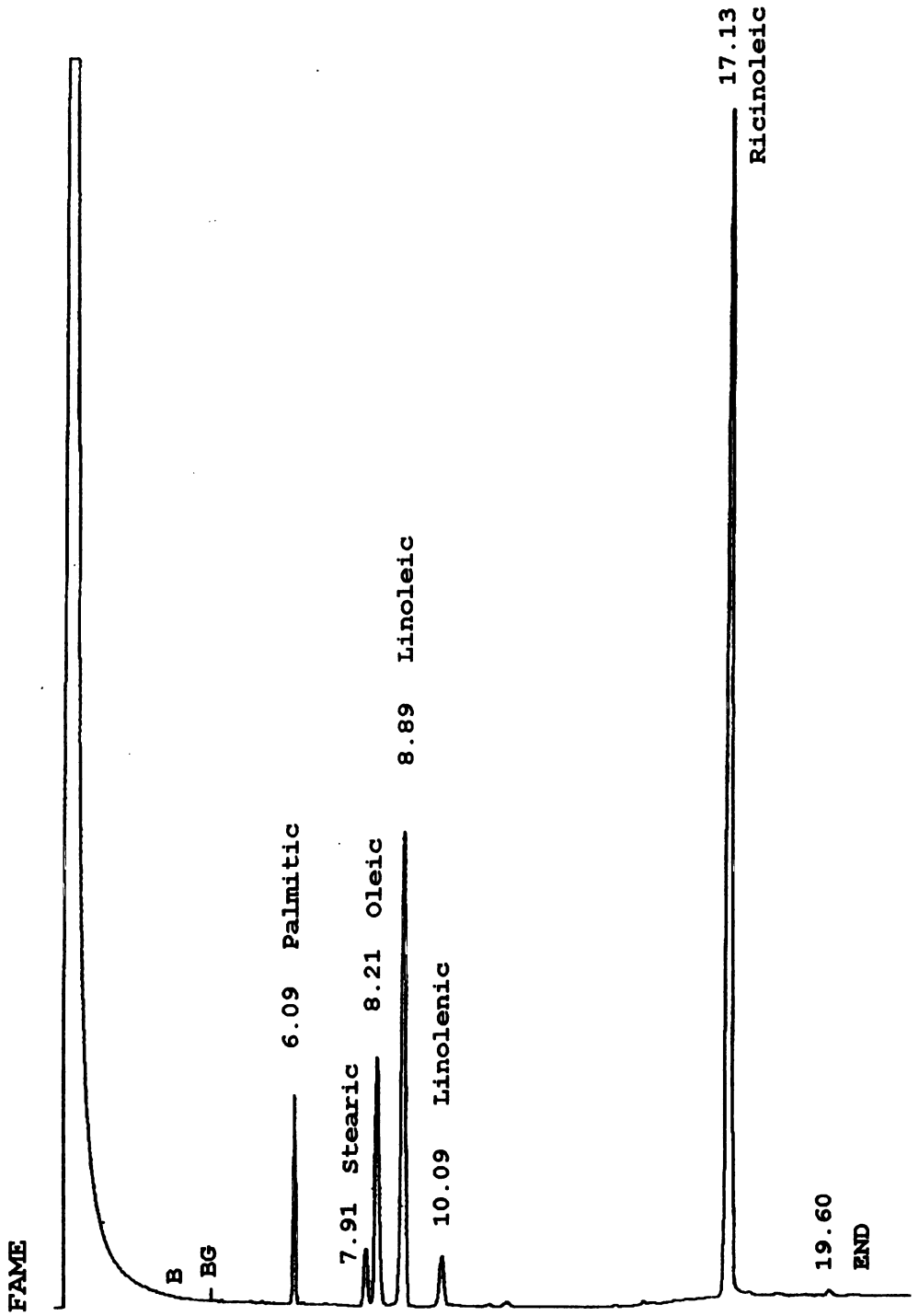

Figure 2.2 Example of Gas Chromatogram of Fatty Acid Methyl Esters
(FAMEs were derivatized from castor-soy (2:1 wt%./wt%.) oil mixture)

Breakthrough behavior – Table 2-4 and Figure 2.3 are the examples of adsorption data and breakthrough curves included in Appendix A. In table 2-4, [a]*Fraction* denotes the sample collected in the experiment, [b]: time (minutes) after fixed-bed starts, [c] : number of bed volumes, [d] : total oil concentration, [e, f, g]: concentrations of total oil (C), ricinolein (C_1), and non-hydroxylated component (C_2) in the effluent compared to their initial C_0 , $C_{1,0}$, $C_{2,0}$. Calculations of Cs are based on 88.1 wt. % of ricinoleic acid in castor oil.

Table 2-4 Sample of Fixed-bed Adsorption Data (Run # 22)

[a]Fraction	[b]Time	[c]Bed Vol	[d]oil %	[e]C/C_0	[f]$C_1/C_{1,0}$	[g]$C_2/C_{2,0}$
1	15	0.620	0.05%	0.021	-	-
2	32	1.323	1.08%	0.448	0.465	0.432
3	48	1.984	1.99%	0.824	0.756	0.840
4	65	2.686	2.21%	0.915	0.937	0.889
5	85	3.513	2.26%	0.933	0.882	0.939
6	115	4.753	2.32%	0.960	-	-
7	133	5.497	2.34%	0.969	1.129	0.880
8	151	6.241	2.35%	0.971	1.291	0.810
11	183	7.563	2.37%	0.978	-	-
12	222	9.175	2.41%	0.996	1.242	0.868

Adsorption capacity – As defined in the previous section, adsorption capacity (q_{max}) of an adsorbent is the maximum amount of the adsorbed component held-up by one gram of that adsorbent. In fixed-bed studies, it was calculated as follows:

$$q_{\max,\, oil} = \frac{\text{amount of adsorbed oil (g)}}{\text{1 gram of adsorbent}} \tag{2.1}$$

$$\text{Amount of adsorbed oil} = \text{total load} * \frac{A_1}{A_1 + A_2} \tag{2.2}$$

$$\text{Total load} = V_{ads} * BedVol * oil\ \% * solution\ density \tag{2.3}$$

where V_{ads}, and *oil %* are already defined above. $BedVol_{sat}$ is the number of bed volumes at saturation point. Because the oil concentration was low, solution density was assumed to be the same as solvent density in calculating the total oil solution loaded into the fixed-bed. A_1 and A_2 are respectively proportional to the amounts of adsorbed and non-adsorbed oil at saturation as shown in Figure 2.3; the $A_1/(A_1 + A_2)$ value in Eqn 2.2 was determined by integration using the paper weight method. Though the concentrations in the bed were not uniform spatially at all times, this method provides a quantitative method to differentiate between various experimental conditions.

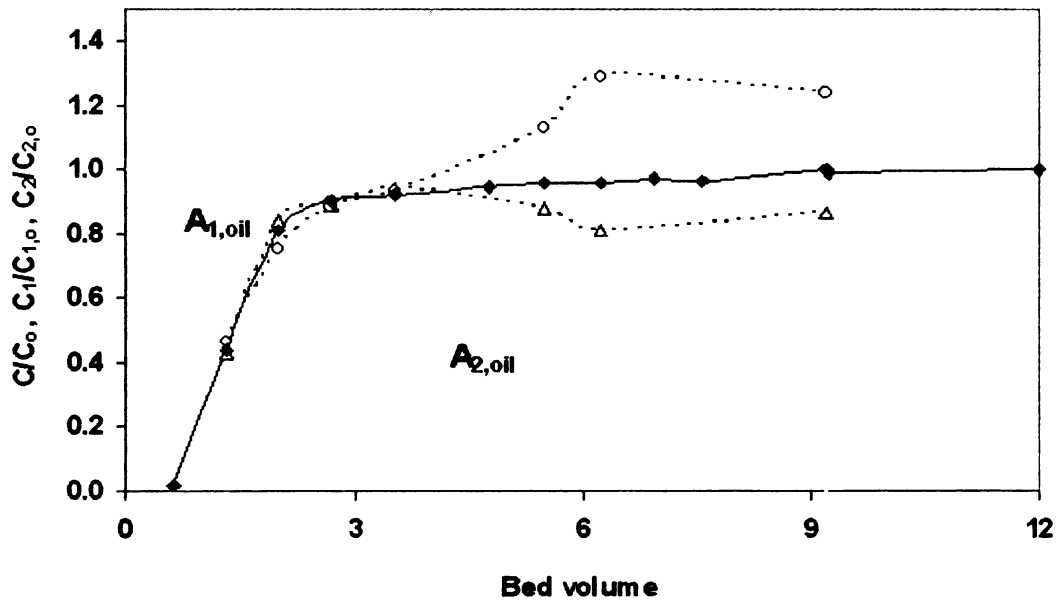

Figure 2.3 Breakthrough Curves of Total Oil and Glycerides (Run # 22)
♦: total oil, ○: hydroxyl, Δ: non-hydroxy, using Florisil and ethanol.

Selectivity of adsorbents – Similar to the relative volatility which measures the simplicity in separations by distillation, a separation factor described below is usually used to determine the equilibrium selectivity in adsorption [30]:

$$\alpha_{AB} = \frac{X_A}{X_B}\frac{Y_B}{Y_A} \tag{2.4}$$

where X_A and Y_A are the mole fractions of component A in adsorbed and fluid phase at equilibrium, respectively. For qualitative analyses in this work, Eqn 2.4 can be modified as follows:

$$\alpha_{OH-nonOH} = \left(\frac{A_{1,OH}}{A_{2,OH}}\right)\left(\frac{A_{2,nonOH}}{A_{1,nonOH}}\right) \tag{2.5}$$

where *OH* and *nonOH* respectively denote hydroxylated and non-hydroxylated components, A_1's and A_2's are the areas enclosed by breakthrough curves of the corresponding glycerides, $C/C_0 = 1$ and *Bed volume* = $BedVol_{sat}$, as illustrated for total oil in Figure 2.3.

2.4.3 – Results and Discussion

Results of fixed bed adsorptions are summarized in Table 2-5. There were five different experiments performed using activated carbon, but data related to this adsorbent were omitted due to their inconsistency as discussed in section 2.3.2.

Table 2-5 Summary of Fixed-bed Adsorption Results

Adsorbent		Solvent	$q_{max,oil}$	$\alpha_{OH\text{-}nonOH}$
Name	Type			
M-43	weak base	ethanol	0.06 ± 0.03	0.78 ± 0.10
L-493	non-polar	ethanol	0.10 ± 0.03	0.45 ± 0.21
XAD-2	non-polar	ethanol	0.10 ± 0.02	0.71 ± 0.20
SD-2	non-polar	propanol	0.08 ± 0.01	0.59 ± 0.18
SD-2	non-polar	ethanol	0.12 ± 0.02	0.55 ± 0.12
SD-2	non-polar	methanol	0.13 ± 0.02	0.54 ± 0.20
Florisil	acidic	ethanol	0.06 ± 0.01	0.26 ± 0.10
Florisil	acidic	hexane	0.17 ± 0.02	6.04 ± 0.99

Non-polar adsorbents have larger adsorption capacities to the total oil (~ 10 wt.%) than basic and acidic adsorbents (~ 6 wt. %). The deviation from multiple runs and deviation in determination of A_1, A_2 using the weight method were combined in calculating the accuracy of $q_{max,oil}$ and $\alpha's$. The values of $\alpha_{OH\text{-}nonOH}$ for all adsorbents are less than 1.0 when alcohols were used as solvents, indicating that non-hydroxylated glycerides were preferentially adsorbed in a fixed-bed. Except for Florisil with hexane, the α's of adsorbents with alcohols are very much the same, showing similar capability for separating glycerides of castor oil. But, separations in alcohols were not very efficient because α's are relatively close to unity.

Effect of solvents – The effect of solvents is significant in adsorption. More oil adsorbs to Florisil and the selectivity of this adsorbent is switched from retaining non-hydroxylated to hydroxylated glycerides if a non-polar solvent such as hexane is substituted for ethanol (Figures 2.3 and 2.4).

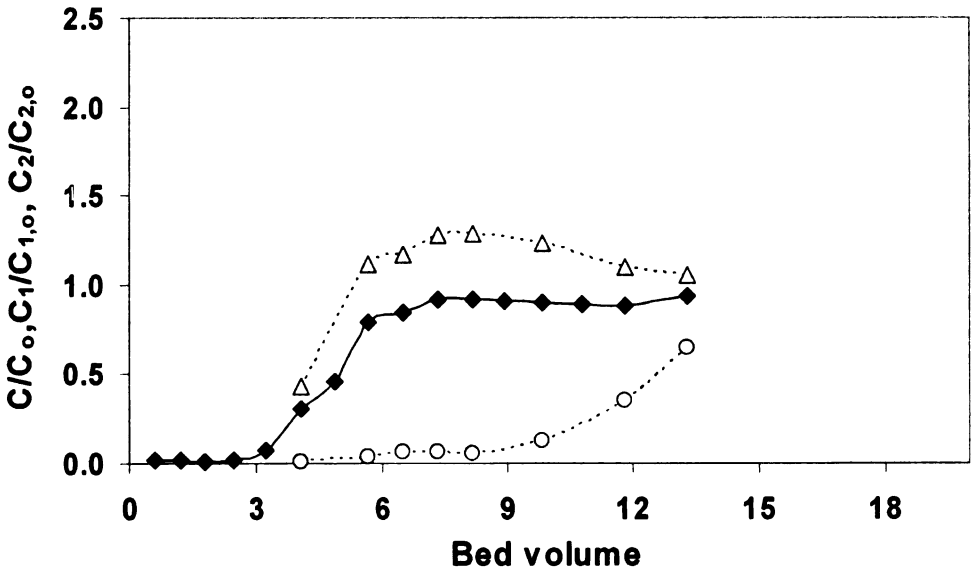

Figure 2.4 Fixed-bed Adsorption Using Hexane and Florisil (Run # 28)
♦: total oil, ○: hydroxyl, Δ: non-hydroxy.

A similar effect to the selectivity of adsorbent is also found in adsorption with SD-2. The $\alpha_{OH\text{-}nonOH}$ value increases when solvent changes from methanol to ethanol and propanol. However, the SD-2 capacity for total oil shifts to the opposite direction compared to the Florisil. More oil adsorbed to Florisil in hexane than in ethanol, but less oil absorbed to SD-2 in propanol than SD-2 in methanol (Table 2-5).

Adsorbents' regenerability – All adsorbents used in the fixed-bed adsorptions can be fully recovered using methanol. In the pairs of runs 1 and 2, 3 and 4, 13 and 17, 14 and 15 (Table 2-3), the first run was performed with fresh adsorbent and the second run used regenerated adsorbents. Results show that regenerated adsorbents provided the same adsorption capacity and selectivity as the fresh adsorbents.

Chapter 3 – Extraction and Purification of SQDG

3.1 – Overview

Extraction of lipids is commonly done using solvent mixture of chloroform-methanol. However, chloroform is very toxic and a possible carcinogen in humans [35]. Isolation of any desired lipids from a multicomponent system requires a series of unit operations. In the recovery of high-value lipids, the cost is often determined by handling large volumes of solvents, thus rapid reduction of volume is preferable.

This chapter presents the results from the two-stage process: (1) extraction and coarse fractionation; and (2) purification of SQDG, using non-chlorinated solvents. The objective of the coarse fractionation in this work was to isolate a glycolipid fraction that could be purified in subsequent steps. Initially, studies were performed using only minor variations from published methods. The initial results are presented to justify the modifications that led to the optimized process.

A proposed method to obtain sulfolipids from alfalfa using non-chlorinated solvents was developed and demonstrated. This method gave a compatible yield of SQDG as it is reported in the literature [11], but used less solvents and chemicals. Significant findings included the use of hot 2-propanol at 50-55 °C to deactivate lipase degradation of lipids during stage (1) of the process. These findings eliminated the need for other reagents used in the literature including dry ice or liquid nitrogen, organic acids, inorganic salts, and Florisil adsorbent.

3.2 – Stage (1) – Extraction and Coarse Fractionation Studies

Solvent selection involves two primary properties: volatility and solvent power.

Following lipid extraction, evaporation is commonly used to concentrate the extract before another separation such as crystallization or adsorption can be performed. Evaporating off solvents, however, cannot be done at high temperature, due to the heat sensitivity of the most biological molecules. As discussed in chapter 1, section 1.2, there is no literature report successfully using a single and non-toxic extraction solvent, with a low boiling point, and compatible with the amphiphilic behavior of plant lipids. Literature extractions use methanol-chloroform (2:1 v/v) predominantly. The starting point in this study was to evaluate the extraction of SQDG using relatively low boiling point blended-methanol solvents which have similar total Hildebrand values as that of chloroform-methanol mixture.

3.2.1 – The Hildebrand Solubility Parameter

The Hildebrand solubility parameter δ [36, 37] is considered the foundation of solution theory, defined as follows:

$$\delta = \sqrt{c} = \left[\frac{\Delta H - RT}{V_m}\right]^{1/2} \tag{3.1}$$

where c is the cohesion energy density, ΔH is heat of vaporization, R is gas constant, T is temperature, and V_m is molar volume. The dimension of δ is $(\text{pressure})^{1/2}$.

As it relates to the cohesion energy density or heat of vaporization, the Hildebrand parameter is strongly affected by molecular interaction forces. It can be described using the Hansen [38] three-parameter approach:

$$\delta^2 = \delta_d^2 + \delta_p^2 + \delta_h^2 \tag{3.2}$$

where δ_d is the dispersion contribution, δ_p is the polar contribution, and δ_h is the hydrogen bonding contribution.

In application, the Hildebrand parameter of a solvent mixture can be theoretically calculated by averaging the Hildebrand parameters of the individual solvents by volume fraction [39]. For example, mixture of 32 vol.% acetone (δ = 20.3 $MPa^{1/2}$) in toluene (δ = 18.2 $MPa^{1/2}$) has δ value = 0.32*20.3 + 0.68*18.2 = 19.0. This approach was used to calculate the mixing ratios for the selected solvent systems.

3.2.2 – Solvent Selection

Toluene, ethyl acetate, and acetone were selected from aromatic hydrocarbons, esters, and ketones for this study. The selection was based on the similarity of the Hildebrand values of these molecules and chloroform's, and also the relatively lower boiling points of these solvents compared to most of their molecular family members. Extraction in chloroform was used as a benchmark to evaluate the selected solvents, and trichloroethylene was used to determine how extraction results changed if the selected solvents were replaced by their homologous molecules.

Table 3-1 Solubility Parameters of Related Solvents [40]

Solvent	δ $(MPa)^{1/2}$	δ_d $(MPa)^{1/2}$	δ_p $(MPa)^{1/2}$	δ_h $(MPa)^{1/2}$
Toluene	18.2	18.0	1.4	2.0
Ethyl acetate	18.6	15.8	5.3	7.2
Trichloroethylene	18.8	18.0	3.1	5.3
Chloroform	19.0	17.8	3.1	5.7
Acetone	20.3	15.5	10.4	7.0
Methanol	29.7	15.1	12.3	22.3
Isopropanol	23.5	15.8	6.1	16.4
n-Hexane	14.9	14.9	0.0	0.0
Water	47.9	15.5	16.0	42.3

Tables 3-1 and 3-2 list the solvent systems and their solubility parameters. The mixing ratios were assigned in order to have the same theoretically calculated Hildebrand value for all systems compared to that of chloroform-methanol (2:1 v/v). The use of formic acid and acetic acid are discussed in section 3.2.6.

Table 3-2 Solvent Systems Used in Extraction Studies

System	Volume Ratio		
	(1)	(2)	(3)
methanol (1) + toluene (2) + formic acid (3)	1	2.09	0.100
methanol (1) + acetone (2) + formic acid (3)	1	1.87	0.000
	1	1.87	0.050
	1	1.87	0.100
methanol (1) + chloroform (2) + formic acid (3)	1	2.00	0.050
	1	2.00	0.100
methanol (1) + ethyl acetate (2) + acetic acid (3)	1	2.04	0.000
	1	2.04	0.050
	1	2.04	0.100
methanol (1) + ethyl acetate (2) + formic acid (3)	1	2.04	0.075
	1	2.04	0.100
	1	2.04	0.050
methanol (1) + trichloroethylelne (2) + formic acid (3)	1	2.02	0.100

3.2.3 – Experimental Preparation

Alfalfa – Alfalfa containing 64-68 wt.% of moisture was harvested in the second week of October 2003, from Michigan State University campus fields. Both stems and leaves were collected to represent a commercial harvest. At the time of collection, a flail harvester chopped the alfalfa stems and leaves into pieces that were about 1-2 inches in length. The chopped alfalfa was pretreated with isopropanol or kept frozen at -5 °C for future use. The moisture of alfalfa was measured using a MB-200 Ohaus moisture balance.

Chemicals – A SQDG [59-1230-7] standard was purchased from Larodan Fine Chemicals Company. Acetone [67-64-1], chloroform [67-66-3], toluene [108-88-3], ethyl actetate [141-78-6] and hexane [110-54-3] were from Burdick & Jackson Company. Methanol [67-56-1] and trichloroethylene [79-01-6] were from Fisher Scientific. Glacial acetic acid [64-19-7], ammonium hydroxide [1336-21-6], and potassium phosphate, monobasic [7778-77-0, crystal] were from EM Science, Inc. Potassium chloride [7447-40-7, crystal, ≥ 99.0% grade] was from Spectrum Quality Products, Inc. Ammonium sulfate [7783-20-2, crystal] was from Columbus Chemical Industrial, Inc. Formic acid [64-18-6, 88 wt.%], sulfuric acid [7664-93-9, 98%], water [7732-18-5, HPLC grade], and thin layer chromatographic plates ["Baker" Si250] were from J.T. Baker, Inc. DEAE-cellulose (diethylaminodiethyl cellulose) [9013-34-7, 100-200 μm pore] was from BioChemika. Myristic acid [544-63-8, crystal, 99-100% grade] and Florisil® [1343-88-0, 16-30 mesh, standard grade] were from Sigma-Aldrich. All solvents and reagents were used as received, if not otherwise specified.

Thin-layer chromatographic plates – Sulfuric acid 50 wt.% and α-naphthol 2.4 wt.% in ethanol-sulfuric acid solution (8:1 v/v) were prepared for sample analyses. The plates were impregnated with 0.15 M ammonium sulfate and dried in air, then activated at 120 °C for 60-90 minutes before use.

3.2.4 – Extraction Procedure

Extraction –Alfalfa was mixed and ground in dry-ice using a mortar and pestle. Extractions were performed on a scale of either 5 g or 50 g basis of alfalfa including leaves and stems. For a 5 g basis, the ground alfalfa was placed in a filter bag, submerged into the selected solvent mixture and squeezed repeatedly to collect the

extract. For a 50 g basis, the ground alfalfa was blended with solvent mixture using a stainless steel blender, and then the extract was filtered though a vacuum funnel. In both cases, fresh solvent was added and the process was repeated until the alfalfa turned light yellow. All the extract was combined after extraction, and carried to the phase separation.

Coarse Fractionation – The inorganic substances and polar lipids being more polar than glycerolipids were eliminated from the extract using either saturated aqueous potassium phosphate, monobasic (KH_2PO_4, d = 1.146 g/ml, pH = 4.02) or potassium chloride solution (KCL, pH = 6.35) [22, 41]. Each volume of the extract was allowed to contact with 0.2 volume of the salt solution, then centrifuged in a benchtop centrifuge at 1500 rpm for 2-3 minutes to completely separate the organic phase from the solid and the aqueous phase.

An alternative method was applied to the methanol + acetone extract, which will be discussed in section 3.2.5. Following coarse fractionation, the extract (organic phase) was then evaporated at room temperature and 10-20 inHg of vacuum to dryness, and the obtainable product called *dry extract*.

3.2.5 – Sample Analysis

To this point, *dry extract* contained not only glycolipids including SQDG, but also phospholipids, chlorophyll, and other pigments. Extractions were evaluated for the SQDG content in the *dry extract* using one-dimensional thin-layer chromatography (TLC) and gas chromatography (GC). Procedures of these analytical analyses and examples of calculations are described below.

TLC Analysis – To minimize the error in using microbalance due to a small

amount of *dry-extract* (~ 0.05 g) obtained from 5 g basis of alfalfa, all *dry extract* was re-dissolved in the same solvent mixture (~ 2 ml) used in the extraction to become *dry extract solution*, (excluding the organic acids).

Samples of *dry extract solution* and standard SQDG were placed on TLC plates in series of 2-3 μL drops, using a micropipet (Gilson, P20 model). The drop size was kept to be less than 3 mm in diameter, and TLC plates were dried under nitrogen between drops. The remainder of the *dry extract solution* was re-evaporated to determine the amount of *dry extract* placed on the TLC plates.

Several mobile phases were evaluated for TLC analyses using acetone-toluene-water (91:38:6 v/v/v, 91:34:7 v/v/v, 91:30:8 v/v/v, 85:66:0 v/v/v, 75:41:1 v/v/v). The mixture acetone-toluene-water (91:34:7 v/v/v) provided the best resolution; the retention factor (R_f) value for lipids of interest were PC < PE < PI < SQDG < DGDG < PG < MGDG.

Glycolipids were visualized by alpha-naphthol and sulfuric acid, in which MGDG and DGDG bands were dark-blue, and SQDG was pink [42]. To locate lipids, the TLC plate was sprayed with sulfuric acid, heated up to 150 °C in a vacuum oven for five minutes then sprayed with the α-naphthol solution. The reaction of SQDG with α-naphthol is irreversible; therefore this reagent would only be used for a qualitative purpose. The color of the lipid bands varied with treatment temperatures and concentration of sulfuric acid. The SQDG band was dark blue or black if the plate was over-sprayed or heated too long.

Phospholipids and SQDG were also identified from light-brown bands when the TLC plate was stained quickly with iodine vapor [22, 43]. This qualitative method of

SQDG was based on the reaction of iodine with unsaturated compounds. It was reversible and there was no effect on the SQDG band, if the contact time was short. The SQDG band was scraped off the TLC plates for further quantitative analysis.

GC Analysis – The collected SQDG band from the TLC plate was derivatized into methyl ester of fatty acids (FAME) for GC analysis. The SQDG sample and 5 μg of myristic acid, an internal standard, were placed in a glass tube, sealed with a Teflon cap and allowed to react with one ml of 1.0 N HCl in methanol at 80 °C for 40 min. Then, the mixture was cooled down, and the FAMEs were extracted into hexane, using 1 ml of hexane and 1ml of sodium chloride 0.09 wt.%.

Gas chromatography was performed at the same condition as described in chapter 2. Results showed that the major FAMEs derivatized from SQDG of alfalfa were palmitate (~ 48 wt.%) and linolenate (~ 42 wt.%), assuming the same GC response factors for all methyl esters including myristate. The C 18:1 (~7 wt.%) and C 18:2 (~3 wt.%) were also found in gas chromatograms, but they were not well recognized in the literature, therefore calculating yield of SQDG only included C 16:0 and C 18:3 contents.

Example of calculation – In the extraction using toluene-methanol (2.09: 1 v/v),

Alfalfa = 4.95 g, total solvent used = 24.7 ml, total dry extract = 0.043 g

TLC sample size = 0.006 g, amount of myristic acid used in GC sample = 5 μg

GC peak areas: C 14:0 = 578.4, C 16: 0 = 1264, C 18: 3 = 855.8

FAME of C 16:0, Mw =256, FAME of C 18:3, Mw = 278

If both R_1 and R_2 of Figure 1.3 are C 16:0, Mw of SQDG = 794

If R_1 is C 16:0 and R_2 is C 18:3, Mw of SQDG = 816

$$\text{Total C16:0 from extraction} = 5\mu g * \frac{1264}{578.4} * \frac{0.043}{0.006} = 54\mu g$$

$$\text{Total C18:3 from extraction} = 5\mu g * \frac{855.8}{578.4} * \frac{0.043}{0.006} = 27.9\mu g$$

$$\text{Total SQDG} = 0.5\mu g * 794\left(\frac{54}{256} - \frac{27.9}{278}\right) + 816 * \frac{27.9}{278} = 125.8\mu g$$

$$\text{Yield} = \frac{125.8}{4.95} = 25.4\frac{\mu g\ SQDG}{1g\ \text{alfalfa}}$$

FAB-MS Analysis – The TLC band which was identified as SQDG using iodine vapor in the extraction with ethyl acetate was also analyzed by Fast Atom Bombardment Tandem Mass Spectrometry (FAB-MS).

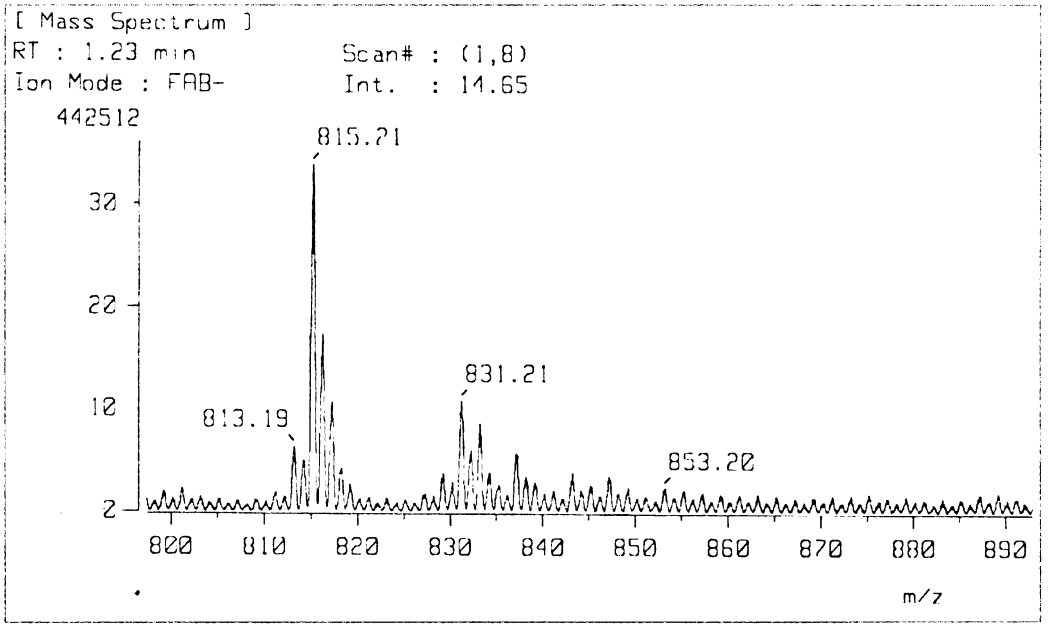

Figure 3.1 FAB-MS Chromatogram of SQDG Sample

Using a similar condition as described by Gage et al. [44], the predominant molecular species $[M-H]^-$ was found at m/z 815 (Figure 3.1). This molecular species fits

the structure of SQDG with palmitic (C 16:0) at *sn*-1 and linolenic (C 18:3) at *sn*-2 positions as described in the literature for alfalfa [11-13].

3.2.6 – Results and Discussion

Results of extractions given in Table 3-3 clearly show that SQDG can be extracted from alfalfa using any solvent systems listed in Table 3-2. The deviation in the reported yield is relatively large, due to the error in weighing small amounts of *dry extracts* and the incidental loss of SQDG during the evaporation process. Extractions using acetone, trichloride ethylene or chloroform gave a similar yield of SQDG, which was apparently higher than that obtained from toluene and ethyl acetate. TLC analyses were used to verify that the variations in yield of SQDG were not due to the loss into the aqueous extraction phase.

Figure 3.2 describes the extraction and evaluation scheme. TLC showed that toluene, the least polar solvent (smallest δ_p), extracted the largest quantity of non-polar lipids and pigments compared to other solvents. However, a very small amount of non-glycophospholipids (polar lipids) was extracted along with SQDG in acetone. All solvent systems listed in Table 3-1 were miscible. Chloroform and trichlorolethylene have higher liquid densities than water, forming a two-liquid-phase extract before salts were added; the lower phase was organic containing the extractable lipids and the upper phase was aqueous. Conversely, the non-chlorinated solvents produced only one liquid-phase extract, and glycolipids migrated to the upper phase when salts were added. In addition, neither potassium phosphate, monobasic nor potassium chloride solution was used for acetone + methanol + formic acid systems as already mentioned. The extract was completely miscible in salt solutions. This behavior of acetone is different from the other

solvents, resulting from the high contribution of δ_h and δ_p in the Hildebrand solubility value. The highly polar carbonyl group in acetone can form H-bonds to glycolipids and solvate to potassium and phosphate monobasic or chloride ions. As further evidence of acetone's polarity, neutral lipids extracted from boar testis are insoluble in acetone at 4 °C [45].

Table 3-3 Result from Extraction Studies

Solvent	Alfalfa	Solvent used	Dry extract	SQDG analysis			Yield
				C16:0	C18:3	SQDG	μg SQDG
	(g)	(ml)	(g)	(μg)	(μg)	(μg)	(per 1g of alfalfa)
Toluene	4.95	24.7	0.043	54	28	126	25.4
Ethyl acetate	5.02	24.3	0.073	64	49	174	34.6
Trichloroethylene	4.99	24.2	0.062	157	95	386	77.4
Chloroform	5.01	36.0	0.065	166	137	463	92.4
Acetone	5.02	23.0	0.078	163	126	442	88.0

* The yield of SQDG in literature is ~ 3 % of the total extractable lipid [11]. This value is equivalent to 30-150 μg SQDG per 1g of alfalfa containing 64-68 wt.% of moisture assuming 1-5 % of alfalfa is extractable lipids [12, 46].

It has been reported that naturally occurring sulfolipase can be activated by grinding or partial degradation of plant tissue [47]. Degradation of plant tissues and/or the activation of sulfolipase in grinding alfalfa were observed from the presence of the extra bands below SQDG when acids were not used in the extraction step. More degradation was seen in extraction using non-chlorinated solvents, especially in extraction using ethyl acetate. The two-liquid phases formed in the extraction with chloroform as described may help to isolate sulfolipid from water and impede hydrolysis and lipase reactions. Increasing the use of dry ice or liquid nitrogen to keep the temperature as low as possible did not eliminate degradation, but bands from degradation products were not shown on the TLCs if formic acid or acetic acid (acid-solvent, 0.02: 1

v/v) was added to solvents. As a result, formic acid was used for most studied cases. Formic acid has a lower boiling point than acetic acid and was easier to remove from the extract using evaporation. In addition, formic acid has been used as a fixative to penetrate the tissue and inactivate the phospholypase [48].

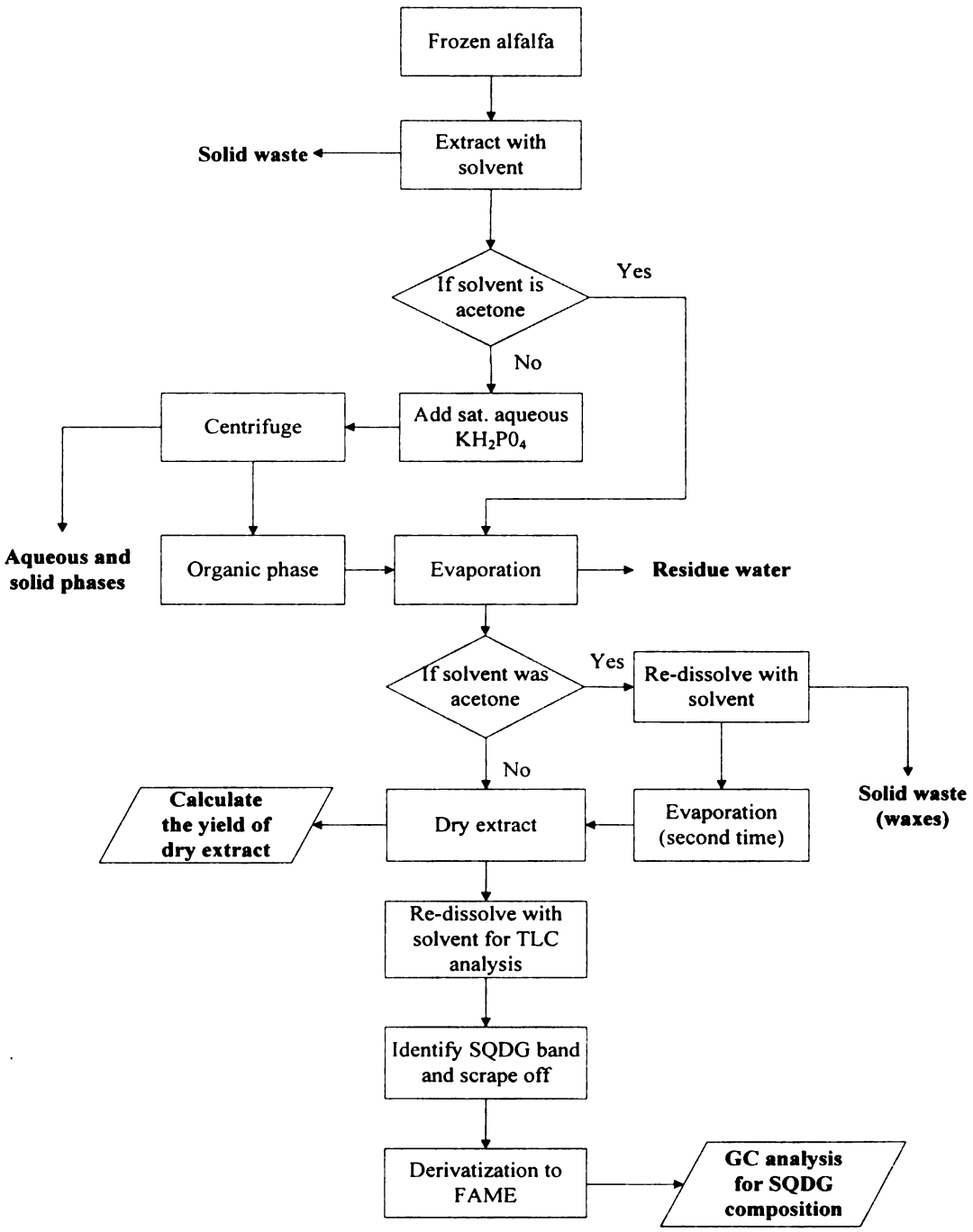

Figure 3.2 Extraction and Evaluation Scheme in Extraction Studies

3.2.7 – Improved Extraction and Coarse Fractionation

Further studies were conducted aimed at either reducing the excessive non-polar lipids, chlorophyll, and pigments in extraction; or efficiently removing them from the extract in phase partitioning. First, extractions were performed using only methanol or acetone. It was found that an insignificant amount of SQDG could be extracted in acetone alone, and no SQDG was extracted using pure methanol. Therefore, extractions were carried out using isopropanol, which has the Hansen hydrogen bonding parameter between the parameters of methanol and acetone. At room temperature, the extract was viscous but it contained SQDG. Assuming the viscosity of extract was due to the low solubility of proteins and non-lipids in isopropanol, extractions were repeated using hot isopropanol. Results showed no extra TLC bands related to degradation of lipids, and a complete extraction could be obtained using hot isopropanol, followed by hexane-methanol (3:5 v/v). No lipids from the residue of extraction with hexane-methanol could further be extracted in chloroform-methanol (2:1 v/v). This indicated the completion of the above extraction using hot isopropanol and hexane-methanol, while simultaneously eliminating lipid degradation.

To improve the coarse fractionation, liquid-liquid partitioning to remove non-polar lipids from the extract was evaluated. When hexane was added together with K_2HPO_4 solution to the extract of alfalfa in acetone + methanol + formic acid (1: 2.04: 0.1 v/v/v), the extract became three phases: the rich pigments and chlorophyll phase was in the top, all extractable lipids including SQDG were in the middle, and solids were in the bottom. Similar results were obtained when replacing acetone with ethyl acetate and hexane by pentane, but SQDG was present in both the top and middle phases.

In a preliminary study to explore options for coarse fractionation, adsorption of the extracts using silica gel [112926-00-8, 150 Å pore] and activated carbon F-400 [7440-44-0] were also studied. Results showed that chlorophyll and pigments were poorly adsorbed onto silica gel, but they could be removed from the extract using activated carbon.

3.3 – Stage (2) – Purification Studies

The *dry extract* was redissolved in solvent for the purification stage of the process. The objective of this work was to find a replacement for chloroform used by Benson [11]. Since acetone-methanol successfully extracted SQDG from alfalfa, the mixture was used as the base solvent in purification studies. First, SQDG, DGDG, and MGDG were separated from pigments, non-polar lipids and phospholipids using Florisil. Then, SQDG was isolated from DGDG and MGDG using DEAE-cellulose ion-exchanger. These adsorption and ion-exchange processes were monitored by TLC as described earlier. Studies were conducted using 5 g basis of alfalfa in extractions.

3.3.1 – Adsorption using Florisil

Experimental procedure – Similar to the procedure described in literature [11], 10 g of Florisil adsorbent (~12 ml in volume) was wetted in methanol, slurry packed into a glass column (50-ml burette, 1.1 cm ID x 64 cm), and washed with 100 ml of methanol followed by 50 ml of acetone. Then, the *dry extract* obtained from a complete evaporation was re-dissolved in acetone-methanol (2:1 v/v) and loaded to the prepared Florisil column. The liquid level in the column was always kept at 0.5 cm above the Florisil and flow rate of solvents through the column was about 2 ml/min.

Results and Discussion – Hexane and acetone-methanol at different gradients were used to elute lipids from the Florisil column. Hexane is a non-polar solvent; selected for elution of chlorophyll and pigments, based on extraction studies showing that toluene (low δ_p) extracted more non-polar lipids than acetone and ethyl acetate. The selection of acetone was based on the observation that phospholipids were sparingly soluble in this solvent, and also because it gave a similar yield of SQDG compared to the yield of extraction using chloroform.

Figure 3.3 illustrates the adsorption scheme giving the best separation of SQDG using Florisil. The elution started with 20 ml of hexane, followed by 22 ml of acetone-methanol (10:1 v/v) and 20 ml of acetone-methanol (2:1 v/v). As expected, the majority of pigments were removed by hexane and the third fraction eluted from Florisil using acetone-methanol (2:1 v/v), was almost free of non-polar lipids.

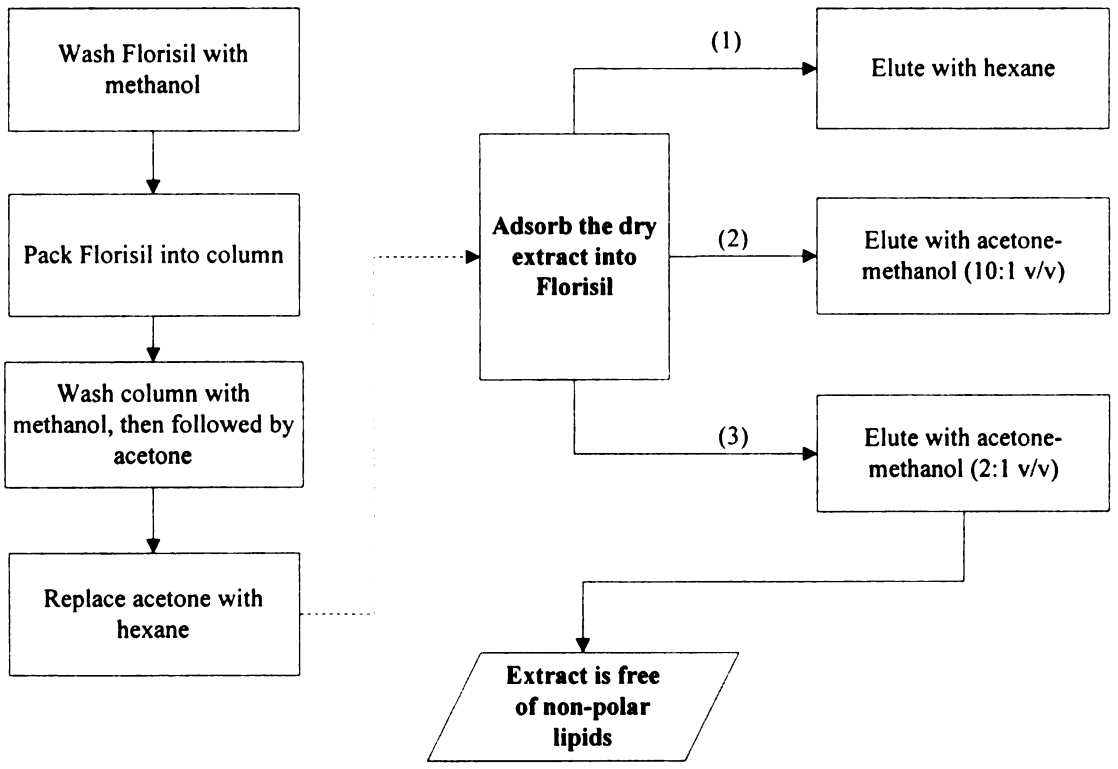

Figure 3.3 Adsorption Using Florisil in Purification Studies

3.3.2 – Ion-exchange Chromatography Using DEAE-cellulose

Experimental procedure – 10 g of DEAE-cellulose was washed and packed into a custom-made column (0.8 cm-ID x 40 cm) using 50 ml of methanol and 50 ml of acetone as described for the Florisil column. Following acetone, 100 ml of glacial acetic acid was used to wash and exchange the DEAE-cellulose to the acetate form. The column was allowed to stand overnight before the glacial acetic acid was removed using 100 ml of methanol and followed by 100 ml of acetone.

The extract, relatively free of non-polar lipids from Florisil was loaded to the pretreated DEAE column. Similar to the procedure used in Florisil adsorption, studies were performed using different solvents to remove non-SQDG from the extract.

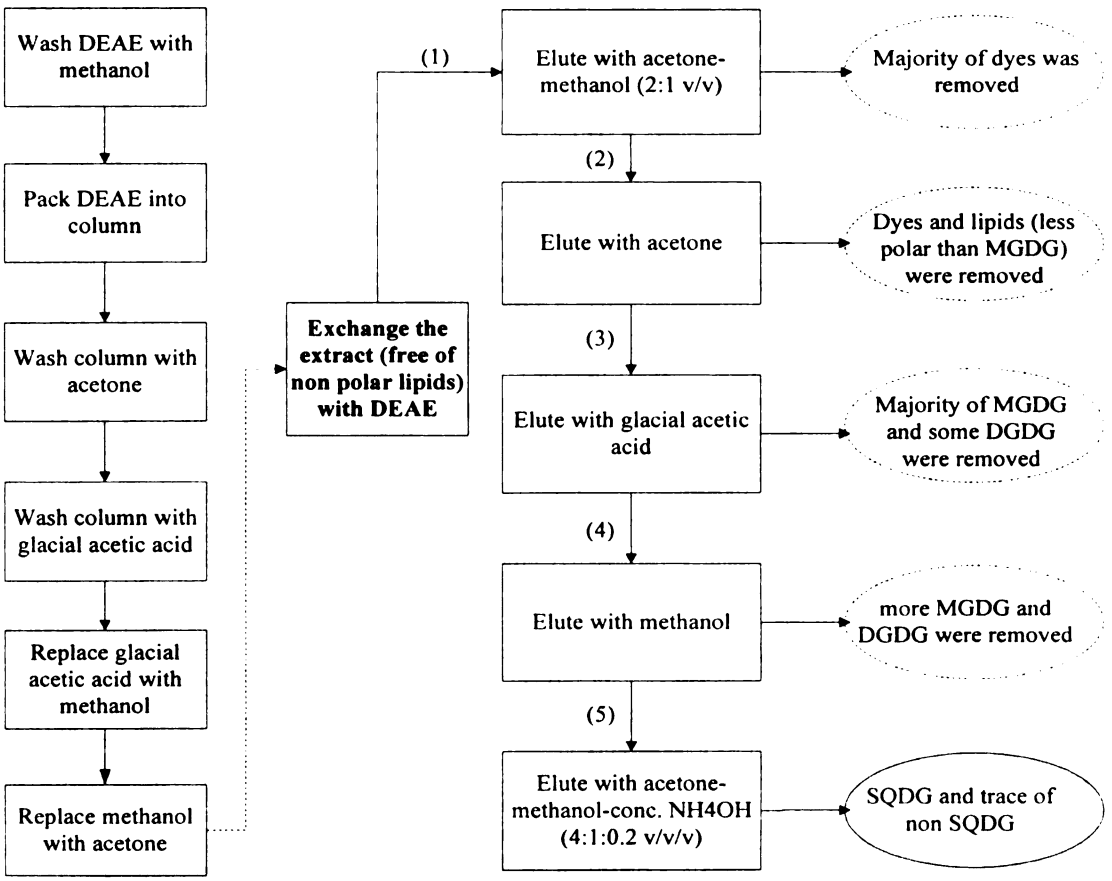

Figure 3.4 Ion-Exchange Using DEAE in Purification Studies

Results and Discussion – The best scheme and result from ion-exchange DEAE-cellulose column is shown in Figure 3.4. For 5 g basis of alfalfa, the first elution used 135 ml of acetone-methanol (2:1 v/v), each elution in the next three steps used 100 ml of the selected solvent, and the last step used 52 ml of acetone-methanol-ammonium hydroxide mixture.

The final effluent from the DEAE column contained mainly SQDG, but ammonium acetate and a small amount of DGDG were also present. The ammonium acetate can be removed from SQDG using the O'Brien [49] dialysis method. In this study, it was eliminated with liquid-liquid partioning using hexane-methanol-water (6:3:1 v/v/v).

3.4 – A proposed Extraction and Purification Scheme

Results from the above studies verified that extraction of SQDG from alfalfa can be done using non-chlorinated solvents. The degradation of extracts can be controlled using hot isopropanol. Non-polar lipids can be removed from the extract using adsorption with activated carbon or phase partitioning with hexane and K_2HPO_4. Phospholipids can be adsorbed onto Florisil or eliminated simultaneously with proteins and water in liquid-liquid partitioning with hexane-methanol-water mixture.

Adsorptions with Florisil or activated carbon require a complete removal of water. To avoid the energy costs involved in the evaporation of water, liquid-liquid partitioning should be used where possible. Therefore, an efficient extraction and purification of SQDG can be done as described here:

I. Enzyme deactivation: Prior to grinding, alfalfa is allowed to contact and partially extracted with preheated isopropanol at 50-55 °C for 5 min.

II. Extraction: The same extraction procedure described in section 3.2.4 should be applied except that the solvent system described in that section is replaced with hexane-methanol (3:5 v/v). No salt is needed, and the extract is filtered out to remove solids and residues.

III. Evaporation: Evaporating as described in section 3.2.4 to remove about 90 vol. % of liquid from the extract and obtain the *wet-extract*. The evaporation is complete if the level of liquid in the evaporator remains the same for five minutes.

IV. Proteins and phospholipids removal: The *wet-extract* is blended with hexane-methanol-water (6:3:1 v/v/v). First, only methanol and hexane are used assuming all liquid remaining in the *wet-extract* is water. Enough hexane-methanol-water mixture is added to completely dissolve and separate the *wet-extract* into two liquid phases. Proteins and most of phospholipids are discarded from the bottom phase. The rich hexane phase containing SQDG is collected and evaporated to dryness.

V. Exchange SQDG with DEAE-cellulose: The DEAE-cellulose is prepared as described in section 3.3.2. The *dry-extract* from step IV is re-dissolved in acetone (2:1 v/v) and loaded to the DEAE column. Elution starts with acetone-methanol (1:1 v/v) to remove chlorophyll, pigments and neutral lipids. Then solvent is changed to isopropanol-acetone-methanol (3:2:5 v/v/v) to elute polar-non SQDG lipids.

VI. Recovery of SQDG: SQDG retained in the column is eluted using isopropanol-methanol-ammonium hydroxide (5:5:1 v/v/v). The trace of PI and ammonium acetate is removed from SQDG using hexane-methanol-water (6:3:1 v/v/v).

Results and strategies of the proposed method are shown in Figures 3.5 and 3.6.

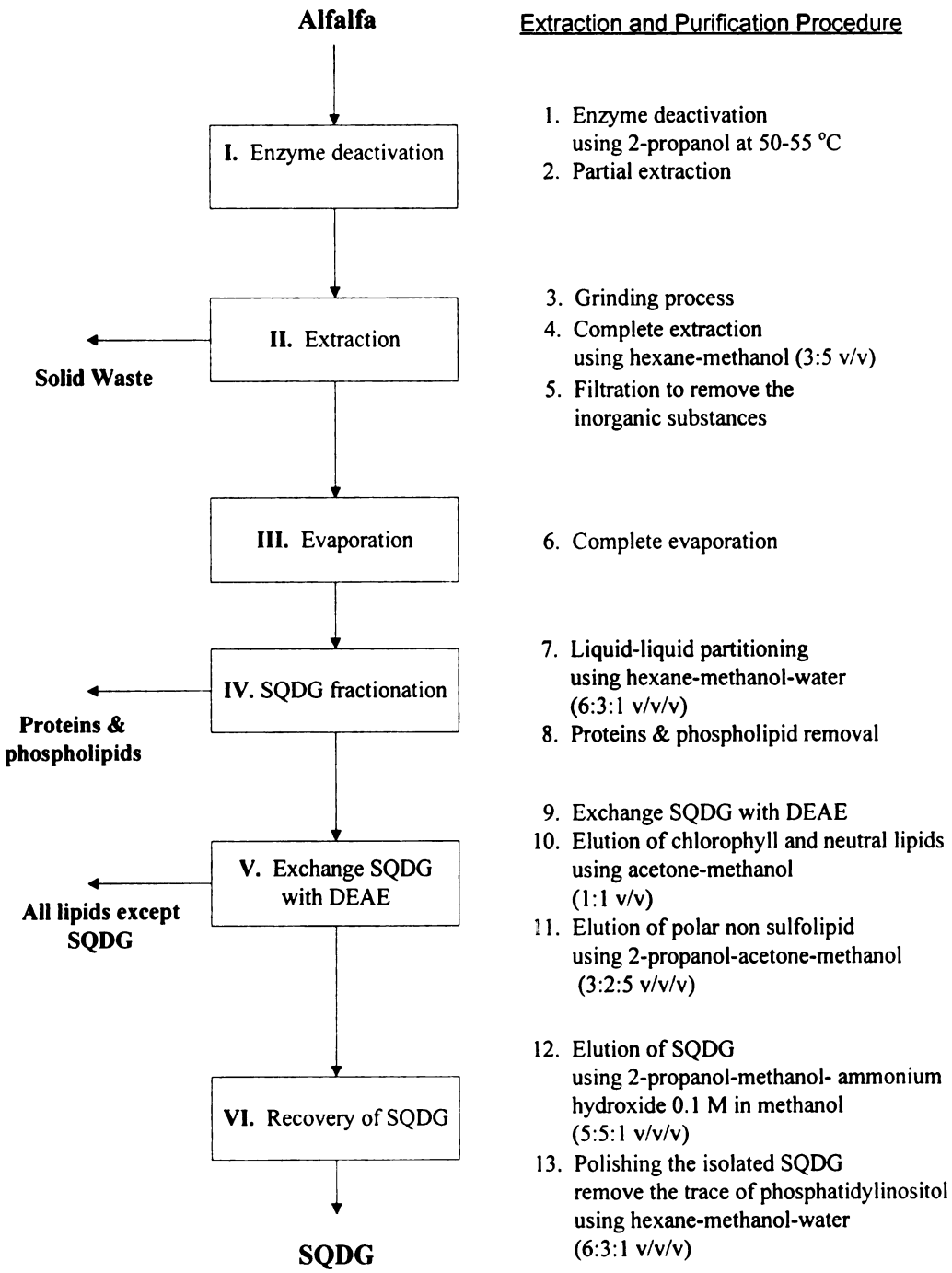

Figure 3.5 A Proposed Extraction and Purification Scheme

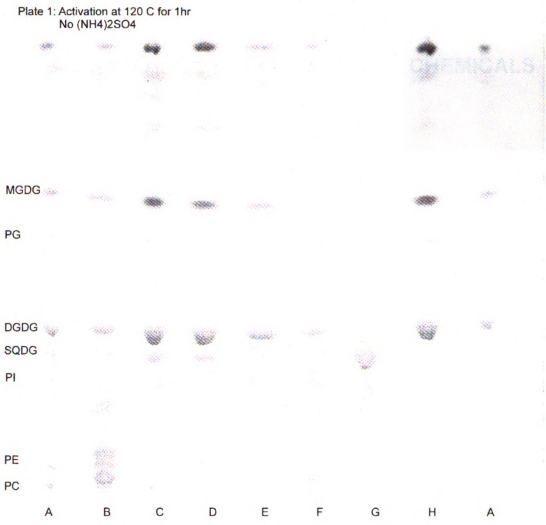

Figure 3.6 Result of Extraction and Purification of SQDG

A – Crude extract obtained by the published method using chlorinated solvents [11].

B – Crude extract obtained in this work prior to step IV described in the proposed scheme.

C, D – After step IV to remove proteins and phospholipids. Path C is after one partitioning, path D is after two partionings.

E, F – Samples from step 11, prior to step 12.

G – Final purified product after step 13.

H – Combination of by-products demonstrating no loss of SQDG.

PART 2:

PROPERTIES OF PLANT-DERIVED CHEMICALS

Chapter 4 – Phase Equilibria and Vapor Pressure

4.1 – Vapor-Liquid Equilibrium Overview

Phase equilibria, particularly the vapor-liquid equilibrium (VLE) are the foundation for a variety of separation methods used in the chemical and petrochemical industries. Separations including simple distillation, azeotropic distillation, reactive distillation, and flash operation cannot be designed and operated efficiently without knowing VLE of the related components in the mixture.

Since the 1970s, many international projects aimed to provide good thermodynamic properties including VLE of pure chemicals, mixtures, and polymers. These projects were sponsored by the Society of Chemical Engineering and Biotechnology (DECHEMA) in Germany, Physical Properties Data Service (PPDS) in the United Kingdom, the Union of Japanese Scientists and Engineers (JUSE) in Japan, and The Design Institute for Physical Property (DIPPR) in the United States [50]. Thermodynamic data for many generic chemicals have become available, but that still cannot entirely satisfy the needs of good experimental VLE data for all chemical process designs. Results from simulations of a distillation depend not only on the thermodynamic model used, but also on the quality of the VLE data.

4.2 – Vapor-Liquid Equilibrium Apparatuses and Measurements

The VLE measurements can be performed at isothermal *(P-x-y: Pressure-liquid and/or vapor compositions)* or isobaric condition *(T-x-y: Temperature-liquid and/or vapor compositions)* depending on the type of VLE apparatus and physical properties of the studied substances. In general, isothermal VLE measurements are performed at low

temperature and more suitable for thermally labile and reactive substances. Also, the possibility of liquid entrainment in the vapor phase is small and there is no concern of superheating of liquid phase at the isothermal condition. In addition, the isothermal VLE data are more easily executed and interpreted, because the measurable variables are directly related to the basic equation of vapor liquid equilibrium: $\gamma_i x_i f_i = \phi_i y_i P$ and f_i is constant across the composition range.

The VLE apparatus is either *static* or *dynamic*, based on how the mixture equilibrated. If the apparatus provides a circulation to liquid, vapor or both phases, it is called the dynamic type, otherwise it is static [51]. In a static apparatus, a fixed overall composition of degassed components is volumetrically or gravimetrically added to a vessel, and the mixture is agitated using an internal stirrer to accelerate the attainment of equilibration. In a dynamic apparatus such as the Fischer still, the studied vapor and liquid phases are disengaged, sampled and recirculated.

The VLE experimental method can be either non-analytical or synthetic. The method is called non-analytical if the phase compositions are pre-determined from pure components and mass calculations. In the analytical method, Gas Chromatograph (GC) and High Pressure Liquid Chromatograph (HPLC) are conventional techniques used to obtain the phase compositions. Complete details of the apparatus and techniques used in the VLE measurements are referred to Hala et al. [52] and Abbot [53].

4.3 – VLE of Pure components and Vapor Pressure Predictions

The VLE of pure compound occurs at its vapor pressure. For many years, scientists and engineers have been seeking reliable methods to estimate the vapor pressure when experimental data are not available. Basically, two different approaches

have been used, either through derivation of the Clausius-Clapeyron equation or through group contribution approaches. The group contribution methods are usually based on the UNIFAC groups, and the methods of predicting vapor pressure using the Clausius-Clapeyron equation commonly require the critical properties, the heat of vaporization and/or the vapor pressure at some reference temperature.

Numerous equations and correlations for the estimation of vapor pressure are reported in the literature [54]. Most of the estimation and correlation methods are only accurate for specific classes of compounds in small ranges of temperature [55-57]. For example, the correlation that has been reported by Chiou and Freed [55] is only valid for aromatic hydrocarbons, organo halogens, aliphatic alcohols, aliphatic acids and chlorinated phenols at 25 °C. The following equations in the next sections have been reported to be the most suitable for use in the largest range of chemicals and vapor pressures.

4.3.1 – Estimation Using the Clausius-Clapeyron Equation

In most cases, the basic equations are derived from integration of the Clausius-Clapeyron equation as follows:

$$\frac{d \ln P_{vp}}{dT} = \frac{\Delta H_v}{\Delta Z \, RT^2} \tag{4.1}$$

Different expressions of vapor pressure (P_{vp}) can be obtained from Eqn. 4.1, depending on the consideration of heat vaporization (ΔH_v) and compressibility (ΔZ).

4.3.1.1 – Assuming that ΔHv/ΔZ is Constant

Re-arranging Eqn. 4.1:

$$d \ln P_{vp} = \frac{\Delta H_v}{R \Delta Z} \left[\frac{dT}{T^2} \right] \tag{4.2}$$

By taking the integral, Eqn 4.2 can be presented in the simplest form as follows:

$$\ln P_{vp} = A_1 - \frac{B_1}{T} \tag{4.3}$$

Using the Antoine equation in the general form that permits representation of curvature in lnP vs. 1/T:

$$\ln P_{vp} = A_2 - \frac{B_2}{T - C_2} \tag{4.4}$$

At the normal boiling point, T = T_b, P_{vp}= 1 atm, or lnP_{vp}= 0, then,

$$A_2 = \frac{B_2}{T_b - C_2} \qquad \text{and} \quad B_2 = \frac{\Delta H_{vb}}{\Delta Z_b \ RT_b^2} (T_b - C_2)^2$$

Eqn 4.4 in a complete form is:

$$\ln P_{vp} = \frac{\Delta H_{vb} (T_b - C_2)^2}{\Delta Z_b \ RT_b^2} \left[\frac{1}{(T_b - C_2)} - \frac{1}{(T - C_2)} \right] \tag{4.5}$$

where P_{vp} is in atm, and ΔZ_b is assumed to be 0.97 [58]. The constant C_2 is estimated, using the Thomson's rule [59] as shown below:

$$C_2 = -18 + 0.19 T_b \tag{4.6}$$

The heat of vaporization at boiling point ΔH_{vb} is evaluated by Fishtine [60], using the modified Kistiakovskii [61] equation as follows:

$$\frac{\Delta H_{vb}}{T_b} = \Delta S_{vb} = K_F (8.75 + R \ln T_b) \tag{4.7}$$

where K_F = 1+ $2\mu/100$, and μ is the dipole moment of molecule. Most of dipole moments fall in the range of 0 to 5 Debye units. The methods of calculating μ are referred to Nelken and Birkett [62].

4.3.1.2 – Using ΔHv/ΔZ Temperature Dependence

The temperature dependence of ΔH_v is considered using a modification of the Watson [63] correlation, as described below:

$$\Delta H_v = \Delta H_{vb}\left(\frac{1-T/T_c}{1-T_b/T_c}\right)^m \tag{4.8}$$

Eqn 4.8 contains the critical temperature (T_c). It has been reported that the ratio T_c/T_b varies from 1.3 to 1.7 for most organic compounds. Therefore, an estimation of $T_c \approx 1.5T_b$ is used, and the derivation of Clausius Clapeyron equation yields:

$$\ln P_{vp} \approx \frac{\Delta H_{vb}}{\Delta Z_b R T_b}\left[1-\frac{(3-2(T/T_b))^m}{(T/T_b)}-2m(3-2(T/T_b))^{m-1}\ln(T/T_b)\right] \tag{4.9}$$

where m = 0.19 is recommended for all liquids.

4.3.1.3 – The Korsten Correlation

Korsten discovered that vapor pressures of homologous compounds converge at a common point (α), and logarithm of vapor pressure (*lnP*) of any chemicals is linear to $(1/T)^{1.30}$ [64]. For example, the common (α) for all the hydrocarbons is (T_α =1994.49 °K, P_α =1867.68 bar). The temperature T_α is the upper limit temperature for vapor pressure, which cannot be exceeded by any component [64].

Substituting (P_α T_α) into Eqn (4.9) yields:

$$\ln P = \ln P_\alpha + B\left(\frac{1}{T^{1.30}}-\frac{1}{T_\alpha^{1.30}}\right) \tag{4.10}$$

The constant *B*, slope of vapor curve in Eqn 4.10, is a characteristic of each component. It is a linear function to molecular weight $M^{0.65}$ within each homologous series. The calculation of *B* and its applications are described by Korsten [64].

4.3.1.4 – Summary of Methods Using the Clausius-Clayperon Equation

The average and maximum errors using the Antoine equation and the modified Watson correlation are summarized in Table 4-1, as shown below. These equations require the values of heat of vaporization and normal boiling point temperature for estimating vapor pressure. The analytical form of vapor pressure is more complex for the temperature dependence of ΔH_v, but the estimation in the range of 10 – 760 mmHg is as accurate as that obtained from a method considering $\Delta H_v/\Delta Z$ as the constant. Both methods predict pressure of gases and liquids limited to 10-760 mmHg with ~ 3% error.

Table 4-1 Errors in Estimating P^{sat} Using the Clausius-Clayperon Equation [54]

Pressure	$\Delta H_v/\Delta Z$ is Constant		$\Delta H_v/\Delta Z$ is Temp. Dependent	
(mmHg)	Average Error (%)	Maximum Error (%)	Average Error (%)	Maximum Error (%)
10 - 760	2.7	6.6	2.5	7.1
10^{-3} - 10	86	100	39	50
10^{-7} - 10^{-3}	Method is not available		47	200

Estimations at low pressures are inaccurate with very large average errors. The average error in estimating vapor pressure using the Clausius-Clapeyron equation can exceed 35% when the boiling point temperature and heat of vaporization are known. If boiling point temperature and heat of vaporization are estimated, the deviation average can be higher than 80%. Error is expected to increase with complexity of molecular structures and low vapor pressures. Reid et al. state that none of the vapor equations in the literature are suitable for estimating the vapor pressure below 10 mmHg within a 10% deviation from the experimental data [56].

Predicting vapor pressure using the Korsten equation requires reliable vapor data of other members of the same homologous series to determine the common point, but data of the homologous series are not always available. However, the linear correlation of molecular weight $M^{0.65}$ and vapor pressure, described by Korsten, can be used to improve the prediction of vapor pressure from the other methods, and Eqn 4.10 can also be used to validate the prediction.

4.3.2 – Highlights of Prediction Methods using Group Contribution

In contrast to molecular structure methods, there is very little literature available for the group contribution methods, which have been commonly based on UNIFAC groups. A typical example of this method is the work of Fredenslund et al. [65, 66].

Predicting vapor pressure based on the group contribution has proved to be a very difficult challenge [67], usually dependent on first estimating critical properties. The deviation has been noted to be very large in predicting vapor pressures using group contribution methods, and it is expected to increase with molecular complexity. Bureau et al. [68] performed the evaluation for seven esters and found deviations averaging near 80% using UNIFAC groups. Similarly, Asher et al. [69] reported deviations averaging near 300% for 76 multi-functional oxygen-containing organic compounds at temperatures of 290-320 ^{o}K. The large deviations in the oxygen-containing compounds indicate the difficult challenges in predicting vapor pressure of esters and acids, which usually form the intra and/or intermolecular hydrogen bonds between molecules.

The indirect approach using a group contribution such as the Constantinous-Gani [70] or Joback [71] with the Clausius-Clapeyron equation also is reported with high deviations in estimating vapor pressure. For example, Ashler et al. [69] reported

deviations averaging near 900% using Joback method and the modified Lee-Kesler equation, for the same data set used in UNIFAC validation.

The ASPEN simulation software usually estimates parameters for the extended Antoine vapor pressure equation through a group contribution, developed by Juan-Carlos Mani of ASPEN [72]. The Mani method uses Riedel's equation [73] to estimate normal boiling point and critical temperatures while Gani's method is used to obtain critical pressures. The Gani [70] method has been reported to be applicable up to the critical temperature, and more accurate than Joback, Lydersen and Ambrose methods [74]. The Mani method accurately correlates vapor pressure curves if some experimental vapor pressure data values are available [75]. However, ASPEN predicted that pressure curves of lactic and di-lactic acids intersect below their critical temperatures; between 493 °K and 503 °K (Table 2.) This vapor pressures contradict the Korsten observation that the common point temperature cannot be exceeded by any component vapor pressure in a homologous series at any pressure [64].

Table 4-2 ASPEN Predicted P^{sat} of Lactic Acid and di-Lactic Acid

Temp (°K)	Lactic acid (kPa)	Di-lactic acid (kPa)	Temp (°K)	Lactic acid (kPa)	Di-lactic acid (kPa)
273	1.51E-05	0.0002	503	153	151
323	0.0073	0.0256	513	204	197
373	0.4350	0.8157	540	420	381
423	7.419	9.801	570	848	727
473	57.65	61.98	600	1581	1289
483	81.19	84.63	660*	4648*	3481
493	112.27	113.74	675*	N/A	4369*

**estimated* critical pressures and temperatures of corresponding components.

The advantage of using the contribution method is that it does not require any experimental data. However, this method in particular is not reliable for multi-functional oxygen containing compounds due to the large error in estimation.

4.4 – Background on Step Potential Equilibria And Dynamics Simulation

In the near future, a possible breakthrough in predicting thermophysical properties of fluids may be realized using molecular simulation. This technology should provide excellent efficiency and accuracy in prediction because molecules are examined at molecular level and state conditions [76]. However, the application of molecular simulation has not been greatly recognized in the industry due to the lack of reliable comparison studies and validation of different methods. To emphasize the capability of utilizing the molecular simulation in engineering correlation and process models, a contest was held in September 2004 by Case Scientific and various experts from industry. Modeling groups around the world were challenged to predict vapor pressure, heat of vaporization, the Henry's law constant, and heats of mixing using the molecular simulation method. Elliott and his co-workers from University of Akron won the first prize for prediction of vapor pressure and heat vaporization. The judges ruled that the Elliott model, SPEAD, is 50 times faster than more conventional molecular simulations [77].

SPEAD is acronym of the Step Potential Equilibria and Dynamics simulation. SPEAD is based on the discontinuous molecular dynamics (DMD) simulation and the thermodynamic perturbation theory (TPT). It is in development by Elliott et al. and is being implemented by ChemStations, Inc. as a physical properties standard model in chemical process simulation [78, 79].

4.4.1 – SPEAD and Discontinuous Molecular Dynamics Algorithm

In the discontinuous molecular dynamics (DMD) simulation, *step potential* refers to the description of molecular interaction energies by a series of discrete steps. The simplest form of a step potential is square-well potential, described below:

$$u_{ij} = \begin{cases} +\infty, & r < \sigma \\ -\varepsilon, & \sigma < r < \lambda\sigma \\ 0, & r > \lambda\sigma \end{cases} \tag{4.11}$$

where u_{ij} is potential function, σ is collision diameter, ε is well depth, and λ is the potential well width.

The square-well potential model has been one of the most commonly considered for computer simulation and statistical mechanical methods, because of its mathematical simplicity [80]. However, research has shown that the simple square-well (one-step) potential model offers limited capacity to characterize the experimental data, which measured physical properties; and the same square-well potential model cannot be transferred to the homologous molecules. On the other hand, the Lennard-Jones [80] potential is more favorable for transferability, and a discrete Lennard-Jones potential can provide properties that are similar to the continuous potential for spheres [81].

To improve the transferability that the one-step square-well potential model cannot provide, the SPEAD method proposes a multi-step united-atom potential for the attractive potentials. This approach is based on the hypothesis that a more transferable discontinuous potential model could be obtained by adding steps of diminishing depth. The attractive potential is divided into an infinite series of wells, with each well width small enough so the energy of each step can be treated as a constant. The SPEAD currently has four step-wells, separated at r/σ = 1.2, 1.5, 1.8, 2.0, shown in Figure 4.1.

SPEAD estimates vapor pressures of hydrocarbons including aromatic hydrocarbons, the low molecular ethers and alcohols, and simple esters with error of less than 10% of the experimental values [78]. In these evaluations, the reduced temperatures are used in the range of 0.45 to 1.0. Results show that the DMD method coupling with the application of TPT theory used in SPEAD, provided an accuracy superior to the published studies using Lennard-Jones model for characterization of vapor pressure. The most accurate prediction of vapor pressure using the transferable Lennard-Jones alternative model has ~15% error of the experimental data, reported by Fuchs et al. However, the Lennard-Jones study is limited in the component types and temperature ranges [82, 83].

SPEAD is a functional group approach applied to molecular simulation. Molecules are broken into a number of interaction sites for computing the dynamics in SPEAD simulation. For example, n-pentane is broken into 2CH3 sites and 3CH2 sites. Each of these united-atom sites is described by a spherical multi-step potential. The interaction sites together form a bonded molecule. All sites are allowed to freely vibrate within their bond wells, and multiple bond wells are used to constrain bond angles. For example, n-pentane is formed by tethering the sites together with wells centered 0.154 nm for adjacent sites. Additional pseudo-bond wells are centered at 0.265 nm for sites two bonds away, confining the C-C-C bond angle to ~110 degrees. To simulate cis-butene, the additional pseudo well is added between the sites that are three bonds distant [78]. Simulations are conducted using infinite wells to represent bonds and pseudo-bonds, and hard cores to represent collisions. Each interaction behaves like independent hard sphere between collisions and changes velocities instantly at collision time, and the

energy of interaction at each distance is described using the potential functions. The NVE simulations (number of molecules, volume, and energy are constant) and Newton's law of motion is applied to molecular interactions.

Following the simulation, the attractive wells are superimposed using perturbation theory described in section 4.4.2. Three parameters are assigned for each interaction site type: the diameter, the depth of the inner well, and the depth of the outer well. The two intermediate wells are interpolated from the inner and the outer wells [84].

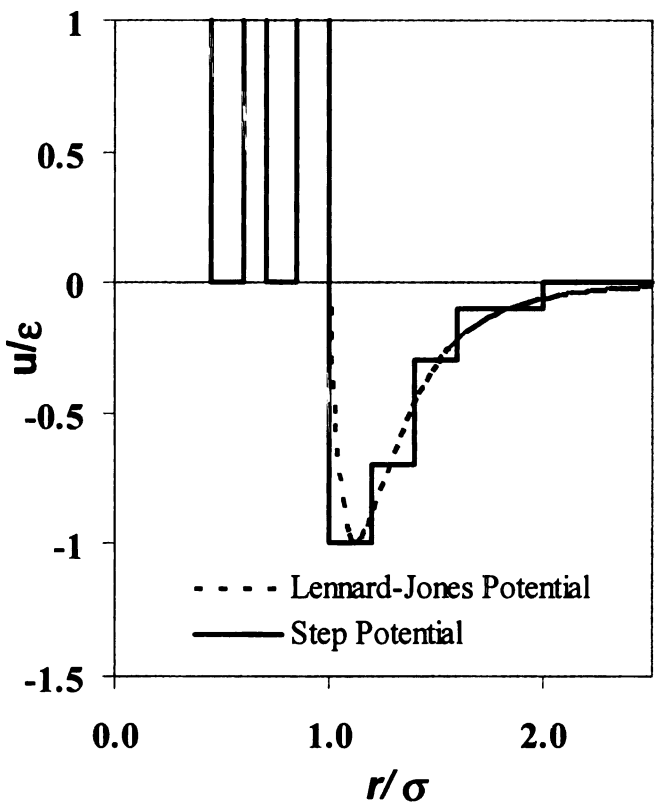

Figure 4.1 Illustration of the Multi-step Potential

4.4.2 – Thermodynamics Perturbation Theory

The thermodynamic perturbation theory is used in SPEAD to simultaneously compute thermodynamics and transport properties of fluid. Mathematically, perturbation

method involves series expansions which are called *asymptotic* expansions in terms of a *small parameter* [85]. This method is found to be very useful in solving the initial and boundary problems when the analytical solution cannot be obtained. In general, an asymptotic expansion has the following form:

$$y(x;\varepsilon) = y_0(x) + \varepsilon y_1(x) + \varepsilon^2 y_2(x) + ... + \varepsilon^n y_n(x) + \mathrm{O}^{n+1}(\varepsilon) \tag{4.12}$$

where ε is a small parameter, and n is the order of the expansion. The well depth is very small in the multi-steps attractive potential; therefore, the free Helmholtz energy can be expressed as an asymptotic expansion of well depth or pair potential energy. This becomes the key to the perturbation theory used in SPEAD. The application of TPT in SPEAD is similar to the work of Baker-Henderson [86]. Basically, it considers that strong repulsive forces play the primary roles in determining fluid structure. The properties of the fluid, therefore, can be calculated by starting with the pure repulsive part (the reference system) and later incorporating the attractive part as a perturbation [87].

Applying the second order of Eqn 4.12 to the molar Helmholtz free energy using a multi-well potential yields:

$$\frac{(A - A_{ig})_{TV}}{RT} = \frac{A_0 - A_{ig}}{RT} + \frac{A_1}{T} + \frac{A_2}{T^2} + \mathrm{O}^3(u_{ijm}) \tag{4.13}$$

where $A_1 = \dfrac{\sum_i^t \sum_j^t \sum_m^w \langle N_{ijm} \rangle_0 u_{ijm}}{N k_B}$ (4.14)

$$A_2 = -\frac{\sum_i^t \sum_j^t \sum_k^t \sum_l^t \sum_m^w \sum_n^w \left(\langle N_{ijm} N_{lkn} \rangle_0 - \langle N_{ijm} \rangle_0 \langle N_{lkn} \rangle_0 \right) u_{ijm} u_{lkn}}{2 N k_B^2} \tag{4.15}$$

In Eqns 4.13 - 4.15, N is the number of particles, and k_B is Boltzmann's constant = 1.38×10^{-23} m^2 kg s^{-2} K^{-1}, A_0 is the Helmholtz energy of the repulsive (reference) fluid. A_{ig}

is the Helmholtz energy of the ideal gas. A_1 and A_2 represent the first and second-order of perturbation terms, m means the m^{th} well, $<N_{ijm}>$ is the ensemble average of the interaction site pairs of sites of types i around sites of type j inside the m^{th} well, t designates the number of site types, w is the number of wells, N_{ijm} is obtained from the reference fluid simulation, and $\langle\ \rangle_0$ denotes an ensemble average of the reference fluid. For a two-site molecule with four wells per site, there are 16 terms in A_1 and 256 terms in A_2. The interaction between two sites or groups of type i and j in well m which is the geometric mean of the group potentials u_{iim} and u_{jjm}, defined as follows:

$$u_{ijm} = \sqrt{u_{iim} \times u_{jjm}} \tag{4.16}$$

The pair group potential energy is the asymptotic parameter, and temperature is specified in Eqn 4.13. Because the reference simulation has no attractive potential energy, the results of the simulation are independent of temperatures; any T can be selected to run the simulation.

4.4.3 – Vapor-Liquid Equilibrium using SPEAD

The thermodynamic correlation between the molar Helmholtz energy (A) and compressibility factor (Z) at constant temperature and volume (in NVE simulation) is described as follows:

$$\frac{\left(A - A_{ig}\right)_{T,V}}{RT} = \int_0^{\rho} \frac{(Z-1)\,d\rho}{\rho} \tag{4.17}$$

where R is the gas constant, V and ρ are respective molar volume and density of fluid at pressure (P) and temperature (T).

By taking the derivative then applying the fundamental theorem of calculus [88],

Eqn 4.17 becomes:

$$Z = 1 + \frac{\rho}{RT}\left[\frac{d}{d\rho}\left(A - A_{ig}\right)_{T,V}\right] \tag{4.18}$$

SPEAD uses packing fraction (η) [89], which is defined as: $\eta = \frac{N_A \rho_m V_w}{M_w}$ where ρ_m is the mass density, V_w is the mass volume, and M_w is the molecular weight. It should be noted that $\frac{\eta}{d\eta} = \frac{\rho_m}{d\rho_m} = \frac{\rho}{d\rho}$. Applying thermodynamic perturbation theory to the Helmholtz free energy in Eqn 4.18 as it is described in Eqn 4.13 yields:

$$Z = 1 + \eta\left(\frac{d(A_0 - A_{ig})}{d\eta}\right) + \eta\frac{dA_1}{d\eta}\left(\frac{1}{T}\right) + \eta\frac{dA_2}{d\eta}\left(\frac{1}{T^2}\right) = Z_o + Z_1\left(\frac{1}{T}\right) + Z_2\left(\frac{1}{T^2}\right) \tag{4.19}$$

where $Z_0 = 1 + \eta\left(\frac{d(A_0 - A_{ig})}{d\eta}\right)$, $Z_1 = \eta\frac{dA_1}{d\eta}$ and $Z_2 = \eta\frac{dA_2}{d\eta}\left(\frac{1}{T^2}\right)$. The following polynomial correlations are used to interpolate simulated results for Z_0, A_1 and A_2 in SPEAD as described below:

$$Z_0 = \frac{1 + a_1\eta + a_2\eta^2 + a_3\eta^3}{(1-\eta)^3} \tag{4.20}$$

$$A_1 = b_1\eta + b_2\eta^2 + b_3\eta^3 + b_4\eta^4 \tag{4.21}$$

$$A_2 = \frac{c_1\eta + c_2\eta^2 + c_3\eta^3 + c_4\eta^4}{1 + 500\eta^4} \tag{4.22}$$

The expression of Z_0 follows the format of Carnahan-Starling [90] equation. The coefficients of Eqn 4.20 are independent of the well depths and are obtained from regression of data provided from hard molecule simulations at 21 different packing fractions (η). The average numbers for site interactions and intermolecular site distances, provided from the simulation data, are combined with the well depths to generate A_1 and

A_2 at each simulation density using Eqns 4.14 and 4.15. To provide the continuous functions that represent the DMD/TPT calculations, the coefficients in Eqns 4.21 and 4.22 are regressed. The polynomial functions A_1 and A_2 are based on the trends of their curves, shown in Figure 4.2. Equations 4.20 – 4.22 provide the smoothed functions for differentiation of the Helmholtz energies at any density subsequently used to generate PVT information.

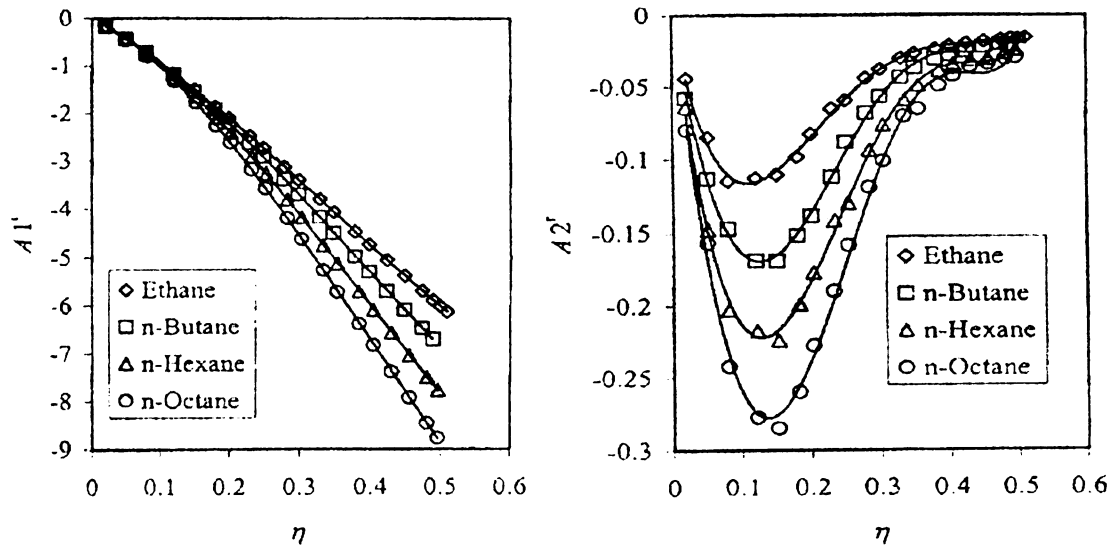

Figure 4.2 Trends of A_1 and A_2 and their Fitted Polynomials Function [84]

Phase equilibrium criteria – At phase equilibrium of any temperature (T) and pressure (P), the following constraints must be satisfied for pure fluids:

$$T^{sat} = T^V = T^L, \qquad P^{sat} = P^V = P^L, \qquad G^{sat} = G^V = G^L \tag{4.23}$$

where L and V respectively denote for liquid and vapor. The vapor pressure (P^{sat}) is determined from:

$$P^{sat} = Z^L RT^{sat}\rho^L = Z^V RT^{sat}\rho^V \tag{4.24}$$

The Helmholtz energy (A) and the Gibbs free energy (G) are related as follows:

$$\frac{\left(G-G_{ig}\right)_{T,P}}{RT}=\frac{\left(A-A_{ig}\right)_{T,V}}{RT}+Z-1-\ln(Z) \tag{4.25}$$

Combining with Eqn. 4.17, Eqn 4.25 becomes:

$$\int_0^{\eta^L}\frac{\left(Z^L-1\right)d\eta}{\eta}+Z^L-\ln Z^L=\int_0^{\eta^V}\frac{\left(Z^V-1\right)d\eta}{\eta}+Z^V-\ln Z^V \tag{4.26}$$

Algorithm in Calculating P^{sat} – Vapor pressure is calculated by the following algorithm: (1) guess P^{sat}; (2) use Eqn. 4.24 to calculate η^L and η^V; (3) use η^L and η^V and Eqns. 4.19 - 4.22 to evaluate each side of the Eqn. 4.26; (4) return to step 1 with a new guess of P^{sat} until the equality of Eqn 4.26 is obtained.

To perform parameter optimization, additional adjustments of the well parameters are included to change the values of A_1 and A_2 that are used in the vapor pressure calculation, and the P^{sat} calculations are performed repeatly to optimize the square-well potentials for individual sites.

4.5 – Objective and Scope of Research

Research on esterification to produce plant-derived esters and bio-diesel products using reactive distillation at Michigan State University has gained reputation and has been recognized with patents [91]. At present, the esters of interest are triethyl citrate, diethyl succinate, ethyl lactate. For biodiesel, acetals of glycerol are of interest. All of these oxygen-bearing compounds are relatively complex and have low vapor pressures; therefore, thermodynamic properties such as binary vapor-liquid equilibrium (VLE) data of components involved in the esterification are either very limited or not accessible in the existing literature. To develop accurate process simulation designs for reactive distillation, MSU must have the reliable phase equilibrium data.

This part of the dissertation focuses on providing substantially reliable thermodynamic properties for economical industrial process designs of reactive distillation to produce the above plant-derived esters and bio-diesel products. The measured and predicted VLE of systems involved in the esterification are presented in chapters 5 and 6, and the SPEAD predicted vapor pressures of components which are not available for direct measurements are in chapter 7.

Chapter 5 – Lactic Acid Oligomers Distribution

5.1 – Overview

Lactic acid (2-hydroxy propanoic acid) contains both hydroxy and carboxylic functional groups. Lactic acid molecules can react to form oligomers as follows [92]:

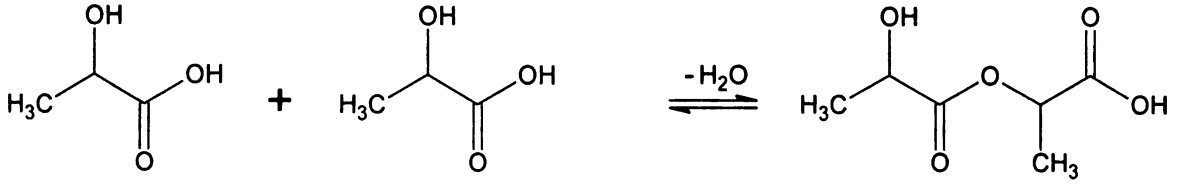

Lactic acid (LA_1) Lactoyllactic acid (LA_2)

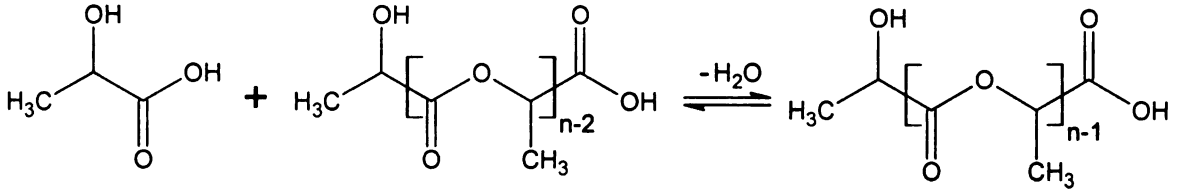

Polylactic acid (LA_{n-1}) Polylactic acid (LA_n)

As described in literature [92-95], this study verified that dilute lactic acid of less than 20 wt.% contains only lactic acid monomer (LA_1), but oligomers exist in equilibrium in concentrated aqueous lactic acid solutions. If pure crystalline lactic acid is stored at room temperature, it spontaneously initiates intermolecular reactions to form water and esters, and the equilibrium mixture is obtained after sufficient time, containing 6 wt.% of water, 47 wt.% of lactic acid monomer (LA_1) and 47 wt.% of polylactic acids of a mean degree of polymerization 2.8. Heating strongly accelerates the reaction without affecting equilibria [96, 97].

Esterification with ethanol producing ethyl lactate requires concentrated lactic acid solution to minimize the amount of water. At the temperature of the reactive distillation, lactic acid oligomers (LA_2, LA_3,..., LA_n) and ethyl lactate oligomers (E_2LA,

E_3LA,..., E_nLA) will co-exist with lactic acid monomer, ethanol, ethyl lactate, and water.

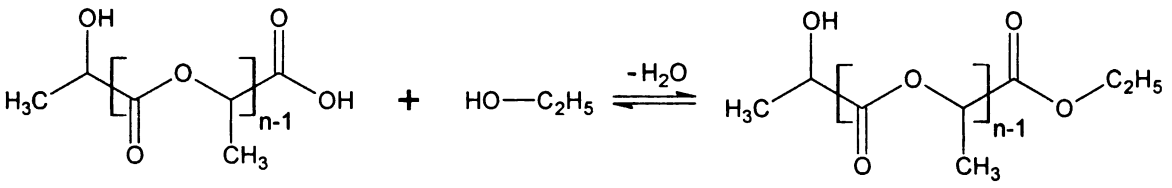

Poly lactic acid (LA_n) Poly ethyl lactate (E_nLA)

To characterize the lactic acid oligomers involved in the esterification of ethyl lactate, a thermodynamic model has been developed using the chemical theory. The model accurately predicts oligomers distribution over the full range of lactic acid concentration. The superficial total lactic acid concentration of any lactic acid solution is reliably determined using HPLC or titratable acidity.

5.2 – The Lactic Acid Oligomers Distribution Model — A Reprint of the Paper "*Oligomer Distribution in Concentrated Lactic Acid Solutions*"

Following is a copy of the paper entitled *Oligomer Distribution in Concentrated Lactic Acid Solutions* by D. T. Vu, A K. Kolah, N. S. Asthana, L. Peereboom, C.T. Lira and D. J. Miller, published in Phase Fluid Equilibria, 236 (2005) 125-135. The paper is reformatted to enlarge the text in figures and tables so that all parts of the dissertation are readable from microfilm.

Available online at www.sciencedirect.com
SCIENCE DIRECT
Fluid Phase Equilibria 236 (2005) 125-135
FLUID PHASE EQUILIBRIA
www.elsevier.com/locate/fluid

Oligomer distribution in concentrated lactic acid solutions

Dung T. Vu, Aspi K. Kolah, Navinchandra S. Asthana, Lars Peereboom, Carl T. Lira*, Dennis J. Miller

Chemical Engineering and Materials Science, Michigan State University 2527 Engineering Building, East Lansing (USA), 48824-1226

Received 21 April 2005; received in revised form 1 June 2005; accepted 3 June 2005
Available online 10 August 2005

Abstract

Lactic acid (2-hydroxypropanoic acid) is a significant platform chemical for the biorenewable economy. Concentrated aqueous solutions of lactic acid (>30 wt.%) contain a distribution of oligomers that arise via intermolecular esterification. As a result, the titratable acidity changes non-linearly with acid concentration. In this work, the oligomer distribution of lactic acid is characterized using GC, GC/MS, and HPLC to extend existing literature data, and titratable acidity is measured via titration with NaOH. A thermodynamic model with a single parameter is proposed that accurately represents oligomer distribution and titratable acidity over the full range of lactic acid concentrations.

Keywords: Lactic acid; Oligomerization; Chemical theory; Esterification; Alpha-hydroxy acid; 2-Hydroxypropionic acid

* Corresponding author. Tel.: +1 517 355 9731; fax: +1 517 432 1105.
E-mail address: lira@egr.msu.edu (C.T. Lira).

1. Introduction

In recent years, there is increasing emphasis on using biorenewable materials as substitutes for petroleum-based feedstocks. This paradigm shift is attributable to rising crude oil prices and the increasing desire to reduce dependence on petroleum. A major building block for the biorenewable economy is lactic acid (2-hydroxypropionic acid), an α-hydroxy acid containing both a hydroxyl and carboxylic acid functional group. For an excellent review on lactic acid the reader is referred to Holten [1]. Lactic acid was first isolated by the Swedish scientist Scheele in 1780 [2], and first produced commercially in 1881 [3]. Applications for lactic acid are found in the food (additive and preservative), pharmaceutical, cosmetic, textile, and leather industries. Lactic acid can be formed either via fermentation of carbohydrate monomers or via a chemical route, but since about 1990 only the fermentation route is practiced commercially. The recent completion of the NatureWorks lactic acid facility for poly-lactic acid production, with an annual capacity of 140,000 metric tonnes of polylactic acid (PLA) [4], has greatly enhanced the stature of lactic acid as a key biorenewable platform.

Polylactic acid [5] is a versatile thermoplastic polymer that has useful mechanical properties including high strength and high modulus. Applications of PLA include household commodity products, polymers used in food contact, biomedical materials like surgical sutures, absorbable bone plates for internal bone fixation, artificial skin, tissue scaffolds, and controlled release drugs. PLA is one of the few polymers whose structure and properties can be modified by polymerizing a controlled composition of the L - and D-isomers to give high molecular weight amorphous or crystalline polymers. PLA has a degradation time of 6 months to 2 years in the environment. For more details on PLA the reader is referred to Garlotta [6].

Esters of lactic acid, formed via combination with alcohols like methanol and ethanol, are finding increased use as environmentally benign solvents. Lactic acid esters are biodegradable, non-toxic, and have excellent solvent proper-ties, which make them attractive candidates to replace halogenated solvents for a wide spectrum of uses. Esterification of lactic acid with alcohol can also be used as a highly efficient method for purification of lactic acid from fermentation broths, especially when lactic acid is desired in concentrated solutions.

It has been observed experimentally that dilute (<20 wt.%) lactic acid solutions contain only lactic acid monomer (LA_1) [7], an observation that has been verified in this paper. However, many processes involving lactic acid, including polymerization and esterification, require concentrated lactic acid solutions, and lactic acid in these solutions undergoes intermolecular self-esterification to form higher oligomers. This oligomerization occurs to an increasing degree at high acid concentration, low water concentration, and high temperature.

In oligomerization, two molecules of lactic acid first react to form a linear dimer, commonly called lactoyllactic acid (LA_2), along with a mole of water.

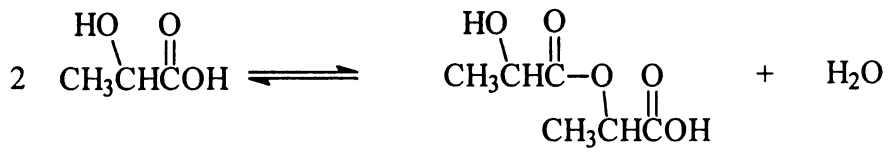

(1)

Lactic Acid (LA_1) Lactoyllactic acid (LA_2)

Lactic acid also forms a cyclic dimer noted as lactide, but this compound is known to be unstable in water [1] and thus is not a concern in this work. Lactoyllactic acid (LA_2) can further esterify

with LA_1 to form the trimer lactoyl-lactoyllactic acid (LA_3); this process can further continue to give higher chain intermolecular polyesters LA_4, LA_5 and so on.

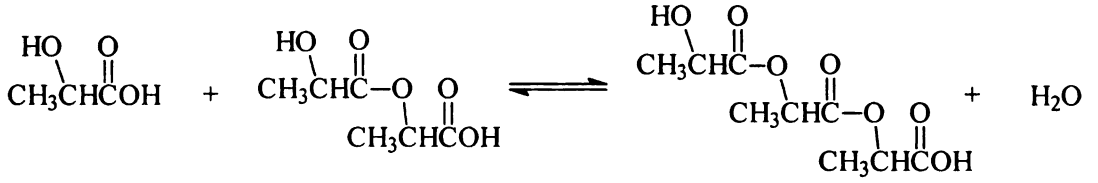

(2)

Lactoyl-lactoyllactic acid (LA_3)

The inherent tendency of aqueous lactic acid to form intermolecular esters in solution poses a formidable obstacle in the modeling of its liquid-phase behavior and vapor-liquid phase equilibria. For design of reaction and separation processes involving concentrated lactic acid solutions, a model to predict thermodynamic properties of these complex chemically reactive mixtures is an indispensable tool. This paper presents such a model that requires only one parameter to adequately represent lactic acid solution behavior over the full range of concentration.

1.1. Definition of concentrations

Experimental work on quantifying concentrations of lactic acid oligomers in aqueous solution has been previously reported by Montgomery [7], Ueda and Terashima [8], and Watson [9], but the methods used in reporting these concentrations and the definitions of concentrations are not always clearly presented. Therefore, we clearly define here the quantities used to describe the concentration of lactic acid and its oligomers in solution.

1.1.1. Equivalent monomer lactic acid

In the literature, it has been found convenient to express the concentration of lactic acid oligomers as a percent of equivalent monomer lactic acid on a water free basis. We abbreviate such a description with the acronym %EMLAj. To illustrate the concept, consider a solution consisting of 50 mol water, 9.20 mol LA_1, 0.343 mol LA_2, and 0.0128 mol LA_3. Upon hydrolysis of the oligomers, $9.20 + 2 \times 0.343 + 3 \times 0.0128 = 9.924$ mol lactic acid monomer would be present. The amount of water present would be $50 - 0.343 - 2 \times 0.0128 = 49.63$ mol H_2O. The lactic acid in the original solution is reported as $9.20 / 9.924 = 92.7\%$ EMLA LA_1, $2 \times 0.343/9.924 = 6.9\%$ EMLA LA_2, and $3 \times 0.0128 / 9.924 = 0.38\%$ EMLA LA_3. Introducing the molecular weight of water and oligomers, the solution has a total mass of $50 \times 18.02 + 9.20 \times 90.08 + 0.343 \times 162.14 + 0.0128 \times 234.21 = 1788.3$ g.

1.1.2. Superficial weight percent

The superficial weight percent of lactic acid is expressed as the weight of total monomer with the corresponding water of hydrolysis divided by total solution weight. For the example above, the superficial wt.% is (9.924 mol LA × 90.08 / 1788.3 = 0.500) 50.0 wt.% lactic acid, and (49.63 × 18.02 / 1788.3 = 0.500) 50.0 wt.% water. When lactic acid is purchased, the concentrations expressed in wt.% should be interpreted as superficial wt.%. In this manuscript, we explicitly label such concentrations superficial wt.% to avoid confusion. When solutions are very concentrated, the superficial concentration of lactic acid can exceed 100 wt.%. The concept of 125 superficial wt.% lactic acid arises from the fact that 100 g of a polymer $(C_3H_4O_2)_n$ upon hydrolysis gives rise to 100 × 90.08 / 72.06 = 125 g of lactic acid, where 90.08 is the molecular weight of lactic acid monomer, and 72.06 is the molecular weight of the ester repeat unit in the

polymer. When an aqueous solution has a lactic acid content exceeding 100 superficial wt.%, the water of esterification (oligomerization) has been removed from the solution, and the solution is thus characterized by a negative superficial wt.% of water.

1.1.3. True weight percent

True weight percent utilizes the mass of a particular sample and the total mass of the individual species within the solution. Using the same example again, the true wt.% values are 46.3 true wt.% LA_1 (9.20 × 90.08 / 1788.3 = 0.463), 3.1 true wt.% LA_2 (0.343 × 162.14 / 1788.3 = 0.031), 0.17 true wt.% LA_3 (0.0128 × 234.21 / 1788.3 = 0.0017), and 50.4 true wt.% H_2O (50 × 18.02 / 1788.3 = 0.504).

2. Experimental

2.1. Chemicals

Analytical grade aqueous lactic acid solutions were used in experiments: 85 superficial wt.% was purchased from J.T. Baker, Inc. and 50 superficial wt.% was purchased from Purac, Inc. HPLC grade water was purchased from J.T. Baker, Inc. HPLC grade acetonitrile was purchased from EMD Chemicals. An aqueous solution of 85 wt.% phosphoric acid was purchased from J. T. Baker, Inc.

2.2. Preparation of oligomer solutions

Solutions of lactic acid below 50 superficial wt.% were prepared by adding water to 50 superficial wt.% lactic acid, whereas solutions between 50 superficial wt.% and 85 superficial wt.% were prepared by mixing the 50% and 85% solutions. After mixing, the solutions were heated at 80 °C for 1 week to increase the rate of formation of various oligomers of lactic acid. To concentrate lactic acid above 85 wt.%, water was removed from 85 wt.% lactic acid at 45 mmHg using a vacuum distillation apparatus. At that pressure, the boiling point temperature started at 30 °C for 90 superficial wt.% solution and rose to 135 °C for solutions of 120 superficial wt.%. Following evaporation, the solutions were equilibrated by refluxing at 100 °C for 30 h.

2.3. Analytical methods

The composition of lactic acid and its oligomers in solution was characterized using a combination of three analytical techniques.

2.3.1. Titration

The composition of dilute solutions containing less than 20 superficial wt.% lactic acid contains > 98% EMLA LA_1 and water [1]. Lactic acid solution containing less than 10 superficial wt.% of lactic acid contains 99.6% EMLA LA_1 [1,10], and direct titration with standardized 0.1N NaOH (Sigma-Aldrich) gave an accurate analysis of LA_1 in solution.

For solutions containing more than 20 but less than 85 superficial wt.% lactic acid, the total free acidity of the solution was determined from titration with standard 0.1N NaOH. In solutions above 85 superficial wt.%, titration with 0.1N NaOH occurred with too little base to accurate determine the endpoint. More reproducible results were found when using 0.01N NaOH. In addition, titrating the lactic solution in ice yielded more reproducible results due to decreased probability of hydrolysis. Ester bonds present in oligomers are susceptible to hydrolysis in the presence of aqueous NaOH at room temperature. This could lead to inconsistencies in determination of total acid content by titration; therefore the solution was titrated in ice to minimize hydrolysis. After titration of free acidity, excess NaOH was added and the solution was heated to about 80 °C to hydrolyze the oligomers to monomeric sodium lactate. Hydrolysis was

carried out for two hours for solutions below 100 superficial wt.% and for four hours for solutions above 100 superficial wt.%. The quantity of unreacted NaOH was determined by back titration of the resultant solution with standardized 0.1N H_2SO_4 solution (Sigma-Aldrich). For concentrations where only monomer and dimmer exist, the quantity of LA_1 in solution was calculated by the difference between NaOH consumed for neutralization of total acid and the quantity of NaOH consumed for the hydrolysis of ester linkage present in oligomers [11,12].

2.3.2. GC analysis and GC/MS analysis

Water concentrations in lactic acid standard solutions were verified using a Varian 3600 gas chromatograph (GC) equipped with a thermal conductivity detector (TCD). The GC column was 3.25 mm OD × 4m long and was packed with 80/100 mesh Porapak-Q. The oven temperature was held constant at 413 K for 2 min, ramped at 20 °C / min to 493 K, and held at 493 K for 6 min. The injector temperature was maintained at 493 K and the TCD block temperature was held at 523 K. Helium was used as the carrier gas. HPLC grade acetonitrile was used as an internal standard. Qualitative analysis of LA_1 and its higher oligomers LA_2, LA_3 LA_4, etc. by GC–MS was carried out on a JEOL AX-505H double-focusing mass spectrometer coupled to a Hewlett-Packard 5890J gas chromatograph via a heated interface. GC separation employed a J&W DB-23 fused-silica capillary column (30 m length × 0.25 m ID. with a 0.25 μm film coating). Splitless injection was used. Helium gas flow was maintained at 1 mL/min. The GC temperature program was initiated at 323 K and was ramped at 10 °C / min to 533 K. MS conditions were as follows: interface temperature 523 K, ion source temperature 523 K, electron energy 70 eV, and scan frequency was 1 Hz over the *m/z* range of 45 – 750. Prior to its injection for analysis by GC–MS, LA_1, LA_2, LA_3, and LA_4 were derivatized with TMS {Propanoic acid, 2-[(trimethylsilyl)oxy - trimethyl silyl ester} to enhance their volatility.

2.3.3. HPLC analysis

The concentration of LA_1 and oligomers in concentrated lactic acid solutions were quantified using a Hewlett Packard 1090 Liquid Chromatograph equipped with an auto sampler, gradient flow pump, oven and a Hitachi-L400H UV detector set at 210 nm. Lactic acid samples below 85 superficial wt.% were analyzed using a mobile phase of water + acetonitrile in gradient concentration at a flow rate 1 mL/min on a Novapak C18 column (3.9mm × 150 mm). Both water and acetonitrile were acidified using 2 mL of 85% (w/v) phosphoric acid in 1 L of solvent. The water was analyzed to be pH 1.3. The column oven temperature was maintained at 40 °C. Beginning with a mobile phase of 100% acidified water, the acetonitrile concentration was ramped linearly to 60 vol.% from zero to 20 min and then ramped linearly up to 90% from 20 min to 25 min. The mobile phase composition was maintained constant at 90% to 28 min and then returned to 100% water.

For analysis of solution concentrations above 85 superficial wt.% lactic acid, the total flow rate and column temperature were maintained as above, but the gradient was modified. The mobile phase was ramped linearly from 10% to 100% acetonitrile from 0 to 25 min. Acetonitrile concentration of mobile phase was brought back to 10% at 35 min.

2.3.3.1. Response factor for LA_1. Dilute solutions of lactic acid (<20 superficial wt.%) contain > 98% EMLA LA_1; their concentrations can be accurately determined by titration as described in Section 2.3.1. To prepare a standard containing only LA_1, a dilute solution containing 7–8 superficial wt.% total lactic acid in water was prepared and heated for 6 h in presence of Amberlyst-15 cation exchange resin to facilitate hydrolysis of any LA_2 or higher oligomers present. Titration of this solution with 0.1N NaOH showed a value of 7.3 true wt.% LA_1. This solution was used to create HPLC calibration standards for LA_1 that spanned the range of LA_1

concentrations (0.1 – 1 true wt. %) used in HPLC analysis. A linear UV response was observed from the calibration curve obtained by sample dilution. The response factor for LA_1 obtained from this calibration was used for quantitative determination of LA_1 in concentrated lactic acid solutions.

2.3.3.2. Response factor for LA_2. A 50 superficial wt.% lactic acid solution, containing LA_1 and LA_2, was titrated/hydrolyzed/back-titrated with standardized 0.1N NaOH solution as described in Section 2.3.1. By this method the composition of LA_1 and LA_2 were quantified as 46 and 3 true wt.%, respectively. HPLC analysis was performed on the sample and LA_1 was quantified using the response factor from calibration described in Section 2.3.3.1. GC analysis of the sample showed the presence of 51 true wt.% water, and closed the material balance. This standardized solution was diluted in water to provide a series of calibration standards that spanned the pertinent range of true wt.% of LA_1 (0.1 to 1 wt.% by appropriate dilution with water) and LA_2. A linear UV response with concentration was observed for LA_2 following prompt analysis. The response factor from this calibration curve for LA_2 was used for quantitative determination of the superficial LA_2 concentration in lactic acid solutions. The ratio of response factors for superficial wt.% was found to be $LA_2 / LA_1 = 1.43$ in all HPLC analyses.

2.3.3.3. Response factors for LA_3 and LA_4. In a solution with approximately 93 superficial wt.% aqueous lactic acid solution, the linear oligomers LA_3 and LA_4 are observed in significant quantities in addition to LA_2. HPLC analyses of the solution showed compositions of 58 and 22 true wt.% for LA_1 and LA_2, respectively, with the remaining lactic acid in the form of higher oligomers. GC analysis of the solution showed the presence of 12 true wt.% water. The presence of lactic acid oligomers up to LA_4 was also verified by GC–MS analysis. The assignment of response factors for higher oligomers was based on the following premises: (1) the difference in successively higher oligomers of lactic acid is the presence of an additional ester group; (2) the UV detector response is related to the presence of carbonyl groups in the ester functionality; and (3) the ratio of LA_2/LA_1 response factors was 1.43. Therefore, the same ratio of response factors was assigned to each of the successively higher oligomers of lactic acid for superficial wt.% ($LA_j/LA_1 = 1.43$). Using these response factor ratios for LA_3 and LA_4, the concentrations of LA_3 and LA_4 were determined from HPLC to be 6 and 2 true wt.% respectively. Using these values, the material balance closed (58 + 22 + 6 + 2 + 12 = 100).

To further test the calibration, a series of dilutions where prepared from a solution that was determined by titration to be 73.8 superficial wt.% lactic acid. The dilutions spanned the range of various wt.% of LA_1, LA_2, LA_3, and LA_4 acids (0.1–1 wt.% by appropriate dilution with water), and the HPLC analysis showed a linear concentration response. Using the response factors determined above, the total superficial concentration was determined to be 74%, in excellent agreement with titration and thus verifying the reliability of the oligomer HPLC response factors.

2.3.3.4. Analysis of higher ($>LA_4$) lactic acid oligomers. High oligomers of lactic acid are insoluble in water, but they are miscible in acetonitrile. Mixtures of acetonitrile + water have intermediate solvent strength. To dilute a sample of 115 superficial wt.% lactic acid to an overall concentration of 2 wt.% in a homogeneous phase, a solution of at least 50 wt.% acetonitrile was needed. However, this composition was not suitable for injection because HPLC could not provide reliable resolution between LA_1 and LA_2 if more than 20 wt.% acetonitrile was present in an injected sample containing large quantities of LA_1 and LA_2. The difficulties did not arise when the quantities of LA_1 and LA_2 were small. To provide reliable results, lactic acid solutions greater than 105 superficial wt.% were analyzed in two fractions. Approximately 0.1 g lactic acid solution was transferred to a microcentrifuge tube and weighed. Approximately 1mL of water was added; the solution was shaken, and then centrifuged at 4000 rpm in a desktop

microcentrifuge for 4 min. The water phase was carefully removed using a pipette. The water extraction was repeated four to five times. This water-soluble fraction was weighed and held for analysis. Next, the water-insoluble high oligomers were recovered in 100% acetonitrile and this acetonitrile phase was weighed. All steps were done at room temperature. The oligomer contents in both water and acetonitrile were combined in calculation of superficial wt.% oligomer distribution in the two fractions, and then combined to calculate the superficial wt.% of the original sample and % EMLAj. The response factors for the higher oligomers where assumed to be the same as the values for LA_3 and LA_4. The HPLC results for total lactic acid content determined by adding the superficial wt.% of the individual oligomers is in good agreement with the results from titration as shown in Table 1.

3. Mathematical model

We present here a model of infinite oligomer formation using chemical theory. There are a few examples in the literature of compounds whose phase equilibria properties have been described with the help of chemical theory or chemical theory along with physical intermolecular forces. The most strikingly related example is that of formaldehyde in aqueous and/or methanolic solutions, which reveals extreme deviations from ideality caused mainly by chemical reactions. Formaldehyde in the presence of water gives methylene glycol and polyoxomethylenes; in the presence of methanol it gives hemiformal and higher hemiformals [13].

VLE for formaldehyde-containing systems has been described using chemical theory by Kogan [14], Kogan and Ogorodnikov [15,16], Brandani et al. [17] and Masamoto and Matsuzaki [18]. Maurer [13] presented for the first time a model in which chemical reactions together with physical intermolecular forces were used successfully to describe the VLE and enthalpy for formaldehyde-containing systems containing both reactive and inert components such as trioxane. Maurer's model was subsequently extended and tested using new data; for an update on the model up to 1992 the reader is referred to Hahnenstein et al. [19]. This approach has also been used by Brandani et al. [20–22].

For the system formaldehyde-water, the mole fraction of compounds in the liquid phase is calculated by modeling the oligomerization as two equilibrium constants—one for methylene glycol formation from formaldehyde and water and the second for subsequent higher methylene glycol oligomer formation.

$$K_1 = \left[\frac{x_{MG}}{(x_w\, x_{FA})}\right]\left[\frac{\gamma_{MG}}{(\gamma_w\, \gamma_{FA})}\right] \tag{3}$$

$$K_n = \left[\frac{x_n\, x_w}{(x_{n\text{-}1}\, x_{MG})}\right]\left[\frac{\gamma_n\, \gamma_w}{(\gamma_{n\text{-}1}\, \gamma_{MG})}\right] \qquad 2 \leq n \tag{4}$$

These assumptions are reasonable since methylene glycol is a chemically different structure than formaldehyde, while the higher oligomers of methylene glycol are chemically similar to each other. The formaldehyde formaldehyde–methanol system is treated in a similar way.

Table 1
Summary of HPLC results and comparison with total superficial acid by titration

Overall superficial wt.% LA%		HPLC analysis (%EMLA)										
Titration	**HPLC**	**LA_1**	**LA_2**	**LA_3**	**LA_4**	**LA_5**	**LA_6**	**LA_7**	**LA_8**	**LA_9**	**LA_{10}**	**LA_4+**
12.24	10.81	99.63	0.37	0.00	0.00	0.00	0.00	0.00	0.00	0.00	0.00	0.00
24.36	26.88	96.31	3.59	0.10	0.00	0.00	0.00	0.00	0.00	0.00	0.00	0.00
44.47	47.62	94.74	5.06	0.20	0.00	0.00	0.00	0.00	0.00	0.00	0.00	0.00
53.43[a]	51.25[a]	94.53[a]	5.28[a]	0.19[a]	0.00	0.00	0.00	0.00	0.00	0.00	0.00	0.00
59.59	62.02	89.95	9.33	0.72	0.00	0.00	0.00	0.00	0.00	0.00	0.00	0.00
70.60	71.93	84.61	13.58	1.65	0.16	0.00	0.00	0.00	0.00	0.00	0.00	0.16
81.46	81.90	75.66	19.49	3.88	0.69	0.28	0.00	0.00	0.00	0.00	0.00	0.97
87.13[b]	89.62[b]	65.92[b]	25.05[b]	6.90[b]	1.63[b]	0.49[b]	0.00	0.00	0.00	0.00	0.00	2.12
88.06	89.63	66.85	24.09	6.87	1.72	0.48	0.00	0.00	0.00	0.00	0.00	2.20
96.75	96.42	54.42	28.56	11.48	3.84	1.38	0.32	0.00	0.00	0.00	0.00	5.55
100.18	102.05	45.19	29.03	14.69	6.49	2.98	1.25	0.37	0.00	0.00	0.00	11.10
103.27	104.43	33.36	30.11	18.97	9.68	4.73	1.87	0.81	0.33	0.14	0.00	17.56
106.41	105.65	33.10	25.33	17.46	10.76	6.30	3.47	1.91	0.96	0.43	0.19	24.11
113.61	108.07	29.29	24.20	17.83	11.74	7.28	4.32	2.54	1.45	0.77	0.42	28.69
115.47	116.25	7.62	10.47	11.44	12.06	12.50	11.86	10.84	9.01	6.72	3.96	70.47
119.57	120.02	2.18	4.49	5.02	5.83	8.25	10.40	13.00	13.81	12.75	10.54	88.31

Percentages by HPLC analysis are calculated as explained in the introduction and are also plotted on Figure 4.
[a] Commercial LA 50%.
[b] Commercial LA 85%.

3.1. Literature models for lactic acid based on chemical theory

Prior modeling work to determine the distribution of lactic acid oligomers in solutions above 20 wt.% concentration has been performed by Bezzi et al. [23] and reported by Holten [1]. In the first modeling approach, only the dimers of lactic acid (LA_2) were considered. This approach, however, becomes inaccurate at higher concentrations of lactic acid (>50 wt.%), where significant oligomerization occurs. In a second modeling approach, polylactic acids were taken into account, giving a more realistic representation at high concentrations. However, this model was limited in that solutions were characterized only by concentration of free lactic acid (LA) and total oligomer species; no distributions of oligomers was generated. This polylactic model works poorly at low concentrations, and is interpretative rather than predictive in its application

We are unaware of published mathematical models, apart from the ones described above, that attempt to represent the liquid phase distribution of lactic acid and its oligomers in solution. Therefore, we propose here a model that is based on chemical theory and incorporates an infinite series of oligomer components. The model accurately predicts liquid phase compositions of lactic acid in a method similar to Maurer's for formaldehyde systems, and represents a clear advancement of the characterization of concentrated lactic acid solutions. In order to compare the present model to those in the literature, this work utilizes the terminology used by Montgomery [7] and Ueda and Terashima [8] as clarified in Section 1.1.

3.2. Infinite series polymer model

From a thermodynamic standpoint, the formation of oligomeric intermolecular esters of lactic acid can be described as the set of successive reactions shown below, where W denotes water

$$2LA_1 \rightleftharpoons LA_2 + W \tag{5}$$

$$LA_2 + LA_1 \rightleftharpoons LA_3 + W \tag{6}$$

$$LA_3 + LA_1 \rightleftharpoons LA_4 + W \tag{7}$$

Generally, oligomer formation can be written as

$$LA_{(j-1)} + LA_1 \rightleftharpoons LA_4 + W \tag{8}$$

The chemical reaction equilibrium constants for the above reactions in the generalized form is given by

$$K_j = \frac{n_{LA_j} n_W}{\left(n_{LA_{(j-1)}} n_{LA_1}\right)} \qquad j > 2 \tag{9}$$

Note that since the number of moles of products and reactants is equivalent regardless of the degree of oligomerization, the equilibrium constant written in Eq. (9) is equivalent to an equilibrium constant written in mole fractions.

Since lactic acid oligomers (LA_2, LA_3, etc.) are all formed via identical reaction pathways and are themselves chemically similar, it is reasonable to assume that the esterification reactions (Eqs. (5) – (8) above) have the same value of equilibrium constant.

$$K = K_1 = K_2 = K_3 = K_4 = \ldots\ldots = K_j \tag{10}$$

This reasoning is analogous to the treatment of the formaldehyde model, where all polyoxomethylenes have the same equilibrium constant since they are chemically very similar but the formaldehyde to methylene glycol reaction involves different chemical structures and therefore has a different equilibrium constant [13].

Eq. (9) can be rearranged to the following form

$$n_{LA_j} = n_{LA_{(j-1)}} r \tag{11}$$

where

$$r = \frac{n_{LA_1} K}{n_W} \tag{12}$$

and it is recognized that n LA1 and n W are properties of the solution, identical for all oligomers at a specific superficial concentration. Because of the recursion, it is possible to write

$$n_{LA_j} = n_{LA} r^{(j-1)} \tag{13}$$

A total lactic acid superficial mole balance is given by

$$\begin{aligned} n_{LA}^i &= \sum j n_{LA_j} = n_{LA_1}(1 + 2r + 3r^2 + 4r^3 + \ldots) \\ &= \frac{n_{LA_1}}{(1-r)^2} \end{aligned} \tag{14}$$

where the left hand side is the superficial number of moles of lactate in solution, the second and third expressions represent the infinite converging series obtained by inserting Eq. (13), and the final term represents the closed form solution. The water superficial mole balance is given by taking the difference between the true moles present, and those consumed by hydrolysis of oligomers

$$\begin{aligned} n_W^i &= n_W - \sum (j-1) n_{LA_j} \\ &= n_W - n_{LA_1} r(1 + 2r + 3r^2 + 4r^3 + \ldots) \\ &= n_W - \frac{n_{LA_1} r}{(1-r)^2} \end{aligned} \tag{15}$$

where Eq. (13) is substituted into the summation between the second expression and the third, and the right hand side is the closed form solution. The left-most variable in Eq. (15) is the superficial number of moles of water. Eq. (14) can be inserted into (15) to give

$$n_W = n_W^i + n_{LA}^i \cdot r \tag{16}$$

Inserting Eqs. (14) and (16) into Eq. (12) provides a relation between K and r in terms of the superficial concentrations of lactic acid and water

$$K = \frac{r\left(n_W^i + n_{LA}^i r\right)}{n_{LA}^i (1-r)^2} \tag{17}$$

Free acid and all oligomers contribute to titratable acidity that can be calculated by

$$\sum n_{LA_j} = n_{LA_1}(1 + r + r^2 + r^3 + \ldots) = \frac{n_{LA_1}}{(1-r)}$$

3.3.Application

To apply the model, an overall superficial number of moles n_W^i, n_{LA}^i and K are specified. Eq. (17) is rearranged as a quadratic in r and solved explicitly for the value of r. The value of r is then used to calculate n_{LA_1} from Eq. (14), and subsequently the distribution of oligomers from Eq. (13) as well as the remaining balances.

The equations can be manipulated to express the various oligomer concentrations in terms of the overall superficial wt.% lactic acid.

The %EMLA for LA is

$$\%EMLA_j = jr^{(j-1)}\left(1 - r^2\right) \tag{19}$$

The superficial wt% of LA_j is

(Superficial wt% of LA_j) = (%$EMLA_j$)(overall superficial wt.% LA) (20)

The true wt.% of water is

(True wt.% water) = 100 + (overall superficial wt.% LA)(0.2r – 1) (21)

The true wt.% of a LA_j is

(True wt% LA_j) = (0.8j + 0.2)(overall superficial wt% LA) $r^{(j-1)}(1-r)^2$ (22)

4. Results and discussion

4.1. Analytical results and modeling

Aqueous solutions of lactic acid were prepared and analyzed for oligomer concentrations up to 120 superficial wt.% lactic acid. Table 1 gives a summary of the HPLC results and a comparison with total acidity of the solution determined by titration. The HPLC results for overall superficial wt.% were calculated by summing the peak areas for the individual oligomers. As a check of the HPLC method, the total acid content by the HPLC and titration agreed within ±3 wt.% for solutions up to 105 wt.% lactic acid.

The value of the equilibrium constant K = 0.2023 was obtained by least squares regression of %EMLA for species LA1 through LA_4 simultaneously. Using this value, the distribution is modeled with an average deviation of ± 0.12% of the reported %EMLA. For each composition

from Table 1, calculated %EMLA of the oligomers is presented in Table 2. From the HPLC results, the material balance provided the superficial number of moles of lactic acid and water. Using the value of K and the superficial moles, the value of r was determined for each overall composition, and then Eq. (19) was applied.

Fig. 1 shows a GC/MS result for an 85 superficial wt.% lactic acid solution, demonstrating by molecular weights that only linear oligomers of lactic acid are present. All four components, namely LA_1, LA_2, LA_3 and LA_4, were identified and verified by their respective mass fragmentation data obtained from GC/MS.

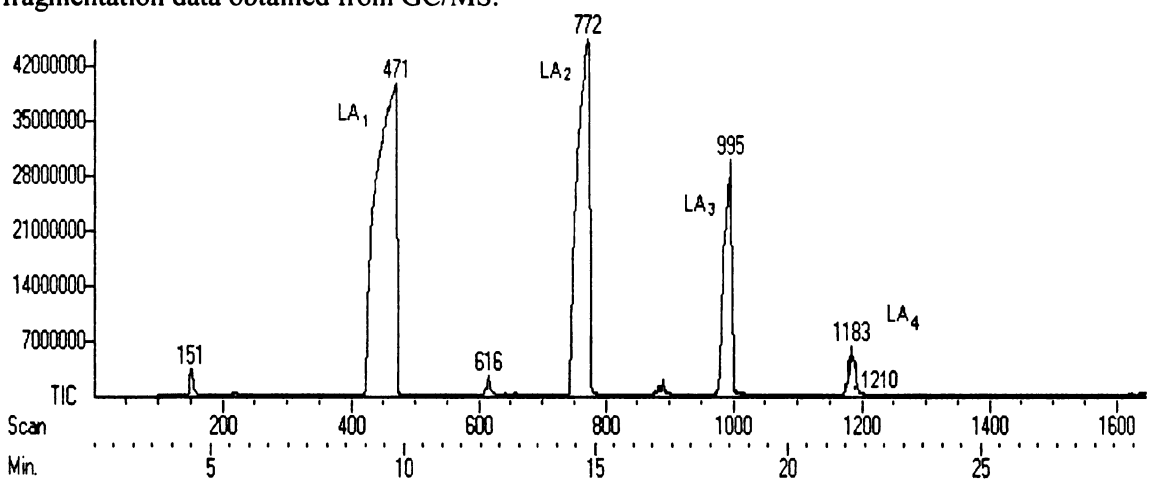

Fig. 1. GC/MS of 85 wt.% LA. The mass fragments (not shown) were used to verify that linear oligomers of LA are present. No lactide was observed.

Fig. 2 shows an example HPLC chromatograph of a 115 superficial wt.% solution of lactic acid. Fig. 3 shows total titratable acidity as a function of lactic acid concentration as summarized by Holten [1] from various sources and from this work. The titratable acidity reflects a balance between increasing total acid content and increasing degree of oligomerization that eliminates free acid groups. The titratable acidity goes through a maximum at about 90 wt.% lactic acid. The model represents the experimental data with an average deviation of ± 2% of titratable acidity.

Fig. 4 shows the experimental distribution of LA_1, LA_2, LA_3 and higher oligomers collected in this work and compared to data from Ueda and Terashima [8] and Montgomery [7]. Higher oligomers are denoted by LA_{4+}, i.e. sum of tetramers and higher oligomers. The abscissa of Fig. 4 denotes the superficial lactic acid concentration; note that it runs through 125% as explained in the introduction. The ordinate of Fig. 4 denotes the %EMLA distribution of lactic acid between monomer and its oligomers on a water-free basis. The percentages are calculated as described in the introduction. The lines shown in Fig. 4 are the calculated values of LA_1, LA_2, LA_3, LA_4 and LA_{4+} from the model. Excellent agreement is seen between the experimental values of this work and the values calculated from the model.

It can be seen from the experimental data of this work and also from Montgomery [7], that there is a maximum value of approximately 15% EMLA LA_3 occurring at 114 superficial wt.% and a maximum value of 29% EMLA LA_2 occurring at 105 superficial wt.%. Experimental data from Ueda and Terashima [8] are also presented; this set of experimental data runs up to 87% total acidity. Watson's [9] experimental data are not plotted because he reports the presence of lactide, which is known to be unstable in aqueous solutions.

Fig. 5 compares the experimental analysis and model concentrations of LA_5 through LA_{10} for solutions with superficial lactic acid content of 80 to 125 wt.%. The agreement is excellent for analyzed solutions up to 108 superficial wt.% of acid. The agreement is not as good for the solutions with superficial concentrations of 116 wt.% and 120 wt.%. These samples were analyzed in two fractions
as discussed above. Since the total acid content is in good agreement by HPLC and titration (Table 1), we believe that the disagreement between the model and HPLC results is due to the incomplete separation of oligomers in the HPLC, even though distinct peaks appear on the HPLC chromatogram. Attempts to refine the HPLC method further for these very high molecular weight solutions have not been successful.

Concentrated solutions of lactic acid (>105 superficial wt.%) are fluid at 120 °C, but are very viscous at room temperature. The solutions had a very slight amber tint, but none of the dark coloration indicated by Montgomery [7]. Our results are in good agreement with those of Montgomery [7] except at the highest concentration. Montgomery reported incomplete separation of LA_3 and higher oligomers—a problem that we experienced only for higher oligomers (>LA_5). To test for hydrolysis under analysis conditions in this work, ethyl lactate was analyzed using the same HPLC method as for the lactic acid oligomers and was found to be stable. Also, our results are also consistent with those of Montgomery, who tested extensively for hydrolysis.

In discussion of the distribution of weight percentages in lactic acid solutions, it is appropriate to express the concentrations in terms of superficial wt.%. The superficial wt.% for oligomers can be quickly calculated from the values in Table 1 by multiplying the total acid superficial wt.% by the % EMLA. A summary of true weight percentages calculated by the oligomer model is shown in Table 3.

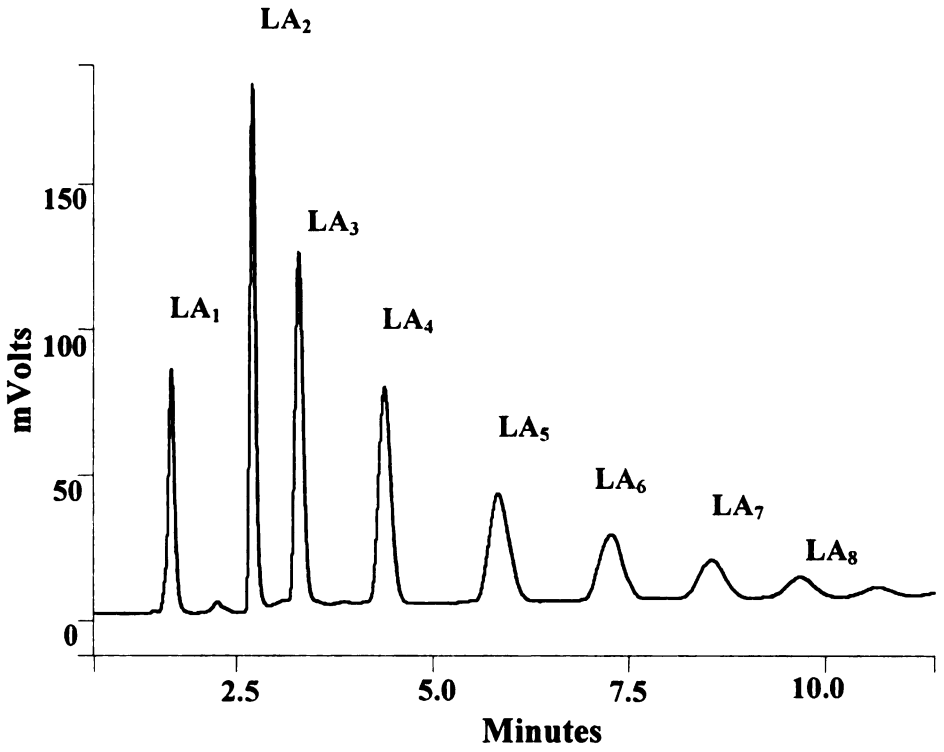

Fig. 2. HPLC chromatograph of the water soluble fraction from 115 superficial wt.% lactic acid demonstrating the separation of oligomers.

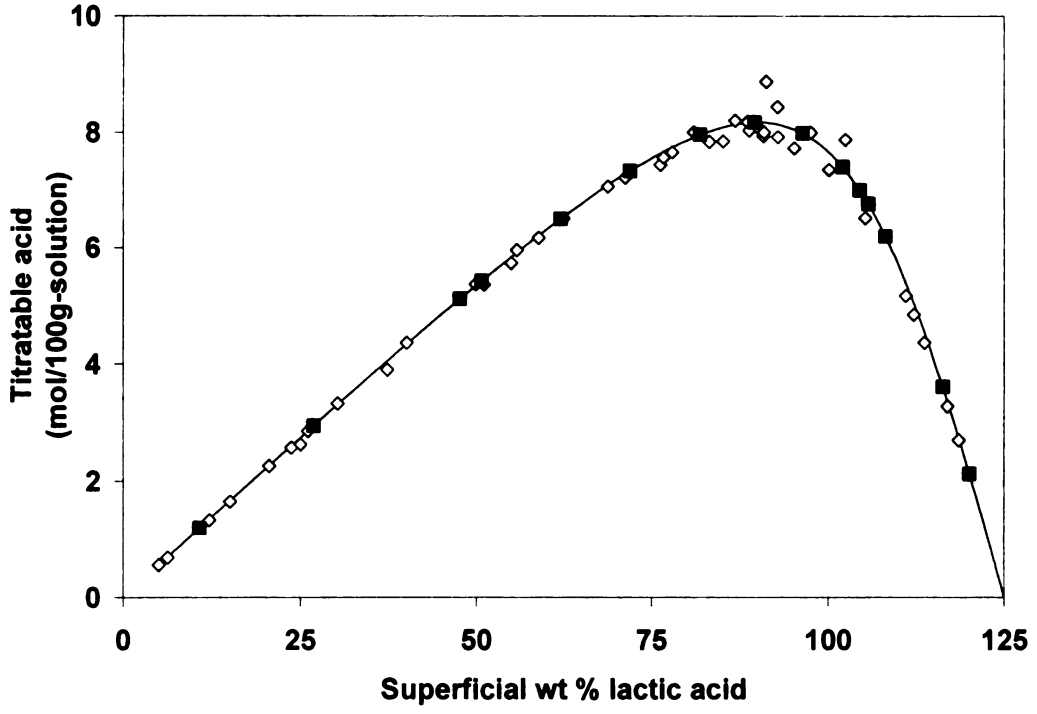

Figure 3. Total titratable acidity tabulated from various workers by Holten [1] and measured in this work compared with the model proposed in this work. □ data compiled by Holten, ■ this work.

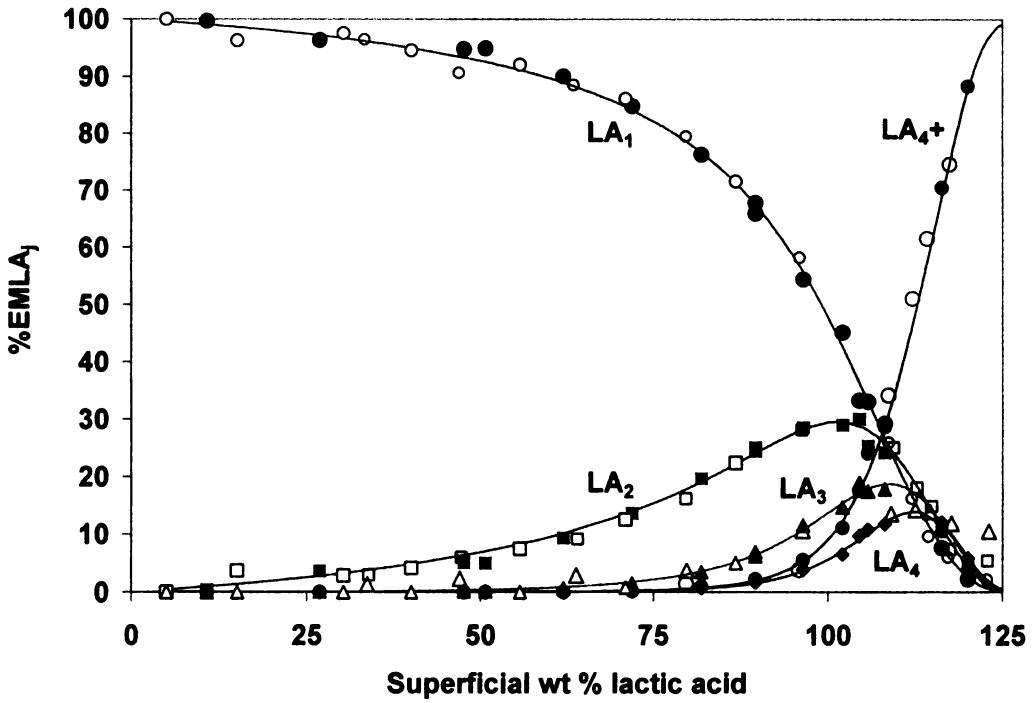

Figure 4. Experimental oligomer distribution compared with the model expressed as %EMLA. Solid lines represent the model, solid symbols are measured in this work and open symbols are from literature as reported by [7] and [16]. The curve labeled LA_{4+} indicates the sum of all oligomers LAj where $j \geq 4$.

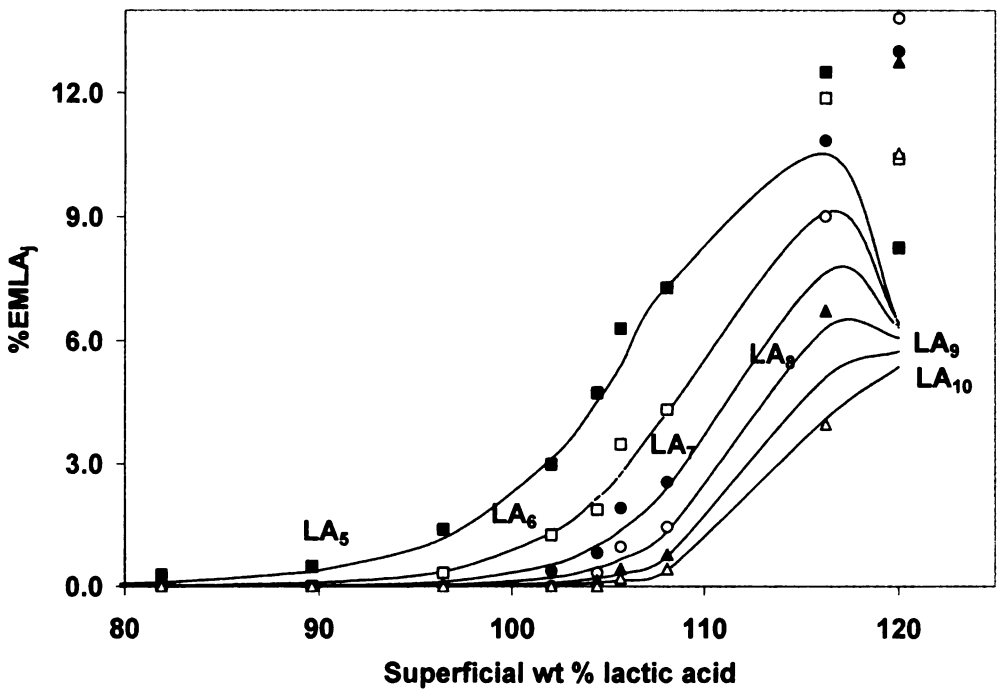

Figure 5. Experimental oligomer distribution compared with the model expressed as %EMLA. Experimental difficulties in analyzing the two highest concentrations are discussed in the text.

Table 2
Summary of calculated %ELMA for oligomers at each of the experimental compositions from Table1

Sample	Acid superficial	n^i_W	n^i_{LA}	r	Calculated (%EMLA$_i$)										
(g)	(wt.%)	(mmol)	(mmol)		LA_1	LA_2	LA_3	LA_4	LA_5	LA_6	LA_7	LA_8	LA_9	LA_{10}	LA_4+
0.081	10.8	3.99	0.097	0.005	99.0	0.96	0.007	0.000	0.000	0.000	0.000	0.000	0.000	0.000	0.000
0.293	26.9	11.9	0.876	0.014	97.1	2.80	0.061	0.001	0.000	0.000	0.000	0.000	0.000	0.000	0.001
0.213	47.6	6.21	1.13	0.034	93.3	6.36	0.326	0.015	0.001	0.000	0.000	0.000	0.000	0.000	0.015
0.112	50.7	3.06	0.631	0.038	92.5	7.07	0.405	0.021	0.001	0.000	0.000	0.000	0.000	0.000	0.022
0.111	62.0	2.34	0.763	0.058	88.8	10.2	0.884	0.068	0.005	0.000	0.000	0.000	0.000	0.000	0.073
0.115	71.9	1.80	0.922	0.084	84.0	14.0	1.76	0.196	0.020	0.002	0.000	0.000	0.000	0.000	0.218
0.107	81.9	1.08	0.977	0.126	76.4	19.2	3.62	0.607	0.095	0.014	0.002	0.000	0.000	0.000	0.719
0.093	89.6	0.533	0.921	0.180	67.3	24.2	6.51	1.56	0.350	0.075	0.016	0.003	0.001	0.000	2.00
0.086	96.4	0.171	0.920	0.255	55.5	28.3	10.8	3.68	1.17	0.358	0.107	0.031	0.009	0.003	5.36
0.081	102.0	-0.093	0.923	0.348	42.5	29.6	15.4	7.16	3.11	1.30	0.527	0.209	0.082	0.032	12.4
0.093	104.4	-0.228	1.07	0.397	36.3	28.9	17.2	9.11	4.52	2.16	1.00	0.454	0.203	0.090	17.6
0.079	105.7	-0.249	0.931	0.425	33.1	28.1	17.9	10.1	5.39	2.75	1.36	0.662	0.316	0.149	20.9
0.054	108.1	-0.240	0.642	0.484	26.6	25.8	18.7	12.1	7.32	4.25	2.40	1.33	0.725	0.390	28.9
0.111	116.2	-1.01.	1.44	0.721	7.80	11.2	12.2	11.7	10.5	9.10	7.65	6.30	5.11	4.09	68.8
0.198	120.0	-2.20	2.64	0.840	2.57	4.32	5.440	6.095	6.402	6.456	6.329	6.078	5.746	5.365	87.7

The first four columns are from experimental results, and the remaining columns are calculated based on the model using K = 0.2023.

Table 3. Model calculations of true wt% of water and lactic acid oligomers for various superficial compositions.

Superficial	Superficial	True weight percent compositions											
wt.% LA	wt.% water	water	LA_1	LA_2	LA_3	LA_4	LA_5	LA_6	LA_7	LA_8	LA_9	LA_{10}	LA_{11+}
5	95	95.0	4.98	0.019	0.000	0.000	0.000	0.000	0.000	0.000	0.000	0.000	0.000
10	90	90.0	9.91	0.079	0.001	0.000	0.000	0.000	0.000	0.000	0.000	0.000	0.000
15	85	85.0	14.8	0.187	0.002	0.000	0.000	0.000	0.000	0.000	0.000	0.000	0.000
20	80	80.0	19.6	0.350	0.005	0.000	0.000	0.000	0.000	0.000	0.000	0.000	0.000
25	75	75.1	24.3	0.575	0.011	0.000	0.000	0.000	0.000	0.000	0.000	0.000	0.000
30	70	70.1	29.0	0.874	0.021	0.000	0.000	0.000	0.000	0.000	0.000	0.000	0.000
35	65	65.1	33.6	1.26	0.038	0.001	0.000	0.000	0.000	0.000	0.000	0.000	0.000
40	60	60.2	38.0	1.75	0.064	0.002	0.000	0.000	0.000	0.000	0.000	0.000	0.000
45	55	55.3	42.3	2.35	0.105	0.004	0.000	0.000	0.000	0.000	0.000	0.000	0.000
50	50	50.4	46.3	3.11	0.167	0.008	0.000	0.000	0.000	0.000	0.000	0.000	0.000
55	45	45.5	50.2	4.03	0.260	0.015	0.001	0.000	0.000	0.000	0.000	0.000	0.000
60	40	40.6	53.8	5.18	0.400	0.028	0.002	0.000	0.000	0.000	0.000	0.000	0.000
65	35	35.8	56.9	6.58	0.611	0.051	0.004	0.000	0.000	0.000	0.000	0.000	0.000
70	30	31.1	59.6	8.31	0.931	0.094	0.009	0.001	0.000	0.000	0.000	0.000	0.000
75	25	26.4	61.5	10.4	1.42	0.175	0.020	0.002	0.000	0.000	0.000	0.000	0.000
80	20	21.9	62.5	13.0	2.18	0.330	0.047	0.007	0.001	0.000	0.000	0.000	0.000
85	15	17.5	62.2	16.2	3.37	0.636	0.113	0.019	0.003	0.001	0.000	0.000	0.000
90	10	13.3	60.1	19.8	5.23	1.25	0.282	0.061	0.013	0.003	0.001	0.000	0.000
95	5	9.49	55.4	23.6	8.04	2.48	0.725	0.204	0.056	0.015	0.004	0.001	0.000
100	0	6.20	47.6	26.6	11.9	4.83	1.85	0.684	0.246	0.087	0.030	0.010	0.005
105	-5	3.61	36.6	27.0	16.0	8.56	4.34	2.12	1.01	0.469	0.216	0.098	0.079
110	-10	1.79	23.7	22.9	17.7	12.4	8.21	5.24	3.25	1.98	1.19	0.708	0.989
115	-15	0.689	11.6	14.3	14.1	12.5	10.6	8.58	6.79	5.27	4.03	3.05	8.55
120	-20	0.149	3.09	4.67	5.66	6.22	6.45	6.44	6.27	5.99	5.64	5.25	44.2
123	-23	0.0219	0.506	0.853	1.15	1.41	1.63	1.82	1.97	2.10	2.20	2.29	84.1

4.2. Implementation of lactic acid model into ASPEN plus

Implementation of the model is extended to ASPEN Plus, which is the most widely used simulation software in the chemical process industry. Use of this model will be shown in future publications for the esterification of lactic acid with ethanol from the authors' laboratories [24].

The proposed model could be incorporated into the process simulator via a user-written subroutine. As an alternative, we assume that oligomerization is adequately approximated by a truncated series. Fig. 4 implies that solutions up to 90 wt.% can be represented by monomer lactic acid and the first four oligomers (LA_2–LA_5). We have used this assumption to simulate a distillation column for the purpose of evaluating its suitability for process simulation.

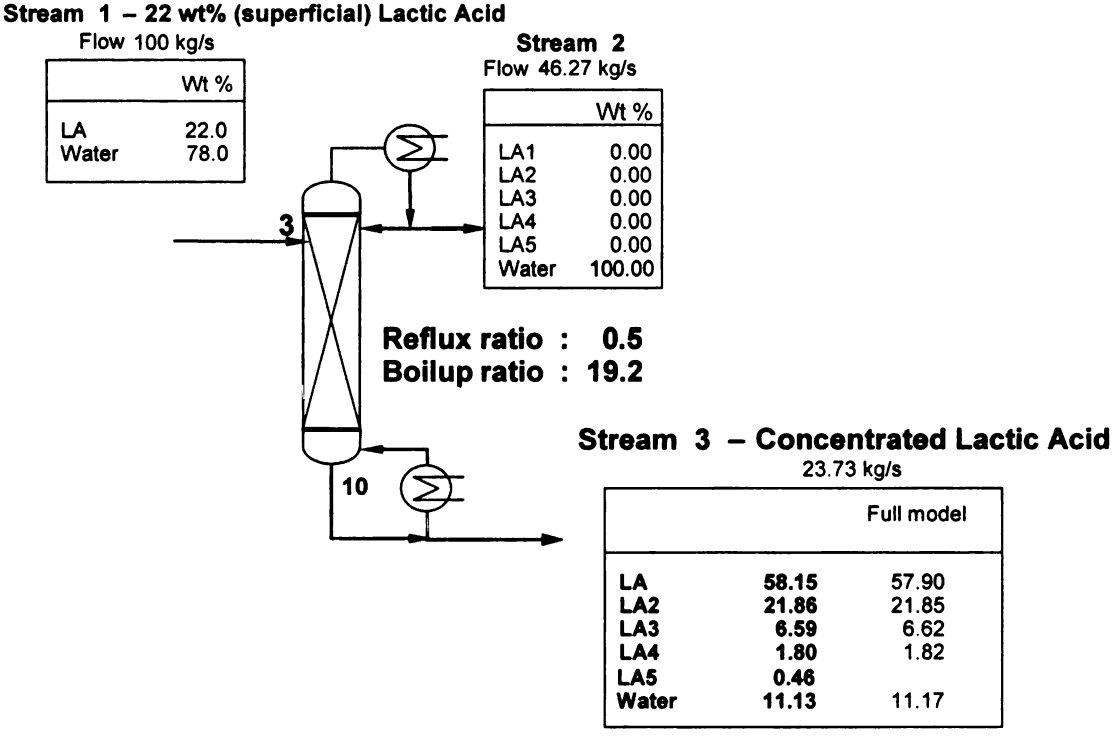

Fig. 6. Process flow diagram and results for the truncated ASPEN simulation compared to the complete oligomer model. The comparisons of composition are for a superficial composition of 92.72 wt.% lactic acid.

Fig. 6 shows the ASPEN Plus simulation to remove water from a 22 superficial wt.% lactic acid solution (non-equilibrated) and form an equilibrated 92.72 superficial wt.% solution. The reactive distillation column is assumed to operate with equilibrium stages, so the bottoms product contains an equilibrium mixture of lactic acid oligomers at an overall concentration of 92.72 superficial wt.%. The oligomer concentrations obtained from the ASPEN Plus simulation with the truncated model compare well with those from the non-truncated oligomer model as summarized in the inset table within Fig. 6. The simulation verifies that the model can be used to model a distillation column where a dilute solution of lactic acid is converted to concentrated solution consistent with oligomer distribution represented by the full model. Other options for comparison of the truncated and full model could have been used, such as an equilibrium reactor with a non-equilibrium feed; the selection of a distillation column was arbitrary.

4.3. Effect of temperature and its effect on equilibrium constant (K)

There are no experimental reports available on heats of formation of oligomers of lactic acid. Other esterification reactions involving carboxylic acids and alcohols are either thermoneutral or have very low heats of formation in the range of 2–6 kJ/mol [25–27], resulting in negligible to modest changes (10–15%) in equilibrium constants with temperature changes of 80 K. In this work, the series of esterification reactions leading to formation of oligomers are assumed to be thermoneutral, resulting in a temperature-independent K= 0.2023. Also, the oligomerization reactions are extremely slow at room temperature, which makes it very difficult to assess the reaction kinetics and time required to reach any redistribution at room temperature [1]. Experiments over a period of eight weeks showed no measurable redistribution of oligomers from the solutions that were prepared at the elevated temperatures reported above.

5. Conclusions

In this work, we provide new data to complement and extend literature data for oligomerization of lactic acid in aqueous solutions. We present a model based on chemical theory that consists of an infinite sequence of equilibriumhomo-esterification reactions between successive oligomers of lactic acid. We show that a single value of the equilibrium constant (K= 0.2023) applied to all oligomerization reactions accurately predicts titratable acidity and oligomer concentrations for solution concentrations ranging from very dilute to greater than 100 superficial wt.% lactic acid. We demonstrate that inclusion of oligomers only up to LA_5 is suitable for process modeling of lactic acid solutions up to 90 wt.%.

List of Symbols

K_j	chemical reaction equilibrium constant for *j* order oligomer
LA_1	monomeric lactic acid
LA_2	dimer lactic acid, lactoyllactic acid
LA_3	trimer lactic acid, lactoyl-lactoyllactic acid
LA_j	polymeric lactic acid consisting on j units of lactic acid
n_j	molar concentration of component j
r	defined by Eq. (12)
x_j	Mole fraction of component j
γ_j	activity coefficient of component j

Superscripts

i	initial (used for superficial number of moles)

Subscripts

FA	formaldehyde
j	component
LAj	polymeric lactic acid consisting of j units of lactic acid
MG	methylene glycol
MG_n	higher polyoxomethylene glycols
n	order of oligomer
W	water

Acknowledgement

The authors extend appreciation to the National Corn Growers Association and the Department of Energy for financial support.

References

[1] C.H. Holten, Lactic acid: Properties and Chemistry of Lactic Acid and Derivatives, Verlag Chemie, 1971.

[2] C.H. Scheele, Om Mjolk: Kgl. Vetenskaps-Academiensnya Handlingar, 1 Stockholm (1780) 116–124.

[3] M.H. Hartmann, in: D.L. Kaplan (Ed.), Biopolymers from Renewal Resources, Springer-Verlag, Berlin, 1998, pp. 367–411.

[4] S.K. Ritter, Chem. Eng. News 82 (22) (2004) 31–34.

[5] W. Robert, Chem. Week. April 10 (2002) 31.

[6] D. Garlotta, J. Polym. Environ. 9 (2002) 63–84.

[7] R. Montgomery, J. Am. Chem. Soc. 74 (1952) 1466–1468.

[8] R. Ueda, T. Terashima, Hakko Kogaku Zaashi. 36 (1958) 371–374.

[9] P.D. Watson, Ind. Eng. Chem. 32 (1940) 399–401.

[10] K. Tanaka, R. Yoshikawa, C. Ying, H. Kita, K. Okamoto, Chem. Eng. Sci. 57 (2002) 1577–1584.

[11] Holten, ibid, pp. 200.

[12] A. Engin, H. Haluk, K. Gurkan, Green Chem. 5 (2003) 460–466.

[13] G. Maurer, AIChE J. 32 (1986) 932–948.

[14] L.V. Kogan, Zhur. Prikl. Khim. 52 (1979) 2149.

[15] L.V. Kogan, S.K. Ogorodnikov, J. Appl. Chem. USSR 53 (1980) 98–101.

[16] L.V. Kogan, S.K. Ogorodnikov, J. Appl. Chem. USSR 53 (1980) 102.

[17] V. Brandani, G.D. Giacomo, P.U. Foscolo, Ind. Eng. Chem. Process. Res. Dev. 19 (1980) 179–185.

[18] J. Masamto, K. Matsuzaki, Chem. Eng. Jpn. 27 (1994) 6–11.

[19] I. Hahnenstein, M. Hasse, Y.-Q. Liu, G. Maurer, AIChE Symp. Ser. 298 (1994) 141–157.

[20] S. Brandani, V. Brandani, G.D. Giacomo, Ind. Eng. Chem. Res. 30 (1991) 414–420.

[21] S. Brandani, V. Brandani, G.D. Giacomo, Fluid Phase Equil. 63 (1991) 27–41.

[22] S. Brandani, V. Brandani, G.D. Giacomo, Ind. Eng. Chem. Res. 31 (1992) 1792–1798.

[23] S. Bezzi, L. Riccoboni, C. Sullam, Mem. cl. sci. fis. mat. nat. 8 (1937) 181–200.

[24] N.S. Asthana, A.K. Kolah, C.T. Lira, D.J. Miller, US. Patent Appl. 2004. Improved Process for Production of Organic Acid Esters.

[25] J. Gangadwala, S. Mankar, S. Mahajani, Ind. Eng. Chem. Res. 42 (2003) 2146–2155.

[26] W. Song, G. Venimadhavan, J.M. Manning, M.F. Malone, M.F. Doherty, Ind. Eng. Chem. Res. 37 (1998) 1917–1928.

[27] W. Jiu, C. Tan, Ind. Eng. Chem. Res. 40 (2001) 3281–3286.

Chapter 6 – Vapor-Liquid Equilibrium

6.1 – Overview

This chapter summarizes the works in vapor-liquid equilibrium measurements, and application of the lactic acid oligomer distribution model to the systems where concentrated lactic acid is used.

A custom-made *P-x-y* apparatus was built to reliably perform isothermal VLE and VLLE measurements down to about 0.7 kPa and temperature up to 80 °C. The use of this apparatus can easily be extended to higher temperatures with a minor modification. Isothermal VLE data of the systems of ethyl lactate + ethanol, ethyl lactate + water, triethyl citrate + water, triethyl citrate + ethanol, and diethyl succinate + ethanol, which did not exist in the open literature, were measured and become readily available using this apparatus.

As reviewed in the previous chapter, isothermal VLE measurements are preferred over the isobaric measurements, and are more suitable for thermally labile and reactive substances. But, for a system with slow kinetics, isobaric VLE measurements using *T-x-y* can be successfully obtained. Therefore, a commercial Fischer still was used to isobarically measure the VLE of the system lactic acid + water and lactic acid + ethanol + ethyl lactate + water. Details of experiments, results and limitations of the *T-x-y* Fischer are presented in the next sections.

6.2 – P-x-y Apparatus and VLE Measurements

Overview of the *P-x-y* apparatus is shown in Figure 6.1. Details of the operating procedure and schematic for this apparatus are described in the paper (*Vu et al., 2006*),

included in section 6.2.1. The additional schematics not included in the published paper are shown in Figures 6.2 and 6.3.

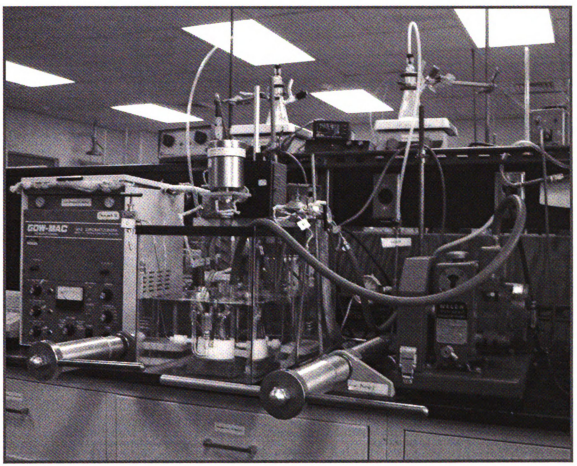

Figure 6.1 Set up of the *P-x-y* apparatus

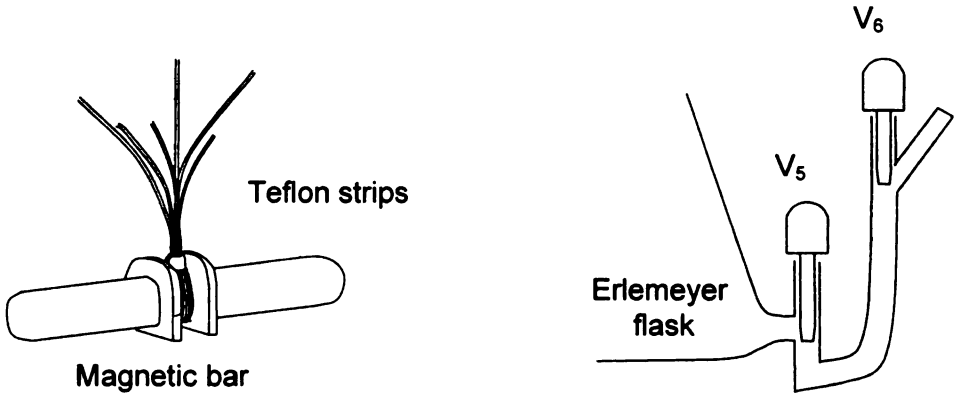

Figure 6.2 Configuration of the Agitator and Liquid Sampling Valves

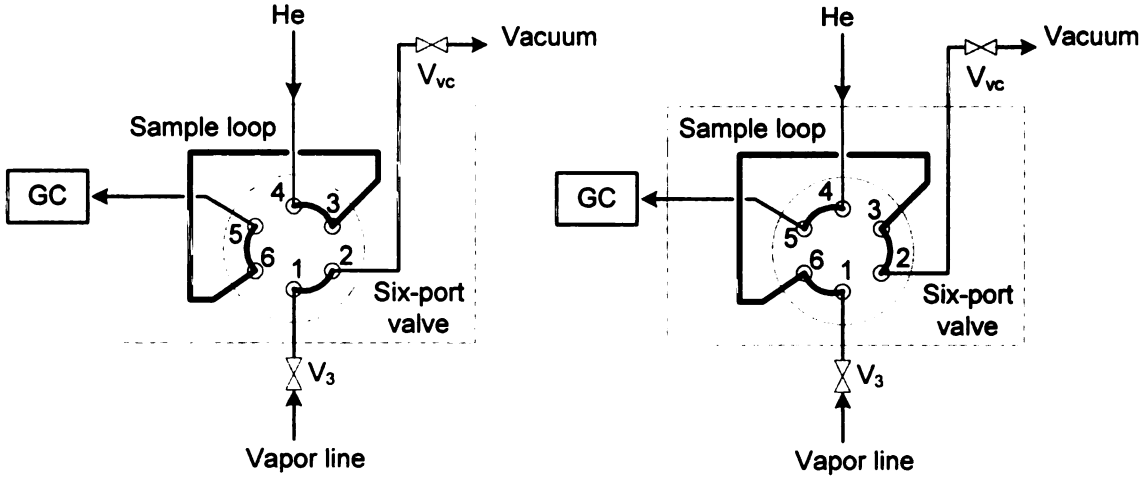

Figure 6.3 Vapor Sampling Valve at the *Inject* (left) and *Load* (right) Position

6.2.1 – P-x-y Data of Ethyl Lactate Systems and (Ethanol + Water at 40 °C) — A Reprint of the Paper *"Vapor-Liquid Equilibria in the Systems Ethyl Lactate + Ethanol and Ethyl Lactate + Water"*

Included in this section is a copy of the paper *Vapor-Liquid Equilibria in the Systems Ethyl Lactate + Ethanol and Ethyl Lactate + Water,* by D.T. Vu, C T. Lira, N. S. Asthana, A. K. Kolah, and D. J. Miller. The paper is reformatted from Journal of Chemical Engineering Data, 2006, 51, 1220-1225, for the same purpose as was explained in section 5.1 of chapter 5.

J. Chem. Eng. Data **2006**, 51, 1220-1225

Vapor-Liquid Equilibria in the Systems Ethyl Lactate + Ethanol and Ethyl Lactate + Water

Dung T. Vu, Carl T. Lira,* Navinchandra S. Asthana, Aspi K. Kolah, and Dennis J. Miller

Department of Chemical Engineering and Materials Science, 2527 Engineering Building, Michigan State University, East Lansing, Michigan 48824

Abstract

A simple vapor-liquid equilibrium (VLE) apparatus has been constructed to successfully measure the VLE of binary ethyl lactate systems that have relatively high differences in volatility ($P_2^{sat}/P_1^{sat} \sim 7.0$). Degassing is done in situ, reducing the experimental time considerably. Isothermal VLE of the ethyl lactate + ethanol system was measured at (40.0, 60.1, and 80.2) °C, and the isothermal VLE of the ethyl lactate + water system was measured at (40.0 and 60.0) °C. The ethyl lactate + ethanol system is slightly nonideal, and the ethyl lactate + water system forms a minimum boiling azeotrope. Isothermal data for ethanol + water were measured at 40.0 °C to demonstrate reliability of the apparatus.

* Corresponding author. Phone: (517)355-9731. E-mail: lira@egr.msu.edu.

Published on Web 06/28/2006

Introduction

Interest in lactate esters is increasing due to emphasis on environmentally friendly solvents from bio-derived sources. Lactate esters (primarily ethyl lactate) have excellent solvent properties and low toxicity and are candidates to replace many halogenated solvents including ozone-depleting CFCs, carcinogenic methylene chloride, toxic ethylene glycol ethers, and chloroform.[1] Lactate esters such as ethyl lactate have the ability to dissolve a wide range of chemicals. They can be used to remove greases, silicone oils, and adhesives in cleaning a variety of metal surfaces for fabrication and coating applications. Because ethyl lactate exists in beer, wine, and soy products, it has been approved by the FDA for use in food industries for many years.

Despite their numerous attractive advantages, the production volume of lactate esters used has been small in industry. Traditional batch processing is expensive compared to the potential for continuous processing. New technologies have been developed to yield lactate esters from carbohydrate feedstocks via esterification using reactive distillation or pervaporation membranes.[2,3]

Esterification usually requires distillation to purify the esters. For column designs and process simulation, thermodynamic properties such as reliable vapor-liquid equilibrium (VLE) data of the related components are valuable. Recently, phase equilibrium of the methyl lactate system has been studied, and VLE of some lactate esters with their associated alcohols at 101.33 kPa were made available.[4,5] However, no information for the ethyl lactate + water system has been found in the existing literature. This work presents the equilibrium *P-x-y* data of the ethyl lactate + ethanol and ethyl lactate + water systems. We have chosen to collect *P-x-y* data isothermally because the temperature can be kept low where the reactive system ethyl lactate + water is kinetically more stable.

Experimental Details

Chemicals. Ethyl (*S*)-(-)-lactate 98 % and ethyl alcohol (200 proof) were purchased from Sigma Aldrich. Water (HPLC grade) was obtained from J. T. Baker, Inc. Water and ethyl alcohol were used as received. Ethyl lactate was further purified by vacuum distillation. Only 85-90 % of the pre-distilled volume was collected for the VLE experiments. Both the first overhead fraction (5-10 %) and the reboiler residue (5 %) were discarded. No detectable water or ethanol remained in the ethyl lactate after distillation as determined using gas chromatography (GC). The GC procedure will be described in the analytical method section.

Apparatus. A *P-x-y* apparatus was constructed for VLE measurements of binary systems from ambient temperature to 353K (Figure 1). The apparatus is based on the design of similar equipment described in the literature.[6] The apparatus has three main sections: an equilibration section, a feed section, and a sampling section.

(a) Equilibrium Chamber and Isothermal Bath. A modified 125 mL Erlenmeyer flask was used as an equilibrium cell. The cell was placed on a submersible stir plate immersed in the isothermal water bath. Temperature was maintained by a PolyScience series 730 circulator. To minimize water bath evaporation, approximately 1 in. of mineral oil was added to the bath to cover the water's surface when conducting experiments at 80 °C. The bath had fluctuations less than ± 0.01 °C at 40 °C below, but the variation was ± 0.05 °C at (60 and 80) °C. Temperature was measured using a thermometer calibrated against a NIST traceable thermometer; the accuracy was better than ± 0.001 °C. Pressure inside the cell was measured using a MKS Baratron model PDR 2000 dual capacitance diaphragm absolute pressure gauge. The pressure gauge provides reliable values between 0.13 and 133 kPa with the resolution of 0.013 kPa and an accuracy of 0.25 % of the reported reading.

The cell was connected to the feed and gas sampling systems using 1/16 in. o.d. 316 stainless steel tubing sealed to the chamber using ACE glass Teflon adapters (Catalog No. 5801-07) and connectors (Catalog Nos. 5854-07 and 5824-24). The Baratron gauge was attached to the top of the cell using a length of glass tubing with a tapered ground glass joint to provide a vacuum tight connection. The Baratron and glass were joined using a Cajon union (SS-4-UT-6).

The liquid and vapor phases were both stirred. Two different vapor-phase stirrer configurations were used in the course of this work. In the first configuration, a vertical length of 1/8 in. stainless steel rod was used to support the vapor-phase agitator. The rod was placed vertically in the center of the equilibrium cell; the bottom end was soldered to a small clip mounted onto a magnetic stir bar. At the middle of the vertical rod, two small arms were created by soldering a wire to the rod. Teflon plumbing tape (1/2 in. × 1 in. × 0.04 in.) was wrapped around the arms to create the agitator. The bar and Teflon tape provided the means of mixing for the liquid and vapor phases simultaneously. However, when the apparatus was modified by adding a liquid-phase sampling section, the equilibrium chamber had to be placed 3/4 in. above the submersible stir plate. Consequently, the magnetic field was considerably reduced, the bottom of the flask was no longer flat, and the vapor stirrer did not work reliably. Thin polypropylene strips (0.06 in. × 3 in. × 0.04 in.) were wrapped around the center of the magnetic stir bar, and small supports were fabricated from Teflon sheet.

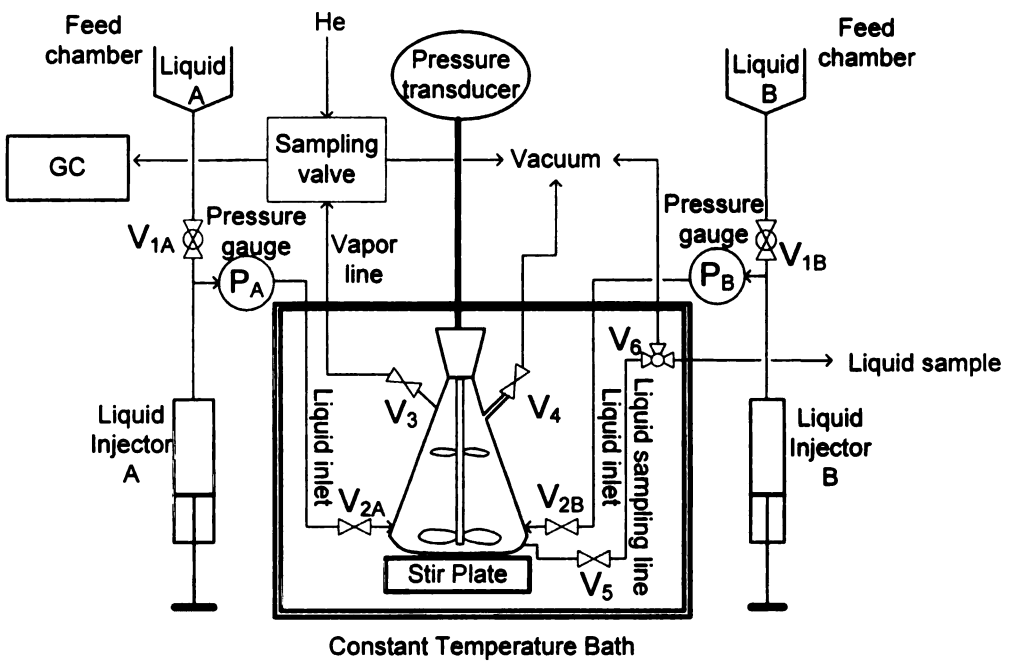

Figure 1. Schematic of the apparatus

(b) Feed Section. Two 125 mL flasks and two liquid injectors were connected using 1/4 in. o.d. polypropylene and 316 stainless steel tubing and Swagelok adapters. Polypropylene tubing provided flexibility for the connection between glass (feed chambers) and stainless steel valves (V_{1A}, V_{1B}) and permitted observation of the liquid level in the feed section. The length of polypropylene tubing was minimized to limit permeability of air from the environment. The flasks were mounted 3 ft above the injectors, providing a hydrostatic head to load the injectors with liquids from the flasks when valves V_{1A} and V_{1B} were opened (Figure 1). The liquid

injectors were 30 mL calibrated pumps (High-Pressure Equipment Company 62-6-10) used to meter liquids to the equilibrium cell with the accuracy of ± 0.003 mL of the injected volume. Pressure of the liquids inside the injectors was monitored using inexpensive pressure gauges.

(c) Liquid-Phase Sampling. Degassing of the liquids in the feed section (flasks and injectors) was tedious. However, we found that the liquids could be degassed reliably within the equilibration chamber. Complete degassing was easy to identify by a reliable stable pressure in the chamber after repeatedly pulling the pressure down about 1 kPa. Because of the expected minor shift in composition during degassing after liquids were charged to the equilibrium chamber, a liquid sampling section was added to the apparatus. This modification was done for the ethyl lactate + water system, reducing considerably the experimental time. High vacuum needle valves, purchased from Chemglass (CG-553-02, CG-534-02) were connected by a 4 in. length of 1/4 in. o.d glass tubing. To take a liquid sample, valve V_6 was first opened to permit evacuation of the sample region. Then valve V_6 was closed before valve V_5 was cracked opened for 10 s to collect approximately 0.2 mL of liquid from the equilibrium cell. No fluctuation in pressure of the equilibration cell was noted when valve V_5 was opened. After sample collection, valve V_5 was closed entirely and valve V_6 was opened fully to permit a narrow Teflon tube connected to a syringe to be inserted for withdrawal of most of the liquid sample. To remove all residual traces of liquid, acetone was added through V_6 and then removed via the syringe apparatus. Any remaining acetone was evaporated under vacuum while the cell was undergoing the next equilibration.

(d) Vapor Phase Sampling. The vapor sample system was based on a Valco six-port switching valve (00V-1375V) positioned immediately above the water bath, approximately 8 in. from the equilibrium cell. A high-temperature rotor (SSAC6WE, 225 °C) and preload nut (PLAW30) were chosen as part of the valve assembly. The vapor line was 1/16 in. stainless steel with a 1/16 in. stainless steel valve. The vacuum line was a 6 in. length of 1/16 in. stainless steel connected to a 1/16 in. valve and adapted to vacuum tubing. The He carrier gas entered through 1/16 in. stainless tubing connected to the outlet of the gas chromatography (GC) injector, and 1/16 in. stainless tubing was used to return the sample to the GC oven where it was fed onto the column. The GC was placed as close as practical to the apparatus, using about 24 in. of tubing between the GC and the sample valve. A 1.8 mL sample loop was created by adapting a coiled length of 1/4 in. tubing to the Valco ports. Each vapor sample was equivalent to about 0.3 μL of the related liquid mixture directly injected into the GC. To avoid condensation of the high boiling components, the vapor line was heat-traced and maintained 15-20 °C above the temperature of the equilibrium cell. To collect a vapor-phase sample, the sample loop was evacuated by placing the valve in the "load" position with the vapor line valve V_3 closed and the vacuum valve V_{vc} opened; then the valve V_{vc} was closed, and the vapor line valve was opened. The loading was done within 1 min, and then the valve V_3 was closed and the sampling valve was switched quickly to the "inject" position. No pressure drop in the equilibrium cell was observed during the course of vapor sampling, since the volume of vapor sample was small as compared to the volume of the chamber. Additional details on the vapor and liquid sampling configurations are available from the corresponding author.

Experimental Procedure. A Sargent-Welch two-stage vacuum pump (model 1400) was used to evacuate the apparatus and sample sections and to provide degassing of liquids. Prior to the experiment, the entire system was evacuated and checked for the leaks. A stable base pressure of 0.07-0.09 kPa for 3-4 h indicated that the chamber was leak tight. Liquids were degassed before they were loaded into the injectors. During the degassing process, fluids in the flasks were shaken and tested using the click test for degassing as described by Van Ness and Abbott[7] and Campbell and Bhethanabotla.[8]

When performing experiments where the liquid composition was determined from the quantities of liquids injected, the following tests supplemented the click test to verify complete degassing in the feed lines and injectors and to verify a leak-tight feed section: (1) Pressure of fully loaded injectors with degassed liquids observed from gauges P_A and P_B had to be steady and equal to the vapor pressure of liquids. If the pump A (or B) was operated while V_{1A} (or V_{1B}) was opened and V_{2A} (or V_{2B}) was closed, the displacement of liquid level in the polypropylene feed line had to be proportional to the displacement inside the injector. (2) If the V_{1A} (or V_{1B}) and V_{2A} (or V_{2B}) were closed, the pressure of the injector A (or B) had to increase instantaneously when the pump started to compress the liquid inside that injector.

To inject liquid A (or B) to the equilibrium cell, pressure P_A (or P_B) was raised to approximately 0.3 MPa before valve V_{2A} (or V_{2B}) was opened. After the pressure of the injector dropped, the valve was closed, the injector pressure was restored, and the injected volume was recorded.

To carry out the experiment, 10-20 mL of component 1 of the studied binary system was charged to the equilibrium cell. After the vapor pressure of this pure liquid was measured, a predetermined quantity of the component 2 was added to the cell. After equilibration, vapor and liquid samples were collected. These steps were continued until the liquid mole fraction of component 1 approached 0.1. Afterward, the equilibrium chamber was emptied; the entire system was cleaned and degassed thoroughly. Then, the process was reversed, charging the equilibrium cell first with component 2 and then adding component 1.

The volume of the initial charge in the experiments with the ethyl lactate + ethanol system was selected to ensure that error in calculation of liquid compositions from the injected volume would be negligible. For the ethyl lactate + water system, 5mL of liquid inside the equilibrium chamber was found to be sufficiently large to ensure accurate composition measurements, because the volumes of liquid injections were not critical with the liquid sampling section in place. Both liquid and vapor of the studied binary mixture were well-mixed and were allowed to reach equilibrium before any measurement was performed. Equilibration was identified by the consistency of the equilibrium pressure reading from the Baratron following vapor withdrawals using vacuum and by the reproducibility of the equilibrium vapor-phase composition.

Analytical Methods. Liquid compositions in the ethanol + water and ethyl lactate + ethanol mixtures were calculated from the known volume of each component charged to the cell. For ethyl lactate + water, samples of the liquid phase were taken via the liquid sampling section, and the compositions were determined from GC analysis. Vapor samples of the studied binary mixtures were injected to the gas chromatograph using the vapor sample valve.
The GOW-MAC 350 gas chromatograph was operated under isothermal conditions using a carrier stream of helium at 35mL/min. The column temperature was 220 °C in experiments involving ethyl lactate, but it was reduced to 150 °C for the ethanol + water system. A thermoconductivity detector was set at 290 °C and 110 mA filament current. The column packing used was Poropak Q 50/80, packed in 6 ft long × 1/8 in. o.d. × 0.085 in. wall stainless steel tubing. To ensure that all vapor samples were analyzed in the column without loss via condensation,1 ft of 1/16 in. o.d. 316 stainless steel tubing was added to the column and used as a precolumn heater within the GC oven.

Calibrations of known compositions of mixtures were done for each binary system to obtain the correlation between the ratio of GC peak areas and the mixture compositions. From the calibration, the unknown compositions of the injected samples were determined. The amounts of each component in the calibrated mixtures were weighed using an electronic balance with its readability of 0.1 mg. The standard mixtures were prepared gravimetrically in an approximate size of 1.0 ± 0.3mg; therefore, the deviation in calculation of molar compositions was negligible. To reduce the error due to the possible evaporation of the more volatile component, two duplicate

mixtures were prepared for each calibration point. Three GC injections were done for every data point, in both calibration and sample analyses. The difference in the ratio of peak areas of the triplicate GC injections was less than ± 0.05 % of the calculated value.

Results and Discussion

Ethanol + Water System. Isothermal VLE data for the ethanol + water system at 40.0 °C were collected and compared to literature data for validation of reliability of the constructed VLE apparatus (Table 1). The ethanol + water system was chosen to study because its components are in the system of interest, and 40.0 °C isothermal literature data are available from two independent sources. Both literature and experimental data were regressed using the Britt-Luecke algorithm, maximum-likelihood principle, provided by ASPEN PLUS 12.1. The area test of Redlich-Kister and point-to-point test of Van Ness and Fredenslund were used to check for data reliability.[9-11] The data are considered to pass the area test if the difference between the positive and negative areas is less than 10 %. However, to pass the point-to-point test, the absolute mean deviation between the calculated and experimental vapor compositions should be ≤ 0.01.

Table 1. VLE data for ethanol (1) + water (2) at 40.0 °C

$P^{40.0}$/kPa	$x_1^{40.0}$	$y_1^{40.0}$	$P^{40.0}$/kPa	$x_1^{40.0}$	$y_1^{40.0}$
7.41	0	0	14.25	0.158	0.541
7.83	0.005	0.036	14.93	0.201	0.573
8.08	0.007	0.069	15.51	0.256	0.598
8.27	0.010	0.096	15.79	0.319	0.612
8.55	0.014	0.133	16.37	0.418	0.655
8.97	0.020	0.181	16.57	0.448	0.660
9.32	0.026	0.221	16.96	0.518	0.697
9.85	0.035	0.269	17.21	0.583	0.730
10.64	0.050	0.332	17.51	0.682	0.767
11.72	0.075	0.407	17.71	0.748	0.805
12.17	0.085	0.421	17.81	0.828	0.841
13.01	0.108	0.478	17.95	0.892	0.893
13.12	0.111	0.474	18.00	0.943	0.960
13.77	0.136	0.519	18.00	1.000	1.000

UNIQUAC with the Hayden and O'Connell (HOC) virial coefficient correlation were used to evaluate thermodynamic consistency. The point-to-point test value was 0.011, significantly smaller than that of 0.063 from Udovenko and Fatkulina[12] and 0.248 from Mertl.[13] In the available literature, these are the only isothermal VLE data that can be found for the ethanol + water system at 40.0 °C. Neither data from Udovenko and Fatkulina nor this work passed the area test, but the value of 10.40 %, which is obtained from this work, is smaller than Udovenko and Fatkulina's value and close to the accepted value. The smoothness of the *P-x-y* curve in Figure 2 and results from the thermodynamic consistency tests show that the VLE data of ethanol + water from this work are very reliable and more consistent than existing literature data at 40 °C.

Ethyl Lactate + Ethanol System. VLE were measured at (40.0, 60.1, and 80.2) °C for this system (Table 2). To minimize the effects of any systematic errors in particular run, the VLE experiments were performed at least five times using different increments and decrements of each

component molar fraction at the reported temperature. All the activity coefficient models listed in Table 3 provide similar correlation of experimental data. The value of R used in the NRTL-HOC equation is 0.3. Figure 3 shows the representation of the UNIQUAC with the HOC correlation. The same nonlinear regression method and consistency tests were used as described. For the HOC method, the η values were assumed to be 1.3 for ethyl lactate + ethanol and 0.53 for ethyl lactate with itself. These values were based on the assumption that solvation of ethyl lactate would be similar to that of ethyl acetate in ethyl acetate + ethanol mixture and that ethyl lactate pure self-interactions would be similar to ethyl acetate pure self-interactions. It should be noted that the calculated vapor fugacity coefficient of ethyl lactate is in the range of 0.990 to 0.998 and that for ethanol is from 0.993 to 0.999 at the system pressure.

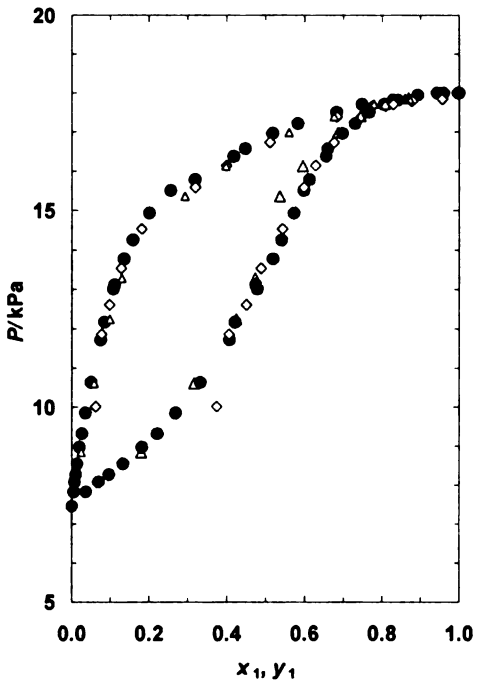

Figure 2. *P-x-y* of ethanol (1) + water (2) at 40.0°C: •-this work, Δ- Udovenko and Fatkulina[12], and ◊-Mertl.[13]

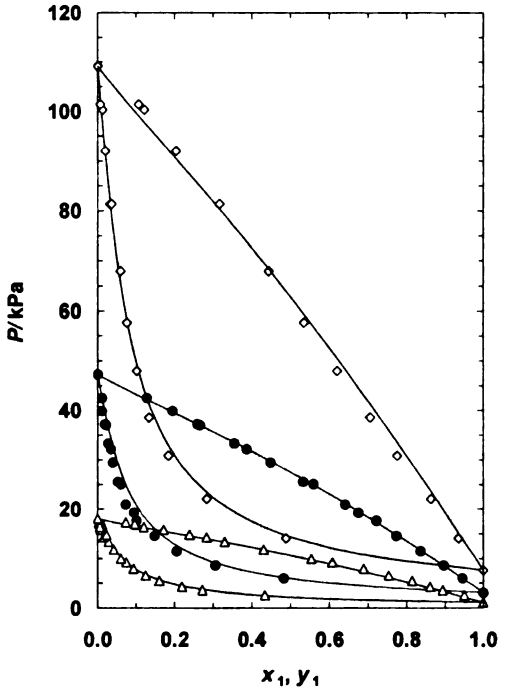

Figure 3. *P-x-y* of ethyl lactate (1) + ethanol (2) system. Δ 40.0°C; •60.1°C; ◊ 80.2°C; solid lines are the representation of UNIQUAC with HOC correlation.

Data are combined from at least five different runs for each reported temperature as described. All P-x-y diagrams are smooth and do not exhibit any trends of systematic error within specific runs. All experimental data satisfied the point-to-point test, but only data at 40.0 °C passed the area test. The area test results were 31 % and 19 % for data at (60.1 and 80.2) °C, respectively. The inconsistency could be due to the error in measuring the vapor phase at low concentration of ethyl lactate where the GC detection was limited. Another potential source of error could be minor decomposition of the ethyl lactate in the GC detector during vapor-phase analysis. It was noted during runs that the outlet lines of the thermal conductivity detector gradually became restricted due to deposits over a period of several hours. The lines were kept clear using a syringe cleaning wire, but this method did not allow determination of the extent of decomposition. Plugging of lines was not noted on the GC used to analyze the liquid samples. Additional experimental runs were consistent with each other, as compiled in the tables and figures, and did not improve the results of the consistency tests.

Table 2. VLE data for ethyl lactate (1) + ethanol (2) systems at (40.0, 60.1, and 80.2) °C

$P^{40.0}$/kPa	$x_1^{40.0}$	$y_1^{40.0}$	$P^{60.1}$/kPa	$x_1^{60.1}$	$y_1^{60.1}$	$P^{80.2}$/kPa	$x_1^{80.2}$	$y_1^{80.2}$
1.12	1.000	1.000						
2.57	0.951	0.433	3.03	1.000	1.000			
3.59	0.893	0.271	5.97	0.946	0.482			
4.28	0.862	0.219	8.55	0.897	0.306			
5.45	0.814	0.16	11.41	0.836	0.205			
6.55	0.754	0.125	14.51	0.774	0.148	7.63	1.000	1.000
7.91	0.689	0.093	17.64	0.722	0.101	14.08	0.935	0.488
9.21	0.608	0.074	19.24	0.675	0.095	22.08	0.863	0.283
9.92	0.554	0.061	20.86	0.641	0.073	30.82	0.775	0.184
11.76	0.43	0.042	25.05	0.559	0.06	38.54	0.705	0.133
13.31	0.329	0.029	25.52	0.532	0.052	47.94	0.62	0.101
14.23	0.283	0.015	29.38	0.448	0.039	57.66	0.534	0.075
14.76	0.239	0.024	32.1	0.386	0.034	67.94	0.443	0.059
15.81	0.172	0.008	33.26	0.354	0.027	81.3	0.316	0.032
16.81	0.102	0.012	36.97	0.266	0.022	81.37	0.316	0.036
16.99	0.097	0.004	37.17	0.259	0.019	92.05	0.203	0.02
17.31	0.073	0.003	39.81	0.195	0.011	100.31	0.121	0.013
16.37	0.120	0.000	42.46	0.128	0.012	101.42	0.106	0.007
18.01	0.000	0.000	47.21	0.000	0.000	109.12	0.000	0.000

Table 3. Binary Parameters of Ethyl Lactate (1) + Ethanol (2) System and Average Absolute Percent Deviation (%) for Equilibrium Pressure (P) and Vapor-Phase Mole Fractions (y_1, y_2)[a]

	Equation	Binary Parameters		Average Absolute Percent Deviation		
		b_{12}/K	b_{21}/K	P/%	y_1/%	y_2/%
UNIQUAC – IG	$\tau_{ij} = \exp(b_{ij}/T)$	-43.00	-23.10	3.3	23.2	1.5
UNIQUAC-HOC	$\tau_{ij} = \exp(b_{ij}/T)$	-40.03	-29.40	3.1	24.7	1.4
NRTL-HOC	$G_{ij} = \exp(-0.3b_{ij}/T)$	-298.69	585.62	3.8	24.8	1.5
Van-Laar-HOC	$A_{ij} = b_{ij}/T$	169.19	65.21	3.3	24.7	1.5
WILSON-HOC	$\Lambda_{ij} = \exp(b_{ij}/T),\ V_i/V_j = 1$	-198.48	71.55	3.7	24.8	1.5

[a] The vapor-phase Hayden-O'Connell parameters are given in the text.

The prediction of isobaric VLE data of ethyl lactate + ethanol at 101.33 kPa using the binary parameters obtained from the reported data are in good agreement with Peña-Tejedor et al.[14] For the ethyl lactate + water system at 40.0 °C, with Peña-Tejedor's binary parameters, the activity coefficients at infinite dilution of ethanol and ethyl lactate are predicted to be 1.38 and 1.35, respectively, using the UNIQUAC-HOC model. From this work, these values are 1.25 and 1.67,

respectively. Similar results were obtained for the data at (60.1 and 80.2) °C.

The P-x bubble line is nearly linear, and the infinite dilution activity coefficients are not large. The ethyl lactate + ethanol system thus can be considered slightly nonideal. This is due to the presence of the hydroxyl group in ethyl lactate, such that the interaction between ethyl lactate molecules is similar to their interaction with the ethanol molecule.

Ethyl Lactate + Water System. VLE at (40.0 and 60.0) °C were measured for the ethyl lactate + water binary system (Table 4). Ethyl lactate was hydrolyzed significantly at 80°C, as verified by the presence of ethanol in GC analyses. Hydrolysis was not detected in the experiments performed at (40.0 and 60.0) °C. The VLE experiments at each listed temperature were performed five times; the same methods as described for the ethyl lactate + ethanol system were used. Figure 4 shows that the system has a minimum boiling azeotrope, occurring at 5-7 mol % ethyl lactate. Due to the narrow phase envelope at high water concentrations, it was not possible to determine the exact azeotrope composition using gas chromatography, even though the analysis was very reproducible.

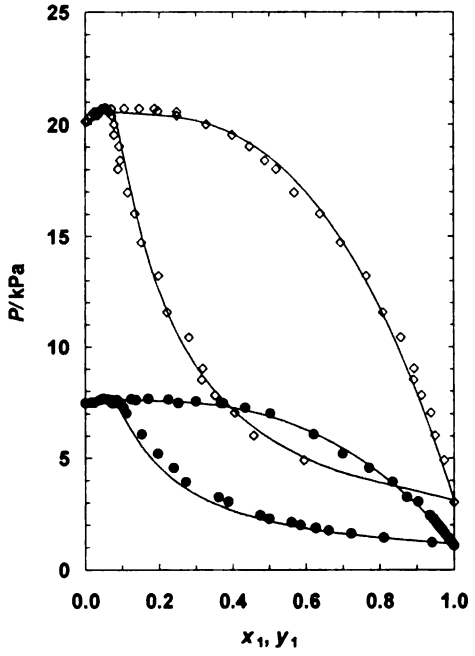

Figure 4. *P-x-y* of ethyl lactate (1) + water (2) system. • 40.0°C; ◊ 60.0°C; solid lines are the representation of UNIQUAC with HOC correlation.

Table 4. VLE data for ethyl lactate (1) + water (2) system at (40.0 and 60.0) °C

$P^{40.0}$/kPa	$x_1^{40.0}$	$y_1^{40.0}$	$P^{60.0}$/kPa	$x_1^{60.0}$	$y_1^{60.0}$
			3.03	1.000	1.000
			4.91	0.973	0.594
			6.01	0.949	0.457
1.12	1.000	1.000	7.04	0.938	0.405
1.23	0.994	0.941	7.83	0.912	0.351
1.44	0.985	0.811	9.04	0.892	0.319
1.63	0.975	0.722	8.53	0.891	0.315
1.76	0.970	0.661	10.44	0.856	0.280
1.87	0.964	0.626	11.56	0.808	0.222
2.00	0.958	0.584	13.21	0.763	0.198
2.12	0.952	0.560	14.72	0.694	0.152
2.28	0.945	0.500	16.03	0.638	0.135
2.44	0.935	0.474	16.97	0.568	0.115
3.05	0.903	0.388	18.01	0.518	0.089
3.25	0.874	0.361	18.40	0.488	0.094
3.93	0.834	0.272	19.04	0.446	0.092
4.56	0.770	0.240	19.55	0.399	0.078
5.20	0.699	0.197	20.01	0.328	0.078
6.07	0.620	0.153	20.40	0.248	0.071
7.01	0.502	0.111	20.57	0.248	0.066
7.27	0.433	0.103	20.61	0.197	0.059
7.47	0.374	0.073	20.70	0.187	0.059
7.48	0.367	0.094	20.70	0.146	0.055
7.56	0.300	0.068	20.72	0.106	0.052
7.48	0.252	0.087	20.69	0.070	0.049
7.64	0.225	0.061	20.68	0.042	0.044
7.67	0.171	0.050	20.41	0.027	0.033
7.61	0.137	0.085	20.48	0.023	0.032
7.65	0.124	0.046	20.56	0.022	0.027
7.61	0.073	0.039	20.33	0.012	0.012
7.49	0.025	0.015	20.15	0.005	0.005
7.47	0.000	0.000	20.01	0.000	0.000

Table 5. Binary Parameters of Ethyl Lactate (1) + Water (2) System and Average Absolute Percent Deviation (%) for Equilibrium Pressure (P) and Vapor-Phase Mole Fractions (y_1, y_2)[a].

	Equation	Binary Parameters		Average Absolute Percent Deviation		
		b_{12}/K	b_{21}/K	P/%	y_1/%	y_2/%
UNIQUAC – IG	$\tau_{ij} = \exp(b_{ij}/T)$	250.51	-133.02	2.4	22	4.1
UNIQUAC-HOC	$\tau_{ij} = \exp(b_{ij}/T)$	248.19	-131.44	2.4	22.2	4.1
NRTL-HOC	$G_{ij} = \exp(-0.3b_{ij}/T)$	-87.07	967.2	3.4	21.6	3.8
Van-Laar-HOC	$A_{ij} = b_{ij}/T$	895.05	307.06	3.4	21.4	4.2
WILSON-HOC	$\Lambda_{ij} = \exp(b_{ij}/T),\ V_i/V_j = 1$	-978.35	-51.56	2.1	22.9	5.0

[a] The vapor-phase Hayden-O'Connell parameters are given in the text.

The data are fitted with several thermodynamic models, and the binary parameters determined are listed in Table 5. All of the selected activity models fit the data equally well; the deviations are given in Table 5. The HOC η value of 1.3 was used for ethyl lactate with water (based on the literature value for ethyl acetate + water), and the same method as described above was applied for data regression. The azeotrope composition is predicted to be at 6.5-6.7 mol% ethyl lactate, based on the UNIQUAC-HOC fit.

The data satisfy the area test but are less satisfactory when analyzed via the point-to-point test. The values of 8.6 % and 0.04 for area and point-to-point tests, respectively, were obtained for the VLE data at 40.0 °C. Likewise, the values for data at 60.0 °C were 4.6% and 0.037. Because the point-to-point test is more significant for isothermal VLE than the area test, the data were carefully reevaluated, including the regression used to generate the GC calibration curve. It was found that the difference in calculation of phase compositions using different representations of the GC calibration curve is negligible. However, the consistency tests are very sensitive to a small change in vapor phase composition. For example, if data point at P = 1.2 kPa in Table 4 is omitted, the value of the point to-point test changes from 0.04 to 0.026. We have also evaluated point-to-point consistency using Legendre polynomials[11] and the Modified Margules[15] method to represent the excess Gibbs energy, but the differences between the calculated and measured values in vapor composition are also larger than the target of 0.01. Consistency failure due to inadequacy of the HOC method is unlikely because the vapor fugacity coefficients are near 0.989 and 0.993 across the composition range for ethyl lactate and water, respectively. Additional experimental runs were consistent with each other as shown in the tables and figures and did not improve the consistency test results.

Fitting of the ethyl lactate + water system is challenging because the infinite dilution activity coefficients are large. These coefficients are 17.7 for ethyl lactate and 2.8 for water from UNIQUAC-HOC in ASPEN 12.1. The UNIQUAC-HOC fails to represent the vapor phase accurately at 40.0 °C and fails to represent the pressure maximum accurately at 60.0 °C, as shown in Figure 4.

The vapor-phase analysis in this system may be subject to the same potential decomposition of ethyl lactate as mentioned earlier. Degradation was more noticeable in this system than in the ethyl lactate + ethanol system.

Summary and Conclusions

This work presents a simple design of an isothermal VLE apparatus that is capable of measuring the vapor pressure of single components down to about 0.7 kPa and the VLE of nonideal binary systems. The P-x-y apparatus is valuable for collecting data at low temperature, where reactive chemicals are kinetically more stable. With the liquid sampling section and the ability to perform the degassing in situ, the apparatus can be extended to multicomponent systems. Data have been evaluated with standard consistency tests, and all data sets passed or nearly passed at least one of the standard tests.

Acknowledgment

The authors are grateful to Professor Scott Campbell (University of South Florida)for suggestions. Appreciation is also extended to Elisabeth Newton for her work in the assembly of an earlier version of the apparatus.

Literature Cited

(1) U.S. Environmental Protection Agency, 1998 Alternative solvents/reaction conditions award, citation to Argonne National Laboratory. http://www.epa.gov/greenchemistry/ascra98.html (Accessed December 2005).

(2) Asthana, N.; Kolah, A. K.; Vu, D. T.; Lira, C. T.; Miller, D. *Org. Process Res. Dev.* **2005**, *9*, 599-607.

(3) Benedict, D. J.; Parulekar, S. J.; Tsai, S.-P. *Ind. Eng. Chem. Res.* **2003**, *42*, 2282-2291.

(4) Sanz, M. T.; Calvo, B.; Beltran, S.; Cabezas, J. L. *J. Chem. Eng. Data.* **2002**, *47*, 1003-1006.

(5) Sanz, M. T.; Beltran, S.; Calvo, B.; Cabezas, J. L. *J. Chem. Eng. Data.* **2003**, *48*, 1446-1452.

(6) Pathare, S.; Bhethanabotla, V.R.; Campbell, S. W. *Ind. Eng. Chem. Res.* **2004**, *49*, 510-513.

(7) Van Ness, H. C.; Abbott, M. M. *Ind. Eng. Chem. Fundam.* **1978**,*17*, 66-67.

(8) Campbell, S. W.; Bhethanabotla, V. R. *Chem. Eng. Educ.* **1997**,34-39.

(9) Redlich, O.; Kister, A. T. *Ind. Eng. Chem.* **1948**, *40*, 345.

(10) Van Ness, H. C.; Byer, S.M.; Gibbs, R.E. *AIChE J.* **1973**, *19*, 238-244.

(11) Fredenslund, A.; Gmehling, J.; Rasmussen, P. *Vapor-Liquid Equilibria using UNIFAC*; Elsevier: Amsterdam, 1971.

(12) Udovenko,V.V.; Fatkulina ,L.G. Zh. Fiz. Khim. 1952, 26,1438.

(13) Mertl, I. *Collect. Czech. Chem. Commun.* **1972**, *37*, 366.

(14) Peña-Tejedor, S.; Murga, R.; Sanz, M.T. ; Beltrán,S. *Fluid Phase Equilib.* **2005**, 230, 197-203.

(15) Prausnitz, J.M.; Lichtenthaler, R.N.; Azevedo,E.G.d. *Molecular Thermodynamics of Fluid-Phase Equilibria*, 3rd ed.; Prentice-Hall: New York, 1999.

Received for review December 23, 2005. Accepted May 19, 2006. The authors thank the National Corn Growers Association and the U.S. Department of Energy for financial support.

JE050537Y

6.2.2 – P-x data of Citrate Systems

Triethyl citrate (99% purity, [CAS 77-93-0]) was purchased from Sigma-Aldrich, and water HPLC grade [CAS 7732-18-5] was from J.T. Baker. All chemicals were used without further purification, and the same experimental procedure [98] described for ethyl lactate systems was applied for citrate systems.

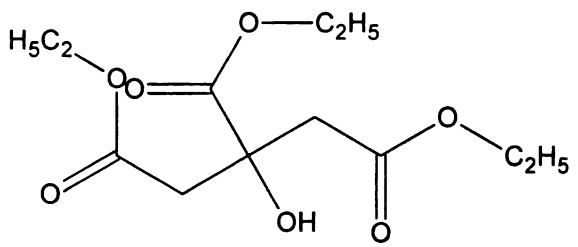

Figure 6.4 Structure of Triethyl Citrate

The structure of triethyl citrate is shown in Figure 6.4. It is the only ethyl ester of citric acid in this study, because no source of pure mono- or diethyl citrate was available for the VLE experiments. Similar to ethyl lactate, triethyl citrate is also an alpha-hydroxy ester. However, citric acid is a white crystalline powder at room temperature, and does not undergo self-esterification like lactic acid; therefore there was no concern of citric acid oligomer involved in the esterification producing citrate esters.

6.2.2.1 – Triethyl Citrate + Water

Phase behavior of triethyl citrate + water systems were studied at 25.0 °C and 60.0 °C, shown in Figure 6.5. Due to the low vapor pressure of triethyl citrate the gas chromatography could not get significant vapor readings, only *P-x* data were obtained.

Results of the VLE measurements are summarized in Table 6-1. It shows that triethyl citrate + water systems are partially miscible, represented by the horizontal

portion of the *P-x* curve. The miscibility slightly changes with temperature, and the mixtures exhibit a positive deviation from Raoult's law in the two-phase, vapor-liquid region.

The system probably does not have an minimum boiling heteroazeotrope because vapor pressure of ethyl citrate and water are very different from each other [99]. To determine whether the triethyl citrate + water system has a minimum or maximum hetero-azeotrope behavior, the normal boiling temperatures of triethyl citrate + water mixtures were carefully measured as molar composition of triethyl citrate was gradually varied between 0 and 0.5. Results showed that the change in temperature was negligible; it was not possible to determine whether the heteroazeotrope boiling point was above or below the boiling point of pure water within the error of uncertainty.

Table 6-1 *P-x* Data of Triethyl Citrate (1) + Water (2) at 25.0 °C and 60.0 °C

$P^{25.0}$/kPa	$x_1^{25.0}$	$P^{25.0}$/kPa	$x_1^{25.0}$	$P^{60.0}$/kPa	$x_1^{60.0}$	$P^{60.0}$/kPa	$x_1^{60.0}$
3.19	0.07			20.11	0.00		
3.19	0.13	3.19	0.64	20.13	0.07	19.84	0.54
3.19	0.17	3.04	0.66	20.14	0.13	18.98	0.57
3.19	0.31	2.81	0.69	20.15	0.18	17.91	0.60
3.19	0.37	2.91	0.69	20.18	0.23	16.50	0.64
3.17	0.43	2.73	0.72	20.19	0.27	15.54	0.69
3.20	0.43	2.65	0.74	20.21	0.31	13.11	0.75
3.21	0.54	2.58	0.75	20.21	0.34	9.74	0.81
3.21	0.60	2.15	0.82	20.46	0.39	5.26	0.89
3.19	0.62	1.33	0.90	20.38	0.48	0.63	1.00

For analyses of the *P-x-y* data, the vapor was assumed to be pure water. ASPEN UNIQUAC model was used to fit data. The binary parameters are b_{12} = -537.32 K, b_{21} = 94.18 K, and $\tau_{ij} = \exp(b_{ij}/T)$.

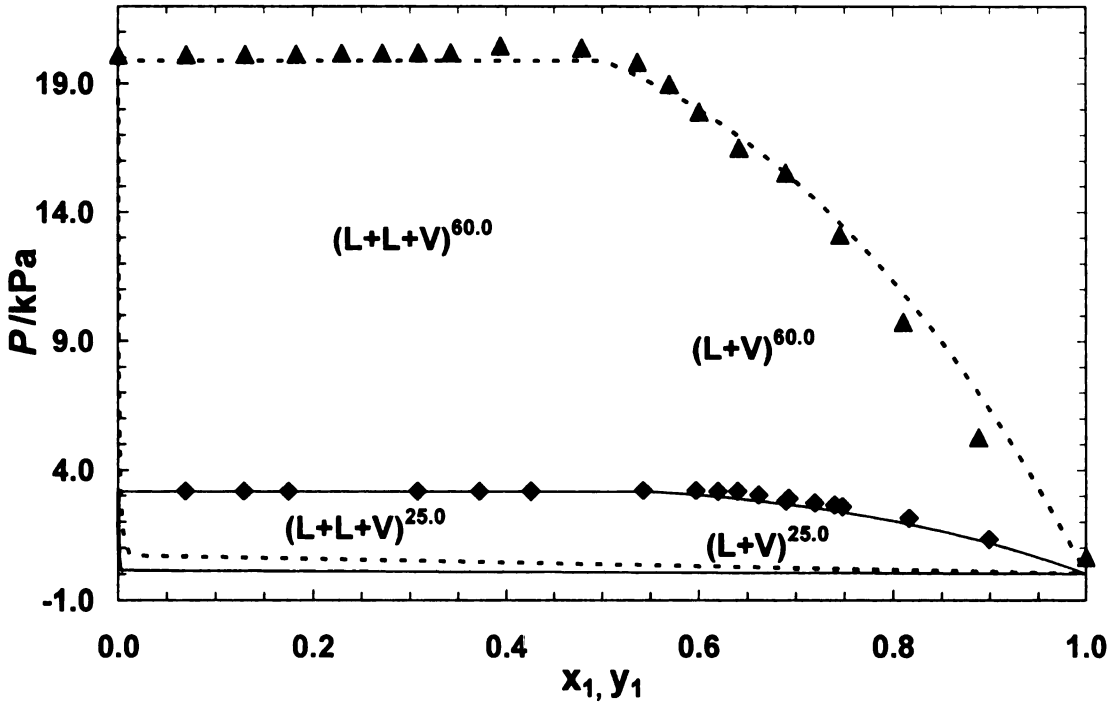

Figure 6.5 *P-x* of Triethyl Citrate (1) + Water (2): ▲, at 60 °C; ♦, at 25 °C
Dashed line and solid line are *P-x-y* representations of ASPEN UNIQUAC. (L+V) and (L+L+V) denote for two-phase and three-phase regions.

6.2.2.2 – Triethyl Citrate + Ethanol

The triethyl citrate + ethanol system was miscible. The *P-x* data at 40 °C are listed in Table 6-2, and Figure 6.6 shows the experimental measurements compared to the UNIQUAC prediction. In fitting data, vapor was assumed to be at least 99 mole% of ethanol, and the binary interaction parameters ($\tau_{ij} = \exp(b_{ij}/T)$) are b_{12} = -294.68 K, and b_{21} = 65.37 K for triethyl citrate (1) + ethanol (2). The UNIQUAC P-x-y generated from ASPEN was consistent with measurements and assumption of vapor molar compositions, but bubble pressure was poorly predicted when molar composition of ethanol is more than 0.5 (Figure 6.6). It should be noticed that a poor prediction for a complex

compound such as triethyl citrate is not atypical, and triethyl citrate was not included in the ASPEN data bank. This compound was defined using molecule connectivity and the UNIFAC functional groups in order to be used with ASPEN.

Table 6-2 P-x Data of Triethyl Citrate (1) + Ethanol (2) at 40.0 °C

$P^{40.0}$/kPa	$x_1^{40.0}$	$P^{40.0}$/kPa	$x_1^{40.0}$	$P^{40.0}$/kPa	$x_1^{40.0}$
18.00	0.00	14.96	0.29	7.67	0.72
17.15	0.11	13.67	0.36	5.00	0.84
16.08	0.24	11.55	0.48	2.96	0.92

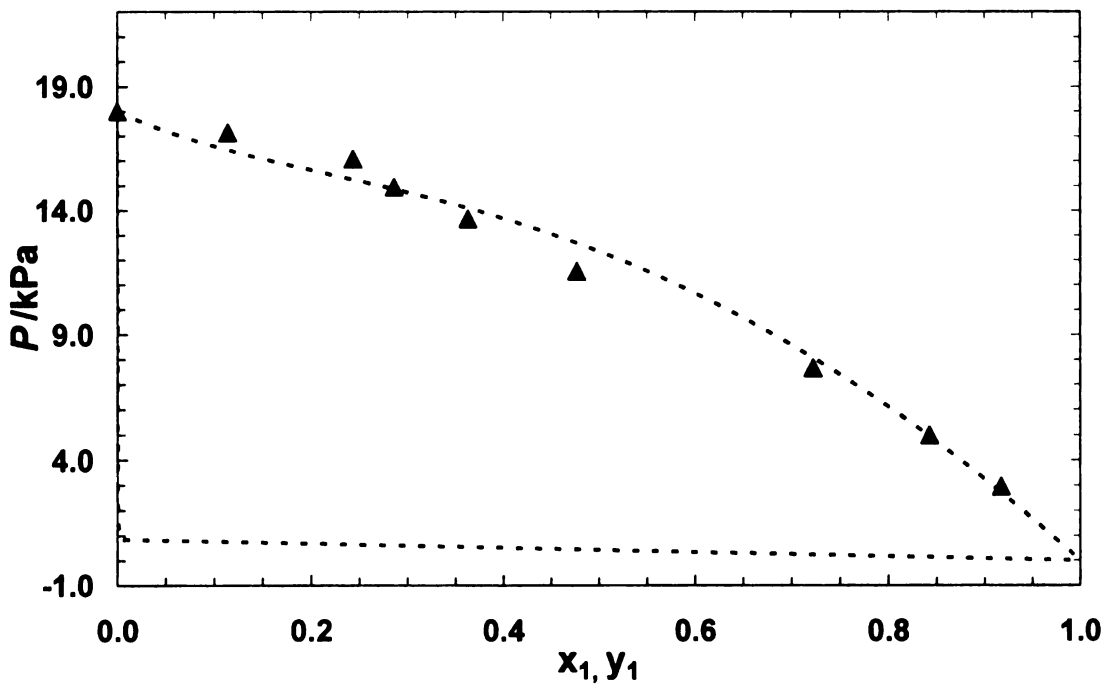

Figure 6.6 *P-x* of Triethyl citrate (1) + Ethanol (2) at 40 °C

▲, measured. Dashed line is *P-x-y* representation of ASPEN UNIQUAC

6.2.3 – P-x Data of Diethyl Succinate System

Diethyl succinate [CAS 123-25-1] was purchased from Sigma-Aldrich and was distilled prior to use. This compound has limited solubility in water [100]. Boiling temperatures of diethyl succinate (1) + water (2) systems were measured using a simple recirculating still. At 98.5 kPa, pure water boiled at 99.2 °C, and both systems of (x_1 = 0.043, x_2 = 0.957) and (x_1 = 0.061, x_2 = 0.939) boiled at 98.0 °C. This result indicated that diethyl succinate + water system has a minimum boiling azeotrope.

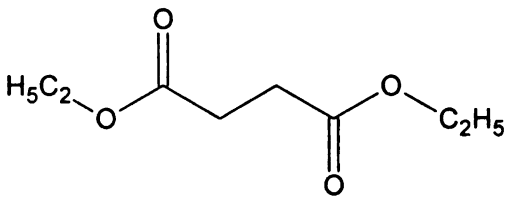

Figure 6.7 Structure of Diethyl Succinate

For the diethyl succinate (1) +ethanol (2) system, due to a low vapor pressure of diethyl succinate only *P-x* measurements could be taken. Table 6-3 lists data measured at 50.0 °C and the ASPEN UNIQUAC prediction is shown in Figure 6.8. In fitting data, vapor was assumed to be at 99.99 % of ethanol. The binary interaction parameters used in the UNIQUAC prediction ($\tau_{ij} = \exp(b_{ij}/T)$) are b_{12} = -149.17 K, and b_{21} = 17.88 K.

Table 6-3 Diethyl Succinate (1) + Ethanol (2) at 50.0 °C

$P^{50.0}$/kPa	$x_1^{50.0}$	$P^{50.0}$/kPa	$x_1^{50.0}$	$P^{50.0}$/kPa	$x_1^{50.0}$
29.53	0.00				
28.20	0.09	20.40	0.48	8.19	0.85
28.06	0.10	17.83	0.58	6.84	0.88
27.00	0.15	15.03	0.67	5.11	0.92
25.46	0.23	12.97	0.72	4.11	0.94
24.33	0.30	12.88	0.72	3.04	0.96
22.93	0.38	9.68	0.81	0.07	1.00

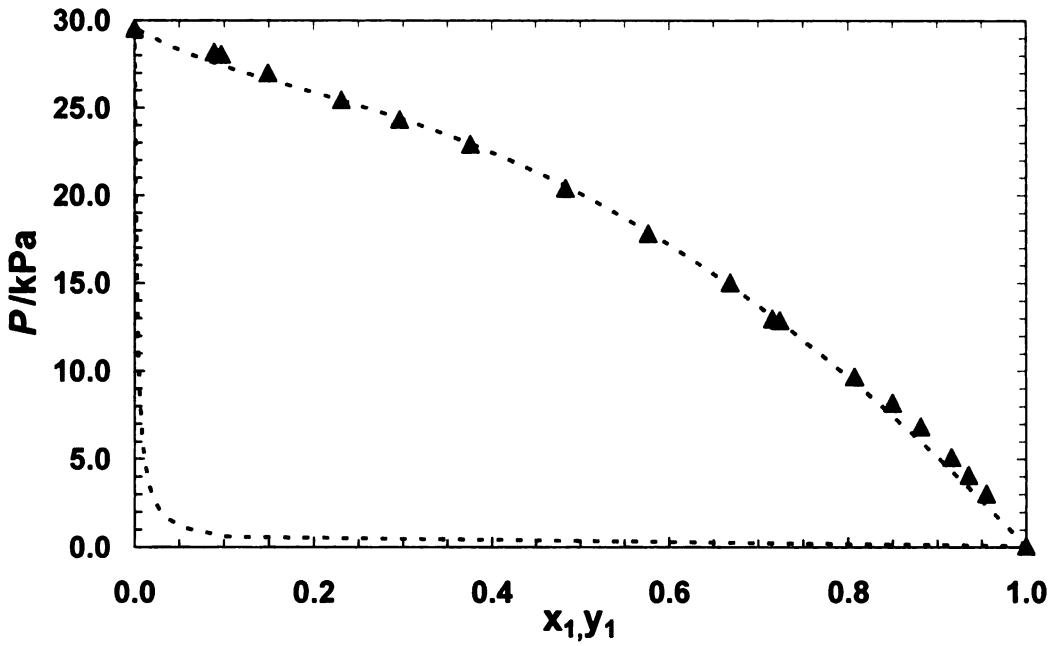

Figure 6.8 *P-x* of Diethyl Succinate (1) + Ethanol (2) at 50 °C
▲: measured, dashed line is *P-x-y* representation of UNIQUAC.

6.3 – T-x-y apparatus and measurements

Isobaric VLE data of lactic acid + water, and lactic acid + ethanol + ethyl lactate + water were obtained using a Fischer still (model VLE 100D) with recirculation of vapor phase, shown in Figures 6.10 and 6.11. The still operated with absolute pressure ranging from 0.25 kPa to 0.4 MPa, and temperature up to 250 °C. The equilibrium temperature was measured with resolution of 0.1 °K, with the temperature sensor positioned above the Cottrell [101] pump. Pressure resolution was 0.01 kPa. Pure water, acetone and ethanol were used to calibrate the pressure and temperature sensors.

Heating was regulated to maintain a mean recirculation speed of 30 drops per minute. Mixtures were equilibrated for at least 12 hours to ensure the equilibrium was reached, before each 0.5 ml sample was taken from condensed vapor and liquid for GC

and/or HPLC analyses. The equilibrium state was indicated by a constant pressure and temperature of the system.

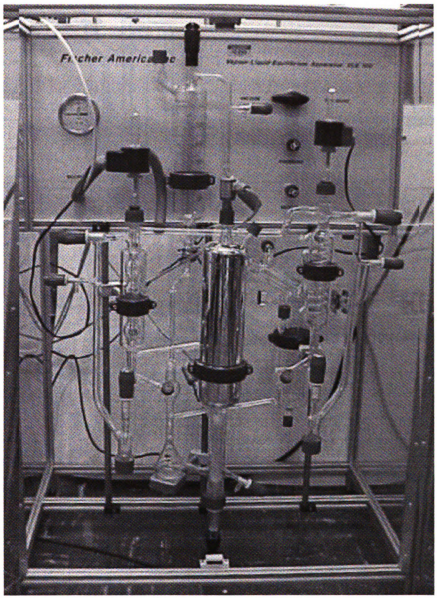

Figure 6.9 Overview of Fischer Recirculating Still

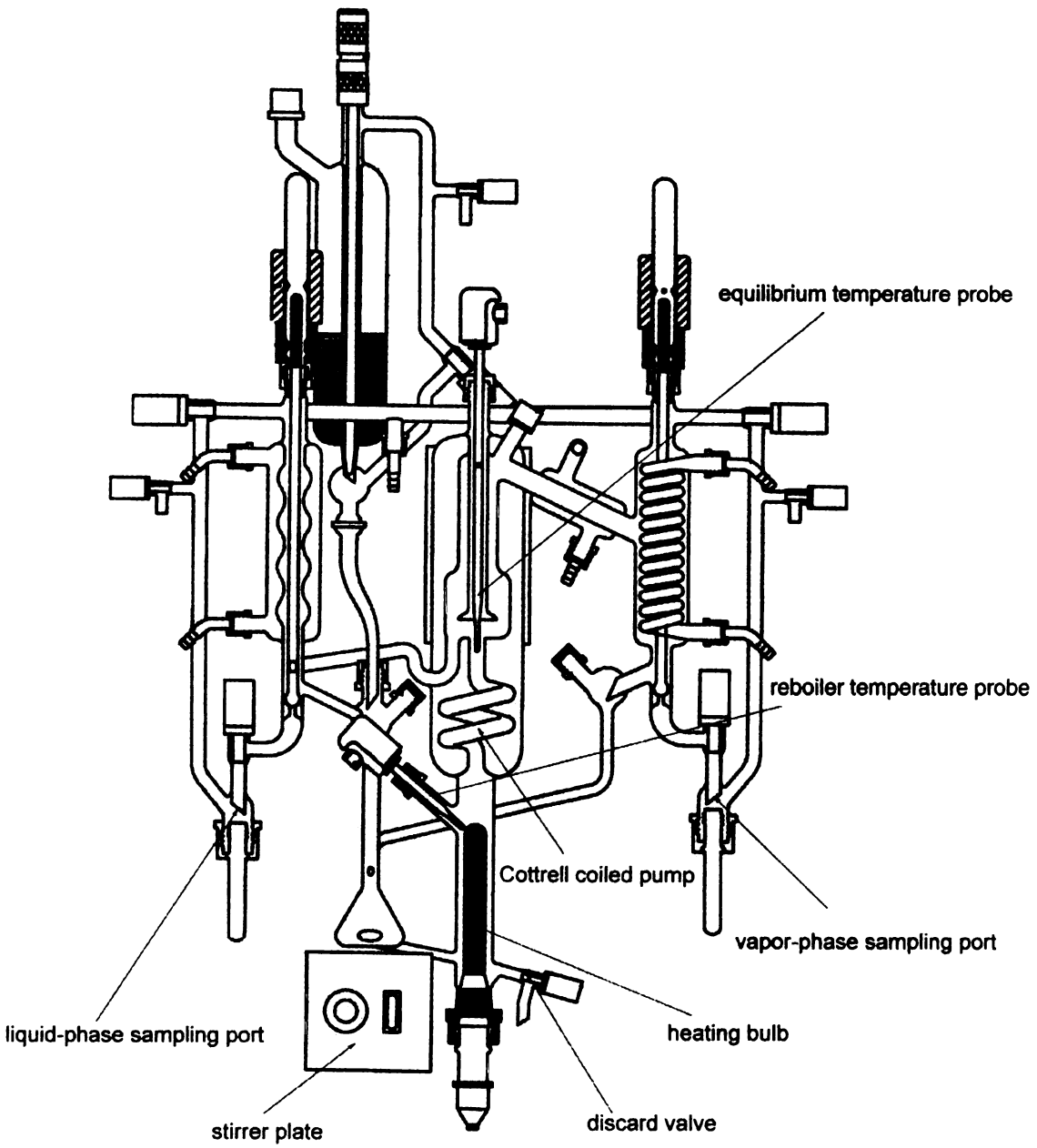

Figure 6.10 Schematic of Fischer Recirculating Still

6.3.1 – T-x-y Data of Lactic Acid + Water System

For the system lactic acid + water, data were collected at 103.33 kPa (Table 6-4). Lactic acid oligomers were quantified using a Hewlett-Packard 1090 Liquid Chromatograph, equipped with UV detection (Hitachi L400H) at a wavelength of 210 nm. The mobile phase was acetonitrile (ACN) + water in a gradient mode (0% ACN (t=0) to 60% ACN (t=20 min) to 90% ACN (t=25 min) to 0% ACN (t=28 min) at 1.0 ml/min. The Novapak C18 column (3.9 mm x 150 mm) was used and both ACN and water are acidified by 2 ml of 85% (w/v) phosphoric acid in one l L of solvent, equivalent to a pH=1.3. Complete details of the HPLC analysis are referred to section 5.1.

Table 6-4 *T-x-y* Data of Lactic acid (1) + Water (2) at 103.33 kPa

Liquid molar composition					
T/K	**water**	**LA_1**	**LA_2**	**LA_3**	**LA_4**
378.25	7.9E-01	1.9E-01	1.5E-02	1.2E-03	1.0E-04
379.25	8.0E-01	1.8E-01	1.4E-02	1.1E-03	8.7E-05
380.25	7.3E-01	2.4E-01	2.4E-02	2.3E-03	2.3E-04
380.75	7.2E-01	2.5E-01	2.5E-02	2.5E-03	2.5E-04
381.75	6.9E-01	2.8E-01	3.0E-02	3.3E-03	3.7E-04
381.85	7.1E-01	2.6E-01	2.7E-02	2.7E-03	3.0E-04
383.35	6.8E-01	2.8E-01	3.2E-02	3.5E-03	4.0E-04
387.35	5.8E-01	3.6E-01	5.4E-02	8.0E-03	1.2E-03
391.65	5.3E-01	3.9E-01	6.6E-02	1.1E-02	1.9E-03
399.85	4.2E-01	4.5E-01	1.0E-01	2.3E-02	5.1E-03
402.25	4.6E-01	4.3E-01	8.7E-02	1.8E-02	3.6E-03
404.05	4.6E-01	4.3E-01	8.8E-02	1.8E-02	3.6E-03
409.15	4.2E-01	4.5E-01	1.0E-01	2.3E-02	5.3E-03

Table 6-4 T-x-y Data of Lactic acid (1) + Water (2) at 103.33 kPa (continued)

Vapor molar composition					
T/K	**water**	**LA_1**	**LA_2**	**LA_3**	**LA_4**
378.25	1.0E+00	5.1E-04	2.9E-07	1.7E-10	9.6E-14
379.25	1.0E+00	7.2E-04	5.8E-07	4.7E-10	3.8E-13
380.25	1.0E+00	1.1E-03	1.5E-06	1.9E-09	2.4E-12
380.75	1.0E+00	8.3E-04	7.8E-07	7.4E-10	6.9E-13
381.75	1.0E+00	9.7E-04	1.0E-06	1.1E-09	1.2E-12
381.85	1.0E+00	1.9E-03	1.0E-04	0.0E+00	0.0E+00
383.35	1.0E+00	2.4E-03	1.0E-04	0.0E+00	0.0E+00
387.35	1.0E+00	3.0E-03	1.0E-04	0.0E+00	0.0E+00
391.65	9.9E-01	1.2E-02	5.0E-04	0.0E+00	0.0E+00
399.85	9.8E-01	2.1E-02	9.0E-04	0.0E+00	0.0E+00
402.25	9.8E-01	2.2E-02	9.0E-04	0.0E+00	0.0E+00
404.05	9.8E-01	1.5E-02	6.0E-04	0.0E+00	0.0E+00
409.15	9.7E-01	3.0E-02	1.3E-03	1.0E-04	0.0E+00

Figure 6.11 shows the measured data in this work and literature values, reported by Sans et al. [102]. As discussed in chapter 5, the amounts of oligomers are significant in concentrated lactic acid solutions. Sans reports lactic acid compositions in terms of only monomers and dimers so the data do not agree with this work at high concentration of lactic acid when plotted vs. mole fraction of lactic acid monomer. However, when the liquid and vapor molar compositions from Sans data are recalculated using the oligomer distribution model discussed earlier, the new values are in excellent agreement with the measured values listed in table 6-4. The following is an example of conversion:

From the reported data [102], at T = 438.13 °K, water (1): x_1 = 0.1940, monomer (2): x_2 = 0.6202, dimer (3): x_3 = 0.1858. Using molecular weights of the species:

$$\textit{Superficial wt.\% LA} = (90x_2 + 162x_3) / (18x_1 + 90x_2 + 162x_3) = 96.09$$

$n^i_{LA} = (90x_2 + 162x_3) / 90 = 0.9546$

and $n^i_w = 0.1940$

Using Eqn. (17) [103] from the oligomer distribution model:

$$K = r\frac{\left(n^i_w + n^i_{LA} r\right)}{n^i_{LA}\left(1-r\right)^2} = 0.2023$$

Solving results in r = 0.2505. Applying Eqn. (22) [103] to calculate for *the true* $wt.\%\ LA_j$, then

$wt.\%\ LA_1$ = 53.98, $wt.\%\ LA_2$ = 24.34, $wt.\%\ LA_3$ = 8.81, $wt.\%\ LA_4$ =2.88,

$wt.\%\ LA_5$ =0.89, and *the true wt.% of water* = 8.72.

Mw_{LA1} = 90, Mw_{LA2} = 162, Mw_{LA3} = 234, Mw_{LA4} = 306

Because LA_5 content is small, assuming the amount of all oligomers higher than LA_4 is negligible. The true liquid molar compositions are:

$$water\ (x_1) = \frac{\frac{true\ wt.\%\ \text{of water}}{18}}{\frac{true\ wt.\%\ \text{of water}}{18} + \sum_{j=1}^{j=4}\frac{wt.\%LA_j}{Mw_{LA_j}}} = 0.38$$

$$LA_j\ (x_{j+1}) = \frac{\frac{wt.\%LA_j}{Mw_{LA_j}}}{\frac{true\ wt.\%\ \text{of water}}{18} + \sum_{j=1}^{j=4}\frac{wt.\%LA_j}{Mw_{LA_j}}}$$

$LA_1\ (x_2)$ = 0.47, $LA_2\ (x_3)$ = 0.12, $LA_3\ (x_4)$ = 0.029, $LA_4\ (x_5)$ = 0.007

The adjusted monomer concentrations of Sanz et al. are shown in Figure 6.11, which are in good agreement with the measurements presented here, and are plotted along with the published monomer concentrations and T-x-y data.

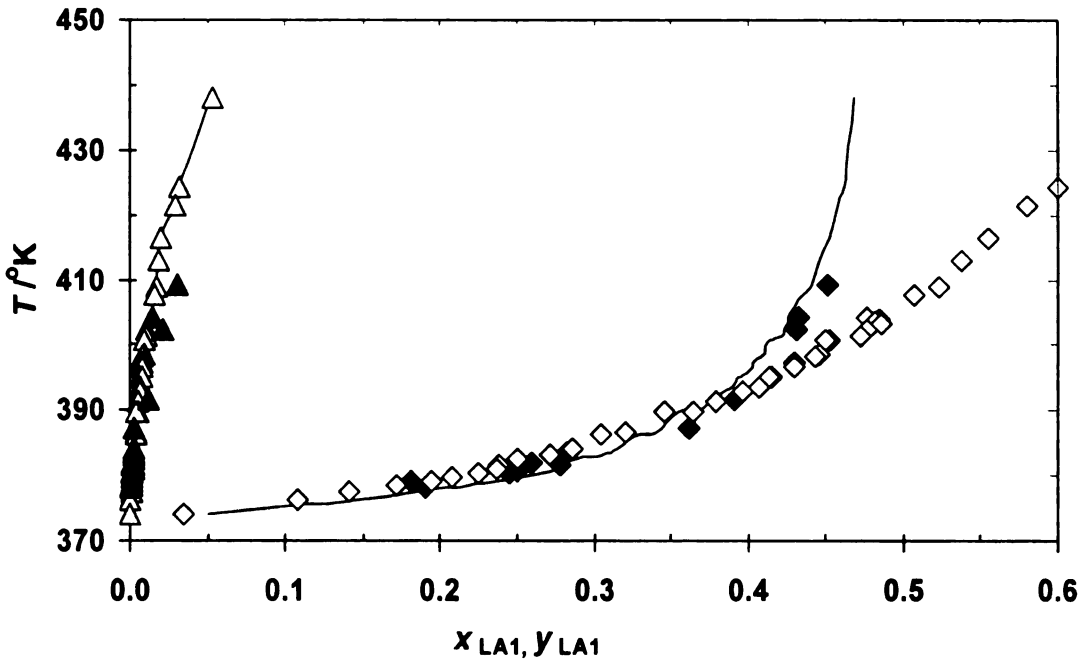

Figure 6.11 *T-x-y* of Lactic acid (1) + Water (2) at 103.33 kPa as a Function of Monomer Concentration

Lines: the true LA1 compositions from Sanz after correction as described above. Solid symbols: measured in this work; open symbols: original data reported by Sanz [102].

6.3.2 – T-x-y Data of Lactic acid + Ethanol + Ethyl lactate + Water System

The Fischer apparatus was also used to obtain isobaric VLE data of lactic acid oligomers (LA_1, LA_2, LA_3, LA_4) + ethanol + ethyl lactate oligomers (E_1LA, E_2LA, E_3LA) + water systems. Ethanol and water contents were determined from Gas Chromatograph (GC Varian 3400, Poropak Q 50/80, 6 ft long x 1/8 in. OD column). Acetonitrile was used as an internal standard. Oligomers of lactic acid and esters were quantified by HPLC.

ASPEN was used to fit the experimental data. Lactic acid tetramer (LA_4), ethyl lactate dimers (E_2LA), and ethyl lactate trimers (E_3LA) were manually entered into the ASPEN data bank, using connectivity of atoms and UNIFAC functional groups. For

example, E_2LA is registered as $C_8H_{14}O_5$, having three-group 1015 (CH3-), one-group 1010 (>CH2), one-group 1005 (>CH-), one-group 1200 (-OH), and two-group 3300 (-COO-). It was noticed that ASPEN assigns the same UNIFAC group for primary, secondary and tertiary hydroxyl groups. There was also a concern that large errors could be involved in estimating vapor pressures of lactic acid dimer (LA_2) and trimer (LA_3), using ASPEN parameters. As shown in Table 6-5 and Figure 6, ASPEN expected vapor pressure of lactic acid trimers about 13 times higher than that of dimer at high temperature, but there was no significant difference between dimer and monomer (LA_1).

Table 6-5 ASPEN Parameters of the Extended Antoine Equation.

	[a]LA1	[b]LA_1	[a]LA_2	[bb]LA_2	[a]LA_3	[bb]LA_3
C1	218.2822	214.9990	94.2322	216.0467	336.2222	213.4113
C2	-18757	-17489	-11976	-17489	-30565	-17489
C3	0	0	0	0	0	0
C4	0	0	0	0	0	0
C5	-28.816	-28.816	-10.528	-28.816	-44.817	-28.816
C6	1.30E-05	1.30E-05	5.07E-18	1.30E-05	1.53E-05	1.30E-05
C7	2	2	6	2	2	2
C8	289.9	373.15	385.7	385.65	312.2	312.2
C9	675.0	438.13	660.0	660	777.0	777.0

[a]: Retrieved from ASPEN ver. 12.1, [b]: from fitting the predicted Antoine coefficient, provided by Sans, [bb]: C2-7 are held the same as parameters in [b]LA_1 (the second column), C1 is adjusted to decrease the vapor pressure of each oligomer by a factor of 10.

$$\ln P = C_1 + \frac{C_2}{T + C_3} + C_4 * T + C_5 * \ln(T) + C_6 * T^{C_7} \quad for \; C_8 < C_9 \tag{6.1}$$

where P is calculated in kPa and T is in Kelvin.

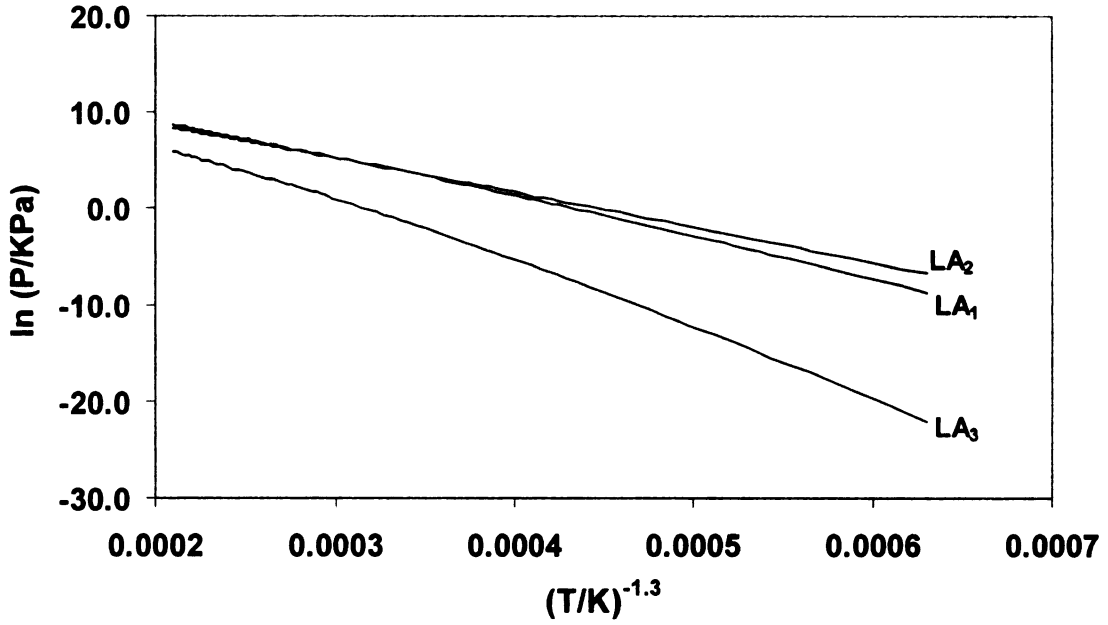

Figure 6.12 ASPEN Predicted P^{sat} of Lactic, di-Lactic, and tri-Lactic Acids

In this work, the Antoine coefficients from the PRO II process simulation database, provided by Sanz et al. [102], were used to refit the extended Antoine vapor pressure equation coefficients for the monomer in ASPEN. The predicted vapor pressures using the fitted ASPEN equation were about 16 % lower than the predicted values using the PRO II coefficients. A fit of the Aspen vapor pressure equation to a curve generated from the PRO II Antoine coefficients provided VLE calculations more consistent with measurements reported by Sans et al. for lactic acid + water systems than use of the original ASPEN vapor pressure coefficients. From the extended Antoine coefficients of the monomer, the C_1 values were adjusted for LA_2, LA_3, and LA_4 assuming vapor pressure of each oligomer decreased by a factor of 10, shown in table 6-5. This ratio is similar to the ASPEN ratio for lactic acid trimer and dimer.

For the ethyl lactate oligomers, parameters were arbitrarily selected to provide low vapor pressures. The molecular area (q) and volume (r) used in the UNIQUAC

activity model were calculated using Bondi's method. The binary interaction parameters, b_{ij} and b_{ji}, of the corresponding compound (i) with water (j) in Eqn: $\tau_{ij} = \exp(b_{ij} / T)$ were obtained by equating the experimental and calculated bubble temperatures. In each case, the liquid composition was specified and the bubble T and vapor composition were predicted.

Table 6-6 Parameters used in ASPEN Prediction

	LA_1	LA_2	LA_3	LA_4	E_1LA	E_2LA	E_3LA
C1	214.999	212.696	210.394	208.091	71.866	10.472	10.334
C2	-17489	-17489	-17489	-17489	-6715	-4382.7	-4852.5
C3	0	0	0	0	0	-58.88	-138.1
C4	0	0	0	0	0		
C5	-28.816	-28.816	-28.816	-28.816	-9.567		
C6	1.3E-05	1.3E-05	1.3E-05	1.3E-05	0.0145		
C7	2	2	2	2	1		
C8	373.15	373.15	373.15	373.15	247		
C9	438.13	438.13	438.13	438.13	588		
q	2.884	4.84	6.796	8.752	10.708	3.928	5.884
r	3.179	5.529	7.879	10.229	12.579	4.456	6.806
bij	-100	-200	-300	-400	279.92	70.81	22.43
bji	135	270	405	540	55.588	-202.36	-148.76

C1-C7: parameters of the extended Antoine equation (Eqn. 6.1) where T is in Kelvin, P is calculated in kPa for LA_1, LA_2, LA_3, LA_4 and E_1LA. For E_2LA and E_3LA, P is calculated in bar. q: molecular area, r: molecular volume. bij and bji: interaction parameters, i: the corresponding compound, j: water.

Table 6-7 Measurement and Prediction of LAs + Ethanol + ELAs + Water Systems

	Experiment 1				Experiment 2			
	Measured		Prediction		Measured		Prediction	
	Liquid	Vapor	Liquid	Vapor	Liquid	Vapor	Liquid	Vapor
LA_1	0.0092	0.0010	0.0093	0.0001	0.0042	0.0023	0.0042	0.0001
LA_2	0.0080	0.0000	0.0080	0.0000	0.0082	0.0064	0.0082	0.0000
LA_3	0.0053	0.0000	0.0054	0.0000	0.0009	0.0000	0.0009	0.0000
LA_4	0.0018	0.0000	0.0018	0.0000	0.0000	0.0000	0.0000	0.0000
E_1LA	0.6575	0.1592	0.6599	0.2139	0.8677	0.4956	0.8677	0.4695
E_2LA	0.1104	0.0000	0.1108	0.0041	0.0415	0.0000	0.0415	0.0035
E_3LA	0.0221	0.0000	0.0222	0.0000	0.0028	0.0000	0.0028	0.0000
Water	0.0088	0.0198	0.0088	0.0303	0.0048	0.0162	0.0048	0.0312
Ethanol	0.1731	0.8199	0.1738	0.7516	0.0698	0.4795	0.0698	0.4957
T(K)	374.3	374.3	373.2	373.2	395.2	395.2	389.9	389.9
P(KPa)	98.7	98.7	98.7	98.7	98.7	98.7	98.7	98.7

	Experiment 3				Experiment 4			
	Measured		Prediction		Measured		Prediction	
	Liquid	Vapor	Liquid	Vapor	Liquid	Vapor	Liquid	Vapor
LA_1	0.0605	0.0002	0.0605	0.0002	0.0488	0.0003	0.0488	0.0002
LA_2	0.0180	0.0011	0.0180	0.0000	0.0145	0.0000	0.0145	0.0000
LA_3	0.0045	0.0001	0.0046	0.0000	0.0039	0.0000	0.0039	0.0000
LA_4	0.0018	0.0007	0.0018	0.0000	0.0005	0.0000	0.0005	0.0000
E_1LA	0.4784	0.1045	0.4784	0.0850	0.6683	0.1873	0.6683	0.1796
E_2LA	0.0421	0.0001	0.0421	0.0005	0.0128	0.0000	0.0128	0.0002
E_3LA	0.0071	0.0004	0.0071	0.0000	0.0012	0.0000	0.0012	0.0000
Water	0.0501	0.0923	0.0501	0.0876	0.0662	0.1944	0.0662	0.1730
Ethanol	0.3375	0.8006	0.3375	0.8267	0.1838	0.6179	0.1838	0.6470
T(K)	358.9	358.9	361.2	361.2	368.1	368.1	367.8	367.8
P(KPa)	99.0	99.0	99.0	99.0	99.2	99.2	99.2	99.2

Table 6-7 (continued)

	Experiment 5				Experiment 6			
	Measured		Prediction		Measured		Prediction	
	Liquid	Vapor	Liquid	Vapor	Liquid	Vapor	Liquid	Vapor
LA_1	0.0095	0.0004	0.0095	0.0001	0.0396	0.0021	0.0396	0.0007
LA_2	0.0006	0.0000	0.0006	0.0000	0.0009	0.0000	0.0009	0.0000
LA_3	0.0000	0.0000	0.0000	0.0000	0.0000	0.0000	0.0000	0.0000
LA_4	0.0000	0.0000	0.0000	0.0000	0.0023	0.0000	0.0023	0.0000
E_1LA	0.8426	0.2711	0.8426	0.3243	0.8221	0.4338	0.8221	0.4939
E_2LA	0.0078	0.0000	0.0078	0.0003	0.0555	0.0000	0.0555	0.0038
E_3LA	0.0000	0.0000	0.0000	0.0000	0.0048	0.0000	0.0048	0.0000
Water	0.0417	0.1974	0.0417	0.1820	0.0396	0.2659	0.0396	0.2495
Ethanol	0.0978	0.5311	0.0978	0.4933	0.0350	0.2982	0.0350	0.2521
T(K)	374.6	374.6	375.6	375.6	384.7	384.7	384.9	384.9
P(KPa)	99.0	99.0	99.0	99.0	98.4	98.4	98.4	98.4

	Experiment 7				Experiment 8			
	Measured		Prediction		Measured		Prediction	
	Liquid	Vapor	Liquid	Vapor	Liquid	Vapor	Liquid	Vapor
LA_1	0.0406	0.0032	0.0406	0.0009	0.0042	0.0121	0.0042	0.0001
LA_2	0.0087	0.0074	0.0087	0.0000	0.0234	0.0058	0.0234	0.0000
LA_3	0.0000	0.0000	0.0000	0.0000	0.0000	0.0004	0.0000	0.0000
LA_4	0.0000	0.0000	0.0000	0.0000	0.0000	0.0000	0.0000	0.0000
E_1LA	0.8470	0.4990	0.8470	0.5682	0.9157	0.4894	0.9157	0.5820
E_2LA	0.0481	0.0000	0.0481	0.0041	0.0021	0.0104	0.0021	0.0002
E_3LA	0.0000	0.0000	0.0000	0.0000	0.0000	0.0000	0.0000	0.0000
Water	0.0298	0.2333	0.0298	0.2182	0.0288	0.2235	0.0288	0.2149
Ethanol	0.0258	0.2571	0.0258	0.2085	0.0258	0.2583	0.0258	0.2029
T(K)	388.2	388.2	361.4	361.4	387.2	387.2	388.4	388.4
P(KPa)	97.3	97.3	97.3	97.3	97.6	97.6	97.6	97.6

6.3.3 – Limitation of T-x-y Fischer Still

The design of the Cottrell coil is excellent in eliminating liquid entrained to equilibrium vapor in measuring saturated vapor pressure of pure components. However, the Cottrell coil is limited to viscous mixtures, in which the heavy components fall back to the reboiler due to gravity. The T-x-y Fisher apparatus does not provide an adequate mixing and superheats the large portion mixture between the tip of the heating bulb and the Cottrell pump. Before the isobaric measurements of the systems involved with lactic acid were taken, vapor pressures of HPLC water, pure acetone, re-distilled absolute ethanol, and re-distilled ethyl lactate were measured to verify the reliability of the T-x-y Fischer still. All the measured P^{sat} were in excellent agreement with the reported values in literature. However, it was noticed that the reboiler temperature (T_{column}) and equilibrium temperature (T_{head}) were the same in experiments with acetone and ethanol, and T_{head} was about 1 °C below T_{column} in experiments with water and ethyl lactate. These temperatures were read from the probes at locations shown in Figure 6.10. The difference between T_{head} and T_{column} became significantly large in experiments with lactic acid + water, especially when the mixtures were highly viscous, for example, T_{head} = 128 °C, T_{column} = 162 °C, and T_{head} = 135 °C, T_{column} = 166 °C. The following calculations were used to determine whether the lactic acid + water mixtures were overheated, causing the differences between T_{head} and T_{column},

Energy balance for adiabatic flashes:

$$n^V H^V + n^L H^L = n^{in} H^{in} \tag{6.2}$$

If the mixture is overheated, then Eqn 6.1 becomes,

$$n^V H^{sat,V} + n^L H^{sat,L} = n^{L,in}(H^{sat,L} + Cp\Delta T) + n^{V,in}(H^{sat,V} + Cp\Delta T) \qquad (6.3)$$

Re-arranging, Eqn. 6.2 becomes,

$$\frac{n^V}{n^T} H^{sat,V} + \frac{n^L}{n^T} H^{sat,L} = \frac{n^{L,in}}{n^T} H^{sat,L} + \frac{n^{V,in}}{n^T} H^{sat,V} + Cp\Delta T \qquad (6.4)$$

where $n^T = n^V + n^L = n^{V,in} + n^{L,in}$. Let reference state = saturated liquid, then

$$H^{sat,V}\left(\frac{n^V - n^{V,in}}{n^T}\right) = Cp\Delta T \qquad (6.5)$$

$$Cp = a + bT + cT^2 + dT^3 + eT^4 \text{ J/Kmol} \qquad (6.6)$$

$$\Delta H^{Vap} = A(1\text{-}T_r)^{B+CT_r+DT_r^2} \text{ J/Kmol} \qquad (6.7)$$

For water: a = 276370, b = -2091.1, c = 8.125, d = 0.01412, e = 9.37 x 10^{-6}, and A = 52.053 x 10^3, B = 0.3199, C = -0.212 , D = 0.25795, and T_c = 647.096 °K.

At 409.15 °K (the last data point in Table 6-4):

Cp(water) = 7.7 x 10^5 J/kmol, ΔH^{Vap}(water) = 3.9 x 10^7 J/Kmol

If all water in the feed was overheated: ΔT = 51 °K

Chapter 7 – Vapor Pressure Prediction using SPEAD

7.1 – Overview

Predicting vapor pressures of the acetals, 5-hydroxy-2-methyl-1,3-dioxane and 4-hydroxymethyl-2-methyl-1,3-dioxolane, and ethyl lactate oligomers for process design of reactive distillations, using SPEAD is an objective in this study. These compounds are involved in the current research at MSU, but they are not available in pure state for direct VLE measurements. Like ethyl lactate, the above acetals have low toxicity and low odor and can be excellent solvents for a wide variety of applications in the pharmaceutical and cosmetic industries [104]. They can also be used as additives in diesel fuel [105].

Vapor pressures of an ethyl lactate oligomer mixture were measured to compare with the SPEAD prediction. This prediction was accomplished using a FORTRAN code, written in this study. The predicted vapor pressures of ethyl lactate were in the same order with the measurements. The normal boiling points for the acetals were predicted within 2 % of the reported values, which are the only information available in literature.

7.2 – SPEAD Simulation Procedure

Prior to simulations, molecules were sketched using ChemSketch software and relaxed to their lowest internal energy [106]. This generated a three dimensional molecular file (*.mol*) for each studied molecule, in which the coordination and connectivity of all atoms were specified. The molecular information in *.mol* files were then carefully transferred into molecular dynamic (*.3md*) files in SPEAD. As described in chapter 4, molecules are broken down into a number of interaction sites in SPEAD simulation. Each interaction site of the simulated molecule is assigned by the repulsive

diameter (*bond diameter*) of the site, followed by an initial set of spatial coordinates (*group-coordinates*), then followed by a three or four digit index (*group ID*) specifying the type of site. Among the described properties of interaction sites, the group ID identifies parameters used to correlate the potential well depth of the interactions in computing the Helmholtz energy after simulation. Therefore, it does not affect the count of number of interactions in wells during simulation. The *.3md* file also contains the bond array showing which potential wells these bonded sites occupy. Sites directly bonded to each other have a value of 2, sites two bonds apart have a value of 4, and sites that are three or more bonds apart have a value of 6 [107]. Layout of the .3md files and complete molecular structures of ethyl lactate oligomers are provided in Appendix C.

To this point, a simulation could be started by choosing *Simulate Molecular Properties* from the *Commands* panel of the SPEAD interface. From the selected *.3md* file, the necessary information for a simulation such as the size of the simulated box corresponding to number of molecules, the effective volume of molecule, time step, etc., was created. In this dissertation, all simulations were performed at 5 ns for 100 molecules, if not otherwise specified.

After simulation, equation of state was generated and vapor pressure of the interested molecule was calculated. Procedures for these calculations are referred to the SPEAD Introduction and Help [78].

7.2.1 – Pair Interaction Sites of the Interested Compounds

The SPEAD interaction sites of ethyl lactate oligomers and acetals were designated as described in Figure 7.1. Each interaction site was specified by a three or four digit index, identifying the main and sub groups. For example, the site 1602 was

made of the main group 16 and the sub group 2.

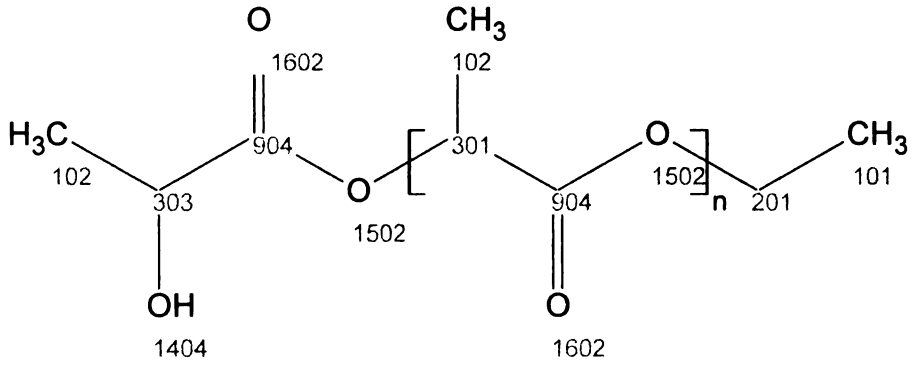

Ethyl Lactate Oligomers

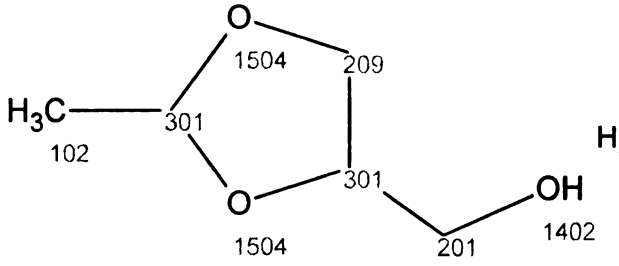

4-hydroxymethyl-2-methyl-1,3-dioxolane

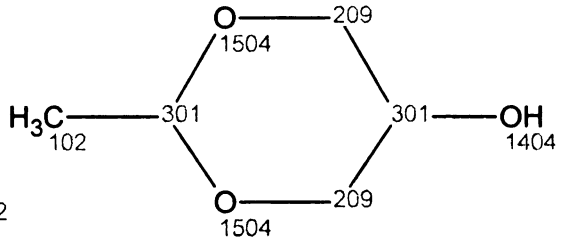

5-hydroxy-2-methyl-1,3-dioxane

Figure 7.1 The Interaction Sites of Ethyl Lactate Oligomers and Acetals

At present, SPEAD has not been fully developed for the multi-oxygen-containing molecules such as ethyl lactate or acetals. Therefore, the site 1404 for secondary –OH group and sites 904, 1502, 1602 for ester groups in Figure 7.1 are not yet parametized. Finding the optimal parameters for these sites was crucial for reliably predicting vapor pressures of acetals and oligomers.

7.2.2 – Approach of Optimizing Secondary -OH and -COO- groups

SPEAD was developed with the premise that parameters are transferable within the homologous compounds. Therefore, the best parameters for secondary –OH and –

COO– groups (shown in Figure 7.2) could be obtained from fitting the good experimental P^{sat} data available in the DIPPR database for 2-alkanols and esters. A datum was considered good if it had the DIPPR notation "*acceptance*" and the DIPPR "*deviation*" of less than 5 %.

Figure 7.2 Group Indices in 2-Alkanols and Base Esters used in Optimization

7.2.3 – Mathematical Methodology

The wells for each group 904, 1404, 1502, and 1602 were characterized by two parameters which were the inner (ε_1) and outer (ε_4) interaction well depth. In addition, group 1404 (-OH) and 1602 (>CO=) formed hydrogen bonds, which were described by the three parameters: the energy (*eHb*), the volume (*BondVol*), and the rate (*BondRate*) of the bonds. As a result, the optimization of secondary -OH and ester groups involved either five or nine parameters, respectively.

The following Eqns (7.1 – 7.4) describe the correlation of hydrogen bonding parameters used in calculation of total Helmholtz energy:

$$\frac{A - A_{ig}}{RT} = \frac{A_0}{RT} + \frac{A_1}{T} + \frac{A_1}{T^2} + A^{assoc} \tag{7.1}$$

$$\frac{A^{assoc}}{Nk_BT} = 2\ln\left(X^A\right) + \left(1 - X^A\right) \tag{7.2}$$

$$X^A = \frac{-1 + \sqrt{1 + 4\alpha}}{2\alpha} \tag{7.3}$$

$$\alpha = \rho \frac{(1-\eta/2)}{(1-\eta)^3} K_{AD} \left[\exp\left(\beta \varepsilon^{AD}\right) - 1 \right] \tag{7.4}$$

where ρ is the molar density, η the packing fraction, K_{AD} the molar hydrogen bonding volume, ε^{AD} the bonding energy, k_B is the Boltzmann's constant and $\beta = 1/k_B T$.

SPEAD parameter file ParmsHb3.txt denotes ε^{AD} as *eHb*, and *BondVol* as *BondV* and *BondRate* as *BondVolSlo* [108]. The correlation of *BondVol* and *BondRate* is defined in Eqn 7.5 below:

$$K_{AD} = BondVol \left[1 + BondRate \left(\frac{n_{h-bonding\ sites}}{n_{sites\ total}} \right)^2 \right] \tag{7.5}$$

As stated by Korsten [64] and also observed, the logarithm of vapor pressure of any compound is linear to $T^{1.3}$. Therefore, a good prediction of P^{sat} for a series of homologous compounds must have a minimum error in both P^{sat} and slope of the $\ln(P^{sat})$ with respect to $T^{1.3}$. Figure 7.3 below illustrates the possible errors in prediction.

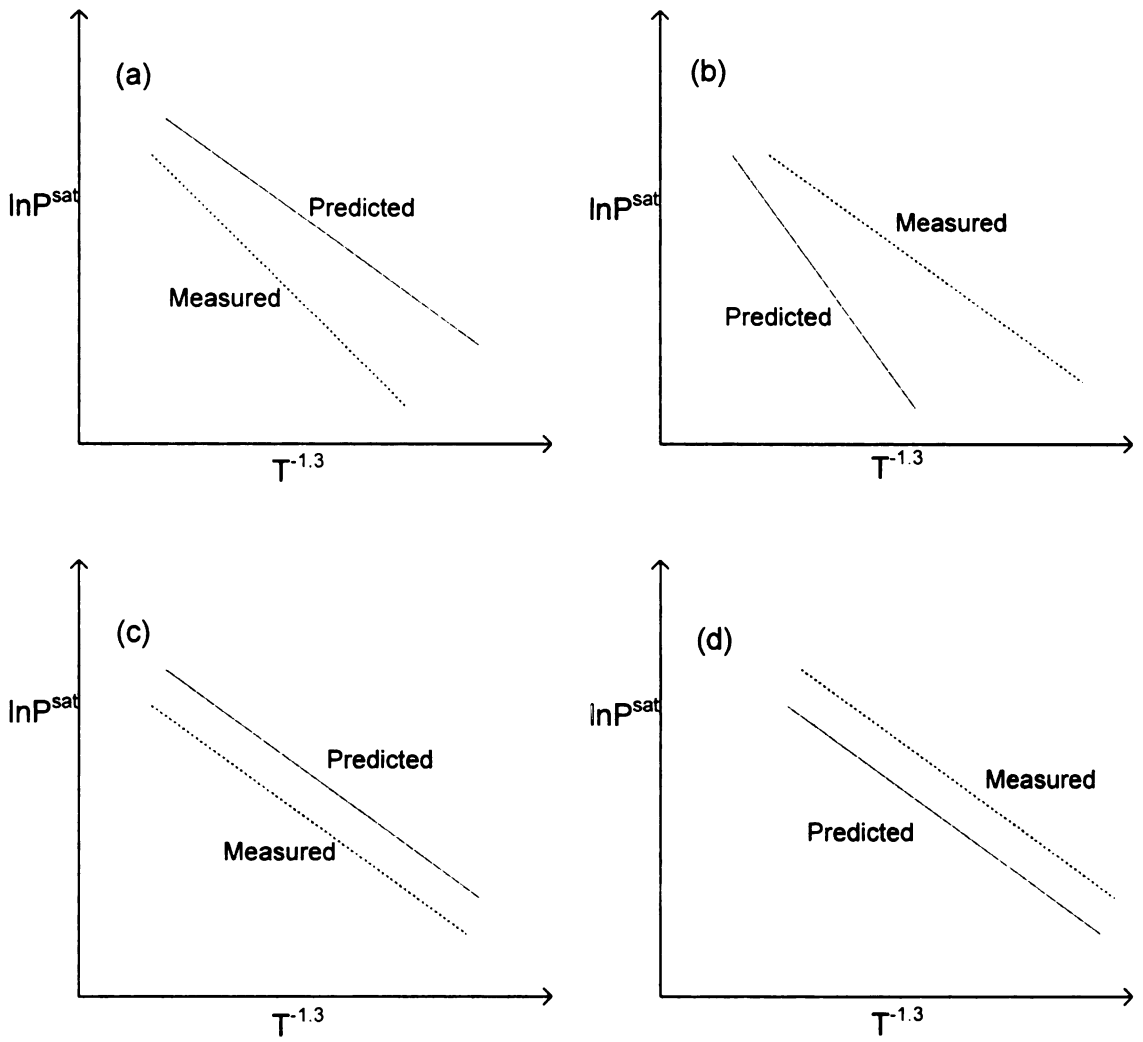

Figure 7.3 Illustration of Error in Prediction of P^{sat}

SPEAD developers used grid search, simplex and recursive random search [109] algorithms for parameterization of hydrocarbons and series of simple homologous compounds. But, these methods were not successful in finding a global optimum for a system with hydrogen bondings.

This dissertation provided a FORTRAN compiler using the routine DBCONF from the International Mathematical and Statistical Library (IMSL) to optimize the five and nine parameters of secondary -OH and ester groups.

To minimize the errors described in Figure 7.3, the objective function $(f \rightarrow \min)$ was defined as follows:

$$f = f_1 * f_2 \tag{7.6}$$

$$f_1 = \left[\sum_{i=1}^{i=n} abs\left(\ln P_{i,pre}^{sat} - \ln P_{i,\exp}^{sat} \right) \right] \tag{7.7}$$

$$f_2 = \left[\frac{1}{n-1} \sum_{i=1}^{i=n} abs\left(\frac{\left(\ln P_{i+1,pre}^{sat} - \ln P_{i,pre}^{sat} \right)}{\left(T_{i+1}^{-1.3} - T_i^{-1.3} \right)} - \frac{\left(\ln P_{i+1,\exp}^{sat} - \ln P_{i,\exp}^{sat} \right)}{\left(T_{i+1}^{-1.3} - T_i^{-1.3} \right)} \right) \right] \tag{7.8}$$

where n was the number of data points, $P_{i,pre}^{sat}$ and $P_{i,\exp}^{sat}$ are the respective predicted and experimental vapor pressures for a datum point i. The function f_1 is created to measure the absolute error in P^{sat}, while f_2 measures the error in the slope.

The DBCONF routine algorithm - DBCONF uses a popular variant of the Quasi-Newton method, which is called the BFGS (Broyden-Fletcher-Goldfarb-Shanno) method and an active set strategy to solve a nonlinear optimization problem subject to simple bounds on the variables [110-113]. The algorithm can be summarized as follows:

An active set **A** containing the indices of the variables at their bounds is built from a given starting point $x^{(0)}$ and an estimate of Hessian matrix $H_0 = \nabla^2 f\left(x^{(0)}\right)$. The routine then computes the search direction for the "free variables", which is not in the active set according to the formula:

$$x^{(k+1)} = x^{(k)} - H_k^{-1} \nabla f\left(x^{(k)}\right) \tag{7.9}$$

$$s^{(k)} = x^{(k+1)} - x^{(k)} \tag{7.10}$$

$$y^{(k)} = \nabla f\left(x^{(k=1)}\right) - \nabla f\left(x^{(k)}\right) \tag{7.11}$$

$$H_{k+1} = H_k - \frac{H_k s^{(k)} \left(s^{(k)}\right)^T H_k}{s^{(k)} \bullet H_k s^{(k)}} + \frac{y^{(k)} \left(y^{(k)}\right)^T}{y^{(k)} \bullet s^{(k)}} \tag{7.12}$$

The active set is changed only when a free variable hits its bounds during iteration or the optimality condition is met for the free variables but not for all variables in **A**, the active set. In the latter case, a variable that violates the optimality condition will be dropped out of **A**.

More details on the DBCONF algorithm can be found in the IMSL documentation. The quasi-Newton method and line search are explained by Dennis and Schnabel [114], and the active set strategy is explained by Gill and Murray [115]. A copy of FORTRAN code to call DBCONF and sample of input and output data files are included in Appendix B.

7.3 – Results of Optimization of the 2nd -OH and -COO- Groups

Existing data were divided into two sets. Some were used for parameter fitting and made up the training set. The other data were used for evaluation of predictive capability and made up the validation set. The training and testing sets, and results of optimization to obtain parameters for the secondary -OH and –COO- interaction sites are summarized in Table 7-1. More details of the output files containing experimental and predicted vapor pressures, generated by the FORTRAN program are in Appendix C.

Table 7-1 Optimization and Validation of –OH and –COO– Sites

Compound Name	Notation	# data points	Deviation in Prediction			References
			σ	Bias	Max	
Training -OH site						
2-propanol	2olC3	33	6	4.1	15.7	[116-118]
2-butanol	2olC4	32	11.3	-11.3	-14.4	[119, 120]
2-pentanol	2olC5	33	3.3	-2	-6.7	[121, 122]
2-hexanol	2olC6	27	5.5	4.6	15.6	[122, 123]
2-octanol	2olC8	33	5.3	3.9	16.6	[122, 124]
2-nonanol	2olC9	2	3	2.7	5.7	[125, 126]
Testing -OH site						
2-heptanol	2olC7	9	4.9	-4.9	-7	[127]
3-pentanol	3olC5	24	24.1	-24.1	-29.8	[122, 128]
3-hexanol	3olC6	22	12	-11.7	-32.2	[122, 127, 128]
3-heptanol	3olC7	6	8	-8	-9.9	[129, 130]
cyclohexanol	c2olC6	33	29.4	29.4	49.9	[117, 131]
cis 2-methylcyclohexanol	c2ol_2_C1C6	3	21.9	21.9	30.9	[132, 133]
cis 4-methylcyclohexanol	c2ol_4_C1C6	2	28.4	28.4	41.7	[134, 135]
2,3-butanediol	diolC4	22	79.4	-79.4	-90.9	[136]
Training -COO- site						
ethyl propionate	C3ateC2	28	5.2	3.3	9	[137]
n-butyl propionate	C3ateC4	32	2.1	0.7	-8.2	[121]
methyl n-butyrate	C4ateC1	30	15.3	-14.9	-38.4	[121, 138]
ethyl n-butyrate	C4ateC2	9	6	-4.7	-24.1	[132]
n-propyl n-butyrate	C4ateC3	28	1.5	-1.4	-3.5	[139, 140]
isobutyl isobutyrate	iC4ateIC4	17	16.7	16.7	22.2	[117, 141]
methyl decanoate	C10ateC1	18	6.3	-6	-13.1	[142, 143]
Testing -COO- site						
n-propyl propionate	C3ateC3	3	5.2	-0.3	-8.2	[137]
n-butyl n-butyrate	C4ateC4	2	13	-4.6	-17.6	[132]
n-propyl isobutyrate	iC4ateC3	1	16	16	16	[144]
n-butyl valerate	C5ateC4	2	5.2	2.5	7.7	[144, 145]
ethyl isovalerate	iC5ateC2	1	18.3	-18.3	-18.3	[132]
methyl laurate	C12ateC1	14	8.7	-1.9	-16.7	[68]
isopropyl laurate	C12ateIC3	7	4.9	3.7	11	[68]
isobutyl laurate	C12ateIC4	11	7	-3.5	-10.9	[68]
2-ethyl hexyl laurate	C12ate2C2C6	9	26.1	-26.1	-36.4	[68]
methyl tetracosanoate	C24ateC1	6	26.7	-26.7	-41.8	[68]

The secondary -OH group – All secondary alcohol data from DIPPR were used in optimization (2-alkanols (C2-C9)). The 2-heptanol was not included in the training set, because its vapor pressures in DIPPR database are not experimental but smoothed data. The average error (σ) in fitting 160 data points of the training set is 6 %. P^{sat} were from 0.01 kPa to 1 MPa.

Parameters obtained from optimization of 2-alkanols were used for prediction of vapor pressure for 3-alkanols and 2-heptanol. As shown in Table 7-1 predictions are in good agreement with the reported values in literature. The errors are large for the 3-pentanol and 3-hexanol, but P^{sat} data of these compounds were measured at low temperature ($P^{sat} < 0.01$ kPa), and they were not in the same range with data used in the training set.

The parameters of 1404 group from 2-alkanols were also tested with cyclohexanol and cyclomethylhexanol to verify if they could be transferable to the secondary OH group, which bonded to a non-aromatic ring. The vapor pressures were overestimated; cyclic alcohols have higher boiling points than the straight chain alcohols, affected by their stronger intermolecular hydrogen bonds and the current version of SPEAD did not represent the effects precisely.

The ester -COO- group – Optimization of the ester groups used 162 data points as summarized in Table 7-1. Deviation of the fitting data is ~ 8 % of the measured values. Experimental P^{sat} were limited, therefore the validation to check for transferability of the obtainable parameters only included 56 data points. Results showed that vapor pressure of esters containing up to 30 carbons could be predicted within 27 % of the measured values, using parameters listed in Table 7-2.

Table 7-2 Parameters used in SPEAD Calculated P^{sat}

Site	Description	Potential Well Depth		Hydrogen Bonding		
		ε_1	ε_4	Bond Vol	Bond Rate	Bond Energy
101	–CH3a	91.871	16.445			
102	–CH3b	55.100	32.400			
106	–CH3f	108.000	11.000			
201	–CH2–	26.558	21.827			
209	–CH2– in a ring	30.000	21.000			
301	>CH– to a Carbon	7.100	6.946			
303	>CH– to the 2nd –OH	31.500	4.400			
*1504	Cyclic ether –O–	140.25	23.65			
*904	=C–	10.209	1.698			
*1404	2nd –OH	142.743	41.760	0.00003587	140.00	4.247
*1502	Ester –O–	100.198	4.087			
*1602	=O	152.632	44.705	0.002	104.65	0.682

Sites with * are optimized in this study.

7.4 – Prediction of Psat for Ethyl Lactate and Methyl Lactate

First, vapor pressure of methyl lactate and ethyl lactate were predicted to compare with experimental values. Results (Table 7-3) showed that SPEAD could not provide an adequate prediction for ethyl and methyl lactates using the above-optimized parameters.

7.4.1 – Effect of Intramolecular H-bonds in Lactates

As shown in Table 7-3, all methods in DIPPR except for Othmer-Yu also underestimated the lactates. These compounds containing both a secondary hydroxyl and an ester group in their molecules, can form intramolecular hydrogen bonds (–OH....O=C<). To verify whether the intramolecular hydrogen bonding could be the cause of underestimation in SPEAD, full atom liquid simulations of 50 ns were

conducted using COMPASS potentials in the NVT ensemble with the Anderson thermostat, provided by Accelrys MS Modeling 4.0. Vibrational and torsional energies were included. Results indicated that liquid phase hydrogen bonds were both intra- and intermolecular.

Table 7-3 Predicted P^{sat} of Methyl Lactate and Ethyl Lactate

	Methyl lactate					
Method	**T = 313.15 K P = 0.0012 MPa**		**T = 333.25 K P = 0.0036 MPa**		**T = 353.35 K P = 0.0094 MPa**	
	Value	% Dev	Value	% Dev	Value	% Dev
Riedel	0.00057	-52%	0.00213	-41%	0.00662	-41%
Othmer-Yu	0.00945	689%	0.02998	731%	0.08191	731%
Gomez-Thodos	0.00027	-78%	0.00129	-64%	0.00483	-64%
Lee-Kesler	0.00054	-55%	0.00204	-43%	0.00644	-43%
Maxwell-Bonnell	0.00182	52%	0.00501	39%	0.01197	39%
[a]SPEAD	0.00003	-97%	0.00015	-96%	0.00058	-94%
[b]SPEAD	0.00110	-8%	0.00340	-6%	0.00900	-6%
	Ethyl lactate					
Method	**T =313.15 K P = 0.0012 MPa**		**T = 333.25 K P = 0.0031 MPa**		**T = 353.35 K P = 0.0076 MPa**	
	Value	% Dev	Value	% Dev	Value	% Dev
Riedel	0.00034	-71%	0.00133	-57%	0.00431	-43%
Othmer-Yu	0.00610	430%	0.01997	538%	0.05607	638%
Gomez-Thodos	0.00012	-89%	0.00067	-79%	0.00277	-64%
Lee-Kesler	0.00032	-73%	0.00127	-60%	0.00417	-45%
Maxwell-Bonnell	0.00098	-15%	0.00295	-6%	0.00761	0.2%
[a]SPEAD	0.00003	-97%	0.00015	-95%	0.00060	-92%
[b]SPEAD	0.00080	-33%	0.00240	-23%	0.00650	-14%

[a]SPEAD: using parameters listed in Table 7-2. [b]SPEAD: same as [a]SPEAD , but the *BondVol = 0, BondRate = 0, and BondEnergy = 0* for site 1404. The experimental P^{sat} of methyl lactate and ethyl lactate were taken from the DIPPR database.

Adjusting for the effect of intramolecular H-bonds in calculating the Helmholtz energy in SPEAD was beyond the scope of this study. However, it was found that SPEAD gives a good prediction for the lactates (still a small underestimation) if all parameters of H-bond in 1404 group were set to zero. Table 7-4 provides an example of P^{sat} predictions for ethyl lactate using the described settings.

The normal boiling point for ethyl lactate is 427.15K, and the predicted value was 428.02 K. Similar results are obtained for methyl lactate (Tb = 417.95 K, predicted value = 418.45 Tb). For the methyl 3-hydroxy butanoate (at P = 0.00132 MPa, T = 336.2 K, and predicted T= 330.2 K).

Table 7-4 Measured *T-P* and SPEAD Prediction for Ethyl Lactate
Using parameters listed in Table 7-2 (except for H-bonding)

T (K)	P (MPa)		T (K)	P (MPa)	
	Measured	SPEAD		Measured	SPEAD
353.15	0.0077	0.0065	317.45	0.0013	0.0010
351.15	0.0072	0.0059	314.65	0.0010	0.0008
349.55	0.0067	0.0055	313.25	0.0011	0.0008
347.15	0.0062	0.0049	312.85	0.0010	0.0007
343.55	0.0053	0.0041	310.45	0.0008	0.0006
341.65	0.0047	0.0037	309.15	0.0007	0.0006
337.45	0.0040	0.0030	308.15	0.0007	0.0006
333.15	0.0031	0.0024	305.65	0.0005	0.0005
330.65	0.0028	0.0021	304.05	0.0005	0.0004
327.35	0.0023	0.0017	303.15	0.0005	0.0004
325.05	0.0021	0.0015	300.05	0.0004	0.0003

7.4.2 – A Common Point for Ethyl Lactate Oligomers

Another evaluation of SPEAD predictions for oligomers was the use of Eqn 4.1,

which was described by Korsten in chapter 4. Vapor pressures were generated for each lactate ester (E_1LA, E_2LA, E_3LA, E_4LA, E_5LA) at temperatures between 300–700 °K (increment of 20 °K), using the parameters listed in Table 7-2 (all parameters for H-bonds of site 1404 were zero, but parameters of site 1602 were not adjusted, because H-bond energy of this site is much lower than the bond energy of site 1404 and has a very minor effect).

Results showed that the SPEAD-predicted vapor pressure curves of lactate oligomers were not completely linear when plotted with Korsten's temperature dependence. However, fitting the predictions with linear equations, the extrapolated vapor pressures for E_2LA, E_3LA, E_4LA, and E_5LA merged at the common point α (T_α = 4947.K, P_α = 2643.3 MPa) as illustrated in Figure 7.4. Therefore, the predictions were generally consistent with the empirical common point analysis of Korsten. The coefficients shown in Eqns 7.1 and 7.2 for slopes of these vapor pressure curves were obtained from regression using the least square method.

$$\ln P = \ln P_\alpha + B\left(\frac{1}{T^{1.30}} - \frac{1}{T_\alpha^{1.30}}\right) \qquad \text{(Eqn. 4.10)}$$

$$B = B_0(\theta_B) + B_1 M^{0.65} = 4669.09 - 321.42\theta_B - 1162.8M^{0.65} \qquad (7.13)$$

$$(T_\alpha = 4947.5 \text{ K},\ P_\alpha = 2643.3 \text{ MPa}),\ \text{and}\ \theta_B = 22.596$$

The above equations can be combined as:

$$\ln P = 7.88 - \left(2593.72 + 1162.8M^{0.65}\right)\left(\frac{1}{T^{1.30}} - \frac{1}{4947.5^{1.30}}\right) \qquad (7.14)$$

where M is molecular weight of the corresponding ethyl lactate oligomer, T is in K, and P is in MPa.

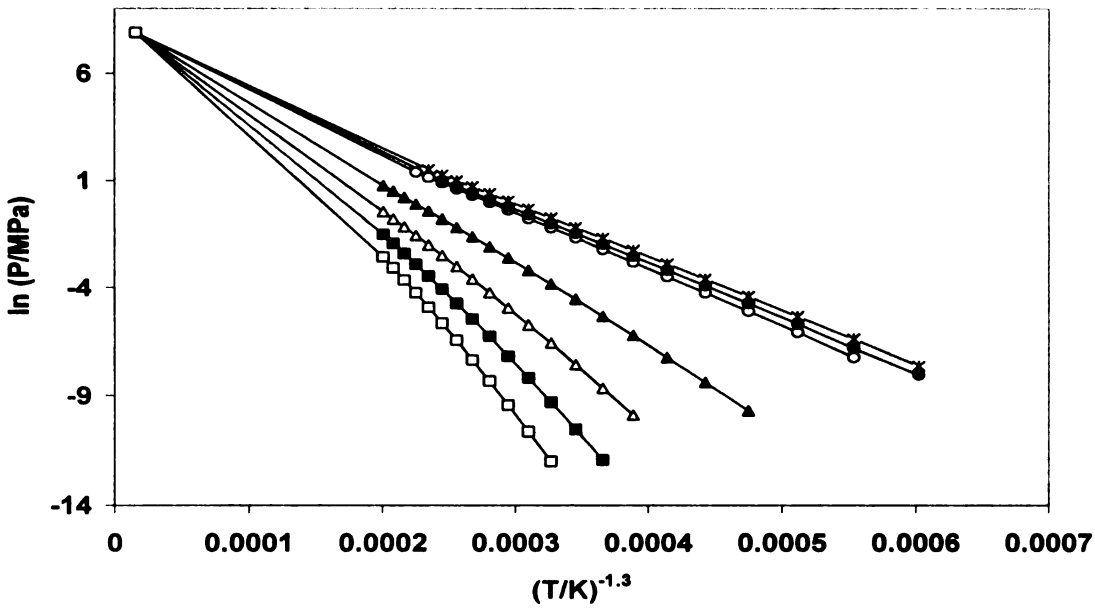

Figure 7.4 Trend of Predicted Vapor Pressure of Ethyl Lactate Oligomers

*: methyl lactate, ○: methyl 3-hydroxy-butyrate, ●: L_1E, ▲: L_2E, Δ: L_3E, ■: L_4E, ◊: L_5E

7.4.3 – A Validation for P^{sat} Prediction of Ethyl Lactate Oligomers

P^{sat} of the ethyl lactate oligomer mixture were measured using *P-x-y* apparatus, which was described in chapter 6. The molar compositions were determined using HPLC. Table 7-5 shows the predicted values using SPEAD regressed with the Korsten correlation as explained above; the measured pressures are the same order of magnitude.

Table 7-5 Vapor Pressure of Ethyl lactate Oligomers Mixtures

Molar compositions: E_1LA = 0.656, E_2LA =0.282, E_3LA = 0.043, E_4LA = 0.019

T(K)	P (kPa)		T (K)	P (kPa)	
	$P_{measured}$	$P_{SPEAD\text{-}Korsten}$		$P_{measured}$	$P_{SPEAD\text{-}Korsten}$
298.0	0.40	0.08	320.7	1.06	0.41
301.2	0.47	0.11	326.6	1.33	0.59
303.7	0.51	0.13	330.7	1.66	0.76
306.2	0.56	0.15	335.1	1.93	0.98
310.9	0.68	0.21	338.2	2.18	1.17
314.7	0.81	0.28	342.1	2.54	1.45
318.5	0.51	0.35	345.8	2.94	1.77

$M_{(E_1LA)} = 118.13$, $M_{(E_2LA)} = 190.18$, $M_{(E_3LA)} = 262.26$, $M_{(E_4LA)} = 334.33$

Using Eqn 7.9 to estimate total vapor pressure of mixture at 345.8 K:

$$P_{monomer} = \exp\left[7.88 - \left(2593.72 + 1162.8 * 118.13^{0.65}\right)\left(\frac{1}{345.8^{1.30}} - \frac{1}{4947.5^{1.30}}\right)\right]$$

$$= 2.69 \times 10^{-3} \text{ MPa}$$

$P_{2\text{-mer}} = 2.85 \times 10^{-5}$ MPa, $P_{3\text{-mer}} = 5.48 \times 10^{-7}$ MPa, $P_{4\text{-mer}} = 0.15 \times 10^{-7}$ MPa

If mixture is an ideal solution, then

$$P_{mixture} = 0.656*(2.69) + 0.282*(0.028) + 0.043*(5.48 \times 10^{-4}) + 0.019*(0.15 \times 10^{-4})$$

$$= 1.77 \text{ kPa}$$

Result is in the same order with the value from measurement.

7.5 – Prediction of P^{sat} for Acetals

Acetals of interest were the 4-hydroxymethyl-2-methyl-1,3-dioxolane (4HMD) and 5-hydroxy-2-methyl-1,3-dioxane (5HMD). These compounds contain two cyclic -O- groups in a molecule. Different from alcohols and esters, the ether oxygen atom does not form intramolecular H-bonds in ethers; therefore vapor pressures of mono-ethers (each molecular containing a single -O- group), such as tetrahydrofuran, are much higher than vapor pressures of alcohols, esters, di-ethers, and the above acetals 4HMD and 5HMD.

The existing SPEAD parameters ($\varepsilon_1 = 287.4$, $\varepsilon_4 = 26.7$) for the cyclic-ether oxygen (group 1504) provided an excellent P^{sat} prediction for tetrahydrofuran. But, using these existing parameters for 1,3-dioxane and 1,4-dioxane, SPEAD underestimated vapor pressures by at least 85 %. In addition to ether oxygens, the 4HMD and 5HMD also contain a hydroxyl group in their structures; therefore if the existing SPEAD parameters were not sufficient for use in 1,3-dioxane and 1,4-dioxane, they were

obviously not suitable for the 4HMD and 5HMD. Thus, optimization was needed for group 1504 assuming the methylene site in a ring (group 209) was already parametized.

Experimental P^{sat} data are very limited for acetals. Table 7-6 lists the compounds found in the DIPPR data bank that have the most similar structure to the 4HMD and 5HMD. The 1,3-dioxane and 1,-4 dioxane were used in optimization; the trioxane and tetrafurfural alcohol were used in validation.

Table 7-6 Optimization and Validation of the Cyclic –O– Site

Compound Name	Structure	# data points	Deviation in Prediction σ	Bias	Max	References
Training –O– site						
1,3-dioxane		15	4.7	4.7	11.7	[146-148]
1,4-dioxane		33	2	0	4.1	[141, 149, 150]
Testing –O– site						
Trioxane (or trioxymethylene)	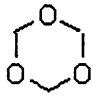	11	3.7	3	6.8	[121, 151]
Tetrahydrofurfuryl alcohol	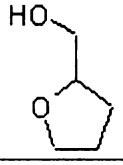	20	15.4	-15.4	46.1	[152-154]

Since the ether group does not associate with H-bond, optimization of the 1504 group only involved two variables, the inner and outer well depths of the site. A minor modification was made in the FORTRAN program for fitting. As discussed in the previous sections, this program was written to optimize either five or nine parameters in alcohol and ester groups. The best parameters for group 1504 were found to be ε_1 = 140.25, and ε_4 = 23.65. Using these parameters, vapor pressures of trioxane and

tetrahydrofurfuryl (testing compounds) were respectively predicted within 4 and 16 % of the reported values in literature.

Table 7-7 summarizes the prediction of P^{sat} for acetals 4HMD and 5HMD using the new well depths for group 1504. There is currently no convergence in the smoothed SPEAD calculation of compressibility factor Z at below 300 °K and above 500 °K for both 4HMD and 5HMD, so the vapor pressures were evaluated only between these temperatures.

Table 7-7 Prediction of Psat for Acetals using SPEAD. $T_{b(dioxane)}$ = 449.15 °K, SPEAD value = 453.15 °K. $T_{b(dioxolane)}$ = 460.15 °K, SPEAD value = 467.96 °K [155].

T (°K)	P (kPa)		T (°K)	P (kPa)	
	5HMD	4HMD		5HMD	4HMD
300	0.038	0.017			
310	0.085	0.040	410	22.9	13.7
320	0.181	0.088	420	33.5	20.3
330	0.365	0.183	430	47.9	29.6
340	0.699	0.360	440	67.0	42.0
350	1.30	0.68	450	92.0	58.5
360	2.30	1.20	460	124.1	80.0
370	3.80	2.10	470	164.6	107.4
380	6.20	3.50	480	214.9	142.0
390	9.90	5.70	490	276.7	185.0
400	5.30	9.00	500	351.6	237.6

*All parameters of H-bond in 1404 group were used as listed in Table 7-2.

As shown in Table 7-7, SPEAD predicted values are very close to the reported boiling points, which are the only VLE data available in literature for 4HMD and 5HMD [155]. The linear trend of predicted vapor pressure curves follows the Korsten correlation. In addition, regression using the least square method shows vapor pressure curves of these homologous isomers 4HMD and 5HMD (same molecular weight and

same functionality) merge at a common point α (T_α = 1024 °K, P_α = 126.7 MPa) and the value of θ_B is 33.49 in Eqn 7.13.

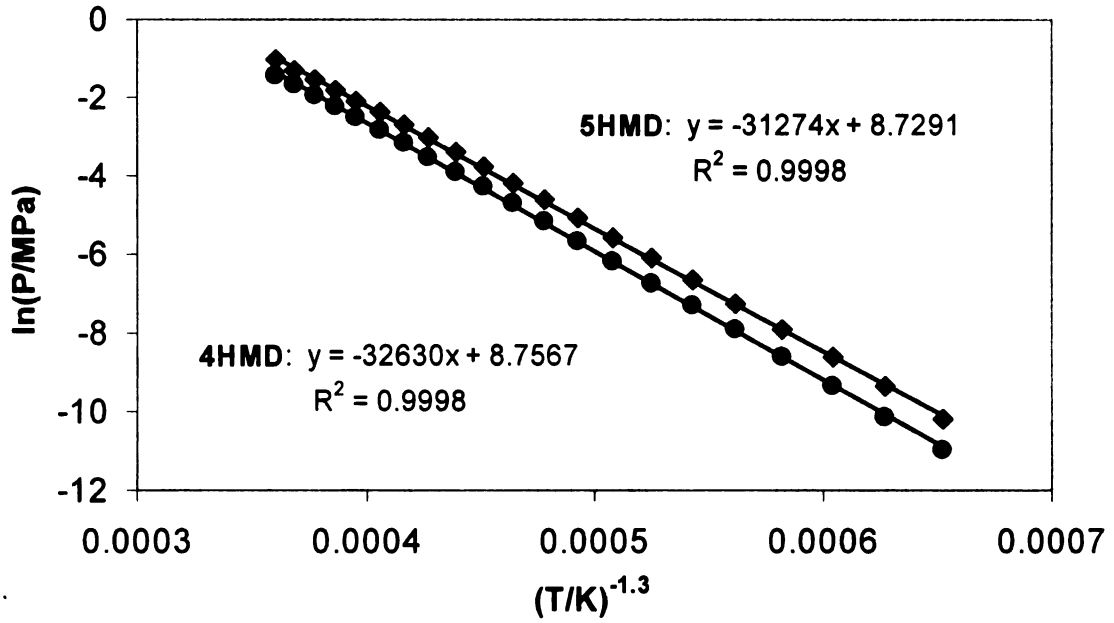

Figure 7.5 SPEAD Predicted Vapor Pressure of Acetals

●: 5HMD, ■: 4HMD. Lines: linear regression

Table 7-8 and Figure 7.6 are predicted VLE of 4HMD and 5HMD mixtures at 373.15 °K. As expected, SPEAD predicts 4HMD and 5HMD form ideal solutions. It will be difficult to separate these acetals using distillation due to their small relative volatility.

Table 7-8 SPEAD Predicted *T-P-x-y* of 4HMD (1) + 5HMD (2) at 373.15 °K

x_1	y_1	P (MPa)	x_1	y_1	P (MPa)
0.0	0.000	0.0025			
0.1	0.167	0.0027	0.6	0.729	0.0037
0.2	0.310	0.0029	0.7	0.807	0.0039
0.3	0.435	0.0031	0.8	0.878	0.0041
0.4	0.545	0.0033	0.9	0.942	0.0043
0.5	0.642	0.0035	1.0	1.000	0.0045

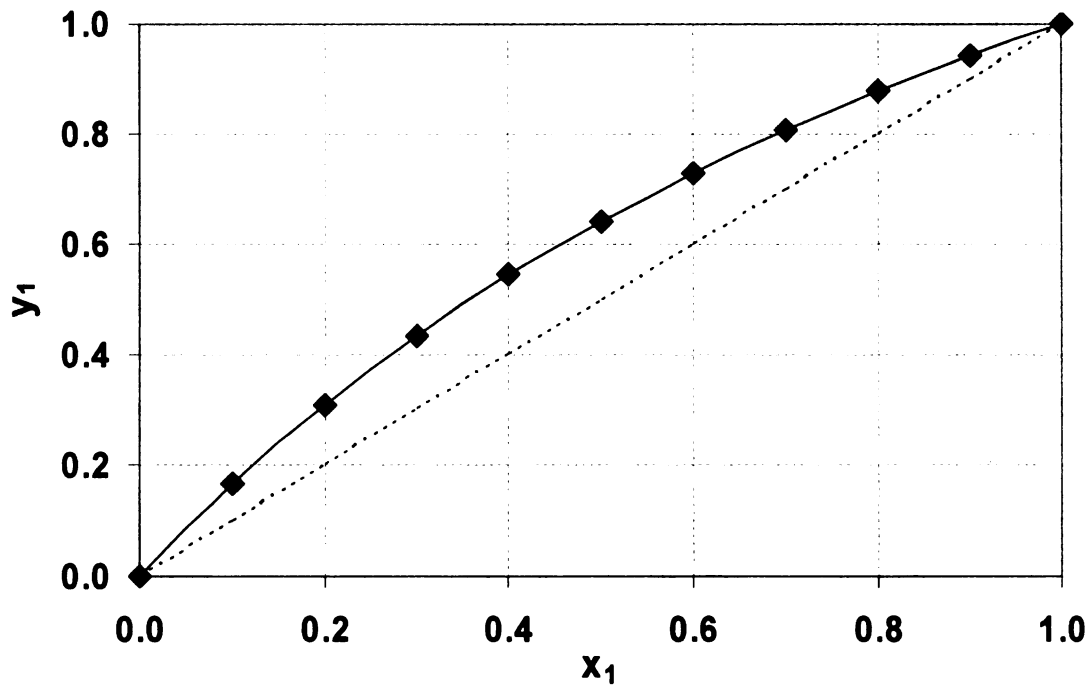

Figure 7.6 Predicted VLE of 5HMD (1) + 4HMD (2) Mixtures at 373 °K.
x, y: liquid and molar compositions.

7.6 – Bias in SPEAD Simulation and Regression of A_2

SPEAD commonly underestimates vapor pressures of the high molecular weight compounds in homologous series. This bias has been seen in P^{sat} predictions of amines, amides, acetates, ketones, and hydrocarbons [67, 108], also shown in the fifth column of Table 7-1.

Error was observed in regression of A_2 for high molecular molecules of homologous series. A maxima of A_2 at high density was apparent in E_3LA, and it increased in size for E_4LA and E_5LA (Figures 7.7). The same trend was found with 2-alkanols and training set esters.

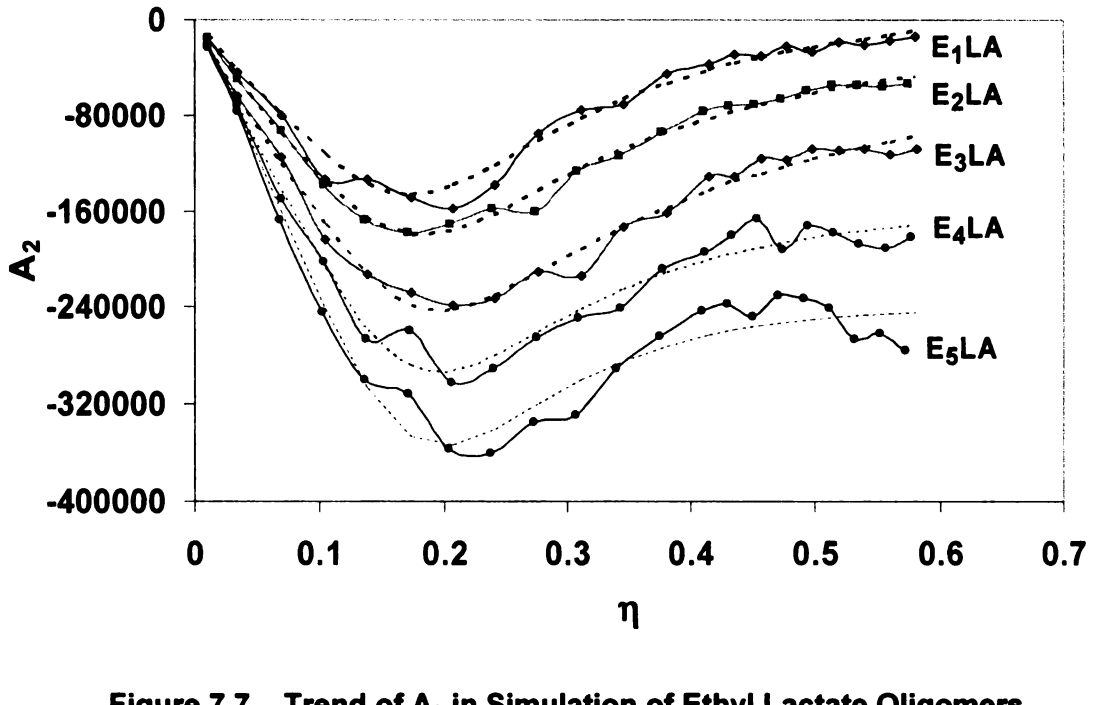

Figure 7.7 Trend of A_2 in Simulation of Ethyl Lactate Oligomers
Notations used in Figures are referred to chapter 5. Solid lines: connecting the values of A_2 in simulation. Dot lines are the regression of A_2.

As it can be seen in Figure 7.7, the values of A_2 from regression at high density are higher than the values originally obtained from simulation (the regression curve is above the actual A_2 curve), resulting in ~25-30 % positive deviation in the values of $\frac{dA_2}{d\eta}$ from regression compared to the original values for $\eta > 0.52$.

Chapter 8 – Conclusion and Recommendations

8.1 – Separation of Ricinolein

This work demonstrates the potential of adsorption can be an alternative separation process to produce ricinolein from castor oil. Recently, a patent has been granted to researchers at Dow Chemical, Inc. for their adsorptive separation method to separate plant oil triglycerides from mixtures [3]. The methodology and result in that patent are similar to the work presented in this dissertation.

Future work on modeling adsorption behavior will be useful for scaling up and processing designs. Solvent mixtures can be used to enhance the solubility of castor oil and/or the selectivity of adsorbents to glycerides. Studies to find the optimal solvent strength for the selected triglycerides is also important. Isohexane which is identified as not a hazardous air pollutant [156] in the United States should be replaced for hexane if it is an option of choice. HPLC should be used to analyze the effluents, since the derivatization of glycerides into FAME for GC analyses limits the detection of di- and mono-ricinolein with non-functional fatty acids in samples.

Separation of ricinolein should be improved using simulated moving beds (SMB). This separation technology has been successful in separating p-xylene from xylene mixtures, used in the petrochemical industry for almost 30 years. The SMB is also used in fructose/glucose separation and olefins/parafins separation [157]. The use of SMB can avoid problems related to pressure drop and solid motion in fixed beds. It is more efficient than the other types of adsorption, since it uses less adsorbent for the same throughput.

8.2 – Extraction and Purification of SQDG

Results from this study show that non-chlorinated solvents can replace chloroform in extraction and recovery of SQDG from alfalfa. Their applications can be extended to any plant extractions. The proposed method in this dissertation uses significantly less chemicals and solvents than the reported amount in literature.

Following this work, isohexane could replace hexane because this solvent is not an environmental concern, and ethanol can be substituted for methanol. Blended solvent mixtures of more than two components, for example a mixture of acetone-hexane-methanol should be tried. The Hansen solubility parameters can be used as the basis in designing an effective solvent system.

Activated carbon or non-polar adsorbents could be used as an alternative technique to remove chlorophyll and pigments from the extracts, depending on the costs of solvent recovery compared to the cost of adsorbent regeneration. Design of solvent recovery and economic analyses should be done to determine the optimal process. Further studies to completely remove proteins prior to the use of adsorption and ion-exchanger in purification of SQDG should be considered. The presence of proteins blocks the adsorption sites, and builds up the pressure of columns.

Recovery of DMDG and DGDG along with SQDG should be evaluated. Alfalfa contains a significant amount of these lipids compared to the SQDG content. Evaluation of ion-exchange DEAE capacity and development of a method for detection of SQDG in the effluent from ion-exchange columns will be useful. Other exchange materials should be investigated since DEAE is relatively expensive. An inert material may also be used to disperse DEAE powder to avoid channeling and high back pressure in the column.

Different sources of SQDG should be evaluated for application of the extraction/purification methods. For example, algae have been reported as a promising source of SQDG with a high content.

8.3 – Measured and Predicted VLE and Vapor Pressure

This work provided VLE and VLLE data and predicted vapor pressure of systems involved in the reactive distillation of ethyl lactate, diethyl succinate, triethyl succinate, and acetals of glycerol for research and industrial process designs. Isothermal measurements were successfully performed using a custom made *P-x-y* apparatus. On the other hand, isobaric measurements were taken from a commercial Fischer *T-x-y* recirculating still. The *P-x-y* apparatus, developed in this study is valuable for reactive chemical systems which cannot be measured at high temperature, and the Fischer *T-x-y* still is effective for systems with slow kinetic, such as lactic acid and water mixtures.

For a successful operation of the *P-x-y* apparatus, the entire system must completely be degassed prior to the VLE measurements. In addition to the procedure, which is described in the journal paper [96] (also included in chapter 5), the following actions are recommended: **1)** Ensure that there is no plugging in the sample loop, and the vapor line, the valve V_3 and the sampling valve are free from impurity of gases and liquids: open V_3 and place the sampling valve at load position then turn on the vacuum pump. If the system is leak-tight and completely degassed, the same reading from Baratron is obtained each time when the sampling valve is switched from *injet* to *load* position. If there is no plugging in the sample loop, pressure reading from the Baratron is quickly reduced as the vacuum pump starts, for example t= 0 min, P= 730 torr, t= 5 sec, P= 450 torr, t=10sec, P=300 torr. **2)** Ensure that there is no air in the liquid lines and

liquids can be instantly ejected from valves V_{2A} and V_{2B} (repeat the test for each valve): turn the *liquid injector* A (or B) to ~30-40 kPa (reading from P_A or P_B), then slightly open valve (V_{2A} or V_{2B}) until the first drop of liquid enters the equilibrium chamber then close valve V_{2A} (or V_{2B}). Record the reading from Baratron and repeat the test. If no liquid was ejected from the valve V_{2A} (or V_{2B}) or readings from the Baratron changed, re-degassing of the feed chamber and liquid line should be considered. The reading from the Baratron should be the pressure of pure liquid A (or B) at the experimental temperature. **3)** Turn the liquid injector in counterclockwise direction (about 1 turn for each 5 turns in clockwise direction) when loading liquid from the feed chamber to an empty injector. This activity provides a quick equilibration inside the injector and allows liquid to be fully loaded. **4)** Intermittently open valve V_4 and turn off the vacuum pump during the evacuation of the equilibration chamber. This activity helps to dilute the gas inside the chamber with fresh air, and reduces the time for a complete evacuation of the chamber.

As discussed in chapter 6, the Fischer recirculating still does not provide adequate mixing, and overheats the large portion mixture between the tip of the heating bulb and the Cottrell pump. These limitations can be reduced by adding a section between the feed chamber and the returning liquid line from the Cottrell pump to recirculate liquid, and provide a good mixing before liquid flows back to the reboiler.

The rate of recirculating vapor is regulated by the *preset* in operating the Fischer apparatus. This parameter should be assigned carefully to reduce the effect of overheating liquid. For a low boiling point liquid ~ 80-100 °C, the preset should be ~ 10 %. For an intermediate boiling point liquid such as ethyl lactate, the preset should

be ~ 15-18 %, and for high boiling point or highly viscosity liquid such as concentrated lactic solution, the preset should be ~25-28 %.

SPEAD molecular simulation demonstrates an excellent capability to predict vapor pressure of complex molecules. A FORTRAN program is provided from this work for use with SPEAD. It can be modified for optimization of a larger number of SPEAD parameters. To obtain the global optimum, the scaling factor which relates to the Hessian matrix used in the DBCONF routine of IMSL must be set in the right order of magnitude to avoid stepping outside the interval. In addition, the order of the initial parameters guesses in the input file should be used carefully, because the routine DBCONF always adjusts parameters in the order in which they are entered before performing simultaneous searches. Different orders were used but no clear trends were observed and no definite recommendations can be made.

Difficulties were encountered in converging SPEAD vapor pressure calculations at high reduced temperatures, which may be due to the fitted A_1 and A_2 terms, or may be due to the iteration method. SPEAD should improve the fitting of A_2 in addition to any weaknesses in the overall simulation or perturbation method. The current expression of $A_2 = \frac{c_1\eta + c_2\eta^2 + c_3\eta^3 + c_4\eta^4}{1 + 500\eta^4}$ indicates that coefficient C_4 is the dominating factor at high density. A different polynomial to obtain a better regression of A_2 at high densities, and/or a correlation to constrain its coefficients should be considered. Fitting of A_2 for the intermediate densities may also need to be improved because the calculated Z shows some deviation from the simulation data in this region. The limitations of the perturbation convergence may be important and should be evaluated. Perhaps third or higher order terms are needed for certain conditions, and a longer simulation should be

performed for large molecules to reduce the apparently random scatter at high densities.

To reduce the underestimation of vapor pressures for high molecular compounds, more investigation should be undertaken to determine the cause of the curvature in the predicted curvature of ln(Psat) versus $T^{-1.3}$. The ratio of A_2/A_1 is known to be a function of molecular weight [84], but the dependence has not been quantified. Such a correlation may be helpful in extending predictive capabilities.

Further studies of both intra and intermolecular hydrogen bonding systems are desirable to extend the reliability of SPEAD for highly oxygenated compounds, which usually have multiple hydrogen bonding sites. These compounds are expected to be developed from natural feedstocks. SPEAD currently does not have a method to differentiate between hydrogen bond donors and hydrogen bond acceptors, and greatly underestimates the vapor pressure of diols, for example the 2,3-butanediol was underestimated by 79 %.

Another interesting modification would involve including the hydrogen bonding in the reference simulation. This modification requires careful thought because the simulations may need to be performed at multiple temperatures. The non-specific attractive potentials could be added as the perturbation, therefore the DMD simulation would still be faster than a simulation with full potentials.

The use of wells at positions 1.2, 1.5, 1.8 and 2.0 σ was dictated by the previously developed SPEAD programs. The position of the wells should be adjusted to more accurately approximate the Lennard-Jones potential. The current *SiteParms.2580.txt* (SPEAD well table) has a number of wells that do not represent the expected Lennard-Jones shape. The well depths could be coupled to reduce the number of adjustable

parameters. The two intermediate wells are currently interpolated from the inner and outer wells, but a large number of variables required adjustments in searching for the optimal parameters of one functional group in some cases.

This work was performed using a compiled version of SPEAD. Therefore, flexibility was limited for investigating the simulation results. For example, it was not possible to explore the intra- and intermolecular events using the current SPEAD version, and SPEAD could not be run on the MSU supercomputers. Also, it was discovered that the code uses a fixed seed for pseudorandom number generations, which exactly provides the same value of Z when the simulation is repeated. Therefore, the scatter in the calculation of A_2 was not eliminated by restarting the simulation. MSU should develop an independent simulation code and smoothing programs.

APPENDIX A

EXPERIMENTAL ADSORPTION DATA

(Reference in Chapter 2)

Run # 6: In ethanol, XAD-2 = 1.9296 g, flowrate = 0.16 ml/min, C = 1.0 %, S = 0%

[a]Fraction	[b]Time	[c]Bed Vol	[d]oil %	[e]C/C_0	[f]$C_1/C_{1,0}$	[g]$C_2/C_{2,0}$
1	20	0.84	0.10%	0.100	-	-
2	40	1.68	0.53%	0.530	-	-
3	59	2.48	0.77%	0.770	-	-
4	79	3.33	0.84%	0.840	-	-
5	99	4.17	0.82%	0.820	-	-
6	119	5.01	0.85%	0.850	-	-
7	149	6.27	0.89%	0.890		
8	189	8.00	0.98%	0.980	-	-

C and S denote for castor and soybean oil. [a] : sample collected in the experiment, [b] : time (minutes) after fixed-bed starts, [c] : number of bed volumes, [d] : total oil concentration, [e, f, g]: concentrations of total oil (C), ricinolein (C_1), and non-hydroxylated component (C_2) in the effluent compared to their initial C_0 , $C_{1,0}$, $C_{2,0}$.

Run # 7: In ethanol, XAD-2 = 2.802 g, flowrate = 0.16 ml/min, C = 2.46 %, S = 0%

[a]Fraction	[b]Time	[c]Bed Vol	[d]oil %	[e]C/C_0	[f]$C_1/C_{1,0}$	[g]$C_2/C_{2,0}$
1	15	0.545	0.07%	0.027	-	-
2	25	0.909	0.06%	0.024	0.026	0.005
3	40	1.455	0.71%	0.290	0.317	0.090
4	56	2.036	1.80%	0.732	0.785	0.341
5	71	2.582	2.09%	0.851	0.866	0.745
7	101	3.673	2.30%	0.934	0.932	0.950
8	116	4.218	2.34%	0.953	0.957	0.925
9	131	4.764	2.36%	0.960	0.907	1.353
10	146	5.309	2.43%	0.989	0.991	0.975
11	162	5.891	2.43%	0.991	0.993	0.972
12	176	6.400	2.45%	0.996	1.002	0.951
13	191	6.945	2.45%	0.997	1.000	0.977
14	206	7.491	2.49%	1.013	1.016	0.994
15	221	8.031	2.48%	1.010	1.017	0.962

C and S denote for castor and soybean oil. [a] : sample collected in the experiment, [b] : time (minutes) after fixed-bed starts, [c] : number of bed volumes, [d] : total oil concentration, [e, f, g]: concentrations of total oil (C), ricinolein (C_1), and non-hydroxylated component (C_2) in the effluent compared to their initial C_0 , $C_{1,0}$, $C_{2,0}$.

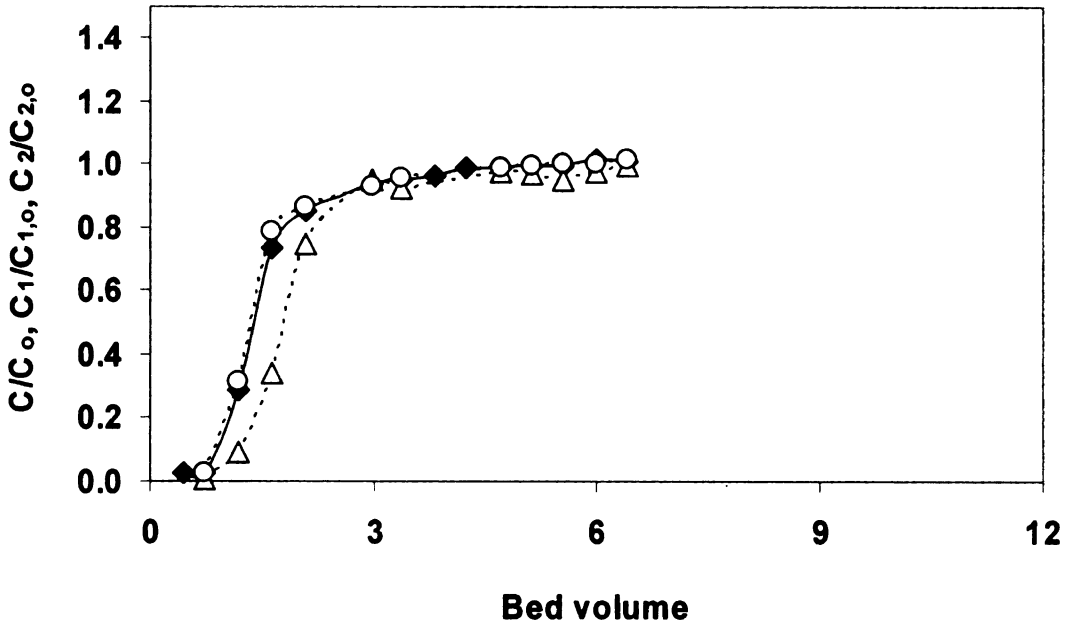

Figure A.1 Fixed-bed Adsorption Using Ethanol and XAD-2 (Run # 7)

♦: total oil, ○: hydroxyl, Δ: non-hydroxy.

Run # 8: In ethanol, SD-2 = 2.833 g, flowrate = 0.18 ml/min, C = 0 %, S = 3.69 %

[a]Fraction	[b]Time	[c]Bed Vol	[d]oil %	[e]C/C_0	[f]$C_1/C_{1,0}$	[g]$C_2/C_{2,0}$
1	12	0.44	0.07%	0.020	0.000	0.020
2	24	0.88	0.00%	0.000	0.000	0.000
3	36	1.32	0.02%	0.004	0.000	0.004
4	51	1.87	0.31%	0.087	0.000	0.087
5	68	2.49	1.28%	0.357	0.000	0.357
6	83	3.04	2.39%	0.663	0.000	0.663
7	97	3.56	2.66%	0.739	0.000	0.739
8	114	4.18	2.92%	0.812	0.000	0.812
9	130	4.77	3.22%	0.896	0.000	0.896
10	148	5.43	3.42%	0.951	0.000	0.951
11	163	5.98	3.49%	0.971	0.000	0.971
12	178	6.53	3.56%	0.988	0.000	0.988

C and S denote for castor and soybean oil. [a] : sample collected in the experiment, [b] : time (minutes) after fixed-bed starts, [c] : number of bed volumes, [d] : total oil concentration, [e, f, g]: concentrations of total oil (C), ricinolein (C_1), and non-hydroxylated component (C_2) in the effluent compared to their initial C_0 , $C_{1,0}$, $C_{2,0}$.

Run # 9: In ethanol, SD-2 = 2.904 g, flowrate = 0.17 ml/min, C = 0.80 %, S = 1.60 %

[a]Fraction	[b]Time	[c]Bed Vol	[d]oil %	[e]C/C_0	[f]$C_1/C_{1,0}$	[g]$C_2/C_{2,0}$
1	16	0.55	-0.01%	-0.006	-	-
2	32	1.11	0.03%	0.012	0.019	0.009
3	51	1.77	0.26%	0.109	-	-
4	67	2.32	0.53%	0.220	-	-
5	82	2.84	0.93%	0.386	0.670	0.267
6	97	3.36	1.27%	0.527	-	-
7	114	3.95	1.58%	0.660	1.008	0.512
8	133	4.61	1.81%	0.754	1.042	0.631
9	150	5.20	1.98%	0.824	-	-
10	166	5.75	2.09%	0.870	-	-
11	181	6.27	2.20%	0.915	-	-
12	196	6.79	2.24%	0.933	-	-
13	214	7.42	2.24%	0.931	0.857	0.960
14	232	8.04	2.15%	0.895	0.938	0.872
16	271	9.39	2.32%	0.968	0.908	0.988
17	293	10.16	2.38%	0.991	-	-
18	319	11.06	2.40%	0.999	-	-

C and S denote for castor and soybean oil. [a] : sample collected in the experiment, [b] : time (minutes) after fixed-bed starts, [c] : number of bed volumes, [d] : total oil concentration, [e, f, g]: concentrations of total oil (C), ricinolein (C_1), and non-hydroxylated component (C_2) in the effluent compared to their initial C_0 , $C_{1,0}$, $C_{2,0}$.

Run # 10: In ethanol, SD-2 = 2.836 g, flowrate = 0.19 ml/min, C = 1.99 %, S = 0.41 %

[a]Fraction	[b]Time	[c]Bed Vol	[d]oil %	[e]C/C_0	[f]$C_1/C_{1,0}$	[g]$C_2/C_{2,0}$
1	16	0.65	0.00%	-0.002	0.000	0.000
2	31	1.26	0.19%	0.078	0.104	0.014
3	46	1.86	0.80%	0.336	0.431	0.098
4	62	2.51	1.32%	0.554	0.692	0.204
5	77	3.12	1.65%	0.690	0.838	0.317
6	92	3.73	1.91%	0.798	0.942	0.435
7	109	4.41	2.05%	0.858	0.935	0.663
8	124	5.02	2.13%	0.891	0.984	0.657
9	139	5.63	2.19%	0.915	0.000	0.000
10	154	6.24	2.19%	0.917	1.019	0.659
11	169	6.84	1.87%	0.781	0.820	0.681
12	186	7.53	2.29%	0.957	0.987	0.880
13	202	8.18	2.32%	0.970	0.000	0.000
14	219	8.87	2.33%	0.973	0.000	0.000
15	235	9.52	2.31%	0.967	0.000	0.000

C and S denote for castor and soybean oil. [a] : sample collected in the experiment, [b] : time (minutes) after fixed-bed starts, [c] : number of bed volumes, [d] : total oil concentration, [e, f, g]: concentrations of total oil (C), ricinolein (C_1), and non-hydroxylated component (C_2) in the effluent compared to their initial C_0 , $C_{1,0}$, $C_{2,0}$.

Run # 11: In ethanol, SD-2 = 2.837 g, flowrate = 0.20 ml/min, C = 0.38 %, S = 1.99 %

[a]Fraction	[b]Time	[c]Bed Vol	[d]oil %	[e]C/C_0	[f]$C_1/C_{1,0}$	[g]$C_2/C_{2,0}$
1	15	0.62	0.00%	-0.002	0.000	0.000
2	30	1.24	0.01%	0.003	0.020	0.001
3	45	1.86	0.24%	0.103	0.403	0.050
4	61	2.52	0.66%	0.276	0.873	0.170
5	77	3.18	1.06%	0.443	0.958	0.353
6	94	3.88	1.43%	0.600	0.000	0.000
7	109	4.50	1.75%	0.734	0.944	0.697
8	126	5.20	1.93%	0.810	1.073	0.763
9	142	5.86	2.09%	0.880	1.103	0.840
10	157	6.48	2.19%	0.921	0.000	0.000
11	174	7.19	2.30%	0.965	1.187	0.925
12	191	7.89	2.26%	0.950	0.000	0.000
13	206	8.51	2.30%	0.965	1.146	0.933
14	221	9.13	2.31%	0.971	0.000	0.000

C and S denote for castor and soybean oil. [a] : sample collected in the experiment, [b] : time (minutes) after fixed-bed starts, [c] : number of bed volumes, [d] : total oil concentration, [e, f, g]: concentrations of total oil (C), ricinolein (C_1), and non-hydroxylated component (C_2) in the effluent compared to their initial C_0 , $C_{1,0}$, $C_{2,0}$.

Run # 12: In ethanol, SD-2 = 2.826 g, flowrate = 0.20 ml/min, C = 0 %, S = 2.44 %

[a]Fraction	[b]Time	[c]Bed Vol	[d]oil %	[e]C/C_0	[f]$C_1/C_{1,0}$	[g]$C_2/C_{2,0}$
1	15	0.66	0.00%	-0.002	0.000	0.000
2	30	1.31	0.02%	0.007	0.000	0.007
3	45	1.97	0.23%	0.094	0.000	0.094
4	60	2.62	0.38%	0.156	0.000	0.156
5	75	3.28	0.85%	0.351	0.000	0.351
6	90	3.93	1.47%	0.606	0.000	0.606
7	105	4.59	1.95%	0.807	0.000	0.820
8	120	5.25	1.98%	0.820	0.000	0.807
9	135	5.90	1.72%	0.807	0.000	0.710
10	154	6.73	2.21%	0.914	0.000	0.914
11	169	7.39	2.36%	0.974	0.000	0.000
12	184	8.04	2.52%	1.042	0.000	0.000
14	214	9.35	2.44%	1.010	0.000	0.000

C and S denote for castor and soybean oil. [a] : sample collected in the experiment, [b] : time (minutes) after fixed-bed starts, [c] : number of bed volumes, [d] : total oil concentration, [e, f, g]: concentrations of total oil (C), ricinolein (C_1), and non-hydroxylated component (C_2) in the effluent compared to their initial C_0 , $C_{1,0}$, $C_{2,0}$.

Run # 13: In ethanol, SD-2 = 2.835 g, flowrate = 0.19 ml/min, C = 0 %, S = 2.42 %

[a]Fraction	[b]Time	[c]Bed Vol	[d]oil %	[e]C/C_0	[f]$C_1/C_{1,0}$	[g]$C_2/C_{2,0}$
1	15	0.63	0.44%	0.168	0.000	0.168
2	30	1.26	0.05%	0.020	0.000	0.020
3	45	1.90	0.46%	0.174	0.000	0.174
4	60	2.53	0.68%	0.257	0.000	0.257
5	75	3.16	1.56%	0.592	0.000	0.592
6	92	3.88	1.47%	0.555	0.000	0.555
7	112	4.72	1.81%	0.687	0.000	0.687
8	127	5.35	2.06%	0.780	0.000	0.000
9	142	5.98	2.22%	0.840	0.000	0.000
10	157	6.61	1.78%	0.674	0.000	0.000
11	172	7.25	2.34%	0.887	0.000	0.000
12	187	7.88	2.47%	0.937	0.000	0.000
13	202	8.51	2.41%	0.915	0.000	0.000
14	217	9.14	2.54%	0.962	0.000	0.000
15	229	9.65	2.63%	0.996	0.000	0.000

C and S denote for castor and soybean oil. [a] : sample collected in the experiment, [b] : time (minutes) after fixed-bed starts, [c] : number of bed volumes, [d] : total oil concentration, [e, f, g]: concentrations of total oil (C), ricinolein (C_1), and non-hydroxylated component (C_2) in the effluent compared to their initial C_0 , $C_{1,0}$, $C_{2,0}$.

Run # 14: In ethanol, SD-2 = 2.832 g, flowrate = 0.19 ml/min, C = 0 %, S = 2.42 %

[a]Fraction	[b]Time	[c]Bed Vol	[d]oil %	[e]C/C_0	[f]$C_1/C_{1,0}$	[g]$C_2/C_{2,0}$
1	15	0.63	0.26%	0.109	0.000	0.109
2	30	1.27	0.08%	0.035	0.000	0.035
3	45	1.90	0.16%	0.067	0.000	0.067
4	60	2.54	0.58%	0.241	0.000	0.241
5	75	3.17	1.03%	0.429	0.000	0.000
6	90	3.80	1.42%	0.590	0.000	0.000
7	105	4.44	1.37%	0.571	0.000	0.000
8	120	5.07	1.92%	0.802	0.000	0.000
9	135	5.71	2.11%	0.880	0.000	0.000
10	150	6.34	1.70%	0.708	0.000	0.000
11	165	6.98	1.23%	0.514	0.000	0.000
12	180	7.61	2.33%	0.970	0.000	0.000
13	195	8.24	2.03%	0.847	0.000	0.000
14	210	8.88	1.80%	0.752	0.000	0.000
15	225	9.51	1.80%	0.749	0.000	0.000

C and S denote for castor and soybean oil. [a] : sample collected in the experiment, [b] : time (minutes) after fixed-bed starts, [c] : number of bed volumes, [d] : total oil concentration, [e, f, g]: concentrations of total oil (C), ricinolein (C_1), and non-hydroxylated component (C_2) in the effluent compared to their initial C_0 , $C_{1,0}$, $C_{2,0}$.

Run # 15: In ethanol, SD-2 = 2.832 g, flowrate = 0.18 ml/min, C = 3.76 %, S = 0 %

[a]Fraction	[b]Time	[c]Bed Vol	[d]oil %	[e]C/C_0	[f]$C_1/C_{1,0}$	[g]$C_2/C_{2,0}$
1	15	0.59	0.07%	0.018	-	-
2	30	1.17	0.31%	0.079	0.085	0.025
3	45	1.76	1.59%	0.409	0.425	0.260
4	60	2.34	2.57%	0.660	0.672	0.546
5	75	2.93	3.07%	0.789	0.819	0.620
6	90	3.51	3.42%	0.877	0.889	0.771
7	105	4.10	3.58%	0.918	0.924	0.863
8	120	4.68	3.67%	0.943	0.970	0.798
9	135	5.27	3.19%	0.819	0.799	0.997
10	150	5.85	3.72%	0.954	0.968	0.826
11	165	6.44	3.72%	0.956	-	-
12	180	7.02	3.71%	0.952	-	-
13	198	7.72	3.78%	0.971	0.992	0.775

C and S denote for castor and soybean oil. [a] : sample collected in the experiment, [b] : time (minutes) after fixed-bed starts, [c] : number of bed volumes, [d] : total oil concentration, [e, f, g]: concentrations of total oil (C), ricinolein (C_1), and non-hydroxylated component (C_2) in the effluent compared to their initial C_0 , $C_{1,0}$, $C_{2,0}$.

Run # 16: In ethanol, SD-2 = 2.834 g, flowrate = 0.19 ml/min, C = 1.20 %, S = 1.21 %

[a]Fraction	[b]Time	[c]Bed Vol	[d]oil %	[e]C/C_0	[f]$C_1/C_{1,0}$	[g]$C_2/C_{2,0}$
1	15	0.62	0.00%	0.002	0.004	0.000
2	30	1.24	0.06%	0.024	0.049	0.004
3	45	1.86	0.34%	0.144	0.293	0.027
4	60	2.48	0.78%	0.327	0.581	0.126
5	75	3.10	1.11%	0.468	0.748	0.246
6	90	3.72	1.49%	0.629	0.928	0.391
7	105	4.34	1.67%	0.704	0.970	0.493
8	120	4.96	1.88%	0.793	1.021	0.613
9	135	5.57	1.99%	0.837	1.003	0.705
10	150	6.19	2.09%	0.879	0.974	0.804
11	165	6.81	1.90%	0.800	0.958	0.674
12	185	7.64	2.28%	0.962	-	-
13	202	8.34	2.24%	0.944	0.989	0.909
14	219	9.04	2.26%	0.951	0.908	0.986
15	239	9.87	2.36%	0.995	1.036	0.962

C and S denote for castor and soybean oil. [a] : sample collected in the experiment, [b] : time (minutes) after fixed-bed starts, [c] : number of bed volumes, [d] : total oil concentration, [e, f, g]: concentrations of total oil (C), ricinolein (C_1), and non-hydroxylated component (C_2) in the effluent compared to their initial C_0 , $C_{1,0}$, $C_{2,0}$.

Run # 17: In ethanol, SD-2 = 2.835 g, flowrate = 0.17 ml/min, C = 2.40 %, S = 0 %

[a]Fraction	[b]Time	[c]Bed Vol	[d]oil %	[e]C/C_0	[f]$C_1/C_{1,0}$	[g]$C_2/C_{2,0}$
1	10	0.37	0.05%	0.019	-	-
2	25	0.94	0.12%	0.050	0.055	0.017
3	42	1.57	0.34%	0.142	0.153	0.062
4	60	2.25	0.99%	0.410	0.433	0.238
5	75	2.81	1.50%	0.623	0.653	0.402
6	91	3.41	1.82%	0.756	0.784	0.552
7	108	4.04	2.36%	0.978	1.006	0.774
8	125	4.68	2.23%	0.924	0.944	0.776
9	140	5.24	2.33%	0.965	0.982	0.841
10	157	5.88	2.37%	0.983	0.997	0.885
11	174	6.51	2.37%	0.981	0.988	0.931
12	194	7.26	2.39%	0.993	1.000	0.939
13	211	7.90	2.41%	1.000	0.995	1.039

C and S denote for castor and soybean oil. [a] : sample collected in the experiment, [b] : time (minutes) after fixed-bed starts, [c] : number of bed volumes, [d] : total oil concentration, [e, f, g]: concentrations of total oil (C), ricinolein (C_1), and non-hydroxylated component (C_2) in the effluent compared to their initial C_0 , $C_{1,0}$, $C_{2,0}$.

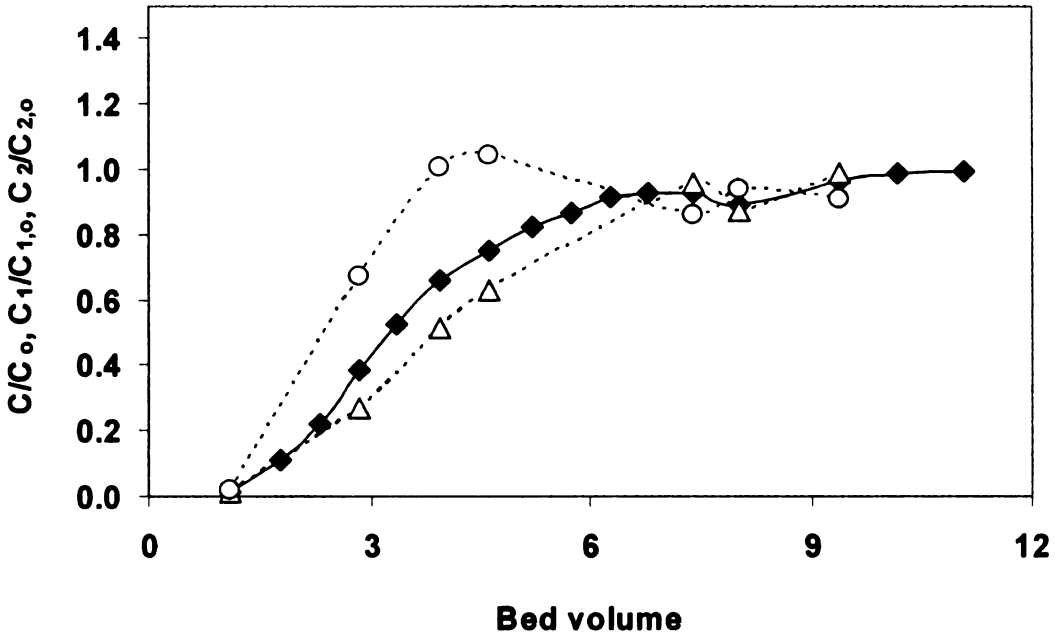

Figure A.2 Fixed-bed Adsorption Using Ethanol and SD-2 (Run # 9)

♦: total oil, ○: hydroxyl, Δ: non-hydroxy.

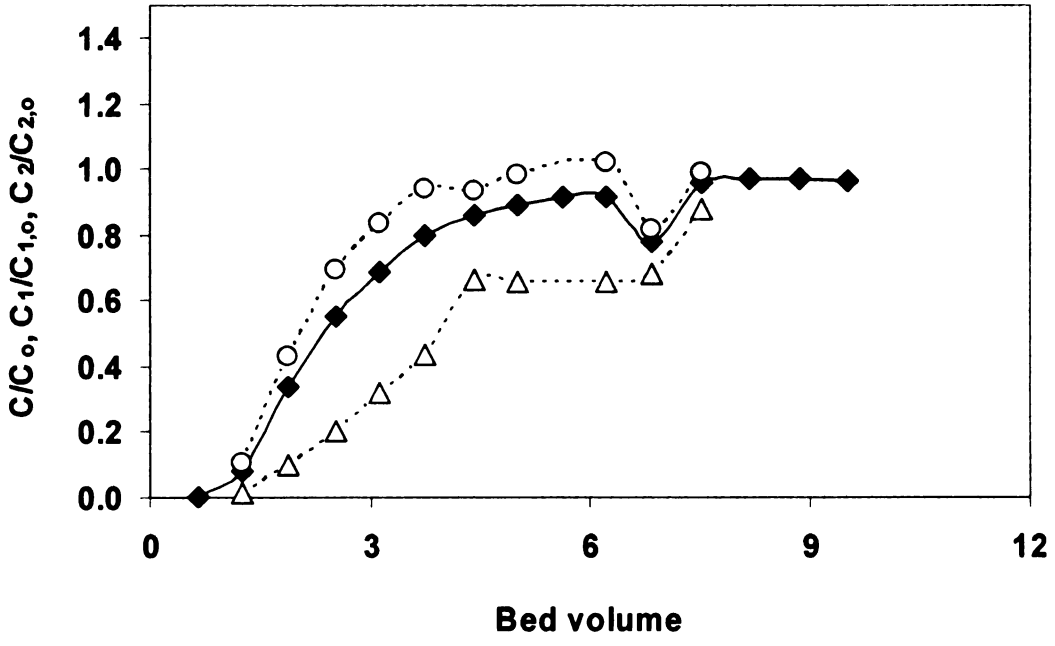

Figure A.3 Fixed-bed Adsorption Using Ethanol and SD-2 (Run # 10)

♦: total oil, ○: hydroxyl, Δ: non-hydroxy.

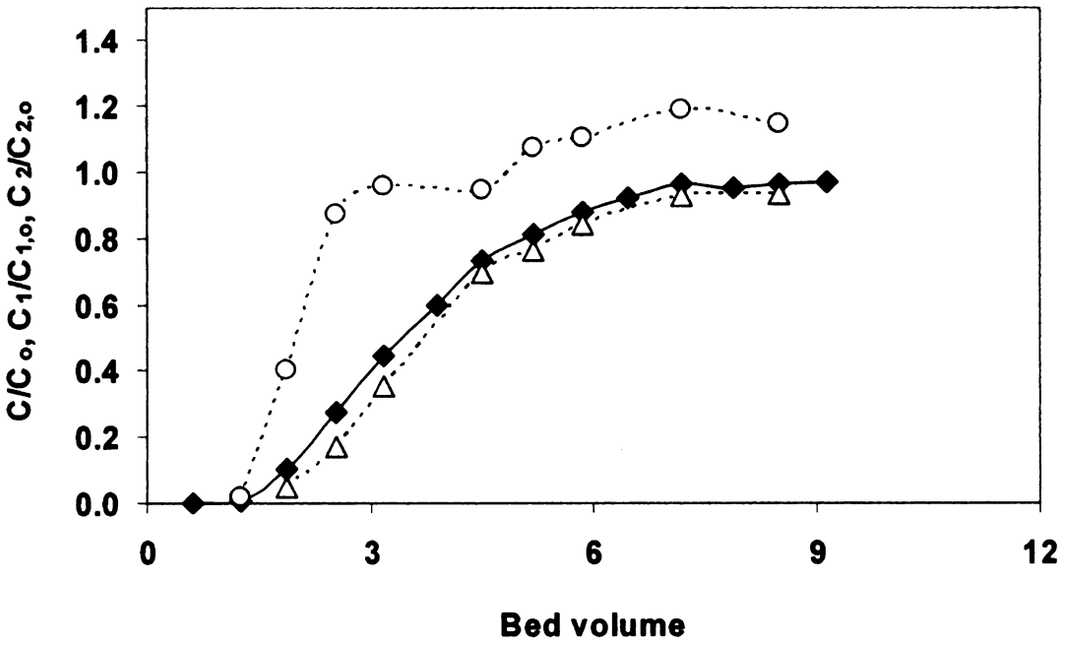

Figure A.4 Fixed-bed Adsorption Using Ethanol and SD-2 (Run # 11)

♦: total oil, ○: hydroxyl, Δ: non-hydroxy.

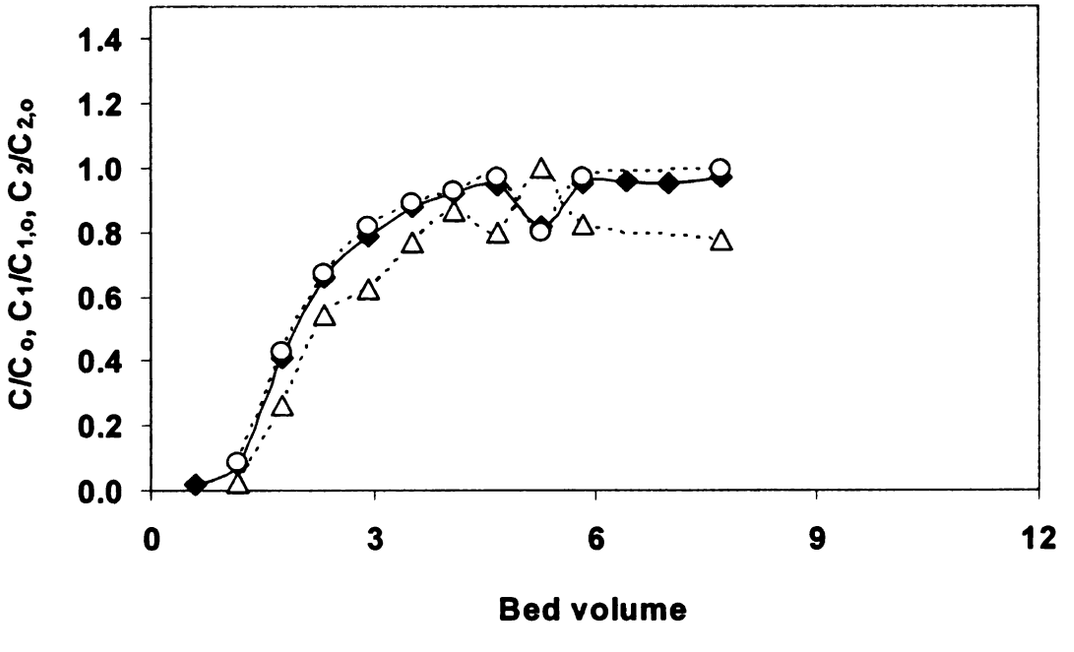

Figure A.5 Fixed-bed Adsorption Using Ethanol and SD-2 (Run # 15)

♦: total oil, ○: hydroxyl, Δ: non-hydroxy.

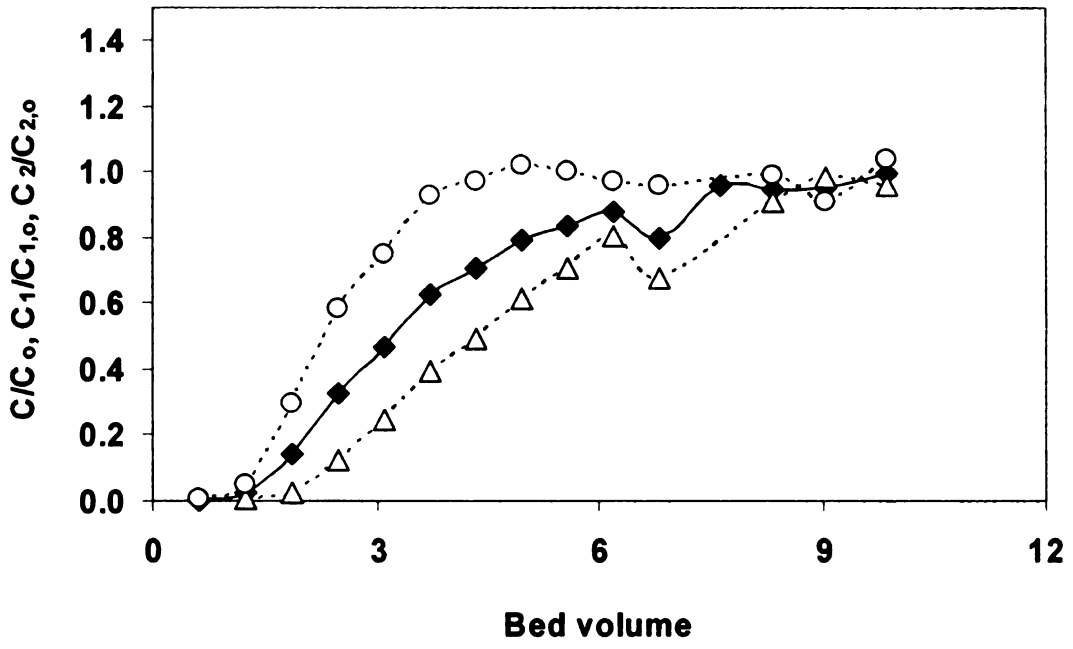

Figure A.6 Fixed-bed Adsorption Using Ethanol and SD-2 (Run # 16)

♦: total oil, ○: hydroxyl, Δ: non-hydroxy.

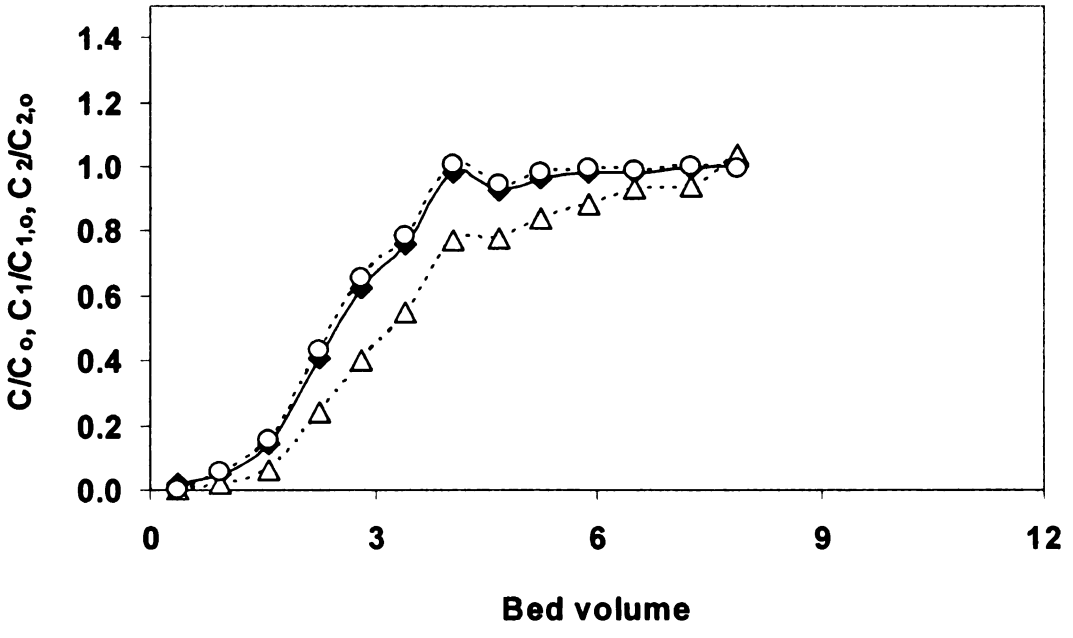

Figure A.7 Fixed-bed Adsorption Using Ethanol and SD-2 (Run # 17)

♦: total oil, ○: hydroxyl, Δ: non-hydroxy.

Run # 18: In ethanol, L-493 = 2.865 g, flowrate = 0.19 ml/min, C = 1.64 %, S = 0.84 %

[a]Fraction	[b]Time	[c]Bed Vol	[d]oil %	[e]C/C_0	[f]$C_1/C_{1,0}$	[g]$C_2/C_{2,0}$
1	15	0.572	-0.01%	-0.003	-	-
2	34	1.296	0.07%	0.029	0.048	0.006
3	54	2.059	0.60%	0.243	0.350	0.114
4	70	2.669	1.23%	0.501	0.682	0.283
5	87	3.317	1.66%	0.676	0.988	0.300
6	102	3.888	1.89%	0.770	-	-
7	121	4.613	2.04%	0.831	1.141	0.459
8	141	5.375	2.14%	0.871	-	-
9	162	6.176	2.22%	0.900	1.054	0.716
10	183	6.976	2.31%	0.939	-	-
11	204	7.777	2.36%	0.960	1.128	0.759
12	228	8.692	2.39%	0.971	-	-
13	251	9.569	2.41%	0.981	-	-
14	274	10.445	2.41%	0.978	1.108	0.822

C and S denote for castor and soybean oil. [a] : sample collected in the experiment, [b] : time (minutes) after fixed-bed starts, [c] : number of bed volumes, [d] : total oil concentration, [e, f, g]: concentrations of total oil (C), ricinolein (C_1), and non-hydroxylated component (C_2) in the effluent compared to their initial C_0 , $C_{1,0}$, $C_{2,0}$

Run # 19: In ethanol, L-493 = 2.827 g, flowrate = 0.19 ml/min, C = 0.82 %, S = 1.63 %

[a]Fraction	[b]Time	[c]Bed Vol	[d]oil %	[e]C/C_0	[f]$C_1/C_{1,0}$	[g]$C_2/C_{2,0}$
1	18	0.661	0.03%	0.008	-	-
2	38	1.396	0.03%	0.012	-	-
3	53	1.947	0.24%	0.098	0.264	0.018
4	74	2.718	0.75%	0.305	0.716	0.106
5	91	3.343	1.28%	0.520	1.018	0.281
6	106	3.894	1.62%	0.663	0.899	0.549
7	120	4.408	1.89%	0.771	0.982	0.670
8	139	5.106	2.09%	0.853	-	-
9	157	5.767	2.19%	0.896	1.012	0.840
10	181	6.649	1.89%	0.772	-	-
11	201	7.384	2.35%	0.960	0.982	0.950
12	223	8.192	2.40%	0.980	-	-
13	243	8.927	2.43%	0.991	1.056	0.960
14	262	9.625	2.36%	0.962	-	-

C and S denote for castor and soybean oil. [a] : sample collected in the experiment, [b] : time (minutes) after fixed-bed starts, [c] : number of bed volumes, [d] : total oil concentration, [e, f, g]: concentrations of total oil (C), ricinolein (C_1), and non-hydroxylated component (C_2) in the effluent compared to their initial C_0 , $C_{1,0}$, $C_{2,0}$.

Run # 20: In ethanol, L-493 = 2.875 g, flowrate = 0.19 ml/min, C = 2.48 %, S = 0 %

[a]Fraction	[b]Time	[c]Bed Vol	[d]oil %	[e]C/C_0	[f]$C_1/C_{1,0}$	[g]$C_2/C_{2,0}$
1	20	0.756	0.12%	0.047	0.049	0.033
2	46	1.740	1.11%	0.447	0.440	0.486
3	62	2.345	1.81%	0.729	-	-
4	79	2.987	2.11%	0.852	0.894	0.601
5	96	3.630	2.29%	0.924	0.936	0.853
6	112	4.235	2.41%	0.971	-	-
7	128	4.840	2.42%	0.975	0.985	0.915
8	148	5.597	2.43%	0.982	-	-
9	163	6.164	2.49%	1.003	1.018	0.910
10	180	6.807	2.47%	0.996	-	-
11	199	7.525	2.46%	0.992	-	-
12	214	8.092	2.48%	1.001	1.007	0.968
13	228	8.622	2.48%	0.998	-	-

C and S denote for castor and soybean oil. [a] : sample collected in the experiment, [b] : time (minutes) after fixed-bed starts, [c] : number of bed volumes, [d] : total oil concentration, [e, f, g]: concentrations of total oil (C), ricinolein (C_1), and non-hydroxylated component (C_2) in the effluent compared to their initial C_0 , $C_{1,0}$, $C_{2,0}$.

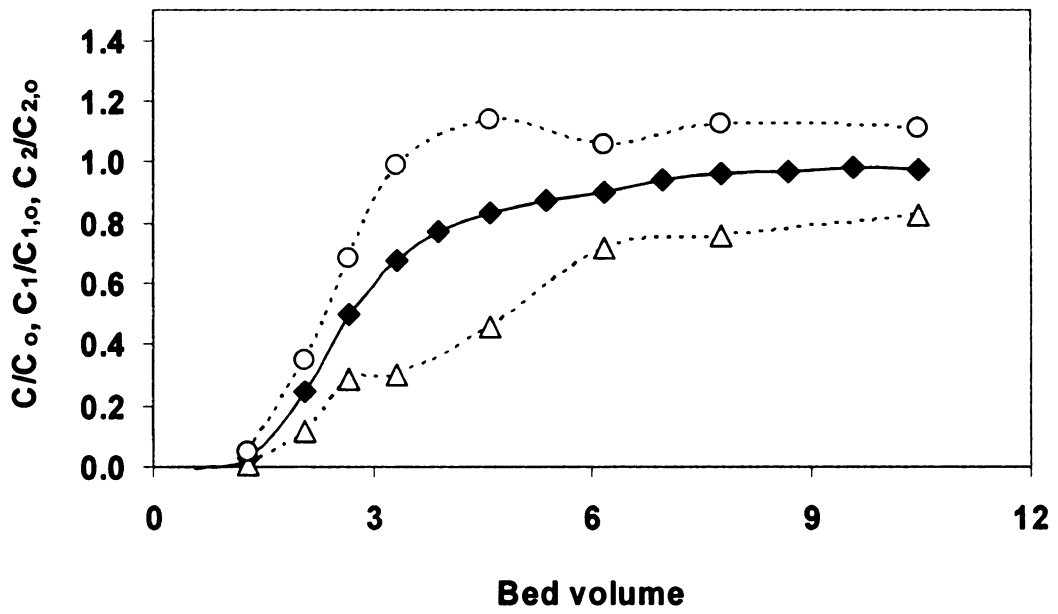

Figure A.8 Fixed-bed Adsorption Using Ethanol and L-493 (Run # 18)

♦: total oil, ○: hydroxyl, Δ: non-hydroxy.

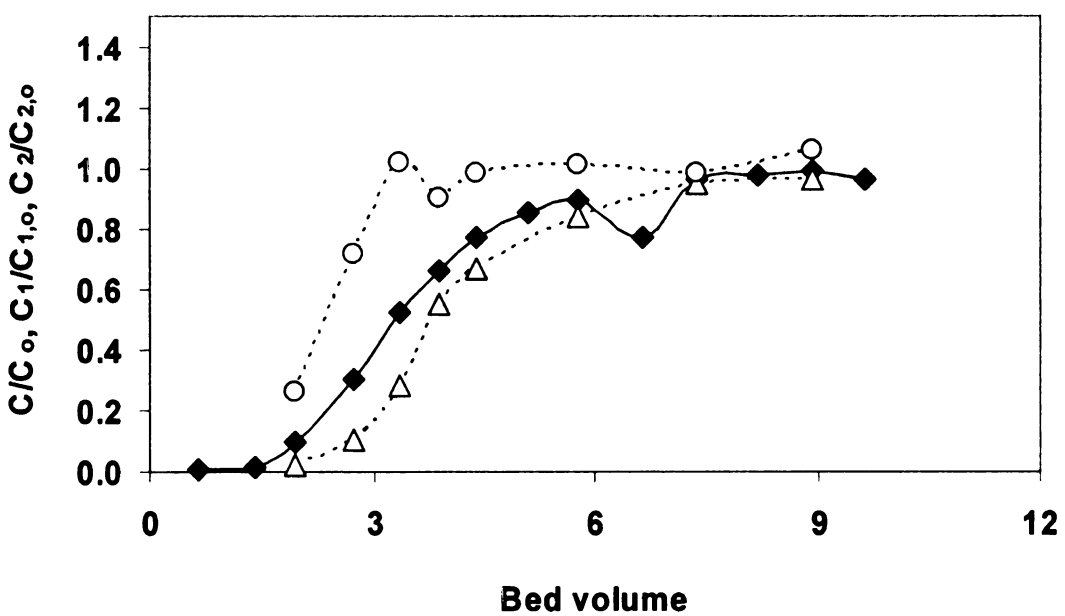

Figure A.9 Fixed-bed Adsorption Using Ethanol and L-493 (Run # 19)

♦: total oil, ○: hydroxyl, Δ: non-hydroxy.

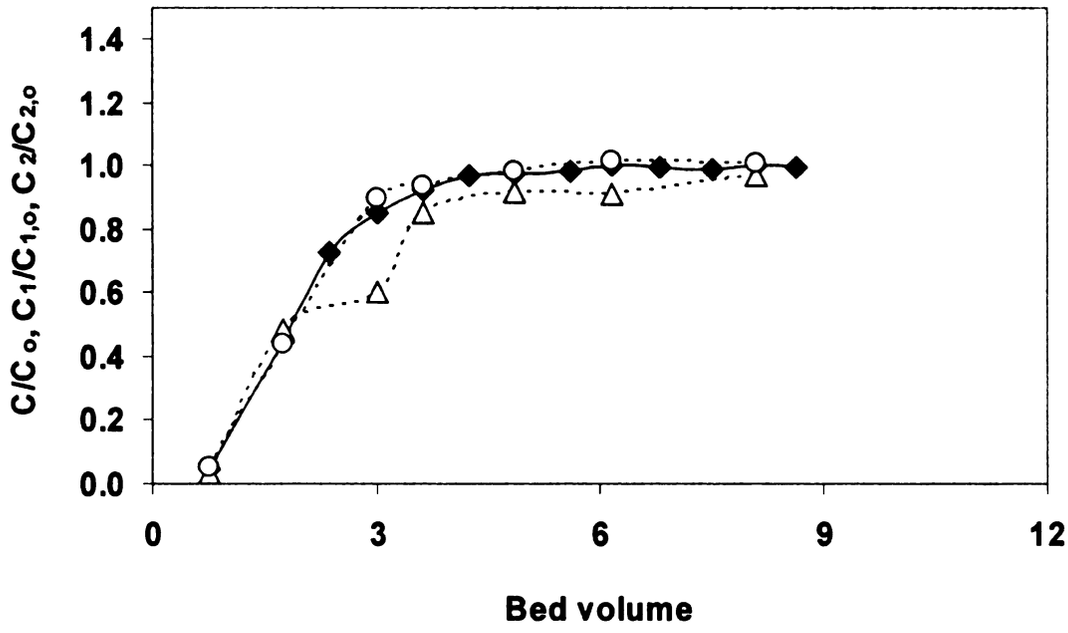

Figure A.10 Fixed-bed Adsorption Using Ethanol and L-493 (Run # 20)

♦: total oil, ○: hydroxyl, Δ: non-hydroxy.

Run # 21: In Ethanol, M-43 = 2.837 g, flowrate = 0.14 ml/min, C = 2.51 %, S = 0%

[a]Fraction	[b]Time	[c]Bed Vol	[d]oil %	[e]C/C_0	[f]$C_1/C_{1,0}$	[g]$C_2/C_{2,0}$
1	16	0.679	0.02%	0.010	0.000	0.000
2	31	1.316	0.97%	0.385	0.387	0.366
3	46	1.953	1.92%	0.765	0.769	0.735
4	62	2.633	2.25%	0.895	0.902	0.838
5	76	3.227	2.27%	0.903	0.910	0.852
6	91	3.864	2.44%	0.973	0.000	0.000
7	106	4.501	2.42%	0.966	0.973	0.912
8	121	5.138	2.42%	0.963	0.958	1.000
9	139	5.902	2.43%	0.967	0.000	0.000
10	156	6.624	2.46%	0.979	0.000	0.000
11	177	7.516	2.45%	0.976	0.000	0.000
12	192	8.152	2.44%	0.973	0.000	0.000
13	209	8.874	2.42%	0.963	0.000	0.000
14	222	9.426	2.41%	0.960	0.000	0.000
15	238	10.106	2.47%	0.983	0.986	0.965

C and S denote for castor and soybean oil. [a] : sample collected in the experiment, [b] : time (minutes) after fixed-bed starts, [c] : number of bed volumes, [d] : total oil concentration, [e, f, g]: concentrations of total oil (C), ricinolein (C_1), and non-hydroxylated component (C_2) in the effluent compared to their initial C_0 , $C_{1,0}$, $C_{2,0}$.

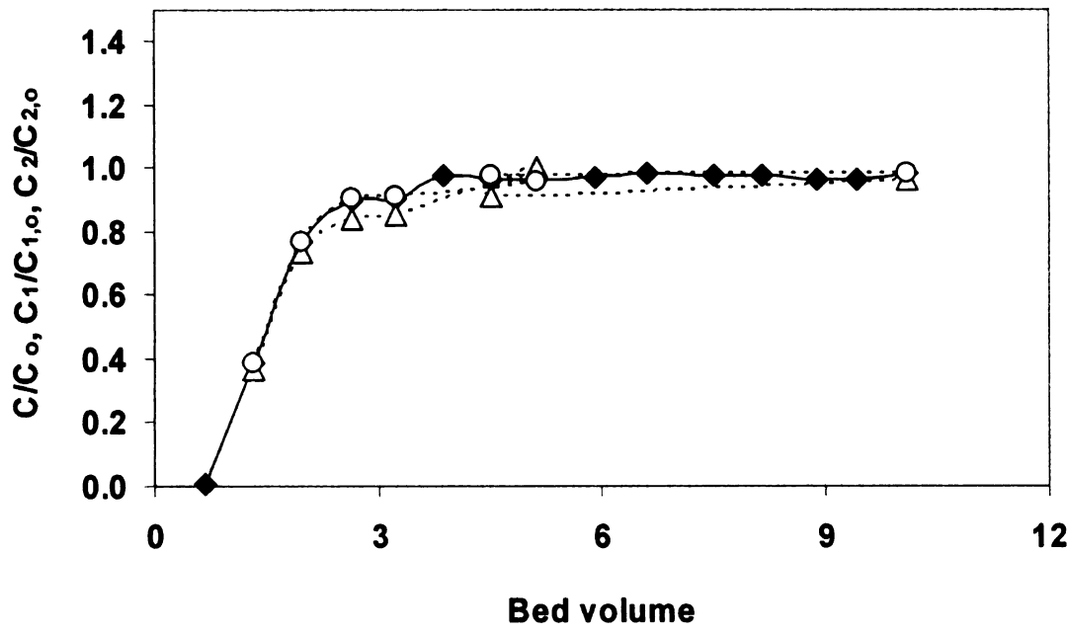

Figure A.11 Fixed-bed Adsorption Using Ethanol and M-43 (Run # 21)

♦: total oil, ○: hydroxyl, Δ: non-hydroxy.

Run # 22: In Ethanol, Florisil = 2.369 g, flowrate = 0.19 ml/min, C = 0.81 %, S=1.61 %

* *Same as Table 2-4 in page 16*

[a]Fraction	[b]Time	[c]Bed Vol	[d]oil %	[e]C/C_0	[f]$C_1/C_{1,0}$	[g]$C_2/C_{2,0}$
1	15	0.620	0.05%	0.021	-	-
2	32	1.323	1.08%	0.448	0.465	0.432
3	48	1.984	1.99%	0.824	0.756	0.840
4	65	2.686	2.21%	0.915	0.937	0.889
5	85	3.513	2.26%	0.933	0.882	0.939
6	115	4.753	2.32%	0.960	-	-
7	133	5.497	2.34%	0.969	1.129	0.880
8	151	6.241	2.35%	0.971	1.291	0.810
9	168	6.943	2.38%	0.983	-	-
11	183	7.563	2.37%	0.978	-	-
12	222	9.175	2.41%	0.996	1.242	0.868

C and S denote for castor and soybean oil. [a] : sample collected in the experiment, [b] : time (minutes) after fixed-bed starts, [c] : number of bed volumes, [d] : total oil concentration, [e, f, g]: concentrations of total oil (C), ricinolein (C_1), and non-hydroxylated component (C_2) in the effluent compared to their initial C_0 , $C_{1,0}$, $C_{2,0}$.

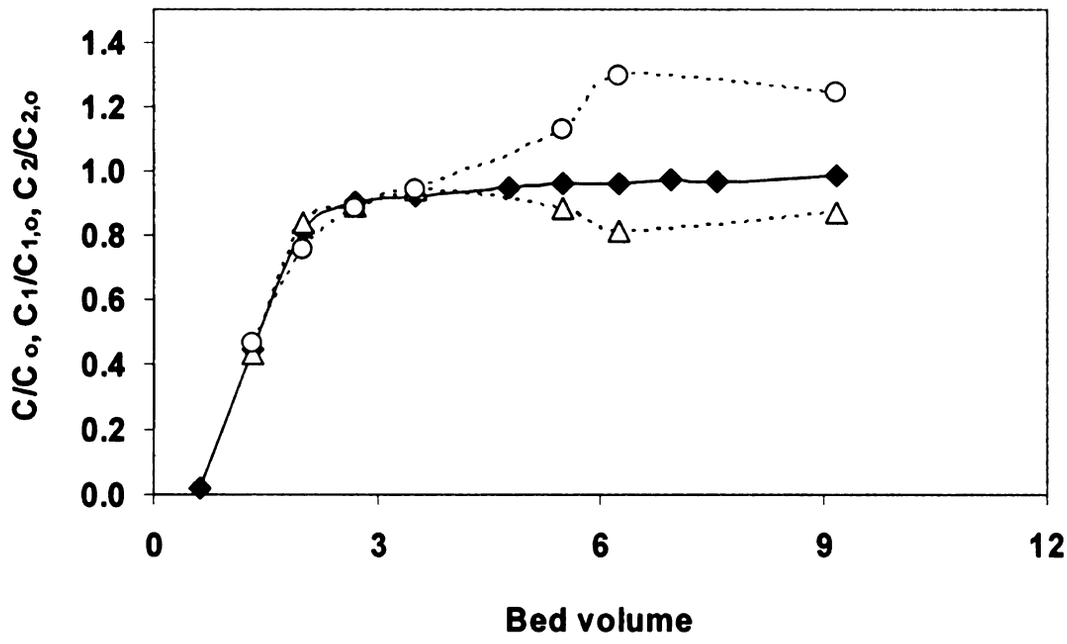

Figure A.12 Fixed-bed Adsorption Using Ethanol and Florisil (Run # 22)

♦: total oil, ○: hydroxyl, Δ: non-hydroxy. * *Same as Figure 2.3 in page 16*

Run # 23: In Hexane, Florisil = 2.408 g, flowrate = 0.14 ml/min, C = 0 %, S = 3.77 %

[a]Fraction	[b]Time	[c]Bed Vol	[d]oil %	[e]C/C_0	[f]$C_1/C_{1,0}$	[g]$C_2/C_{2,0}$
1	17	0.50	0.02%	0.005	0.000	0.005
2	37	1.08	0.01%	0.003	0.000	0.003
3	59	1.72	0.01%	0.001	0.000	0.001
4	79	2.31	0.01%	0.003	0.000	0.003
5	95	2.77	0.09%	0.024	0.000	0.024
6	115	3.36	0.82%	0.219	0.000	0.219
7	139	4.06	2.08%	0.553	0.000	0.553
8	161	4.70	2.97%	0.789	0.000	0.789
9	179	5.23	3.00%	0.797	0.000	0.797
10	199	5.81	3.88%	1.033	0.000	1.033
11	219	6.39	3.93%	1.046	0.000	1.046

C and S denote for castor and soybean oil. [a] : sample collected in the experiment, [b] : time (minutes) after fixed-bed starts, [c] : number of bed volumes, [d] : total oil concentration, [e, f, g]: concentrations of total oil (C), ricinolein (C_1), and non-hydroxylated component (C_2) in the effluent compared to their initial C_0 , $C_{1.0}$, $C_{2.0}$.

Run # 24: In Hexane, Florisil = 2.407 g, flowrate = 0.14 ml/min, C = 0 %, S = 2.46 %

[a]Fraction	[b]Time	[c]Bed Vol	[d]oil %	[e]C/C_0	[f]$C_1/C_{1,0}$	[g]$C_2/C_{2,0}$
1	15	0.46	-0.05%	-0.019	0.000	-0.019
2	38	1.17	-0.02%	-0.007	0.000	-0.007
3	55	1.69	0.04%	0.014	0.000	0.014
4	70	2.16	0.01%	0.003	0.000	0.003
5	87	2.68	0.10%	0.039	0.000	0.039
6	107	3.30	0.60%	0.244	0.000	0.244
7	123	3.79	1.06%	0.429	0.000	0.429
8	138	4.25	1.33%	0.537	0.000	0.537
9	157	4.84	1.30%	0.527	0.000	0.527
10	173	5.33	2.21%	0.892	0.000	0.892
11	192	5.92	2.32%	0.936	0.000	0.936
12	214	6.59	2.43%	0.981	0.000	0.981
13	234	7.21	2.46%	0.994	0.000	0.994
14	254	7.83	2.46%	0.993	0.000	0.993
15	274	8.44	2.49%	1.008	0.000	1.008
16	296	9.12	2.49%	1.005	0.000	1.005
17	318	9.80	2.51%	1.014	0.000	1.014

C and S denote for castor and soybean oil. [a] : sample collected in the experiment, [b] : time (minutes) after fixed-bed starts, [c] : number of bed volumes, [d] : total oil concentration, [e, f, g]: concentrations of total oil (C), ricinolein (C_1), and non-hydroxylated component (C_2) in the effluent compared to their initial C_0 , $C_{1,0}$, $C_{2,0}$.

Run # 25: In Hexane, Florisil = 2.427 g, flowrate = 0.21 ml/min, C = 1.43 %, S = 0 %

[a]Fraction	[b]Time	[c]Bed Vol	[d]oil %	[e]C/C_0	[f]$C_1/C_{1,0}$	[g]$C_2/C_{2,0}$
1	17	0.75	0.05%	0.033	-	-
2	34	1.51	0.09%	0.063	-	-
3	49	2.17	0.03%	0.024	-	-
4	68	3.01	0.01%	0.008	-	-
5	89	3.94	0.03%	0.020	-	-
6	107	4.74	0.02%	0.017	-	-
7	123	5.45	0.00%	0.003	-	-
8	144	6.38	0.00%	0.000	-	-
9	164	7.26	0.06%	0.045	-	-
10	181	8.02	0.19%	0.131	0.085	0.442
11	200	8.86	0.39%	0.272	0.193	0.803
12	221	9.79	0.61%	0.422	0.295	1.266
13	246	10.90	0.85%	0.591	0.465	1.440
14	266	11.78	0.84%	0.583	-	-
15	283	12.53	0.96%	0.667	-	-
16	298	13.20	1.01%	0.705	0.589	1.477
17	315	13.95	1.11%	0.770	-	-
18	339	15.02	1.12%	0.782	-	-
19	357	15.81	1.18%	0.822	0.597	2.332
20	375	16.61	1.22%	0.852	-	-
21	394	17.45	1.15%	0.798	-	-
22	413	18.29	1.28%	0.893	0.710	2.122

C and S denote for castor and soybean oil. [a] : sample collected in the experiment, [b] : time (minutes) after fixed-bed starts, [c] : number of bed volumes, [d] : total oil concentration, [e, f, g]: concentrations of total oil (C), ricinolein (C_1), and non-hydroxylated component (C_2) in the effluent compared to their initial C_0 , $C_{1,0}$, $C_{2,0}$.

Run # 26: In Hexane, Florisil = 2.413 g, flowrate = 0.18 ml/min, C = 1.29 %, S = 1.3 %

[a]Fraction	[b]Time	[c]Bed Vol	[d]oil %	[e]C/C_0	[f]$C_1/C_{1,0}$	[g]$C_2/C_{2,0}$
1	20	0.77	0.02%	0.006	-	-
2	40	1.55	0.03%	0.010	-	-
3	64	2.47	0.08%	0.031	-	-
4	87	3.36	0.14%	0.051	-	-
5	109	4.21	0.75%	0.278	-	-
6	132	5.10	1.14%	0.420	-	-
7	154	5.95	1.38%	0.509	-	-
8	174	6.72	2.02%	0.747	-	-
9	197	7.61	2.08%	0.767	-	-
10	220	8.50	2.33%	0.861	-	-
11	238	9.20	2.35%	0.868	-	-
12	253	9.78	2.40%	0.886	-	-
14	294	11.36	1.77%	0.654	-	-

C and S denote for castor and soybean oil. [a] : sample collected in the experiment, [b] : time (minutes) after fixed-bed starts, [c] : number of bed volumes, [d] : total oil concentration, [e, f, g]: concentrations of total oil (C), ricinolein (C_1), and non-hydroxylated component (C_2) in the effluent compared to their initial C_0 , $C_{1,0}$, $C_{2,0}$.

Run # 27: In Hexane, Florisil = 2.413 g, flowrate = 0.18 ml/min, C = 1.66 %, S =0.85 %

[a]Fraction	[b]Time	[c]Bed Vol	[d]oil %	[e]C/C_0	[f]$C_1/C_{1,0}$	[g]$C_2/C_{2,0}$
1	18	0.66	-0.02%	-0.006	-	-
2	35	1.28	-0.01%	-0.003	-	-
3	55	2.01	0.06%	0.024	-	-
4	75	2.75	0.16%	0.061	-	-
5	96	3.52	0.48%	0.183	0.008	0.419
6	119	4.36	1.06%	0.407	0.030	0.913
7	142	5.20	1.49%	0.569	0.048	1.269
8	166	6.08	1.76%	0.673	0.188	1.325
9	191	6.99	1.80%	0.687	-	-
10	217	7.95	1.78%	0.682	-	-
11	243	8.90	1.80%	0.687	0.438	1.023
12	270	9.89	1.89%	0.723	-	-
13	295	10.80	1.93%	0.739	0.633	0.880
14	313	11.46	2.03%	0.775	-	-
15	330	12.08	2.05%	0.785	0.618	1.011
16	358	13.11	2.02%	0.771	-	-
17	375	13.73	2.09%	0.799	-	-
18	400	14.65	2.17%	0.829	0.664	1.050
19	420	15.38	2.20%	0.841	-	-

C and S denote for castor and soybean oil. [a] : sample collected in the experiment, [b] : time (minutes) after fixed-bed starts, [c] : number of bed volumes, [d] : total oil concentration, [e, f, g]: concentrations of total oil (C), ricinolein (C_1), and non-hydroxylated component (C_2) in the effluent compared to their initial C_0 , $C_{1,0}$, $C_{2,0}$.

Run # 28: In Hexane, Florisil = 2.462 g, flowrate = 0.14 ml/min, C = 0.80 %, S =1.68 %

[a]Fraction	[b]Time	[c]Bed Vol	[d]oil %	[e]C/C_0	[f]$C_1/C_{1,0}$	[g]$C_2/C_{2,0}$
1	17	0.60	0.04%	0.017	-	-
2	34	1.20	0.04%	0.015	-	-
3	51	1.79	0.02%	0.008	-	-
4	70	2.46	0.05%	0.018	-	-
5	92	3.24	0.17%	0.068	-	-
6	115	4.05	0.77%	0.306	0.010	0.431
7	138	4.86	1.15%	0.459	-	-
8	161	5.66	1.98%	0.790	0.032	1.111
9	185	6.51	2.11%	0.841	0.062	1.171
10	208	7.32	2.30%	0.916	0.066	1.277
11	232	8.16	2.31%	0.921	0.054	1.288
12	253	8.90	2.29%	0.913	-	-
13	279	9.82	2.27%	0.903	0.125	1.232
14	306	10.77	2.23%	0.890	-	-
15	335	11.79	2.20%	0.877	0.353	1.099
17	378	13.30	2.34%	0.932	0.646	1.053

C and S denote for castor and soybean oil. [a] : sample collected in the experiment, [b] : time (minutes) after fixed-bed starts, [c] : number of bed volumes, [d] : total oil concentration, [e, f, g]: concentrations of total oil (C), ricinolein (C_1), and non-hydroxylated component (C_2) in the effluent compared to their initial C_0 , $C_{1,0}$, $C_{2,0}$.

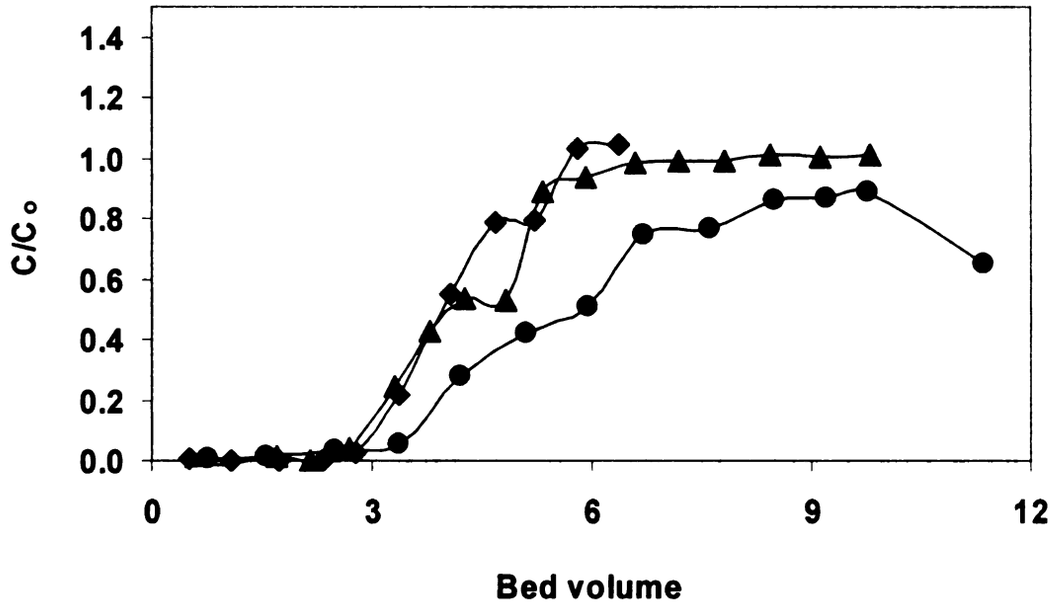

Figure A.13 Fixed-bed Adsorption Using Hexane and Florisil (Runs # 23, 24, 26)

♦: total oil (Run # 23), ▲: total oil (Run # 24), ●: total oil (Run # 26)

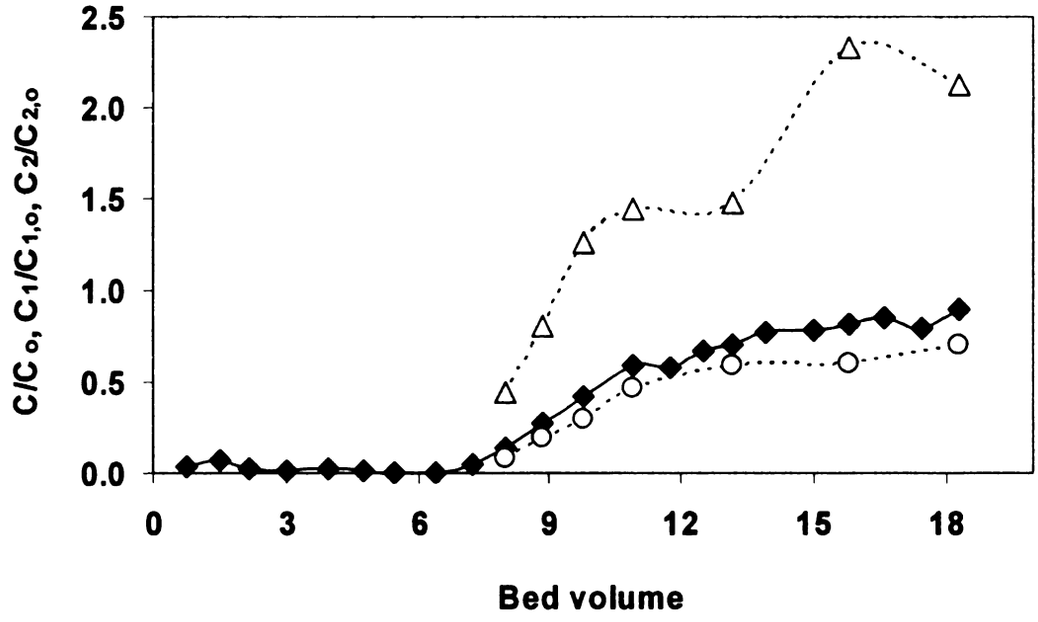

Figure A.14 Fixed-bed Adsorption Using Hexane and Florisil (Run # 25)

♦: total oil, ○: hydroxyl, Δ: non-hydroxy.

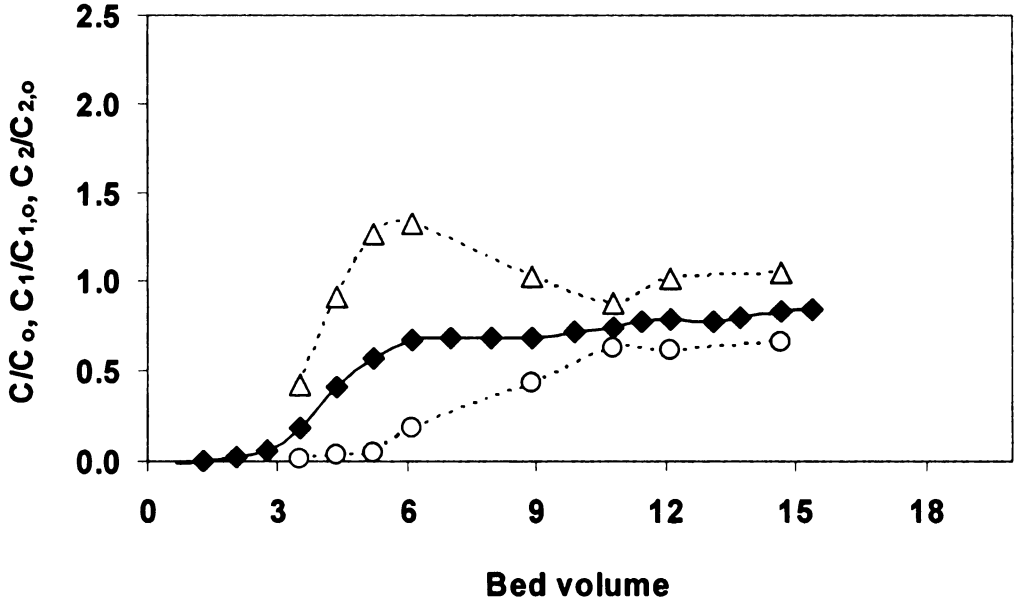

Figure A.15 Fixed-bed Adsorption Using Hexane and Florisil (Run # 27)

♦: total oil, ○: hydroxyl, Δ: non-hydroxy.

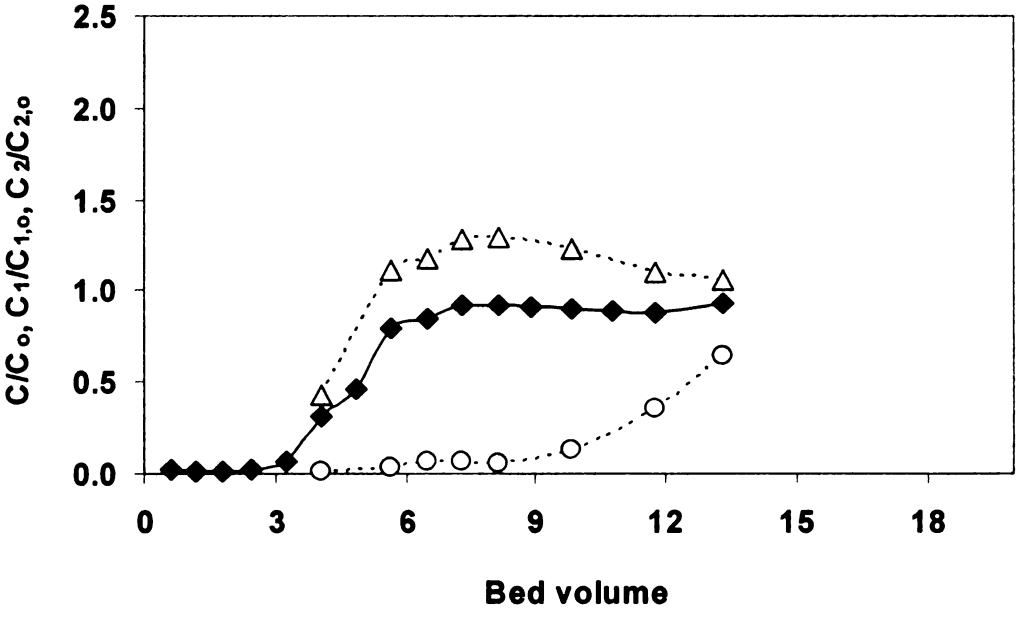

Figure A.16 Fixed-bed Adsorption Using Hexane and Florisil (Run # 28)

♦: total oil, ○: hydroxyl, Δ: non-hydroxy.

Run # 29: In Methanol, SD-2 = 2.835 g, flowrate = 0.20 ml/min, C = 2.44 %, S = 0 %

[a]Fraction	[b]Time	[c]Bed Vol	[d]oil %	[e]C/C_0	[f]$C_1/C_{1,0}$	[g]$C_2/C_{2,0}$
1	15	0.60	0.01%	0.003	0.000	0.000
2	30	1.19	0.00%	-0.002	-0.002	-0.002
3	45	1.79	0.05%	0.019	0.019	0.022
4	60	2.38	0.23%	0.093	0.101	0.039
5	75	2.98	0.76%	0.308	0.327	0.169
6	90	3.57	1.33%	0.538	0.000	0.000
7	106	4.21	1.82%	0.737	0.775	0.454
8	118	4.68	2.09%	0.846	0.000	0.000
9	133	5.28	2.25%	0.911	0.954	0.590
10	145	5.76	2.33%	0.940	0.000	0.000
11	157	6.23	2.37%	0.960	0.998	0.675
12	177	7.03	2.38%	0.964	0.000	0.000
13	197	7.82	2.39%	0.964	0.000	0.000
14	217	8.61	2.46%	0.992	0.985	1.051
15	237	9.41	2.40%	0.971	0.000	0.000

C and S denote for castor and soybean oil. [a] : sample collected in the experiment, [b] : time (minutes) after fixed-bed starts, [c] : number of bed volumes, [d] : total oil concentration, [e, f, g]: concentrations of total oil (C), ricinolein (C_1), and non-hydroxylated component (C_2) in the effluent compared to their initial C_0 , $C_{1,0}$, $C_{2,0}$.

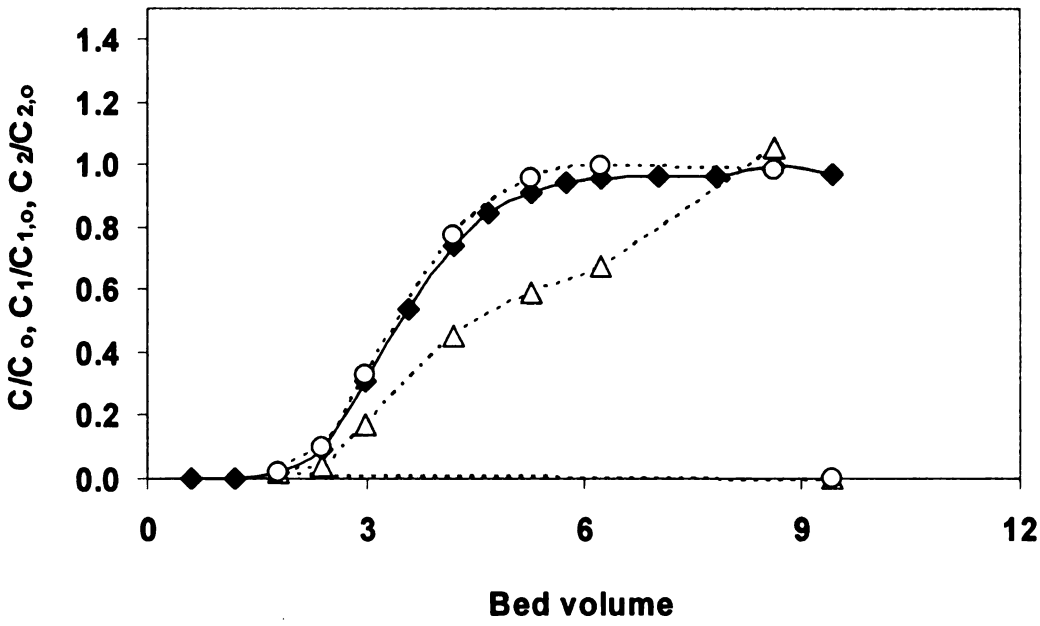

Figure A.17 Fixed-bed Adsorption Using Methanol and SD-2 (Run # 29)

♦: total oil, ○: hydroxyl, Δ: non-hydroxy.

Run # 30: In Propanol, SD-2 = 2.838 g, flowrate = 0.20 ml/min, C = 2.38 %, S = 0 %

[a]Fraction	[b]Time	[c]Bed Vol	[d]oil %	[e]C/C_0	[f]$C_1/C_{1,0}$	[g]$C_2/C_{2,0}$
1	18	0.72	0.04%	0.015	-	-
2	33	1.31	0.76%	0.314	0.292	0.469
3	48	1.91	1.58%	0.648	0.654	0.612
4	64	2.55	2.00%	0.823	0.827	0.792
5	80	3.18	2.09%	0.860	-	-
6	98	3.90	2.17%	0.894	0.907	0.806
7	114	4.54	2.22%	0.914	-	-
8	129	5.13	2.28%	0.939	-	-
9	143	5.69	2.29%	0.941	-	-
10	161	6.41	2.32%	0.955	-	-
11	185	7.36	2.31%	0.951	-	-
12	207	8.24	2.32%	0.955	0.964	0.892
13	229	9.12	2.33%	0.957	-	-
14	253	10.07	2.36%	0.971	0.975	0.944

C and S denote for castor and soybean oil. [a] : sample collected in the experiment, [b] : time (minutes) after fixed-bed starts, [c] : number of bed volumes, [d] : total oil concentration, [e, f, g]: concentrations of total oil (C), ricinolein (C_1), and non-hydroxylated component (C_2) in the effluent compared to their initial C_0 , $C_{1,0}$, $C_{2,0}$.

Run # 31: In Propanol, SD-2 = 2.856 g, flowrate = 0.16 ml/min, C = 1.63 %, S =0.84 %

[a]Fraction	[b]Time	[c]Bed Vol	[d]oil %	[e]C/C_0	[f]$C_1/C_{1,0}$	[g]$C_2/C_{2,0}$
1	17	0.54	0.00%	0.000	-	-
2	36	1.15	0.51%	0.207	0.297	0.075
3	54	1.73	1.34%	0.540	0.735	0.254
4	75	2.40	1.78%	0.718	0.897	0.456
5	95	3.04	2.04%	0.821	-	-
6	121	3.87	2.18%	0.880	1.027	0.664
7	144	4.60	2.29%	0.923	-	-
8	168	5.37	2.33%	0.941	0.944	0.936
9	193	6.17	2.40%	0.968	-	-
10	213	6.81	2.40%	0.967	0.988	0.937
11	238	7.61	2.40%	0.969	-	-
12	263	8.41	2.43%	0.979	1.038	0.894
13	287	9.18	2.49%	1.003	-	-
14	317	10.14	2.47%	0.995	-	-

C and S denote for castor and soybean oil. [a] : sample collected in the experiment, [b] : time (minutes) after fixed-bed starts, [c] : number of bed volumes, [d] : total oil concentration, [e, f, g]: concentrations of total oil (C), ricinolein (C_1), and non-hydroxylated component (C_2) in the effluent compared to their initial C_0 , $C_{1,0}$, $C_{2,0}$.

Run # 32: In Propanol, SD-2 = 2.835 g, flowrate = 0.19 ml/min, C = 0.81 %, S =1.63 %

[a]Fraction	[b]Time	[c]Bed Vol	[d]oil %	[e]C/C_0	[f]$C_1/C_{1,0}$	[g]$C_2/C_{2,0}$
1	17	0.65	0.00%	0.000	-	-
2	34	1.30	0.41%	0.172	0.316	0.113
3	52	1.99	1.20%	0.498	0.657	0.433
4	70	2.67	1.65%	0.686	0.777	0.649
5	88	3.36	1.92%	0.800	-	-
6	110	4.20	2.11%	0.878	0.941	0.851
7	131	5.00	2.21%	0.922	-	-
8	149	5.69	2.28%	0.951	0.978	0.939
9	176	6.72	2.33%	0.972	0.995	0.963
10	198	7.56	2.36%	0.984	-	-
11	218	8.32	2.37%	0.989	0.975	0.994
12	242	9.24	2.39%	0.994	-	-
13	265	10.12	2.38%	0.993	0.952	1.009
15	291	11.11	2.41%	1.003	1.037	0.989

C and S denote for castor and soybean oil. [a] : sample collected in the experiment, [b] : time (minutes) after fixed-bed starts, [c] : number of bed volumes, [d] : total oil concentration, [e, f, g]: concentrations of total oil (C), ricinolein (C_1), and non-hydroxylated component (C_2) in the effluent compared to their initial C_0 , $C_{1,0}$, $C_{2,0}$.

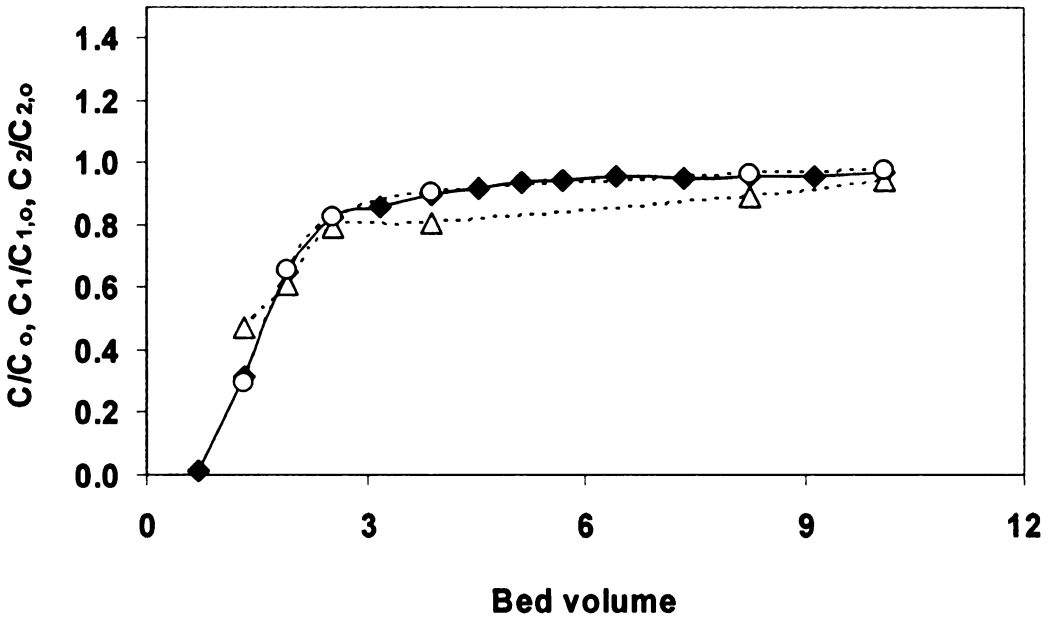

Figure A.18 Fixed-bed Adsorption Using Propanol and SD-2 (Run # 30)

♦: total oil, ○: hydroxyl, Δ: non-hydroxy.

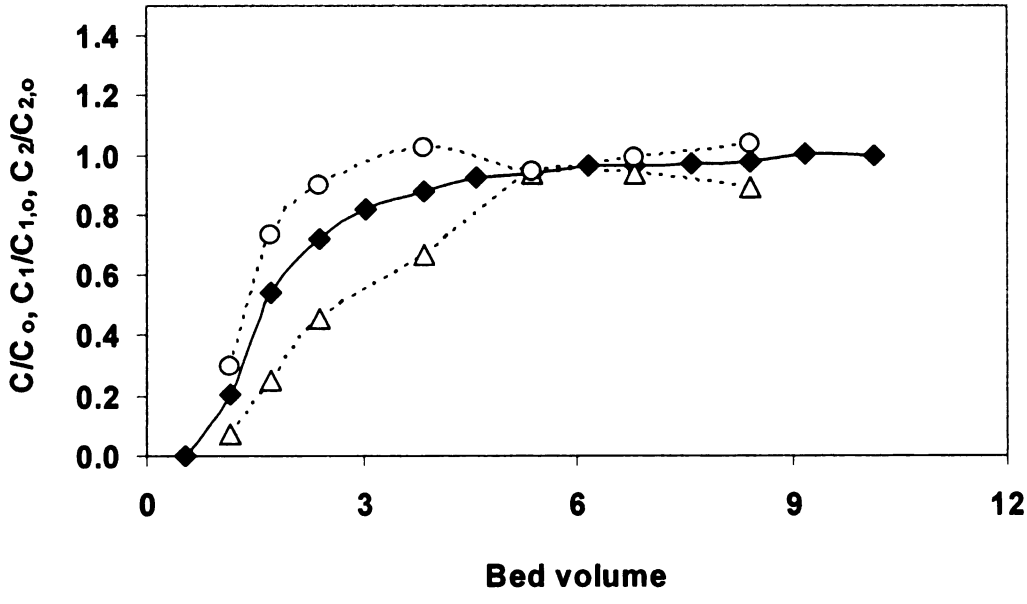

Figure A.19 Fixed-bed Adsorption Using Propanol and SD-2 (Run # 31)

♦: total oil, ○: hydroxyl, Δ: non-hydroxy.

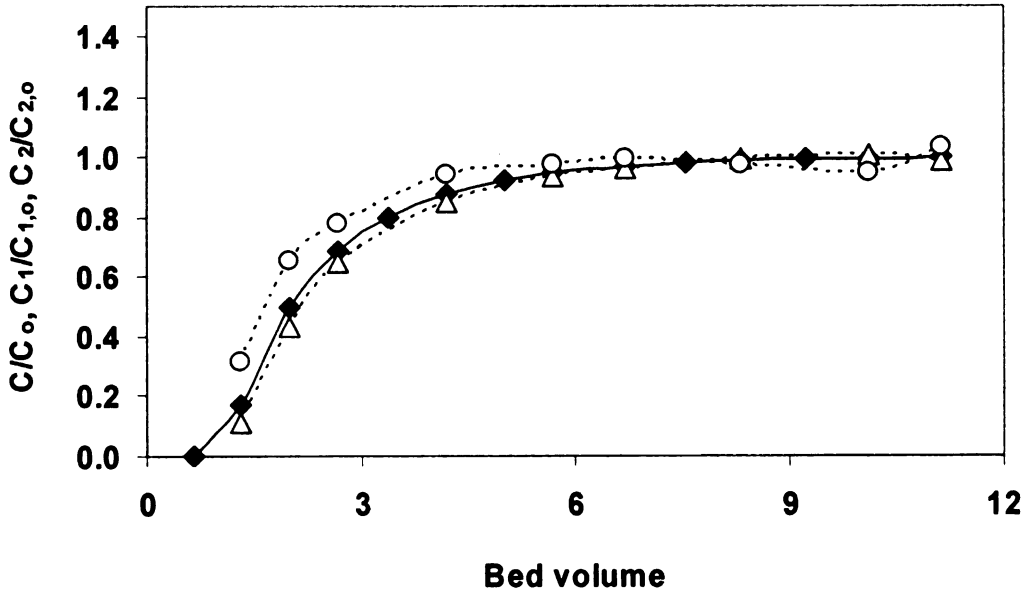

Figure A.20 Fixed-bed Adsorption Using Propanol and SD-2 (Run # 32)

♦: total oil, ○: hydroxyl, Δ: non-hydroxy.

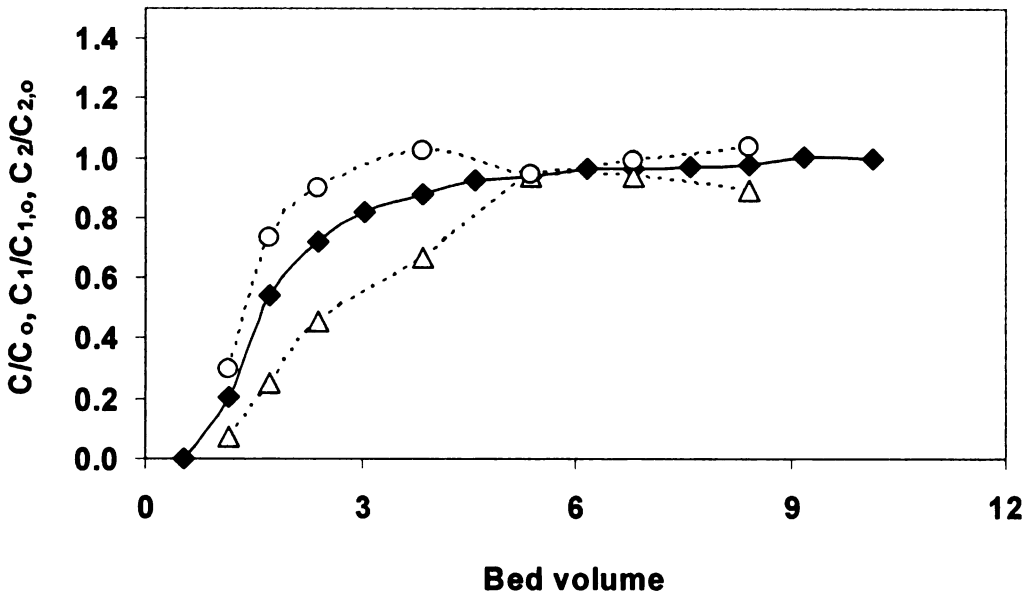

Figure A.19 Fixed-bed Adsorption Using Propanol and SD-2 (Run # 31)

♦: total oil, ○: hydroxyl, Δ: non-hydroxy.

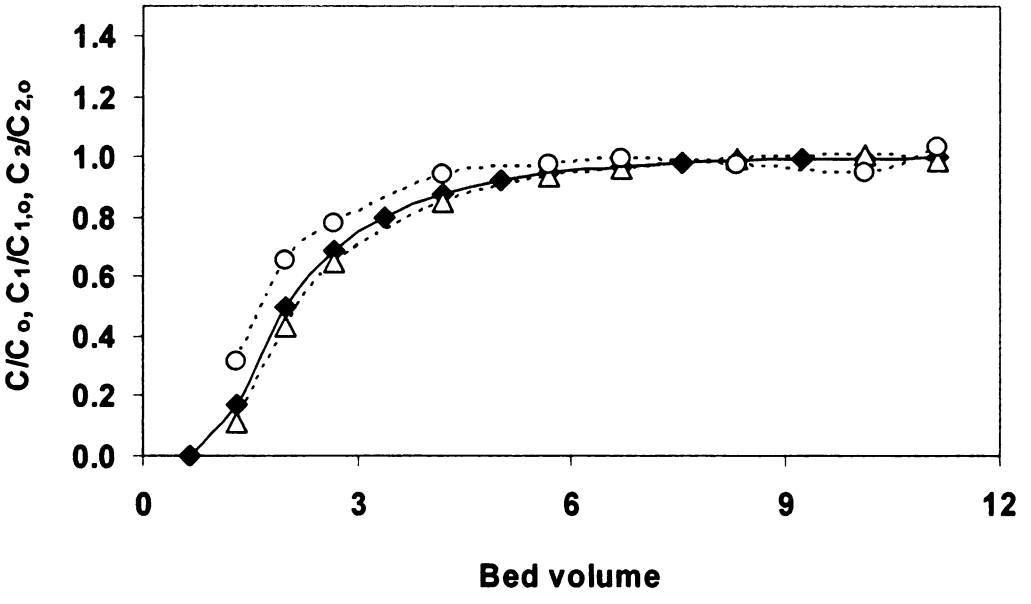

Figure A.20 Fixed-bed Adsorption Using Propanol and SD-2 (Run # 32)

♦: total oil, ○: hydroxyl, Δ: non-hydroxy.

APPENDIX B

FORTRAN PROGRAM

(Reference in Chapter 7)

```
Program Opt2olEster
!**********************************************************************
! There are 5 subroutines, and two functions named and used in the following order:
!       1. ConvertData.f90
!       2. CalcSlope.f90
!       3. DungErrCalc.f90
!               4. ErrFunction.f90:  Function error.f90
!               5. CalcLnPsat.f90:  Function  lnPErr ()
!       6. WriteParmsHb3.f90
!       7. WriteRegEoK.f90
!**********************************************************************
USE MSFLIB          !To use runQQ and changeDIRQQ
USE MSIMSL          !To use IMSL functions

implicit none
character compName*16(200)
integer k(20),L,n,nComponent,nPoint,NumAdj_2ol,NumAdj_Ester,Nout,option
double precision T(200),ln_expP(200), ln_preP(200), AveExpSlope(200),
AveSpeadSlope(200)
logical status, result

common/C/n,k,CompName,nComponent,nPoint
common/V/T,ln_expP,ln_preP,AveExpSlope,AveSpeadSlope
common/P/Param1,Param2
common/O/option

parameter (NumAdj_2ol=5, NumAdj_Ester=9)
integer IPARAM(7), IBTYPE
double precision PsatErr, RPARAM(7), XLB1(NumAdj_2ol), XUB1(NumAdj_2ol),
ParamGuess1(NumAdj_2ol), Param1(NumAdj_2ol), ParamScale1(NumAdj_2ol),
ErrScale1, XLB2(NumAdj_Ester), XUB2(NumAdj_Ester), ErrScale2,
ParamGuess2(NumAdj_Ester), Param2(NumAdj_Ester), ParamScale2(NumAdj_Ester)

data ParamGuess1/0.0000368d0,130.d0,4.3d0,152.d0,30.d0/, ErrScale1/0.000001d0/,
ParamScale1/1.D0, 1.D-8, 1.D-7, 5.D-9, 1.D-8/
data XLB1/.00000D0, 0.D0, 0.D0, 0.D0,0.D0/
data XUB1/.00006D0, 200.D0, 10.D0, 200.D0,60.D0/

data ParamGuess2/0.00001573d0,104.65d0,.8d0,10.8D0,  0.6D0, 100.2d0,5.d0,
152.6d0,44.7d0/, ErrScale2/0.0000001d0/, ParamScale2/1.D-3, 1.D-8, 1.D-7, 5.D-9, 1.D-
7,5.D-9, 1.D-8, 5.D-9, 1.D-8/
data XLB2/.0D0,  0.D0, .0D0,  0.D0,  .0D0,  0.D0,  0.D0,  0.D0,0.D0/
data XUB2/.002D0,  140.D0, 3.D0, 20.D0,  5.D0,  200.D0,40.D0, 200.D0,100.D0/

external  DungErrCalc
IBTYPE=0
```

```
call DU4INF(IPARAM, RPARAM)
open (7,file='C:\spead\CalcEos\Input\Parmsrecord.txt')
write(7,*) (IPARAM(L),L=1,7)
write(7,*) (RPARAM(L),L=1,7)
close(7)
!*** Set non default values for desired IPARAM and RPARARM elements.  Using the
same set up as in the example UMINF/DUMINF
write(*,*) 'Enter (1): optimization of 2-ols'
write(*,*) 'Enter (2): optimization of esters'

read (*,*) option

if (option .EQ.1) then
        call            DBCONF(DungErrCalc,NumAdj_2ol,ParamGuess1,IBTYPE,XLB1,
XUB1,ParamScale1,ErrScale1,IPARAM,RPARAM,Param1,PsatErr)
        call WriteParmsHb3(14,4,param1)
        call WriteRegEok(14,4, param1(4),param1(5))
        status = CHANGEDIRQQ('C:\DmdTpt\BaseAlcohol\2ols')
        result=RUNQQ('C:\DmdTpt\BaseAlcohol\2ols\RegSteps3v.Exe','-1 -r')
        status = CHANGEDIRQQ('C:\Temp\dung\try')

else if (option .EQ.2) then
        call        DBCONF(DungErrCalc,NumAdj_Ester,ParamGuess2,IBTYPE,XLB2,
XUB2,ParamScale2,ErrScale2,IPARAM,RPARAM,Param2,PsatErr)
        call WriteParmsHb3(16,2,param2)
        call WriteRegEok(9,4, param2(4),param2(5))
        call WriteRegEok(15,2, param2(6),param2(7))
        call WriteRegEok(16,2, param2(8),param2(9))
        status = CHANGEDIRQQ('C:\DmdTpt\BaseEsters')
        result=RUNQQ('C:\DmdTpt\BaseEsters\RegSteps3v.Exe','-1 -r')
        status = CHANGEDIRQQ('C:\Temp\dung\try')
endif

call UMACH (2, NOUT)
write (NOUT,100) PsatErr, (IPARAM(L),L=3,5)
100 format (' The Psat Error','value is', F15.3, //, ' The number of iterations is',I3, //,' The
number of function evaluations is ', I3, //, ' The number of gradient evaluations is', I3)

End
!**********************************************************************

Subroutine ConvertData
! Reading data from TPRhoResults.txt
! Converting text type to numeric, calculating and saving T,P,Rho, T^(-1.3), lnP(exp),
ln(Pspead) in the Convert.txt
```

```
implicit none
character colHead*16(200,6),compName*16(200),Name*16(200)
integer i,j,k(20),n,nComponent,nPoint,option
double precision T(200),ln_expP(200), ln_preP(200), AveExpSlope(200),
AveSpeadSlope(200), col(200,5)
common/C/n,k,CompName,nComponent,nPoint
common/V/T,ln_expP,ln_preP,AveExpSlope,AveSpeadSlope
common/O/option

i=0
n=0
k(1)=1
nPoint=0
if (option == 1) then
        open(1,file='C:\DmdTpt\BaseAlcohol\2ols\TPRhoResults.txt')
else if (option == 2) then
        open(1,file='C:\DmdTpt\BaseEsters\TPRhoResults.txt')
endif
open(2,file='c:\temp\dung\try\Convert.txt')

do while (.not.EOF(1))
        i=i+1
        read(1,*) (colHead(i,j),j=1,6)
        compName(i)= colHead(i,1)
        if (i .EQ.1) then
                write (2,201) (colHead(i,j),j=1,6),' (1/Texp)^(-1.3),  ln(exp_P),  ln(pre_P)'
        else
                do j=2,6
                        read(colHead(i,j),*) col (i,j)
                enddo
                T(i)= (col (i,2))**(-1.3)
                ln_expP(i)= log(col (i,3))
                ln_preP(i)=log(col(i,5))
                write (2,202) colHead(i,1),(col(i,j),j=2,6), T(i),ln_expP(i),ln_preP(i)
                nPoint=nPoint+1
        endif
!counting number of data point for each component. This info is written at the end of the
file Covert.txt.
        if ((i .GT. 1) .and. (compName(i)/=compName(i-1))) then
                n=n+1
                k(n)=1
        else
                k(n)=k(n)+1
        endif
        Name(n)=CompName(i)
```

```
enddo
write (2,204)'**********','There are ',nPoint,' data points and ',n-1, ' components.'
write(2,*)'Below is number of data points for each component:'

do i=2,n
        write(2,203)i-1,Name(i),k(i)
enddo
nComponent=n
close(1)
!close(2) will be closed in ErrFunction
201 format (A12,A8,A10,A15,A10,A10,A40)
202 format(A16,F5.1,5X,4F8.5,5X,E13.6,5X,2F13.6)
203 format (I3,5x,A16,I3)
204 format (//A10//A11,I3,A17,I2,A12)
End subroutine ConvertData
!************************************************************************

Subroutine CalcSlope
!Calculating the average experimental and predicted slopes.  Writing info onto inter1.txt

implicit none
character CompName*16(200)
integer i,j,k(20),m,n,nComponent,nPoint
double precision SumExpSlope(200),SumSpeadSlope(200),ln_expP(200), ln_preP(200),
AveExpSlope(200),AveSpeadSlope(200),ExpSlope(200),SpeadSlope(200),T(200)
common/C/n,k,CompName,nComponent,nPoint
common/V/T,ln_expP,ln_preP,AveExpSlope,AveSpeadSlope

m=1
do i=1,nComponent
        SumSpeadSlope(i)=0.d0
        SumExpSlope(i)=0.d0
        if (k(i)>1) then
                do j=2,k(i)
                !calculate and compare the average experimental slope with predicted
                        m=m+1
                        if (T(m+1)-T(m) ==0.d0) then
                                k(i)=k(i)-1
                                ExpSlope(m)=(ln_expP(m+2)-ln_expP(m+1))/(T(m+2)-
T(m+1))
                                SpeadSlope(m)=(ln_preP(m+2)-ln_preP(m+1))/(T(m+2)-
T(m+1))
                        else
                                ExpSlope(m)=(ln_expP(m+1)-ln_expP(m))/(T(m+1)-T(m))
                                SpeadSlope(m)=(ln_preP(m+1)-ln_preP(m))/(T(m+1)-
T(m))
```

```
                    endif
                    SumSpeadSlope(i)=SumSpeadSlope(i)+ SpeadSlope(m)
                    SumExpSlope(i)=SumExpSlope(i)+ ExpSlope(m)
                enddo
                AveExpSlope(i)=SumExpSlope(i)/(k(i)-1)
                AveSpeadSlope(i)=SumSpeadSlope(i)/(k(i)-1)
        endif
enddo

open(3,file='c:\temp\dung\try\inter1.txt')
!unit 3 will be kept open until error is evaluated in ErrFunction
do i=1,nComponent
        write(3,301)AveExpSlope(i),AveSpeadSlope(i)
enddo
301 format (2F25.8)

End subroutine CalcSlope
!**************************************************************************
Subroutine DungErrCalc(NumAdj,Parms,PsatErr)
! Reading data from TPRhoResults.txt. Converting text type data to numeric, calculating
and saving T,P,Rho, T^(-1.3), lnP(exp), ln(Pspead), and calculating slope

USE MSFLIB          !To use runQQ and changeDIRQQ
USE MSIMSL          !To use IMSL functions
implicit none
character compName*16(200)
integer k(20),n,nComponent,nPoint,NumAdj,option
double precision T(200), ln_expP(200), ln_preP(200), AveExpSlope(200), PsatErr,
PsatErr1, PsatErr2, lnPErr,AveSpeadSlope(200), error, Param1(5), Param2(9), Parms(9)
common/C/n,k,CompName,nComponent,nPoint
common/V/T,ln_expP,ln_preP,AveExpSlope,AveSpeadSlope
common/P/Param1,Param2
common/O/option
external error, lnPErr
logical result, status

if (option .EQ.1) then
        NumAdj =5
        call WriteParmsHb3(14,4,Parms)
        call WriteRegEok(14,4, param1(4),param1(5))
        status = CHANGEDIRQQ('C:\DmdTpt\BaseAlcohol\2ols')
        result=RUNQQ('C:\DmdTpt\BaseAlcohol\2ols\RegSteps3v.Exe','-1 -r')
        status = CHANGEDIRQQ('C:\Temp\dung\try')
else if (option .EQ.2) then
        NumAdj =9
```

```
        call WriteParmsHb3(16,2,Parms)
        call WriteRegEok(9,4, param2(4),param2(5))
        call WriteRegEok(15,2, param2(6),param2(7))
        call WriteRegEok(16,2, param2(8),param2(9))
        status = CHANGEDIRQQ('C:\DmdTpt\BaseEsters')
        result=RUNQQ('C:\DmdTpt\BaseEsters\RegSteps3v.Exe','-1 -r')
        status = CHANGEDIRQQ('C:\Temp\dung\try')
endif
call ConvertData
call CalcSlope
PsatErr1= error(3,AveExpSlope,AveSpeadSlope,nComponent)
PsatErr2= lnPErr()
PsatErr=PsatErr1*PsatErr2
open (7,file='C:\spead\CalcEos\Input\Parmsrecord.txt',access='append')
write(7,*)PsatErr1, PsatErr2, PsatErr
write(7,*)
close(7)
End subroutine DungErrCalc
!*************************************************************************

Function error(location,parm1,parm2,times)

integer location, times
double precision parm1(200), parm2(200)

rewind (location)

error=0.d0
do i=1,times
        read(location,*)parm1(i),parm2(i)
        error=error+abs(parm1(i)-parm2(i))
enddo

close(3)
return

End function error
!*************************************************************************

Function  lnPErr ()

implicit none
character CompName*16(200)
integer i,k(20),n, nComponent, nPoint

double precision lnPErr, ln_expP(200), ln_preP(200), AveExpSlope(200),
```

```
AveSpeadSlope(200), T(200)

common/C/n,k,CompName,nComponent,nPoint
common/V/T,ln_expP,ln_preP,AveExpSlope,AveSpeadSlope

lnPErr=0
do i=1,nPoint
        lnPErr=lnPErr+abs(ln_expP(i)-ln_preP(i))
        enddo

End function  lnPErr
!**************************************************************************

Subroutine WriteParmsHb3(main,sub,parms)
Use MSFLIB

character note*10(200)
integer  mainType(200),subType(200), nDs(200),nAs(200),sub,main
integer countline
double precision bondVol(200),bondSlope(200),bondEnergy(200),parms(9)

open (6,file='C:\spead\CalcEos\Input\ParmsHb3.txt')
open (7,file='C:\spead\CalcEos\Input\Parmsrecord.txt',access='append')

rewind(6)

i=0
countline=0
do while (.not.EOF(6))
        i=i+1
        countline=countline+1
        if (i .EQ.1) then
                read (6,*)mainType(i)
        else
                read(6,*)       mainType(i),subType(i),         nDs(i),nAs(i),bondVol(i),
bondSlope(i), bondEnergy(i),note(i)
                if      ((mainType(i)==main) .and.(subType(i)==sub)) then
                        if ((parms(1)*parms(2)*parms(3)) .GT. 0.D0) then
                                bondVol(i)= parms(1)
                                bondSlope(i) = parms(2)
                                bondEnergy(i)=parms(3)
                        endif

                        write(7,602)mainType(i),subType(i),     nDs(i),nAs(i),bondVol(i),
bondSlope(i), bondEnergy(i),note(i)
                endif
```

```
        endif
enddo

rewind(6)
write (6,601) mainType(1), ' nDs    nAs    bondVNm3    bVolSlo        eHbKcal_mol'
do i=2,countline
        write(6,602)mainType(i),subType(i),   nDs(i),nAs(i),bondVol(i),   bondSlope(i),
bondEnergy(i),note(i)
enddo

close(6)
close(7)

601 format (I3,A40)
602 format(4I3,3x,F15.8,3x, 2F15.3,3x,3A10)

End subroutine WriteParmsHb3
!*************************************************************************

Subroutine WriteRegEoK(ID1,ID2,parm1,parm2)
implicit none
character note*10(200)
integer ID1,ID2,option,count,i,mainType(200),subType(200),step1(200),step4(200)
double precision parm1, parm2, eok1High(200), eok1Low(200), eok4High(200),
eok4Low(200)
common/O/option

if (option ==1) then
        open (4,file='C:\DmdTpt\BaseAlcohol\2ols\RegEoK.txt')
        open (5,file='C:\DmdTpt\BaseAlcohol\2ols\RegEoKrecord.txt',access='append')
else if (option ==2) then
        open (4,file='C:\DmdTpt\BaseEsters\RegEoK.txt')
        open (5,file='C:\DmdTpt\BaseEsters\RegEoKrecord.txt',access='append')
endif
open (7,file='C:\spead\CalcEos\Input\Parmsrecord.txt',access='append')

i=0
count=0
do while (.not.EOF(4))
        i=i+1
        count=count+1
        read(4,*)note(i)
        if (index(note(i),'#') .EQ. 0)then
                backspace (4)
                read
(4,*)mainType(i),subType(i),eok1High(i),eok1Low(i),step1(i),eok4High(i),eok4Low(i),st
```

```
ep4(i)
                        if ((mainType(i)==ID1) .and.(subType(i)==ID2))then
                              if (parm1 .GT. parm2 .and. (parm1*parm2 .GT. 0.D0)) then
                                    eok1High(i)=parm1
                                    eok4High(i)=parm2
                                    eok1Low(i)= eok1High(i)
                                    eok4Low(i)=  eok4High(i)
                                    write       (5,201)       mainType(i),subType(i),
eok1High(i),eok1Low(i),step1(i),eok4High(i),eok4Low(i),step4(i)
                                    write       (7,201)       mainType(i),subType(i),
eok1High(i),eok1Low(i),step1(i),eok4High(i),eok4Low(i),step4(i)
                               endif
                         endif
        endif
enddo

rewind(4)
write(4,101)'#The epsilons to regress.  The type description is in the SiteParms.txt file.'
write(4,102)"#Please put these in ascending order.  I'm not going to bother writing code"
write(4,103)'#to sort these things into the proper order.'
write(4,104)'#Main Type      Sub Type      eok1Low      eok1High      eok1Step
        eok4Low      eok4High      eok4Step'
i=5
do i=5,count-1
        write                    (4,201)                    mainType(i),subType(i),
eok1High(i),eok1Low(i),step1(i),eok4High(i),eok4Low(i),step4(i)
enddo
write (4,105)'#END'

101 format(a77)
102 format(a75)
103 format(a44)
104 format(a71)
105 format(a4)
201 format (2I4,2F15.3,I4,3x,2F15.3,I4)
close(4)
close(5)
close(7)
End subroutine WriteRegEoK
!*****************************************************************
```

APPENDIX C

MISCELLANEOUS DOCUMENTATION

(Reference in Chapter 7)

C.1 – Vapor Pressure Data (predicted and experimental)

The tables in this section are ouput files (TptCoeff.txt) from SPEAD and the FORTRAN program. Notations are described bellows:

compName: Name of component (referred to Tables 7.1 and 7.4).

TextpK: experimental temperature (^{o}K)

PexpMPa: experimental vapor pressure (MPa)

RhoLexpG_cc: experimental liquid density (g/cm^3)

Ptpt: SPEAD predicted vapor pressure (MPa)

Rhotpt: SPEAD predicted liquid density (g/cm^3)

C.1.1 – Training –OH Site

compName	TexpK	PexpMPa	RhoLexpG_cc	Ptpt	Rhotpt
2olC3.dat	415.8	.707000	.6461	.675817	.6543
2olC3.dat	407.3	.579000	.6583	.543495	.6653
2olC3.dat	403.6	.516000	.6635	.491923	.6700
2olC3.dat	400.0	.466000	.6684	.445497	.6745
2olC3.dat	395.9	.412000	.6739	.396436	.6797
2olC3.dat	392.6	.374000	.6782	.361008	.6837
2olC3.dat	386.5	.308000	.6861	.300577	.6911
2olC3.dat	382.7	.272000	.6908	.267468	.6957
2olC3.dat	375.0	.210000	.7003	.208824	.7048
2olC3.dat	374.1	.205000	.7014	.202622	.7059
2olC3.dat	364.9	.147000	.7122	.147967	.7165
2olC3.dat	363.1	.136000	.7143	.138799	.7185
2olC3.dat	362.4	.133000	.7151	.135144	.7194
2olC3.dat	359.7	.120000	.7182	.122408	.7224
2olC3.dat	355.1	.100000	.7235	.102924	.7276
2olC3.dat	354.8	.099000	.7238	.101673	.7280
2olC3.dat	353.1	.092200	.7256	.095564	.7298
2olC3.dat	350.0	.081300	.7291	.084468	.7333
2olC3.dat	349.6	.080000	.7296	.083137	.7337
2olC3.dat	345.3	.066600	.7343	.069818	.7385
2olC3.dat	343.1	.060600	.7366	.063923	.7408
2olC3.dat	340.2	.053400	.7397	.056533	.7440
2olC3.dat	333.9	.040000	.7464	.042936	.7507
2olC3.dat	333.1	.038500	.7472	.041420	.7516
2olC3.dat	325.5	.026500	.7552	.028989	.7597
2olC3.dat	325.0	.025900	.7557	.028343	.7602
2olC3.dat	323.1	.023600	.7576	.025915	.7622
2olC3.dat	313.1	.014100	.7676	.015600	.7726

2olC3.dat	303.1	.007880	.7774	.008998	.7828
2olC3.dat	300.0	.006480	.7805	.007495	.7860
2olC3.dat	298.1	.005870	.7822	.006716	.7879
2olC3.dat	293.1	.004320	.7870	.004951	.7929
2olC3.dat	283.1	.002270	.7963	.002586	.8029
2olC4.dat	453.1	.993000	.6148	.851507	.6445
2olC4.dat	443.5	.794000	.6300	.689902	.6569
2olC4.dat	443.2	.794000	.6305	.685073	.6573
2olC4.dat	433.2	.624000	.6456	.542036	.6700
2olC4.dat	432.8	.623000	.6462	.537211	.6705
2olC4.dat	423.6	.491000	.6595	.426711	.6819
2olC4.dat	422.1	.474000	.6616	.410726	.6837
2olC4.dat	387.2	.169000	.7073	.148148	.7250
2olC4.dat	382.3	.143000	.7133	.125749	.7306
2olC4.dat	380.3	.133000	.7158	.117193	.7329
2olC4.dat	377.5	.121000	.7192	.106219	.7360
2olC4.dat	375.8	.114000	.7212	.099914	.7380
2olC4.dat	372.7	.101000	.7249	.089305	.7414
2olC4.dat	370.4	.093100	.7276	.082152	.7439
2olC4.dat	367.9	.084500	.7305	.074696	.7467
2olC4.dat	364.2	.073300	.7348	.064907	.7507
2olC4.dat	363.1	.070100	.7361	.062120	.7519
2olC4.dat	358.4	.057800	.7415	.051375	.7571
2olC4.dat	356.5	.053400	.7436	.047575	.7591
2olC4.dat	353.6	.047400	.7469	.042228	.7622
2olC4.dat	349.8	.039900	.7512	.035731	.7663
2olC4.dat	348.9	.038600	.7521	.034503	.7672
2olC4.dat	344.3	.031200	.7573	.027993	.7721
2olC4.dat	340.9	.026600	.7610	.023931	.7757
2olC4.dat	339.6	.025000	.7624	.022556	.7770
2olC4.dat	335.0	.019900	.7674	.018046	.7818
2olC4.dat	331.4	.016700	.7712	.015136	.7855
2olC4.dat	327.2	.013300	.7757	.012161	.7899
2olC4.dat	323.0	.010700	.7801	.009769	.7941
2olC4.dat	317.9	.008000	.7855	.007365	.7992
2olC4.dat	311.0	.005330	.7926	.004946	.8061
2olC4.dat	301.9	.003000	.8018	.002814	.8151
2olC5.dat	391.9	.099300	.7160	.092845	.7336
2olC5.dat	387.7	.085100	.7204	.080343	.7384
2olC5.dat	383.9	.074200	.7243	.070352	.7426
2olC5.dat	383.4	.073400	.7249	.068910	.7432
2olC5.dat	383.3	.073400	.7250	.068885	.7432
2olC5.dat	379.9	.064000	.7285	.060878	.7470
2olC5.dat	375.8	.054600	.7327	.052191	.7516
2olC5.dat	374.3	.052000	.7341	.049331	.7532
2olC5.dat	374.3	.052000	.7342	.049312	.7532
2olC5.dat	371.7	.046400	.7368	.044543	.7561
2olC5.dat	367.5	.039000	.7410	.037672	.7607
2olC5.dat	364.0	.034100	.7444	.032688	.7644
2olC5.dat	364.0	.034100	.7444	.032674	.7644
2olC5.dat	363.4	.032900	.7450	.031950	.7650
2olC5.dat	359.5	.027700	.7488	.027013	.7693
2olC5.dat	355.3	.022900	.7529	.022479	.7738
2olC5.dat	353.7	.021600	.7543	.021004	.7754
2olC5.dat	353.7	.021600	.7544	.020995	.7754
2olC5.dat	351.0	.018800	.7569	.018564	.7783
2olC5.dat	346.8	.015300	.7609	.015231	.7828

2olC5.dat	343.4	.013200	.7641	.012976	.7863
2olC5.dat	343.4	.013200	.7641	.012970	.7863
2olC5.dat	342.4	.012300	.7650	.012344	.7874
2olC5.dat	338.6	.010100	.7686	.010200	.7914
2olC5.dat	335.1	.008000	.7718	.008538	.7950
2olC5.dat	334.8	.008230	.7721	.008365	.7954
2olC5.dat	333.3	.007720	.7735	.007734	.7969
2olC5.dat	333.3	.007720	.7735	.007730	.7969
2olC5.dat	330.4	.006670	.7761	.006614	.7999
2olC5.dat	326.9	.005264	.7792	.005485	.8034
2olC5.dat	323.2	.004320	.7826	.004442	.8072
2olC5.dat	323.2	.004320	.7826	.004440	.8072
2olC5.dat	322.2	.004008	.7835	.004176	.8083
2olC6.dat	415.1	.108190	.7013	.105188	.7172
2olC6.dat	413.3	.101630	.7033	.099371	.7192
2olC6.dat	413.1	.101390	.7034	.099009	.7193
2olC6.dat	408.1	.086286	.7086	.084789	.7247
2olC6.dat	407.4	.084227	.7094	.082933	.7254
2olC6.dat	401.9	.069861	.7151	.069359	.7314
2olC6.dat	398.1	.060662	.7189	.061154	.7354
2olC6.dat	396.6	.057912	.7205	.057952	.7371
2olC6.dat	391.1	.047425	.7260	.047894	.7429
2olC6.dat	388.1	.042730	.7289	.043053	.7460
2olC6.dat	385.7	.038501	.7314	.039290	.7487
2olC6.dat	380.4	.031216	.7365	.032206	.7542
2olC6.dat	378.1	.028838	.7387	.029509	.7566
2olC6.dat	375.1	.025077	.7416	.026189	.7598
2olC6.dat	370.2	.020232	.7464	.021365	.7650
2olC6.dat	368.1	.018665	.7483	.019636	.7671
2olC6.dat	364.7	.015822	.7515	.016928	.7707
2olC6.dat	358.1	.011466	.7577	.012646	.7775
2olC6.dat	354.3	.009617	.7612	.010580	.7814
2olC6.dat	349.6	.007576	.7655	.008440	.7863
2olC6.dat	348.1	.007066	.7668	.007854	.7878
2olC6.dat	345.1	.005970	.7696	.006743	.7909
2olC6.dat	341.0	.004770	.7733	.005454	.7951
2olC6.dat	338.1	.004400	.7759	.004687	.7980
2olC6.dat	336.9	.003787	.7770	.004386	.7992
2olC6.dat	328.1	.002507	.7847	.002676	.8081
2olC6.dat	318.1	.001333	.7934	.001455	.8181
2olC8.dat	473.3	.172000	.6619	.165363	.6820
2olC8.dat	464.4	.137000	.6713	.132844	.6906
2olC8.dat	453.5	.103000	.6825	.099930	.7011
2olC8.dat	453.1	.102000	.6829	.098964	.7014
2olC8.dat	447.2	.085800	.6888	.084026	.7072
2olC8.dat	446.6	.084300	.6894	.082624	.7077
2olC8.dat	442.8	.075600	.6932	.074252	.7113
2olC8.dat	440.0	.069400	.6959	.068403	.7141
2olC8.dat	434.0	.057700	.7017	.057292	.7198
2olC8.dat	432.6	.055200	.7031	.054781	.7212
2olC8.dat	427.8	.047200	.7077	.047169	.7258
2olC8.dat	423.7	.041400	.7115	.041463	.7296
2olC8.dat	421.6	.038400	.7135	.038716	.7316
2olC8.dat	415.8	.031300	.7189	.031859	.7372
2olC8.dat	413.9	.029400	.7206	.029886	.7390
2olC8.dat	410.0	.025300	.7243	.026024	.7428
2olC8.dat	404.8	.020800	.7290	.021533	.7478

2olC8.dat	403.9	.020100	.7297	.020907	.7486
2olC8.dat	400.1	.017400	.7332	.018131	.7522
2olC8.dat	398.0	.015800	.7351	.016692	.7543
2olC8.dat	394.8	.014000	.7379	.014727	.7574
2olC8.dat	392.7	.012700	.7398	.013564	.7594
2olC8.dat	391.8	.012300	.7406	.013061	.7603
2olC8.dat	388.2	.010500	.7437	.011304	.7637
2olC8.dat	386.6	.009720	.7451	.010567	.7652
2olC8.dat	384.4	.008840	.7470	.009639	.7673
2olC8.dat	380.8	.007450	.7502	.008236	.7708
2olC8.dat	379.6	.007130	.7512	.007814	.7720
2olC8.dat	376.5	.006090	.7538	.006821	.7749
2olC8.dat	373.9	.005420	.7561	.006046	.7775
2olC8.dat	371.5	.004760	.7581	.005414	.7798
2olC8.dat	367.5	.003830	.7615	.004473	.7836
2olC8.dat	366.3	.003700	.7625	.004232	.7847
2olC9.dat	364.1	.001733	.7664	.001836	.7889
2olC9.dat	358.1	.001333	.7714	.001331	.7945

C.1.2 – Testing –OH Site

compName	TexpK	PexpMPa	RhoLexpG_cc	Ptpt	Rhotpt
2olC7.dat	424.9	.084121	.7008	.078249	.7180
2olC7.dat	410.4	.053077	.7153	.049515	.7329
2olC7.dat	397.3	.033489	.7281	.031323	.7463
2olC7.dat	385.1	.021130	.7396	.019709	.7587
2olC7.dat	374.3	.013332	.7496	.012614	.7697
2olC7.dat	364.3	.008413	.7586	.008066	.7798
2olC7.dat	354.9	.005307	.7669	.005152	.7892
2olC7.dat	346.1	.003349	.7746	.003266	.7980
2olC7.dat	337.9	.002113	.7817	.002072	.8062
3olC5.dat	245.1	.000007	.8619	.000006	.8892
3olC5.dat	249.8	.000013	.8580	.000010	.8848
3olC5.dat	258.1	.000033	.8510	.000025	.8771
3olC5.dat	262.8	.000053	.8470	.000040	.8727
3olC5.dat	267.4	.000084	.8431	.000062	.8684
3olC5.dat	283.4	.000353	.8292	.000254	.8533
3olC5.dat	290.3	.000627	.8231	.000440	.8467
3olC5.dat	293.8	.000807	.8200	.000574	.8433
3olC5.dat	317.7	.003839	.7982	.002908	.8200
3olC5.dat	321.8	.004922	.7943	.003729	.8159
3olC5.dat	325.5	.006091	.7908	.004618	.8122
3olC5.dat	329.1	.007452	.7874	.005654	.8086
3olC5.dat	334.0	.009707	.7828	.007372	.8037
3olC5.dat	338.7	.012416	.7782	.009440	.7989
3olC5.dat	343.5	.015793	.7735	.012012	.7940
3olC5.dat	348.3	.019930	.7688	.015189	.7890
3olC5.dat	353.0	.024810	.7641	.018942	.7841
3olC5.dat	358.1	.031050	.7590	.023763	.7788
3olC5.dat	363.0	.038285	.7539	.029390	.7736
3olC5.dat	368.0	.046950	.7488	.036148	.7683
3olC5.dat	373.4	.057937	.7432	.044780	.7626
3olC5.dat	378.2	.069435	.7381	.053895	.7575
3olC5.dat	384.1	.086016	.7317	.067112	.7510
3olC5.dat	388.7	.100990	.7267	.079047	.7460
3olC6.dat	398.1	.071700	.7209	.064848	.7429

3olC6.dat	388.1	.050760	.7310	.045425	.7536
3olC6.dat	378.1	.035200	.7409	.030971	.7642
3olC6.dat	370.0	.032700	.7487	.022174	.7728
3olC6.dat	368.1	.023410	.7505	.020495	.7748
3olC6.dat	360.1	.014500	.7581	.014386	.7831
3olC6.dat	358.1	.015300	.7599	.013121	.7852
3olC6.dat	356.1	.016600	.7618	.011951	.7872
3olC6.dat	353.0	.013300	.7647	.010284	.7905
3olC6.dat	348.1	.009530	.7692	.008100	.7955
3olC6.dat	341.1	.008000	.7755	.005643	.8026
3olC6.dat	339.0	.007280	.7775	.005029	.8048
3olC6.dat	338.1	.005870	.7782	.004802	.8056
3olC6.dat	333.1	.004900	.7827	.003637	.8107
3olC6.dat	330.0	.003270	.7855	.003035	.8139
3olC6.dat	318.1	.001549	.7958	.001470	.8257
3olC6.dat	313.3	.001121	.8001	.001066	.8305
3olC6.dat	311.5	.001020	.8016	.000947	.8322
3olC6.dat	308.4	.000821	.8042	.000764	.8352
3olC6.dat	305.4	.000656	.8068	.000618	.8382
3olC6.dat	303.2	.000563	.8087	.000526	.8403
3olC6.dat	299.3	.000423	.8119	.000394	.8441
3olC6.dat	296.3	.000327	.8144	.000313	.8470
3olC6.dat	293.3	.000253	.8169	.000248	.8498
3olC6.dat	290.3	.000200	.8194	.000194	.8527
3olC6.dat	287.4	.000152	.8218	.000153	.8555
3olC6.dat	284.3	.000119	.8244	.000117	.8584
3olC6.dat	283.2	.000120	.8253	.000106	.8595
3olC6.dat	281.3	.000090	.8268	.000090	.8613
3olC6.dat	278.3	.000067	.8293	.000069	.8641
3olC6.dat	273.1	.000051	.8334	.000043	.8689
3olC6.dat	263.1	.000022	.8415	.000016	.8783
3olC7.dat	429.9	.100000	.6899	.091404	.7211
3olC7.dat	429.1	.098100	.6907	.089406	.7219
3olC7.dat	429.1	.098730	.6908	.089142	.7220
3olC7.dat	339.1	.002400	.7827	.002162	.8127
3olC7.dat	337.6	.002200	.7841	.001983	.8142
3olC7.dat	303.2	.000196	.8160	.000194	.8478
c2ol_2_C1C6.dat	440.1	.100390	.7936	.116149	.7937
c2ol_2_C1C6.dat	338.1	.002133	.8964	.002020	.8978
c2ol_2_C1C6.dat	333.6	.001600	.9006	.001547	.9024
c2ol_4_C1C6.dat	441.6	.099325	.7776	.114277	.7875
c2ol_4_C1C6.dat	345.6	.002000	.8760	.002834	.8848
c2olC6.dat	444.5	.137140	.8086	.159662	.8122
c2olC6.dat	440.0	.120710	.8134	.141446	.8171
c2olC6.dat	434.7	.103620	.8189	.122457	.8228
c2olC6.dat	434.2	.101850	.8195	.120484	.8234
c2olC6.dat	433.9	.099192	.8198	.119439	.8237
c2olC6.dat	428.9	.086046	.8250	.103566	.8291
c2olC6.dat	428.8	.086544	.8251	.103326	.8292
c2olC6.dat	424.8	.076327	.8293	.091797	.8335
c2olC6.dat	421.9	.069487	.8322	.084149	.8366
c2olC6.dat	418.7	.062690	.8355	.076250	.8400
c2olC6.dat	415.6	.056449	.8387	.069187	.8433
c2olC6.dat	415.2	.055883	.8390	.068488	.8437
c2olC6.dat	411.4	.049053	.8428	.060629	.8477
c2olC6.dat	409.4	.045356	.8449	.056631	.8499
c2olC6.dat	404.9	.038859	.8493	.048746	.8546

c2olC6.dat	404.1	.037543	.8501	.047432	.8555
c2olC6.dat	398.2	.030307	.8559	.038648	.8617
c2olC6.dat	393.5	.025221	.8605	.032544	.8667
c2olC6.dat	393.5	.025265	.8605	.032544	.8667
c2olC6.dat	389.9	.021813	.8640	.028470	.8704
c2olC6.dat	385.9	.018252	.8679	.024353	.8747
c2olC6.dat	385.8	.018418	.8680	.024286	.8747
c2olC6.dat	381.1	.015041	.8725	.020150	.8797
c2olC6.dat	378.0	.013159	.8754	.017764	.8829
c2olC6.dat	375.3	.011609	.8780	.015855	.8857
c2olC6.dat	372.9	.010426	.8803	.014325	.8882
c2olC6.dat	371.7	.009872	.8814	.013610	.8894
c2olC6.dat	367.9	.008251	.8849	.011543	.8933
c2olC6.dat	366.0	.007522	.8867	.010611	.8952
c2olC6.dat	361.9	.006125	.8905	.008783	.8995
c2olC6.dat	357.1	.004803	.8949	.007014	.9043
c2olC6.dat	354.3	.004130	.8975	.006101	.9072
c2olC6.dat	350.8	.003420	.9007	.005125	.9108
diolC4.dat	468.1	.159990	.8002	.042083	.8739
diolC4.dat	462.1	.133320	.8085	.033824	.8794
diolC4.dat	459.1	.119990	.8125	.030234	.8821
diolC4.dat	455.1	.106660	.8179	.025952	.8857
diolC4.dat	454.6	.103990	.8187	.025357	.8862
diolC4.dat	454.1	.102660	.8192	.024966	.8865
diolC4.dat	453.9	.101320	.8196	.024676	.8868
diolC4.dat	453.4	.099992	.8201	.024295	.8872
diolC4.dat	453.1	.098658	.8207	.023918	.8875
diolC4.dat	452.1	.095992	.8218	.023088	.8883
diolC4.dat	451.4	.093325	.8229	.022371	.8890
diolC4.dat	447.1	.079993	.8284	.018909	.8927
diolC4.dat	441.1	.066661	.8361	.014761	.8980
diolC4.dat	435.1	.053329	.8437	.011417	.9032
diolC4.dat	423.1	.033331	.8586	.006634	.9134
diolC4.dat	417.1	.026664	.8659	.004979	.9185
diolC4.dat	410.1	.019998	.8743	.003513	.9243
diolC4.dat	389.1	.007999	.8986	.001119	.9416
diolC4.dat	381.1	.005333	.9076	.000693	.9480
diolC4.dat	375.1	.004000	.9143	.000476	.9528
diolC4.dat	367.1	.002666	.9231	.000282	.9592
diolC4.dat	355.1	.001333	.9360	.000121	.9686

C.1.3 – Training –COO– Site

compName	TexpK	PexpMPa	RhoLexpG_cc	Ptpt	Rhotpt
C3ateC2.dat	533.1	2.776400	.4773	2.971444	.5752
C3ateC2.dat	523.1	2.395800	.5189	2.577247	.5980
C3ateC2.dat	513.1	2.056500	.5510	2.223511	.6184
C3ateC2.dat	503.1	1.752500	.5780	1.906773	.6371
C3ateC2.dat	493.1	1.492500	.6019	1.624263	.6546
C3ateC2.dat	483.1	1.260700	.6235	1.373538	.6711
C3ateC2.dat	473.1	1.057400	.6433	1.152323	.6869
C3ateC2.dat	463.1	.882460	.6619	.958436	.7021
C3ateC2.dat	453.1	.731540	.6794	.789748	.7168
C3ateC2.dat	443.1	.600620	.6960	.644176	.7311
C3ateC2.dat	433.1	.487560	.7118	.519671	.7451

C3ateC2.dat	423.1	.389300	.7269	.414226	.7587
C3ateC2.dat	413.1	.308770	.7415	.325885	.7721
C3ateC2.dat	403.1	.240110	.7556	.252748	.7852
C3ateC2.dat	393.1	.184780	.7693	.192988	.7982
C3ateC2.dat	383.1	.139720	.7825	.144859	.8110
C3ateC2.dat	373.1	.104660	.7954	.106712	.8236
C3ateC2.dat	363.1	.075927	.8080	.077006	.8362
C3ateC2.dat	353.1	.053809	.8203	.054323	.8486
C3ateC2.dat	343.1	.037317	.8322	.037374	.8610
C3ateC2.dat	333.1	.025065	.8440	.025013	.8733
C3ateC2.dat	323.1	.016399	.8555	.016236	.8856
C3ateC2.dat	313.1	.010386	.8668	.010187	.8979
C3ateC2.dat	303.1	.006366	.8779	.006156	.9101
C3ateC2.dat	293.1	.003700	.8888	.003567	.9224
C3ateC2.dat	283.1	.002073	.8995	.001973	.9347
C3ateC2.dat	273.1	.001107	.9100	.001035	.9470
C3ateC2.dat	263.1	.000540	.9204	.000512	.9594
C3ateC4.dat	417.4	.099490	.7511	.101984	.7766
C3ateC4.dat	416.7	.097520	.7519	.099904	.7774
C3ateC4.dat	416.0	.095690	.7527	.097942	.7782
C3ateC4.dat	415.4	.094120	.7533	.096262	.7789
C3ateC4.dat	414.8	.092620	.7541	.094522	.7796
C3ateC4.dat	414.1	.090860	.7548	.092753	.7803
C3ateC4.dat	413.5	.089160	.7556	.090931	.7811
C3ateC4.dat	412.8	.087430	.7563	.089085	.7819
C3ateC4.dat	412.1	.085730	.7571	.087320	.7827
C3ateC4.dat	411.3	.083920	.7580	.085381	.7835
C3ateC4.dat	410.7	.082370	.7587	.083725	.7842
C3ateC4.dat	410.2	.081220	.7592	.082512	.7848
C3ateC4.dat	409.1	.078650	.7605	.079816	.7860
C3ateC4.dat	408.1	.076530	.7616	.077542	.7871
C3ateC4.dat	407.4	.074990	.7623	.075963	.7879
C3ateC4.dat	407.1	.074200	.7627	.075137	.7883
C3ateC4.dat	406.1	.072120	.7638	.072970	.7894
C3ateC4.dat	405.2	.070310	.7647	.071028	.7903
C3ateC4.dat	404.5	.068880	.7655	.069556	.7911
C3ateC4.dat	403.8	.067300	.7663	.067919	.7920
C3ateC4.dat	403.0	.065820	.7672	.066312	.7928
C3ateC4.dat	366.1	.019732	.8062	.018108	.8337
C3ateC4.dat	359.9	.014932	.8125	.014095	.8405
C3ateC4.dat	354.4	.011732	.8179	.011231	.8464
C3ateC4.dat	349.9	.009333	.8224	.009233	.8513
C3ateC4.dat	343.3	.006933	.8290	.006816	.8586
C3ateC4.dat	337.4	.005200	.8346	.005178	.8650
C3ateC4.dat	330.6	.003733	.8412	.003696	.8724
C3ateC4.dat	323.6	.002533	.8478	.002564	.8801
C3ateC4.dat	317.1	.001733	.8541	.001784	.8873
C3ateC4.dat	309.4	.001133	.8612	.001148	.8956
C3ateC4.dat	305.6	.000867	.8648	.000906	.8999
C4ateC1.dat	513.1	1.897200	.5854	1.938385	.6568
C4ateC1.dat	503.1	1.613900	.6093	1.649130	.6732
C4ateC1.dat	493.1	1.371200	.6307	1.393173	.6889
C4ateC1.dat	483.1	1.157800	.6504	1.167923	.7039
C4ateC1.dat	473.1	.971520	.6687	.970943	.7183
C4ateC1.dat	463.1	.808330	.6858	.799897	.7323
C4ateC1.dat	453.1	.669280	.7021	.652530	.7459
C4ateC1.dat	443.1	.548090	.7175	.526654	.7592

C4ateC1.dat	433.1	.443700	.7323	.420150	.7722
C4ateC1.dat	423.1	.354240	.7464	.330972	.7849
C4ateC1.dat	413.1	.279980	.7601	.257153	.7975
C4ateC1.dat	403.1	.216910	.7733	.196815	.8098
C4ateC1.dat	393.1	.166390	.7861	.148178	.8221
C4ateC1.dat	383.1	.125460	.7985	.109568	.8341
C4ateC1.dat	375.4	.101720	.8079	.085552	.8434
C4ateC1.dat	375.6	.101590	.8076	.086254	.8431
C4ateC1.dat	375.4	.101500	.8079	.085552	.8434
C4ateC1.dat	373.1	.093419	.8106	.079436	.8461
C4ateC1.dat	363.1	.067594	.8223	.056355	.8579
C4ateC1.dat	353.1	.048183	.8338	.039038	.8697
C4ateC1.dat	343.1	.033370	.8451	.026342	.8815
C4ateC1.dat	333.1	.022331	.8561	.017267	.8932
C4ateC1.dat	323.1	.014619	.8669	.010962	.9048
C4ateC1.dat	313.1	.009226	.8774	.006716	.9165
C4ateC1.dat	303.1	.005593	.8878	.003957	.9281
C4ateC1.dat	302.8	.005333	.8882	.003870	.9286
C4ateC1.dat	293.1	.003273	.8980	.002231	.9398
C4ateC1.dat	283.1	.001840	.9080	.001198	.9514
C4ateC1.dat	273.1	.000973	.9179	.000609	.9632
C4ateC1.dat	263.1	.000473	.9276	.000291	.9750
C4ateC2.dat	392.9	.101240	.7719	.098826	.8016
C4ateC2.dat	394.4	.100920	.7700	.103568	.7997
C4ateC2.dat	392.4	.096285	.7724	.097482	.8021
C4ateC2.dat	392.4	.095445	.7725	.097186	.8022
C4ateC2.dat	373.4	.052782	.7945	.052692	.8244
C4ateC2.dat	339.9	.015945	.8312	.014445	.8633
C4ateC2.dat	321.9	.006693	.8499	.006274	.8841
C4ateC2.dat	321.9	.006666	.8499	.006274	.8841
C4ateC2.dat	298.1	.002267	.8739	.001721	.9116
C4ateC3.dat	415.8	.101450	.7460	.102267	.7776
C4ateC3.dat	412.7	.093430	.7496	.093531	.7810
C4ateC3.dat	412.3	.092480	.7500	.092523	.7815
C4ateC3.dat	411.6	.090680	.7508	.090693	.7822
C4ateC3.dat	410.6	.088160	.7519	.088055	.7833
C4ateC3.dat	409.7	.085730	.7530	.085554	.7844
C4ateC3.dat	408.6	.083260	.7543	.082813	.7856
C4ateC3.dat	407.2	.079940	.7559	.079443	.7871
C4ateC3.dat	406.8	.078860	.7564	.078368	.7876
C4ateC3.dat	405.9	.076830	.7574	.076230	.7886
C4ateC3.dat	404.9	.074900	.7584	.074163	.7896
C4ateC3.dat	404.3	.073290	.7592	.072608	.7903
C4ateC3.dat	402.2	.068970	.7615	.068164	.7925
C4ateC3.dat	400.4	.065500	.7635	.064488	.7945
C4ateC3.dat	398.1	.061320	.7661	.059837	.7970
C4ateC3.dat	395.8	.057170	.7687	.055568	.7996
C4ateC3.dat	394.2	.054400	.7704	.052764	.8013
C4ateC3.dat	392.5	.051310	.7723	.049894	.8031
C4ateC3.dat	391.1	.049200	.7738	.047627	.8046
C4ateC3.dat	389.7	.046990	.7753	.045444	.8062
C4ateC3.dat	381.1	.033690	.7847	.033713	.8155
C4ateC3.dat	373.0	.025330	.7933	.025146	.8241
C4ateC3.dat	370.1	.022740	.7964	.022490	.8273
C4ateC3.dat	366.9	.020160	.7998	.019852	.8307
C4ateC3.dat	364.4	.018430	.8023	.018056	.8333
C4ateC3.dat	358.4	.014520	.8086	.014102	.8398

C4ateC3.dat	357.3	.013910	.8097	.013484	.8410
C4ateC3.dat	354.8	.012580	.8123	.012144	.8436
iC4ateIC4.dat	441.3	.174650	.6879	.206712	.7120
iC4ateIC4.dat	432.9	.142250	.6983	.168105	.7215
iC4ateIC4.dat	423.9	.112390	.7095	.132498	.7316
iC4ateIC4.dat	414.8	.088259	.7206	.103103	.7417
iC4ateIC4.dat	409.6	.076260	.7268	.088786	.7474
iC4ateIC4.dat	401.1	.058795	.7367	.069037	.7566
iC4ateIC4.dat	393.4	.046263	.7457	.054182	.7649
iC4ateIC4.dat	382.6	.032397	.7582	.037661	.7766
iC4ateIC4.dat	378.9	.028531	.7623	.033208	.7805
iC4ateIC4.dat	373.6	.023731	.7684	.027342	.7862
iC4ateIC4.dat	367.1	.018665	.7756	.021517	.7930
iC4ateIC4.dat	358.9	.013332	.7847	.015586	.8017
iC4ateIC4.dat	354.4	.010932	.7897	.012902	.8066
iC4ateIC4.dat	347.9	.007999	.7968	.009774	.8135
iC4ateIC4.dat	338.4	.005733	.8070	.006390	.8234
iC4ateIC4.dat	298.1	.000640	.8494	.000707	.8661
iC4ateIC4.dat	293.1	.000427	.8546	.000511	.8715
C10ateC1.dat	433.8	.013332	.7523	.013152	.7906
C10ateC1.dat	427.9	.010666	.7577	.010606	.7958
C10ateC1.dat	421.8	.008186	.7634	.008357	.8013
C10ateC1.dat	415.9	.006666	.7688	.006632	.8064
C10ateC1.dat	410.9	.005333	.7733	.005398	.8109
C10ateC1.dat	403.8	.003986	.7798	.003967	.8173
C10ateC1.dat	395.9	.002866	.7868	.002797	.8242
C10ateC1.dat	387.1	.002000	.7946	.001845	.8319
C10ateC1.dat	380.4	.001440	.8004	.001323	.8379
C10ateC1.dat	369.8	.000800	.8096	.000753	.8473
C10ateC1.dat	366.6	.000667	.8124	.000632	.8502
C10ateC1.dat	362.3	.000533	.8161	.000495	.8540
C10ateC1.dat	350.1	.000267	.8263	.000240	.8648
C10ateC1.dat	339.1	.000133	.8354	.000118	.8746
C10ateC1.dat	331.6	.000080	.8416	.000070	.8813
C10ateC1.dat	326.1	.000053	.8462	.000047	.8864
C10ateC1.dat	316.9	.000027	.8536	.000023	.8946
C10ateC1.dat	308.6	.000013	.8603	.000012	.9021

C.1.4 – Testing –COO– site

compName	TexpK	PexpMPa	RhoLexpG_cc	Ptpt	Rhotpt
C3ateC3.dat	394.3	.101720	.7712	.103306	.7982
C3ateC3.dat	395.3	.100660	.7699	.106452	.7970
C3ateC3.dat	292.6	.001333	.8825	.001224	.9168
C4ateC4.dat	438.6	.098100	.7309	.106271	.7555
C4ateC4.dat	328.3	.001730	.8390	.001425	.8660
iC4ateC3.dat	407.1	.100260	.7439	.116323	.7607
C5ateC4.dat	457.1	.100000	.7118	.107715	.7404
C5ateC4.dat	291.1	.000047	.8691	.000045	.9043
iC5ateC2.dat	298.1	.001053	.8611	.000861	.9040
C12ateC1.dat	452.0	.007848	.7397	.008647	.7791
C12ateC1.dat	442.0	.005357	.7485	.005894	.7876
C12ateC1.dat	432.0	.003597	.7573	.003920	.7960
C12ateC1.dat	422.0	.002343	.7660	.002541	.8045
C12ateC1.dat	412.0	.001476	.7745	.001606	.8129

C12ateC1.dat	411.9	.001600	.7745	.001604	.8129
C12ateC1.dat	401.8	.000969	.7831	.000978	.8215
C12ateC1.dat	391.8	.000611	.7914	.000581	.8299
C12ateC1.dat	381.9	.000357	.7995	.000336	.8382
C12ateC1.dat	371.5	.000203	.8081	.000181	.8470
C12ateC1.dat	362.4	.000111	.8154	.000102	.8547
C12ateC1.dat	355.5	.000074	.8210	.000064	.8606
C12ateC1.dat	345.5	.000037	.8289	.000032	.8691
C12ateC1.dat	335.5	.000018	.8368	.000015	.8777
C12ateIC3.dat	452.1	.004698	.7735	.005215	.7617
C12ateIC3.dat	442.1	.003219	.7806	.003481	.7699
C12ateIC3.dat	432.1	.002104	.7877	.002266	.7781
C12ateIC3.dat	422.3	.001405	.7945	.001450	.7861
C12ateIC3.dat	412.0	.000885	.8015	.000885	.7945
C12ateIC3.dat	401.9	.000535	.8084	.000526	.8027
C12ateIC3.dat	391.9	.000313	.8151	.000304	.8109
C12ateIC4.dat	452.2	.002591	.7457	.002835	.7650
C12ateIC4.dat	442.2	.001726	.7582	.001845	.7730
C12ateIC4.dat	432.2	.001137	.7623	.001168	.7810
C12ateIC4.dat	412.1	.000433	.7684	.000427	.7971
C12ateIC4.dat	402.0	.000255	.7756	.000245	.8052
C12ateIC4.dat	391.8	.000142	.7847	.000135	.8134
C12ateIC4.dat	381.7	.000078	.7897	.000072	.8215
C12ateIC4.dat	371.7	.000041	.7968	.000037	.8296
C12ateIC4.dat	361.8	.000020	.8070	.000018	.8377
C12ateIC4.dat	355.4	.000013	.8494	.000011	.8429
C12ateIC4.dat	345.3	.000006	1.4543	.000005	.8511
C12ate2C2C6.dat	452.0	.000472	.7675	.000409	.7833
C12ate2C2C6.dat	442.0	.000290	.7748	.000241	.7908
C12ate2C2C6.dat	432.0	.000173	.7821	.000138	.7983
C12ate2C2C6.dat	422.0	.000099	.7894	.000076	.8058
C12ate2C2C6.dat	412.0	.000055	.7966	.000040	.8133
C12ate2C2C6.dat	402.1	.000030	.8037	.000021	.8208
C12ate2C2C6.dat	392.0	.000015	.8109	.000010	.8284
C12ate2C2C6.dat	381.8	.000007	.8181	.000005	.8361
C12ate2C2C6.dat	371.6	.000003	.8252	.000002	.8438
C24ateC1.dat	452.2	.000017	1.7881	.000010	.8023
C24ateC1.dat	442.3	.000008	1.8220	.000005	.8093
C24ateC1.dat	442.2	.000008	1.8220	.000005	.8093
C24ateC1.dat	432.2	.000003	1.8555	.000002	.8164
C24ateC1.dat	432.2	.000003	1.8555	.000002	.8164
C24ateC1.dat	422.1	.000001	1.8883	.000001	.8235

C.2 – Structure of Ethyl Lactate and its Oligomers

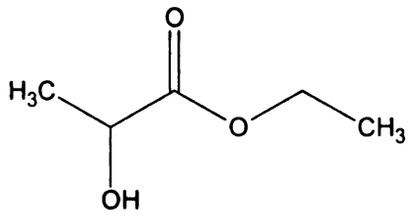

Ethyl lactate

ethyl 2-hydroxypropanoate

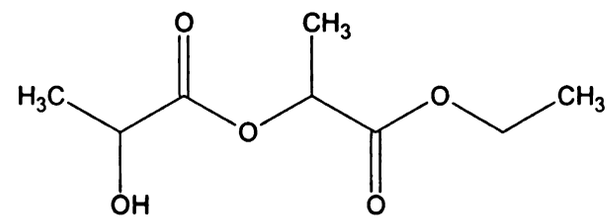

Ethyl lactate *Dimer*

2-ethoxy-1-methyl-2-oxoethyl 2-hydroxypropanoate

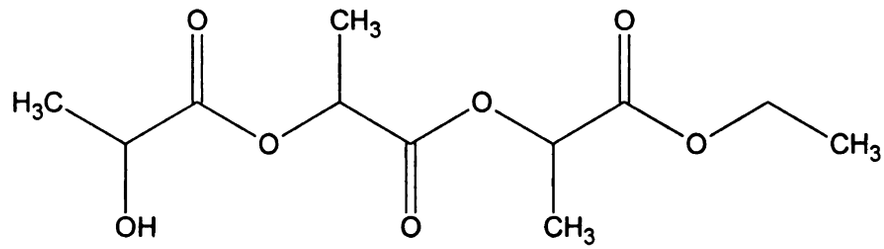

Ethyl lactate *Trimer*

2-(2-ethoxy-1-methyl-2-oxoethoxy)-1-methyl-2-oxoethyl 2-hydroxypropanoate

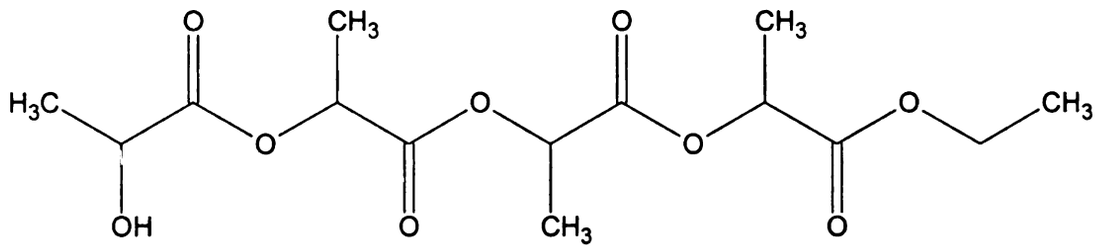

Ethyl lactate *Tetramer*

2-[2-(2-ethoxy-1-methyl-2-oxoethoxy)-1-methyl-2-oxoethoxy]-1-methyl-2-oxoethyl 2-hydroxypropanoate

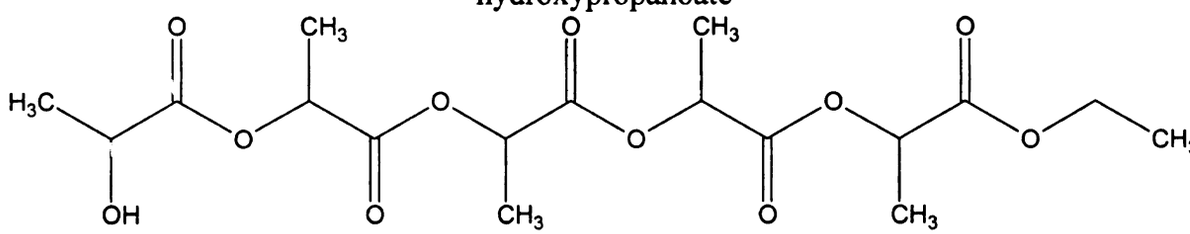

Ethyl lactate *Pentamer*

Ethyl 14-hydroxy-2,5,8,11-tetramethyl-4,7,10,13-tetraoxo-3,6,9,12-tetraoxapentadecan-1-oate

C.3 – The .m3d Files used in P^{sat} Predictions

C.3.1 – Ethyl Lactate Dimer. 3md

1. Interaction sites, n= 13

Bond radius	Group-coordinates			Group ID	
	x	y	z	Main group	Sub group
0.285	0.65588	0.00000	0.00000	14	4
0.390	0.52621	0.05991	-0.02242	3	3
0.363	0.40938	0.11646	0.04292	1	2
0.345	0.47677	-0.02100	-0.13928	9	4
0.270	0.49160	-0.05429	-0.25944	16	2
0.270	0.46124	-0.14741	-0.08840	15	2
0.390	0.33557	-0.17536	-0.03036	3	20
0.345	0.25117	-0.20569	-0.14276	9	4
0.363	0.32966	-0.30924	0.04143	1	2
0.270	0.15709	-0.10846	-0.15196	15	2
0.270	0.21697	-0.26136	-0.24874	16	2
0.357	0.03174	-0.11630	-0.10087	2	1
0.363	0.00000	0.00000	0.00000	1	1

2. Bond Matrix

	0	1	2	3	4	5	6	7	8	9	10	11
1	2											
2	4	2										
3	4	2	4									
4	6	4	6	2								
5	6	4	6	2	4							
6	6	6	6	4	6	2						
7	6	6	6	6	6	4	2					
8	6	6	6	6	6	4	2	4				
9	6	6	6	6	6	6	4	2	6			
10	6	6	6	6	6	6	4	2	6	4		
11	6	6	6	6	6	6	6	4	6	2	6	
12	6	6	6	6	6	6	6	6	6	4	6	2

C.3.2 – Ethyl Lactate Trimer. 3md

1. Interaction sites, n= 18

Bond radius	Group-coordinates			Group ID	
	x	y	z	Main group	Sub group
0.285	0.82500	-0.10234	0.22100	14	4
0.390	0.81527	-0.04031	0.09983	3	3
0.363	0.91205	0.00000	0.00000	1	2
0.345	0.73146	0.07980	0.13413	9	4
0.270	0.73418	0.17905	0.21498	16	2
0.270	0.63387	0.10412	0.04838	15	2
0.390	0.53727	0.00527	0.02053	3	20
0.345	0.42286	0.08670	-0.03130	9	4
0.363	0.54661	-0.11142	-0.08145	1	2
0.270	0.31415	0.04083	0.03105	15	2
0.270	0.38275	0.18021	-0.10763	16	2
0.390	0.28141	0.03173	0.16284	3	20
0.345	0.15079	-0.03662	0.16725	9	4
0.363	0.34997	-0.01765	0.28444	1	2
0.270	0.09165	-0.13605	0.22339	16	2
0.270	0.05192	0.04560	0.12031	15	2
0.357	0.00000	0.00000	0.00000	2	1
0.363	0.05158	-0.12339	-0.07990	1	1

2. Bond Matrix

	0	1	2	3	4	5	6	7	8	9	10	11	12	13	14	15	16
1	2																
2	4	2															
3	4	2	4														
4	6	4	6	2													
5	6	4	6	2	4												
6	6	6	6	4	6	2											
7	6	6	6	6	6	4	2										
8	6	6	6	6	6	4	2	4									
9	6	6	6	6	6	6	4	2	6								
10	6	6	6	6	6	6	4	2	6	4							
11	6	6	6	6	6	6	6	4	6	2	6						
12	6	6	6	6	6	6	6	6	6	4	6	2					
13	6	6	6	6	6	6	6	6	6	4	6	2	4				
14	6	6	6	6	6	6	6	6	6	6	6	4	2	6			
15	6	6	6	6	6	6	6	6	6	6	6	4	2	6	4		
16	6	6	6	6	6	6	6	6	6	6	6	6	4	6	6	2	
17	6	6	6	6	6	6	6	6	6	6	6	6	6	6	6	4	2

C.3.3 – Ethyl Lactate Tetramer. 3md

1. Interaction sites, n = 23

Bond radius	Group-coordinates			Group ID	
	x	y	z	Main group	Sub group
0.363	1.18538	0.00000	0.00000	1	1
0.285	0.21606	-0.00092	0.13672	14	4
0.390	0.15150	-0.01614	0.01336	3	3
0.363	0.00000	0.00000	0.00000	1	2
0.345	0.16659	-0.16314	-0.00495	9	4
0.270	0.13132	-0.27999	0.03315	16	2
0.270	0.26707	-0.19608	-0.08527	15	2
0.390	0.40473	-0.16235	-0.04931	3	20
0.345	0.46757	-0.23992	-0.15746	9	4
0.363	0.45018	-0.02212	-0.08116	1	2
0.270	0.59382	-0.26893	-0.11509	15	2
0.270	0.46812	-0.29037	-0.27660	16	2
0.390	0.62454	-0.34400	-0.00107	3	20
0.345	0.71075	-0.24401	0.06991	9	4
0.363	0.52397	-0.39057	0.09579	1	2
0.270	0.70730	-0.13888	0.14405	16	2
0.270	0.82769	-0.30396	0.08193	15	2
0.390	0.91459	-0.29869	-0.03879	3	20
0.363	0.88646	-0.42092	-0.13489	1	2
0.345	1.02727	-0.35253	0.04474	9	4
0.270	1.08707	-0.43113	0.12028	16	2
0.270	1.09711	-0.24145	0.07588	15	2
0.357	1.15519	-0.15309	-0.01526	2	1

2. Bond Matrix

	0	1	.....	21
1	6			
2	6	2		
3	6	4	2	
4	6	4	2	4
5	6	6	4	6	2
6	6	6	4	6	2	4
7	6	6	6	6	4	6	2
8	6	6	6	6	6	6	4	2
9	6	6	6	6	6	6	4	2	4
10	6	6	6	6	6	6	6	4	2	6
11	6	6	6	6	6	6	6	4	2	6	4
12	6	6	6	6	6	6	6	6	4	6	2	6
13	6	6	6	6	6	6	6	6	6	6	4	6	2
14	6	6	6	6	6	6	6	6	6	6	4	6	2	4
15	6	6	6	6	6	6	6	6	6	6	6	6	4	2	6
16	6	6	6	6	6	6	6	6	6	6	6	6	4	2	6	4
17	6	6	6	6	6	6	6	6	6	6	6	6	6	4	6	6	2
18	6	6	6	6	6	6	6	6	6	6	6	6	6	6	6	6	4	2
19	6	6	6	6	6	6	6	6	6	6	6	6	6	6	6	6	4	2	4
20	6	6	6	6	6	6	6	6	6	6	6	6	6	6	6	6	6	4	6	2
21	4	6	6	6	6	6	6	6	6	6	6	6	6	6	6	6	6	4	6	2	4
22	2	6	6	6	6	6	6	6	6	6	6	6	6	6	6	6	6	6	6	4	6	2

C.3.4 – Ethyl Lactate Pentamer. 3md

1. Interaction sites, n = 28

Bond radius	Group-coordinates			Group ID	
	x	y	z	Main group	Sub group
0.345	0.08076	-0.09219	0.03199	9	4
0.285	0.99207	0.25405	-0.00236	14	4
0.390	0.98110	0.16311	-0.10459	3	3
0.363	1.00510	0.13702	-0.25105	1	2
0.345	1.05847	0.05614	-0.03250	9	4
0.270	1.17048	0.00000	0.00000	16	2
0.270	0.98713	-0.00689	0.05169	15	2
0.390	0.87015	-0.07672	-0.00130	3	20
0.345	0.80529	-0.08187	0.13130	9	4
0.363	0.90450	-0.22855	-0.03154	1	2
0.270	0.67346	-0.09869	0.11164	15	2
0.270	0.81811	-0.04284	0.25128	16	2
0.390	0.60069	-0.21425	0.10818	3	20
0.345	0.56016	-0.22269	0.25166	9	4
0.363	0.62052	-0.35008	0.05876	1	2
0.270	0.60637	-0.26066	0.36467	16	2
0.270	0.44013	-0.17823	0.28202	15	2
0.390	0.41802	-0.04203	0.25083	3	20
0.363	0.50561	0.07024	0.31366	1	2
0.345	0.28714	-0.03116	0.30773	9	4
0.270	0.20969	0.01436	0.39889	16	2
0.270	0.19267	-0.04209	0.20844	15	2
0.390	0.15397	-0.15525	0.14194	3	20
0.363	0.05175	-0.25290	0.21374	1	2
0.270	0.14117	-0.11408	-0.08815	15	2
0.270	0.00000	0.00000	0.00000	16	2
0.357	0.09034	-0.21832	-0.16249	2	1
0.363	0.15233	-0.31923	-0.24503	1	1

2. **Bond Matrix**

	0	1	.....	26
1	6			
2	6	2		
3	6	4	2	
4	6	4	2	4
5	6	6	4	6 2
6	6	6	4	6 2 4
7	6	6	6	6 4 6 2
8	6	6	6	6 6 6 4 2
9	6	6	6	6 6 6 4 2 4
10	6	6	6	6 6 6 6 4 2 6
11	6	6	6	6 6 6 6 4 2 6 4
12	6	6	6	6 6 6 6 6 4 6 2 6
13	6	6	6	6 6 6 6 6 6 6 4 6 2
14	6	6	6	6 6 6 6 6 6 6 4 6 2 4
15	6	6	6	6 6 6 6 6 6 6 6 6 4 2 6
16	6	6	6	6 6 6 6 6 6 6 6 6 4 2 6 4
17	6	6	6	6 6 6 6 6 6 6 6 6 6 4 6 6 2
18	6	6	6	6 6 6 6 6 6 6 6 6 6 6 6 6 4 2
19	6	6	6	6 6 6 6 6 6 6 6 6 6 6 6 6 4 2 4
20	6	6	6	6 6 6 6 6 6 6 6 6 6 6 6 6 6 4 6 2
21	4	6	6	6 6 6 6 6 6 6 6 6 6 6 6 6 6 4 6 2 4
22	2	6	6	6 6 6 6 6 6 6 6 6 6 6 6 6 6 6 6 4 6 2
23	4	6	6	6 6 6 6 6 6 6 6 6 6 6 6 6 6 6 6 6 4 2
24	2	6	6	6 6 6 6 6 6 6 6 6 6 6 6 6 6 6 6 6 6 4 6
25	2	6	6	6 6 6 6 6 6 6 6 6 6 6 6 6 6 6 6 6 6 6 4 6 4
26	4	6	6	6 6 6 6 6 6 6 6 6 6 6 6 6 6 6 6 6 6 6 6 2 6
27	6	6	6	6 6 6 6 6 6 6 6 6 6 6 6 6 6 6 6 6 6 6 6 4 6 2

C.3.5 – Dioxane. 3md (5-hydroxy-2-methyl-1,3-dioxane or 5HMD)

Interaction sites, n= 8

Bond radius	Group-coordinates			Group ID	
	x	y	z	Main group	Sub group
0.39	0.38061	0.01813	0.06592	3	1
0.27	0.30861	-0.11056	0.03568	15	1
0.357	0.21754	-0.10558	-0.07610	2	1
0.39	0.12777	0.02395	-0.06059	3	1
0.357	0.22643	0.14493	-0.06764	2	1
0.27	0.32506	0.13956	0.02941	15	1
0.363	0.51032	0.00000	0.00000	1	2
0.285	0.00000	0.00000	0.00000	14	4

C.3.6 – Dioxolane. 3md (4-hydroxymethyl-2-methyl-1,3-dioxolane or 4HMD)

Interaction sites, n = 8

Bond radius	Group-coordinates			Group ID	
	x	y	z	Main group	Sub group
0.39	0.38970	0.02521	0.03615	3	4
0.27	0.35938	0.12730	-0.07242	15	1
0.357	0.25062	0.08419	-0.16080	2	1
0.39	0.09236	-0.08703	-0.05174	1	6
0.357	0.22984	-0.07035	-0.12540	3	4
0.27	0.31654	-0.09858	-0.00529	15	1
0.363	0.54307	0.00000	0.00000	1	2
0.285	0.00000	0.00000	0.00000	14	2

Bond Matrix (for 5HMD)

	0	1	2	3	4	5	6
1	2						
2	4	2					
3	6	4	2				
4	4	6	4	2			
5	2	4	6	4	2		
6	2	4	6	6	6	4	
7	6	6	4	2	4	6	6

Bond Matrix (for 4HMD)

	0	1	2	3	4	5	6
1	2						
2	4	2					
3	6	6	4				
4	4	4	2	2			
5	2	4	4	4	2		
6	2	4	6	6	6	4	
7	6	6	4	2	4	6	6

LIST OF REFERENCES

1. Campell & Co., *Castor oil & Castor Oil Derivatives*, http://www.campbell-uv.com/castor.html (Accessed December, 2005).

2. Baker, *Urethanes - Castor oil - Chemical Derivatives*, in *CasChem Technical Bulletin 100*. 1982. p. 1-3.

3. Lysenko, Z., et al., *Separation of Plant Oil Triglyceride Mixtures by Solid Bed Adsorption.* U.S. Patent 7,097,770 B2, 2006.

4. Sonntag, N.O.V., *Structure and Composition of Fats and Oils*, in *Bailey's Industrial Oil and Fat Products*, D. Swern, Editor. 1979, John Wiley & Sons: New York. p. 1-98.

5. Smith, M., M. H., and L. Kunst, *Production of Hydroxy Fatty Acids in The Seeds of Arabidopsis Thaliana.* Biochem. Soc. Trans., 2000. **28**: p. 947-950.

6. Offeman, R.D., Stephenson, Serena K. , Robertson, George H., Orts, William J., *Solvent Extraction of Ethanol from Aqueous Solutions Using Biobased Oils, Alcohols, and Esters.* Journal of the American Oil Chemists' Society, 2006. **83**(2): p. 153-157.

7. Browse, J. and C. Somerville, *Glycerolipid Synthesis: Biochemistry and Regulation.* Annual Review of Plant Physiology and Plant Molecular Biology, 1991. **42**: p. 467-506.

8. Kates, M., *Glycolipids, Phosphoglycolipids, and Sulfolipids.* Handbook of Lipid Research, ed. D.J. Hanahan. Vol. 6. 1990: Plenum Press. 520.

9. Haines, T.H., *The Chemistry of The Sulfolipids.* Prog. Chem. Fats Other Lipids, 1971. **11**: p. 297.

10. Benson, A.A., *The Plant Sulfolipid.* Advances in Lipid Research, 1963: p. 387-394.

11. Benson, J.S., *Isolation and Fatty Acid Composition of the Plant Sulfolipid and Galactolipids.* Journal of Lipid Research, 1964. **5**: p. 432-436.

12. Norman, H.A., Mischke, Charles F, Allen, Bertha, Vincent, James S., *Semi-Preparative Isolation of Plant Sulfoquinovosyldiacylglycerols by Solid Phase Extraction and HPLC Procedure.* Journal of Lipid Research, 1996. **37**: p. 1372-1375.

13. Mudd, B.J. and K.F. Kleppinger-Sparace, *The Biochemistry of Plants*, P.K.

Stumpf and E.E. Conn, Editors. 1987, Academic Press: New York. p. 159-173.

14. Allen, C.F., Good, P., Davis, H.F., Chisum, P., *Methodology for the Separation of Plant Lipids and Application to Spinach Leaf and Chloroplast Lamellae.* The Journal of The American Oil Chemists' Society, 1966. **43**: p. 223-231.

15. Benning, C., *Biosysthesis and Function of The Sulfolipid Sulfoquinovosyl Diacylglycerol.* Annu. Rev. Plant Physiol. Plant Mol. Biol., 1998. **49**: p. 53-75.

16. Johnson, A.R. and J.B. Davenport, *Biochemistry and Methodology of Lipids.* 1971: Willey-Interscience. 578.

17. Kim, Y.H., J.S. Yoo, and M.S. Kim, *Structural Characterization of Sulfoquinovosyl, Monogalactosyl and Digalactosyl Diacylglycerols by FAB-CID-MS/MS.* Journal of Mass Spectrometry, 1997. **32**: p. 968-977.

18. Carter, H.E., R.A. Hendry, and N.Z. Stanacev, *Wheat Flour Lipids. III. Structure Determination of Mono- and Digalactosyl Diglycerides.* J. Lipid Res., 1961. **2**: p. 223.

19. Murray, R.K., M. Levine, and M.J. Kornblatt, *Sulfatides: Principle Glycolipids of the Testis, Spermatozoa of Chordates*, in *Glycolipid Methodology*, L.A. Witting, Editor. 1976, American Oil Chemists' Society: Champaign, Illinois. p. 305-327.

20. Gustafson, K.R., et al., *Aids-Antiviral Sulfolipids from Cyanobacteria (Blue-Green-Algae).* Journal of the National Cancer Institute, 1989. **81**(16): p. 1254-1258.

21. Fishwick, M.J. and A.J. Wright, *Comparison of Methods for the Extraction of Plant Lipids.* Biochemistry, 1977: p. 1507-1510.

22. Harwood, J.L., *Synthesis of Sulfoquinovosyl Diacylglycerol by Higher Plants.* Biochimica et Biophysica Acta, 1975. **398**: p. 224-230.

23. Barber J. and Gournaris K., *What Role Does Sulphollipid Play within the Thylakoid Membrane?* Photosynth. Res., 1986. **9**: p. 239-249.

24. Harwood, J.L., Jones A. L., *Lipid Metabolism in Algae.* Adv. Bot. Res., 1989. **16**: p. 1-53.

25. Andrews, J. and J. Ohlrogge, in *Plant Physiology, Biochemistry and Molecular Biology*, D.T. Dennis and D.H. Turpin, Editors. 1990, Longman Scientific & Technical, Singapore. p. 339.

26. Kates, M., *Plant Phospholipids and Glycolipids.* Adv. Lipid Res, 1970. **8**: p. 225.

27. Sigma-Aldrich, *Technical Information Bulletin - Ion-exchange Resins and Related polymeric Adsorbents*, http://www.sigmaaldrich.com/Brands/Aldrich/Tech_Bulletins/AL_142/Amberlite___Amberlyst.html (Accessed September, 2006).

28. Krishnankutty, N. and M.A. Vannice, *Effect of Pretreatment on Surface Area, Porosity, and Adsorption Properties of a Carbon Black.* Chem. Matter, 1995. **7**: p. 754-763.

29. Zweig, G. and J. Sherma, *Lipids.* CRC Handbook of Chromatography, ed. H.K. Mangold. Vol. 1. 2000, Boca Raton, Florida: CRC Press, Inc. 601.

30. Douglas M. Ruthven, *Principles of Adsorption and Adsorption Process.* 1984, New York: John Wiley & Sons, Inc. 433.

31. Yao, J.K. and G.M. Rastetter, *Microanalysis of Complex Tissue Lipids by High-Performance Thin-layer Chromatography.* Analytical Biochemistry, 1985. **150**(1): p. 111-16.

32. The Dow Chemical Company, *FILMTEC™ Membranes, DOWEX™ Ion Exchange Resins*, http://www.dow.com/liquidseps/prod/prd_dowx.htm (Accessed September, 2006).

33. AOCS official method Ce 2-66: Preparation of Methyl Esters of Long-chain Fatty Acids, in *Official Methods and Recommended Practices of the American Oil Chemists' Society*, D. Firestone, Editor. 1994, AOCS: Champaign, IL.

34. Baber, T.M., D.T. Vu, and C.T. Lira, *Liquid-Liquid Equilibrium of the Castor Oil + Soybean oil + Hexane Ternary System.* Journal of Chemical and Engineering Data, 2002. **47**(6): p. 1502-1505.

35. Levesque, B.A., Pierre; Tardif, Robert; Ferron, Liliane; Gingras, Suzanne; Schlouch, Emmanuelle; Gingras, Guy; Levallois, Patrick; Dewailly, Eric., *Cancer Risk Associated with Household Exposure to Chloroform.* Journal of Toxicology and Environmental Health, Part A, 2002. **65**(7): p. 489-502.

36. Hildebrand, J.H., *Solubility. XII. Regular Solutions.* J. Am. Chem. Soc, 1929. **51**(1): p. 66-80.

37. Hildebrand, J.H., *A History of Solution Theory.* Annual Review of Physical Chemistry, 1981. **32**: p. 1-23.

38. Hansen, C.M., *Three-Dimensional Solubility Parameter-Key to Paint-Component Affinities: I. Solvents, Plasticizers, Polymers, and Resins.* Journal of Paint Technology, 1967. **39**: p. 104-17.

39. Burke, J., *Solubility Parameters: Theory and Application.* The Book & Paper Group Annual, 1984. **3**: p. 13-58.

40. Barton, A.F.M., *CRC Handbook of Solubility Parameters and other Cohesion Parameters*. 1983: CRC Press. 594.

41. P. Dormann, S.H.-B., I. Balbo, and C. Benning, *Isolation and Characterization of an Arabidopsis Mutant Deficient in the Thylakoid Lipid Digalactosyl Diacylglycerol.* Plant Cell, 1995. **7**: p. 1801-1810.

42. Siakotos, A.N., *Analytical Separation of Nonlipid Water Soluble Substances and Gangliosides from Other Lipids by Dextran Gel Column Chromatography.* journal of American Oil Chemists' Society, 1965. **42**: p. 913-919.

43. Härtel, K., P. Dörmann, and C. Benning, *DGD1-Independent Biosynthesis of Extraplastidic Galatolipids after Phosphate Deprivation in Arabidopsis.* PNAS, 2000. **97**(19): p. 10649-54.

44. Gage, D.A., Z.-H. Huang, and C. Benning, *Comparison of Sulfoquinovosyl Diacylglycerol from Spinach and the Purple Bacterium Rhodobacter sphaeroides by Fast Atom Bombardment Tandem Mass Spectrometry.* Lipids, 1992. **27**(8): p. 632-636.

45. Ishizuka, I., Suzuki, M.,Yamakawa, T, *Isolation and Characterization of a Novel Sulfoglycolipid, 'Seminolipid,' from Boar Testis and Spermatozoa.* J. Biochem., 1973. **73**(1): p. 77-87.

46. E. Choe, J.L., K. Park, S. Lee, *Effects of Heat Treatment on Lipid and Pigments of Freeze-Dried Spinach.* Food Chemistry and Toxicology, 2001. **66**(8): p. 1074-1079.

47. Benson, A.A., *Plant sulfolipid. V. Lysolipid Formation.* Biochimica et Biophysica Acta, 1962. **57**: p. 601-603.

48. Benning, C., *Formic Acid in Extractions of Plant Lipids.* A Personal Communication, 2003.

49. O'Brien, J.S., Fillerup, Dorothy L., Mead, James F., *Brain Lipids: 1. Quantification and Fatty Acid Composition of Cerebroside Sulfate in Human Cerebral Gray and White Matter.* Journal of Lipid Research, 1964. **5**: p. 109-116.

50. Thomson, G.H. and A.H. Larsen, *DIPPR: Satisfying Data Needs.* J. Chem. Eng. Data, 1996. **41**: p. 930-934.

51. Dvoskin, N., *Thermodynamic Equilibrium of New Organic Mixtures for Absorption Heat Pumps*, in *Mechanical Engineering*. 2004, Ben-Gurion

University. p. 121.

52. Hala, E., et al., *Vapor Liquid Equilibrium.* 2nd ed. 1967: Pergamon Press, Oxford.

53. Abbott, M.M., *Low-Pressure Phase Equilibria: Measurement of VLE.* Fluid Phase Equilibria, 1986. **29**: p. 193-207.

54. Lyman et al., *Vapor Pressure*, in *Handbook of Chemical Property Estimation Methods.* 1982. p. 14-1, 14-20.

55. Chiou, C.T. and V.J. Freed, *Chemical Studies on Bench Mark Industrial Chemicals.* Annaual Report to National Science Foundation on Contract AEN7617700, Report No. NSF/RA-770286, National Science Foundation, Washington D.C., 1977.

56. Reid, R.C., J.M. Prausnitz, and T.K. Sherwood, *The Properties of Gases and Liquids*, ed. rd. 1977, New York: McGraw-Hill Book Co.

57. Pandharipande, S.L., Laxminarayan Institute of Technology, and N. Nagpur University, India,, *Artificial neural network: Prediction of vapor pressure of phenol series.* Chemical Engineering World, 2004. **39**(7): p. 70-72.

58. Miller, D.G., *Estimating Vapor Pressure - a Comparison of Equations.* Ind. Eng. Chem, 1964. **56**: p. 46.

59. Thomson, G.W., *Techniques of Organic Chemistry*, A. Weissberger, Editor. 1959, Interscience: New York. p. 473.

60. Fishtine, S.H., *Reliable Latent Heats of Vaporization.* Ind. Eng. Chem, 1963. **55**(47).

61. Kistiakovskii, V.A., *Latent Heats of Vaporization.* J. Russ. Phys. Chem. Soc., 1921. **53**(1): p. 256-64.

62. Nelken, L.H. and D. Birkett, *Dipole Moment*, in *Handbook of Chemical Property Estimation Methods*. p. 25-1 - 25-22.

63. Watson, K.M., *Thermodynamics of the Liquid State - Generalized Prediction of Properties.* Ind. Eng. Chem, 1943. **35**: p. 398.

64. Korsten, H., *Internally Consistent Prediction of Vapor Pressure and Related Properties.* Ind. Eng. Chem, 2000. **39**: p. 813-820.

65. Yair, O.B. and A. Fredenslund, *Extension of the UNIFAC Group-Contribution Method for the Prediction of Pure-Component Vapor Pressure.* Ind. Eng. Chem. Process Des. Dev., 1983. **22**: p. 433-436.

66. Jensen, T., A. Fredenslund, and P. Rasmussen, *Pure-Component Vapor-Pressures Using UNIFAC Group Contribution.* Industrial & Engineering Chemistry Fundamentals, 1981. **20**(3): p. 239-246.

67. Gray, N.H., Z.N. Gerek, and J.R. Elliott, *Molecular Modeling of Isomer Effects in Naphthenic and Aromatic Hydrocarbons.* Fluid Phase Equilibria, 2005. **228**: p. 147-153.

68. N. Bureau, J.J., I. Mokbel, and J-C. de Hemptinne, *Vapour Pressure Measurements and Prediction for Heavy Esters.* J. Chem. Thermodynamics, 2001. **33**(11): p. 1485-1498.

69. William. E. Asher, J.F.P., Garnet. B. Erdakos, and John. H. Seinfeld, *Estimating the vapor pressures of multi-functional oxygen-containing organic compounds using group contribution methods.* Atmospheric Environment, 2002. **36**(9): p. 1483-1498.

70. Constantinou, L. and R. Gani, *New Group Contribution Method for estimatiing Properties of Pure Compounds.* AIChE J., 1994. **40**(10): p. 1697-1709.

71. Joback, K.G. and R.C. Reid, Chem. Eng. Commun., 1987. **57**: p. 233-243.

72. Aspen Technologies, *Physical Property Methods and Models*, in *Aspen Physical Property System 2004.1 User Manual.* p. 8-4 - 8-5.

73. Riedel, L.A., *A New Universal Vapor Pressure Equation.* Chem. Ing. tech, 1954. **26**: p. 83.

74. D. Ambrose and J. Walton, *Vapor-Pressure up to Their Critical Temperatures of Normal Alkanes and Alkanols.* Pure & Appl. Chem. **61**: p. 1395-1403.

75. Aspen Technology, I., *Physical Property Reference Manuals.* Aspen Physical Property System 2004.1, April 2005.

76. T. B. Thompson (Ed.) at tbthompson@dow.com, *Chemical Industry of the Future, Technology Roadmap for Computational Chemistry.* 1999.

77. Fiona Case, et al., *The second industrial fluid properties simulation challenge.* Fluid Phase Equilibria, 2005. **236**: p. 1-14.

78. Elliott, J.R., *SPEAD 1.03. 1.04, Intro and Help.*

79. J. R. Elliott, *SPEAD Progress Report, June 2003.* 2003.

80. Prausnitz, J.M., R.N. Lichtenthaler, and E.G.d. Azevedo, *Molecular*

Thermodynamics of Fluid-Phase Equilibria. 3rd ed. In The Physical and Chemical Engineering Sciences, ed. P.H. International. 1999: Prentice-Hall, Inc. 860.

81. Chapela, G.A., L.E. Scriven, and H.T. Davis, *Molecular Dynamics for Discontinuous Potential. IV. Lennard Jonesium.* J. Chem. Phys., 1989. **91**: p. 4307.

82. Mackie, A.D., et al., *Vapour-liquid phase equilibria predictions of methane-alkane mixtures by Monte Carlo simulation.* Molecular Simulation, 1997. **19**(1): p. 1-15.

83. Goujon, F., Malfreyt, P., Boutin, A. and Fuchs, A. H., *Vapour-liquid phase equilibria of n-alkanes by direct Monte Carlo simulations.* Molecular Simulation, 2001. **27**(2): p. 99-114.

84. Cui, J.Y. and J.R. Elliott, *Phase Diagrams for a Multistep Potential Model of n-Alkanes by Discontinuous Molecular Dynamics and Thermodynamic Perturbation Theory.* Journal of Chemical Physics, 2002. **116**(19): p. 8625-8631.

85. Rice, R.G. and D.D. Do, *Approximate Solution Methods for ODE: Perturbation Methods*, in *Applied Mathematics and Modeling for Chemical Engineers.* 1995, John Willey & Sons, Inc. p. 184-189.

86. Barker, J.A. and D. Henderson, *Perturbation Theory and Equation of State for Fluids: The Square-Well Potential.* J. Chem. Phys., 1967. **47**(8): p. 2856-2861.

87. Cui, J.Y. and J.R. Elliott, *Phase envelopes for variable width square well chain fluids.* Journal of Chemical Physics, 2001. **114**(16): p. 7283-7290.

88. George B. Thomas, J. and R.L. Finney, *Calculus and Analytic Geometry.* 2003, Library of Congress Cataloging-in-Publication Data. p. 333.

89. Hu, L.G., Rangwalla, H., Cui, J. Y., and Elliott, J. R., *Vapor-liquid equilibria of vibrating square well chains.* Journal of Chemical Physics, 1999. **111**(3): p. 1293-1301.

90. Carnahan, N.F. and K.E. Starling, *Equation of State for Nonactracting Rigid Spheres.* J. Chem. Phys., 1969. **51**: p. 635-636.

91. Miller, D.J.A., Navinchandra S. ; Kolah, Aspi; Lira, Carl T. (Board of Trustees of Michigan State University, USA), *Process for Production of Organic Acid Esters by Reactive Distillation*, in *U.S. Pat. Appl. Publ.* 2006. 20 pp.

92. Holten, C.H., *Lactic acid: Properties and Chemistry of Lactic Acid and Derivatives.* Verlag Chemie. 1971.

93. Vidler, W., *The Kinetics of Polymer Formation and Hydrolysis in Lactic Solutions.* Report to Stichting Ilra., 1959. **Personal Communication.**

94. Van Ness, J.H., *Hydroxy Carboxylic Acids.* Encyclopedia of Chemical Technology. Kirk Othmer. Vol. 13. 1981, New York: Willey.

95. Montgomery, R., *Acidic Constituents of Lactic Acid-Water Systems.* J. Am. Chem. Soc., 1952. **74**(6): p. 1466 -1468.

96. LockWood, L.B., D.E. Yoder, and M. Zienty, *Lactic Acid.* Ann. N.Y. Acad. Sci., 1965. **119**: p. 854-867.

97. Eder, R. and F. Kutter, *Gleichgewicht von Milchsäure und Milchsäure-anhydrid in Handelsmilchsäure.* Helv. chim. Acta, 1926. **9**: p. 355-364.

98. Vu, D.T., et al., *Vapor-liquid Equilibria in the Systems Ethyl Lactate + Ethanol and Ethyl Lactate + Water.* Journal of Chemical and Engineering Data, 2006. **51**(4): p. 1220-1225.

99. Elliott, J.R. and C.T. Lira, *Introductory Chemical Engineering Thermodynamics.* 1999: Prentice Hall PTR. 660.

100. Hefter, G.T., *Solubility data. Diethyl Succinate - Water System.* Solubility Data Series, 1992. **49**: p. 91-4.

101. Cottrell, F., *On the Determination of Boiling Points of Solutions.* J. Am. Chem. Soc., 1919. **41**: p. 721-729.

102. Sanz, M.T., et al., *Vapor Liquid Equilibria of the Mixtures Involved in the Esterification of Lactic Acid with Methanol.* Journal of Chemical and Engineering Data, 2003. **48**(6): p. 1446-1452.

103. Vu, D.T., et al., *Oligomer Distribution in Concentrated Lactic Acid Solutions.* Fluid Phase Equilibria, 2005. **236**: p. 125-135.

104. Ferreira, A.C.D., J.C. Barbe, and A. Bertrand, *Heterocyclic Acetals from Glycerol and Acetaldehyde in Port Wines: Evolution with Aging.* Journal of Agricultural and Food Chemistry, 2002. **50**(9): p. 2560-2564.

105. Delfort, B., et al., *Diesel Fuel Compounds Containing Glycerol Acetals, Pub. No: US 2003/0163949 A1*, in *United States Patent Application Publication.* Sep. 4, 2003: France.

106. Advanced Chemistry Development, *ChemSketch 8.17 Freeware.*

107. Gray, N.H., *Layout of M3D File.* Report to J. Richard Elliott, 2006. **Personal Communication**.

108. Baskaya, F.S., et al., *Transferable step potentials for amines, amides, acetates, and ketones.* Fluid Phase Equilibria, 2005. **236**: p. 42-52.

109. Ye, T. and S. Kalyanaraman. *A Recursive Random Search Algorithm for Large-Scale Network Parameter Configuration.* in *ACM SIGMETRICS International Conference on Measurement and Modeling of Computer Systems.* 2003. San Diego, CA, USA.

110. Broyden, G., *the Convergence of a Class of Double-Rank Minimization Algorithms, Parts I and II.* J. Inst. Math. Appl., 1970. **6**: p. 76-90 and 222-231.

111. Shanno, D.F., *Conditioning of Quasi-Newton Methods for Function Minimization.* Mathematics of Computation, 1970. **24**: p. 647-656.

112. Goldfrab, D., *A Family of Variable Metric Methods Derived by Variational Means.* Mathematics of Computation, 1970. **24**: p. 23-26.

113. Fletcher, R., *A New Approach to Variable Metric Algorithms.* Computer Journal, 1970. **13**: p. 317-322.

114. Dennis, J.E. and R.B. Schnabel, *Numerical Methods for Unconstrained Optimization and Nonlinear Equations*. Computational Mathematics. 1983: Prentice-Hall. 378.

115. Gill, P.E., W. Murray, and M.H. Wright, *Practical Optimization*. 1981: Academic Press. 401.

116. Ambrose, D., Sprake, C.H.S., *Vapor Pressure of Alcohols.* J. Chem. Thermo., 1970. **2**: p. 631.

117. Timmermans, J., *Physico-Chemical Constants of Pure Organic Substances*. 2nd ed. 1965: Elsevier, New York.

118. Ambrose, D., Counsell, J.F., Laurenson, I.J., Lewis, G.B.,, *Thermodynamic Properties of Organic Oxygen Compounds. XLVII. Pressure, Volume, Temperature Relations and Thermodynamic Properties of Propan-2-ol.* J. Chem. Thermo., 1978. **10**: p. 1033.

119. Lyons, R.L., *The Determination of Critical Properties and Vapor Pressure of Thermally Stable and Unstable Compounds.* M.S. Thesis, Dept. of Chem. Eng. The Pennsylvania State University, May 1985.

120. Ambrose, D. and R. Townsend, *Thermodynamic Properties of Organic Oxygen*

Compounds. Part IX. The Critical Properties and Vapour Pressures above Five Atmospheres of Six Aliphatic Alcohols. J. Chem. Soc., 1963: p. 3614.

121. Boublik, T., Fried, V., Hala, E., *The Vapour Pressures of Pure Substances.* 1973: Elsevier, New York.

122. Sachek, A.I., Markovnik, V.S., Peshchenko, A.D., Shvaro, O.V., Andreevskii, D.N., *Vapor Pressure of Secondary C5 - C8 Alcohols of Normal Structure.* Sov. Chem. Ind., 1984. **16**: p. 705.

123. Hovorka, F., Lankelma, H.P., Stanford, S.C., *Thermodynamic Properties of the Hexyl Alcohols. II. Hexanols-1, -2, -3 and 2-Methylpentanol-1 and -4.* J. Amer. Chem. Soc., 1938. **60**: p. 820.

124. Ambrose, D., Ghiassee, N.B., *Vapor Pressures, Critical Temperatures, and Critical Pressures of Benzyl Alcohol, Octan-2-ol, and 2-Ethylhexan-1-ol.* J. Chem. Thermo., 1990. **22**: p. 307.

125. McKillop, A., Ford, M.E., *Mercury-Assisted Solvolyses of Alkyl Halides. Simple Procedure for the Preparation of Nitrate Esters, Acetate Esters, Alcohols and Ethers.* Tetrahedron, 1974. **30**: p. 2467-2475.

126. Polgar, N., Robinson, R., *Synthetical Experiments Bearing on the Constitution of Phthioic Acid.* J. Chem. Soc., 1945: p. 393.

127. Thomas, L.H., Meatyard, R., *Viscosity and Molecular Association. Part IV. Association of Monohydric Alcohols and Some Hindered Phenols.* J. Chem. Soc., 1986: p. 1963.

128. Thomas, L.H., Meatyard, R., Smith, H., Davies, G.H., *Vapor Pressures and Molar Entropies of Vaporization of Monohydric Alcohols.* J. Chem. Eng. Data, 1979. **24**(3): p. 159.

129. N'Guimbi, J., Berro, C., Mokbel, I., Rauzy, E., Jose, J., *Experimental vapour pressures of 13 secondary and tertiary alcohols--correlation and prediction by a group contribution method.* Fluid Phase Equilibria, 1999. **162**: p. 143-158.

130. Sherrill, M.L., *An Investigation of a Series of Derivatives of Normal Heptane. I. Preparation, Identification and Physical Constants.* J. Amer. Chem. Soc., 1982. **52**: p. 1930.

131. Ambrose, D., Ghiassee, N.B., *Vapor Pressures and Critical Temperatures and Critical Pressures of C5 and C6 Cyclic Alcohols and Ketones.* J. Chem. Thermo., 1987. **19**: p. 903.

132. Riddick, J.A., Bunger, W.B., Sakano, T.K., *Organic Solvents: Physical*

Properties and Methods of Purification. 4th ed. 1986: Wiley Interscience, New York.

133. Huckel, W., Hubele, A., *Cis- and trans-1-Methyl-2-Cyclohexanol.* Liebigs Ann. Chem., 1958. **27**: p. 613.

134. Eliel, E.L., Haber, R.G., *the Boiling Points of the Methylcyclohexanols - an Exception to the Conformational Rule.* J. Org. Chem., 1958. **23**: p. 2041.

135. Matyschok, H., Pritzkow, W., Radeglia, R., *Untersuchungen zur Sulfochlorierung von Paraffinen. II. Untersuchungen uber die Reaktion von Aliphatischen Sulfochloriden mit Nucleophilen.* J. Prakt. Chem., 1977. **319**: p. 46.

136. *Selected Values of Properties of Chemical Compounds, Data Project.* Thermodynamics Research Center, Texas A&M University, College Station, Texas, loose-leaf data sheets, 1980-extant.

137. Young, S., *the Vapour-Pressure, Specific Volumes, Heats of Vaporization, and Critical Constants of Thirty Pure Substances.* Royal Dublin Society, Scientific Proceedings, Ser. A. Vol., 1910. **12**: p. 374.

138. Gonzalez, E., Ortega, J., *Densities and Isobaric Vapor-Liquid Equilibria of Butyl Esters (Methanoate to Butanoate) with Ethanol at 101.32 KPa.* J. Chem. Eng. Data, 1995. **40**: p. 1178.

139. Ortega, J., Galvan, S., *Vapor-Liquid Equilibria and Densities for Propyl Butanoate + Normal Alcohols at 101.32 kPa.* J. Chem. Eng. Data, 1995. **40**: p. 699.

140. Farkova, J., Wichterle, I., *Vapour Pressures of Some Ethyl and Propyl Esters of Fatty Acids.* Fluid Phase Equil., 1993. **90**: p. 143.

141. Riddick, J.A., Bunger, W.B., Sakano, T.K., *Organic Solvents: Physical Properties and Methods of Purification.* 3rd ed. ed. 1970: Wiley Interscience, New York.

142. Bonhorst, C.W., Althouse, P.M., Triebold, H.O., *Esters of Naturally Occurring Fatty Acids. Physical Properties of Methyl, Propyl and Isopropyl Esters of C6 to C10 Saturated Fatty Acids.* Ind. Eng. Chem., 1948. **40**: p. 2379.

143. Gros, A.T., Feuge, R. O., *Surface and Interfacial Tensions, Viscosities, and other Physical Properties of Some n-Aliphatic Acids and their Methyl and Ethyl Esters.* J. Amer. Oil Chem. Soc, 1952. **29**: p. 313-17.

144. Vogel, A.I., *Physical Properties and Chemical Constitution. Part XIII. Aliphatic Carboxylic Esters.* J. Chem. Soc., 1948: p. 624.

145. Bronsted, J.N., Colmant, P., *Molekulgrosse und Phasenverteilung. III.* Z. Phys. Chem. (A), 1934. **168**: p. 381.

146. Walker, R., Davidson, D.W., *The Dielectric Constant and Dipole Moment of 1,3-Dioxane.* Can. J. Chem., 1959. **37**: p. 492.

147. Fletcher, S.E., Mortimer, C.T., Springall, H.D., *Heats of Combustion and Molecular Structure. Part VII. 1:3 Dioxa- and 1:3:5-Trioxa-cycloalkanes.* J. Chem. Soc. London, 1959: p. 580.

148. Arbusov, B.A., Vinogradova, V.S., *Parachors of the Cyclic Esters of Carbonic Sulfurous and Phosphorous Acids.* Izv. Akad. SSSR, 1950. **297**.

149. Kobe, A.K., Ravicz, A.E., Vohra, S.P., *Critical Properties and Vapor Pressures of Some Ethers and Heterocyclic Compounds.* J. Chem. Eng. Data, 1956. **1**(1): p. 50.

150. Crenshaw, J.L., Cope, A.C., Finklestein, Rogan, R., *The Dioxanates of the Mercuric Halides.* J. Amer. Chem. Soc., 1938. **60**: p. 2310.

151. Melia, T.P., Bailey, D., Tyson, A., *Thermodynamics of Addition Polymerisation. I. The System Trioxane-Polyoxymethylene.* J. Appl. Chem., 1967. **17**: p. 15.

152. Komatsu, S., Masumoto, M., *Studies on Catalytic Action at High Pressure and Temperature. Catalytic Hydrogenation of Ethers.* Bull. Chem. Soc. Jap., 1930. **5**: p. 241.

153. Quaker Oats Chemicals Inc., *Tetrahydrofurfuryl Alcohol.* Bulletin 206-A, Chicago, IL, 1960.

154. Kaufmann, W.E., Adams, R., *the Use of Platinum Oxide as a Catalyst in the Reduction of Organic Compounds. IV. Reduction of Furfural and its Derivatives.* J. Amer. Chem. Soc., 1923. **45**: p. 3029.

155. *CRC Handbook of Chemistry and Physics.* 63 ed, ed. M.J.A. Robert C. Weast. 1982-1983: CRC Press.

156. Wakelyn, P.J., Wan, Peter J., National Cotton Council, Washington, DC, USA., *Edible Oil extraction Solvents: FDA Regulatory Considerations.* Inform., 2004. **15**(1): p. 22-23.

157. Cavalcante, C.L., Jr., *Industrial Adsorption Separation Processes: Fundamentals, Modeling and Applications.* Latin American Applied Research, 2000. **30**(4): p. 357-364.